

[IMD Overview](#)

[What's New in Version 4](#)

[Chapter 1. Getting Started](#)

[1.1 System requirements](#)

[1.2 Downloading IMD](#)

[1.3 Installing IMD](#)

[1.4 Starting IMD](#)

[Chapter 2. Modeling](#)

[2.1 Designating materials and optical constants](#)

- [Browsing the IMD optical constants database](#)
- [Material designation method 1: by reference to an optical constants file](#)
- [Material designation method 2: by specification of density and composition](#)

[2.2 Defining a structure: specifying](#)

IMD

Version 4.1, December 1998

David L. Windt

windt@bell-labs.com

www.bell-labs.com/user/windt/idl

Copyright (c) 1997-1998, David L. Windt, Bell Laboratories, Lucent Technologies. All rights reserved

Overview - What is IMD and what can it do?

IMD is a point-and-click IDL application that can calculate specular and non-specular (diffuse) optical functions of an arbitrary multilayer structure, i.e., a structure consisting of any number of layers of any thickness, and of any material. **IMD** includes a database of optical constants for over 150 materials, spanning the X-ray region to the infrared. It's also easy to use your own optical constants if necessary, or to create new X-ray optical constants for any compound, using tabulated atomic scattering factors for 92 elements. **IMD** can be used for both modeling and for parameter estimation by nonlinear, least-squares curve-fitting (including confidence interval generation) to your own measured data.

The **IMD** graphical user interface allows you to quickly define the multilayer structure you wish to consider. The general multilayer structure consists of any number of individual layers, which can be grouped together to create periodic (and optionally depth-graded) multilayers, if desired. You can even create 'groups of groups' of layers, with no limit on nesting depth. Layers and periodic multilayers can be inserted or removed anywhere in the stack.

Specular optical functions - reflectance, transmittance, absorbance, electric

parameters

- [Ambient](#)
- [Multilayer stack](#)
 - [Layers](#)
 - [Periodic multilayers](#)
 - [Depth-graded multilayers](#)
 - [Nested multilayers](#)
 - [Layer-data files](#)
- [Substrate](#)
- [Interfaces](#)
 - [Modified Fresnel coefficients: interface widths and interface profile functions](#)
 - [Power-Spectral-Density functions](#)
 - [Graded interfaces](#)

2.3 Specifying variables and coupled parameters

- [Dependent variables](#)
 - [Specular optical functions / Electric fields](#)
 - [User-defined specular optical functions](#)
 - [Non-specular](#)

field intensities, phase shifts, and ellipsometric psi and delta functions - are computed using an algorithm that is based on recursive application of the Fresnel equations [1], modified to include interfacial roughness and/or diffuseness [2,3]. Non-specular reflected intensities can be computed using either a dynamical Born approximation vector theory [4], or the so-called 'Distorted-Wave Born Approximation' formalism [5-8], a scalar theory which is nonetheless valid below the critical angle of total external reflection in the X-ray region. For both specular and non-specular computations, a stochastic model of film growth and erosion [9] can be used to account for the evolution of interfacial roughness through the film stack. Alternatively, a more conventional roughness model [10] can be used, with the option of defining depth-graded roughness and correlation length parameters.

The specular and non-specular optical functions can be calculated not just as a function of incidence angle and/or wavelength, but also as a function of any of the parameters that describe the multilayer structure (i.e., optical constants, densities, layer thicknesses, roughness parameters, etc.) and/or the incident 'beam' (i.e., polarization, and spectral or angular resolution) You can designate as many as eight independent variables simultaneously. In addition, individual structure parameters can be coupled to one another, so that a single independent variable (or fit parameter) can be used to vary multiple parameters.

An interactive visualization tool, **IMDXPLOT**, allows you to view, analyze and print 1D or 2D 'slices' through multi-dimensional optical functions; with this visualization tool, it's possible to vary a given parameter and see the resulting effect on the optical functions in real time. **IMDXPLOT** makes it easy to overlay multiple optical functions on a single plot, and to include a variety of labels and legends; 2D 'slices' can be viewed as either surface or contour plots You can also overlay your own measured data in order to compare interactively your measurements to the calculations.

Parameter estimation is afforded by fitting an optical function to your own experimental data, using nonlinear, least-squares curve-fitting, with an unlimited number of adjustable parameters: any of the parameters that describe the multilayer structure or the incident beam can be fit. Multi-dimensional confidence intervals associated with the best-fit parameter values can be estimated as well, and **IMDXPLOT** can be used to view confidence interval 'slices' in parameter space.

The **IMD** interface was created with the hope that you will not need to consult this documentation very much. Nonetheless, contained in the chapters that follow is a detailed description of how to use **IMD** for modeling and

[optical functions](#)

- [Independent variables](#)
 - [Independent variables specific to electric field calculations](#)
 - [Independent variables specific to non-specular optical functions](#)
- [Coupled parameters](#)

[2.4 Performing the computation](#)

[2.5 Viewing, printing and saving the results](#)

- [Saving the Results](#)
- [Viewing and Printing the Results - IMDXPLOT](#)
 - [Fixed Curves](#)
 - [Statistics: estimating film thicknesses, feature widgets, etc.](#)
- [Examples](#)
 - [Reflectance and transmittance contours of a Y/Al multilayer](#)
 - [Electric field intensity contours of a Mo/Si](#)

parameter estimation. In addition, a variety of example files are included with the IMD distribution, which illustrate some of IMD's unique modelling and visualization capabilities. You might also have a look at the preprint of reference [11], to learn a bit more about the inner workings of IMD (as of version 3.1, that is.)

[next](#)

Last Updated: **1-Dec-1998**

[dlw](#)

- [multilayer](#)
 - [Reflectance of a depth-graded C/Ni multilayer, using coupled parameters](#)
 - [Normal incidence non-specular scattering for a Mo/Si multilayer using the BA](#)
 - [Grazing incidence non-specular scattering for a W/Si multilayer using the DWBA](#)
-

[Chapter 3. Measured Data and Parameter Estimation](#)

[3.1 Using your measured data](#)

[3.2 Specifying fit parameters](#)

[3.3 Curve-fitting](#)

[3.4 Confidence intervals](#)

[Chapter 4. Problem Solving, and](#)

[Reporting Bugs](#)

[Appendix A - Optical Constants](#)

[A.1 The IMD optical constants database](#)

[A.2 Using your own optical constants](#)

[A.3 Creating new X-ray optical constants](#)

[Appendix B- Notes for IDL programmers](#)

[B.1 Customizing the installation](#)

[B.2 Some IMD functions and procedure](#)

[B.3 Reading measured data files](#)

[B.4 IMD COMMON block variables](#)

[References](#)

[Preprint of *Computers in Physics* article on IMD](#)

IMD

Version 4.1, December 1998

David L. Windt

windt@bell-labs.com

www.bell-labs.com/user/windt/idl

Copyright (c) 1997-1998, David L. Windt, Bell Laboratories, Lucent Technologies. All rights reserved

Overview - What is IMD and what can it do?

IMD is a point-and-click IDL application that can calculate specular and non-specular (diffuse) optical functions of an arbitrary multilayer structure, i.e., a structure consisting of any number of layers of any thickness, and of any material. **IMD** includes a database of optical constants for over 150 materials, spanning the X-ray region to the infrared. It's also easy to use your own optical constants if necessary, or to create new X-ray optical constants for any compound, using tabulated atomic scattering factors for 92 elements. **IMD** can be used for both modeling and for parameter estimation by nonlinear, least-squares curve-fitting (including confidence interval generation) to your own measured data.

The **IMD** graphical user interface allows you to quickly define the multilayer structure you wish to consider. The general multilayer structure consists of any number of individual layers, which can be grouped together to create periodic (and optionally depth-graded) multilayers, if desired. You can even create 'groups of groups' of layers, with no limit on nesting depth. Layers and periodic multilayers can be inserted or removed anywhere in the stack.

Specular optical functions - reflectance, transmittance, absorbtance, electric field intensities, phase shifts, and ellipsometric psi and delta functions - are computed using an algorithm that is based on recursive application of the Fresnel equations [1], modified to include interfacial roughness and/or diffuseness [2,3]. Non-specular reflected intensities can be computed using either a dynamical Born approximation

vector theory [4], or the so-called 'Distorted-Wave Born Approximation' formalism [5-8], a scalar theory which is nonetheless valid below the critical angle of total external reflection in the X-ray region. For both specular and non-specular computations, a stochastic model of film growth and erosion [9] can be used to account for the evolution of interfacial roughness through the film stack. Alternatively, a more conventional roughness model [10] can be used, with the option of defining depth-graded roughness and correlation length parameters.

The specular and non-specular optical functions can be calculated not just as a function of incidence angle and/or wavelength, but also as a function of any of the parameters that describe the multilayer structure (i.e., optical constants, densities, layer thicknesses, roughness parameters, etc.) and/or the incident 'beam' (i.e., polarization, and spectral or angular resolution) You can designate as many as eight independent variables simultaneously. In addition, individual structure parameters can be coupled to one another, so that a single independent variable (or fit parameter) can be used to vary multiple parameters.

An interactive visualization tool, **IMDXPLOT**, allows you to view, analyze and print 1D or 2D 'slices' through multi-dimensional optical functions; with this visualization tool, it's possible to vary a given parameter and see the resulting effect on the optical functions in real time. **IMDXPLOT** makes it easy to overlay multiple optical functions on a single plot, and to include a variety of labels and legends; 2D 'slices' can be viewed as either surface or contour plots You can also overlay your own measured data in order to compare interactively your measurements to the calculations.

Parameter estimation is afforded by fitting an optical function to your own experimental data, using nonlinear, least-squares curve-fitting, with an unlimited number of adjustable parameters: any of the parameters that describe the multilayer structure or the incident beam can be fit. Multi-dimensional confidence intervals associated with the best-fit parameter values can be estimated as well, and **IMDXPLOT** can be used to view confidence interval 'slices' in parameter space.

The **IMD** interface was created with the hope that you will not need to consult this documentation very much. Nonetheless, contained in the chapters that follow is a detailed description of how to use **IMD** for modeling and parameter estimation. In addition, a variety of example files are included with the **IMD** distribution, which illustrate some of **IMD**'s unique modelling and visualization capabilities. You might also have a look at the preprint of reference [11], to learn a bit more about the inner workings of **IMD** (as of version 3.1, that is.)

[next](#)

Last Updated: **1-Dec-1998**

[dlw](#)

References

1. M. Born and E. Wolf, *Principles of Optics*, sixth edition, Pergamon Press, Oxford, 1980.
2. D. G. Stearns, 'The scattering of X-rays from non-ideal multilayer structures', *J. Appl. Phys.* **65**, 491-506 (1989).
3. L. Nevot and P. Croce, 'Caracterisation des surface par reflexion rasante de rayons X. Application a l'etude du polissage de quelques verres silicates.', *Revue. Phys. Appl.*, **15**, 761-779 (1980).
4. D. G. Stearns, 'X-ray scattering from interfacial roughness in multilayer structures', *J. Appl. Phys.*, **71**, 4286-4298 (1992); D. G. Stearns, D. P. Gaines, D. W. Sweeney, and E. M. Gullikson, 'Nonspecular X-ray scattering in a multilayer-coated imaging system.', *J. Appl. Phys.* **84**, 1003-1028 (1998). Click [here](#) to view a reprint.
5. S. K. Sinha, E. B. Sirota, S. Garoff, and H. B. Stanley, 'X-ray and neutron scattering from rough surfaces', *Phys. Rev. B*, **38**, 2297-2311 (1988).
6. V. Holy, J. Kubena, I. Ohlidal, K. Lischka, and W. Plotz, 'X-ray reflection from rough layered systems', *Phys. Rev. B*, **47**, 15896-15903 (1993).
7. V. Holy and T. Baumbach, 'Nonspecular X-ray reflection from rough multilayers.', *Phys. Rev. B*, **49**, 10668-10676 (1994).
8. D. K. G. de Boer, 'X-ray scattering and x-ray fluorescence from materials with rough interfaces', *Phys.Rev. B*, **53**, 6048-6064 (1996).
9. D. G. Stearns, 'Stochastic model for thin film growth and erosion', *Appl. Phys. Lett.* **62**, 1745-1747 (1993).
10. D. K. G. de Boer, 'X-ray reflection and transmission by rough surfaces.', *Phys. Rev. B*, **51**, 5297-5305 (1995).
11. D. L. Windt, 'IMD - Software for modelling the optical properties of multilayer films.', *Computers in Physics*, to be published, (Jul/Aug 1998). Click [here](#) to view a preprint.
12. B. L. Henke, E. M. Gullikson, and J. C. Davis, 'X-ray interactions: photabsorption, scattering, transmission, and reflection at E=50-30,000 eV, Z=1-92', *Atomic Data and Nuclear Tables*, **54** (1993). In addition to the data contained therein, the Center for X-Ray Optics (CXRO), Lawrence Berkeley Laboratory, maintains an active database of atomic scattering factors; these data are available at <<http://www-cxro.lbl.gov>>, and have been included in IMD, courtesy of E. M. Gullikson.
13. High-energy atomic scattering factors are available from the Lawrence Livermore National Laboratory, at <http://www-phys.llnl.gov/V_Div/scattering/asf.html>.
14. D. W. Marquardt, 'An algorithm for least-squares estimation of nonlinear parameters', *J. Soc. Ind. Appl. Math.*, **11**, 431-441 (1963).
15. P. R. Bevington, *Data Reduction and Error Analysis for the Physical Sciences*, McGraw-Hill, New York, 1969.
16. M. Lampton, B. Margon and S. Bowyer, 'Parameter estimation in X-ray astronomy', *Ap. J.*, **208**, 177 (1976).
17. W. Cash, 'Generation of confidence intervals for model parameters in X-ray astronomy', *Astron. & Astrophys.*, **52**, 307 (1976).

18. *Handbook of Optical Constants of Solids*, edited by E. D. Palik, Academic Press, Inc., 1985.
 19. MINPACK-1, Jorge More', FORTRAN code available at<<http://www.netlib.org>>; *Optimization Software Guide*, Jorge More' and Stephen Wright, SIAM, **Frontiers in Applied Mathematics**, 14.
-

[Contents](#)

Nonspecular x-ray scattering in a multilayer-coated imaging system

D. G. Stearns,^{a)} D. P. Gaines,^{b)} and D. W. Sweeney

Lawrence Livermore National Laboratory, P.O. Box 808, Livermore, California 94550

E. M. Gullikson

Center for X-Ray Optics, Lawrence Berkeley Laboratory, 1 Cyclotron Road, Berkeley, California 94720

(Received 6 January 1998; accepted for publication 11 April 1998)

We present a rigorous theoretical treatment of nonspecular x-ray scattering in a distributed imaging system consisting of multilayer-coated reflective optics. The scattering from each optical surface is obtained using a vector scattering theory that incorporates a thin film growth model to provide a realistic description of the interfacial roughness of the multilayer coatings. The theory is validated by comparing calculations based on measured roughness to experimental measurements of nonspecular scattering from a Mo–Si multilayer coating. The propagation of the scattered radiation through the optical system is described in the context of transfer function theory. We find that the effect of nonspecular scattering is to convolve the image with a point spread function that is independent of the coherence of the object illumination. For a typical soft x-ray imaging system, the scattering within the image field from the multilayer coatings is expected to be slightly greater than for single surfaces (as normalized to the reflectivity). This is because the roughness of the coatings includes both replication of the substrate roughness and the intrinsic roughness of the multilayer growth process. Our analysis indicates that the current multilayer coating technology is capable of producing soft x-ray imaging systems that have acceptably low levels of scattering, provided that the optical substrates are sufficiently smooth. [S0021-8979(98)02214-2]

I. INTRODUCTION

Advancement in areas such as extreme ultraviolet (EUV) lithography¹ and x-ray astronomy² are spurring dramatic improvement in the performance of optical imaging systems for the soft x-ray regime ($1 < \lambda < 100$ nm). The ultimate goal is to achieve high throughput with resolution near the diffraction limit. This requires the use of all reflective, distributed imaging systems working near normal incidence. However, the normal incidence reflectivity of all materials is very low at soft x-ray wavelengths. The problem is overcome by coating the optical surfaces with multilayer films, which increases the reflectivity by several orders of magnitude in comparison to a single surface. There are yet many potential problems that can degrade the image formation and limit the resolution. One of the most important of these is the nonspecular scattering from the multilayer coatings.

The ultimate resolution of a soft x-ray imaging system depends in detail on the nonideal nature of the optical substrate and the interfaces in the multilayer coatings. These structures are imperfect at all spatial frequencies. The errors at frequencies less than ~ 10 cm⁻¹ are called figure error and are treated deterministically. The figure errors produce an aberration of the image that can be calculated using ray tracing techniques. The errors at higher frequency are called roughness (or surface finish) and are usually treated statisti-

cally. The effect of the roughness is to remove intensity from the image (the specular field) and scatter it throughout the image field. This nonspecular scattering is problematic for two reasons: (1) it decreases the useful throughput of the optical system and, (2) it produces a background halo which reduces the contrast of the image.

Soft x-ray imaging systems are particularly susceptible to nonspecular scattering. The first reason is that the optics are by necessity all reflective. The second reason is the well-known λ^{-4} dependence of the cross section for dipole scattering. For a given interfacial roughness, the nonspecular scattering increases rapidly with decreasing wavelength. The implications for high resolution imaging are clear: the optical substrates and multilayer coatings must be very smooth to avoid significant scattering. But how smooth is smooth enough? The answer to this question is of both fundamental and practical interest. Fundamentally, there has been until now a general lack of understanding of the effects of scattering in a multilayer-coated imaging system. From a practical perspective, the time and cost of producing figured optical substrates increases dramatically with the smoothness of the surface. An accurate model of scattering is needed to derive realistic specifications for surface finish that can be used as a guideline for manufacturing precision optical components.

The problem of nonspecular scattering of x rays from multilayer films has been addressed by many authors in recent years.^{3–7} It is now understood that the scattering from a multilayer film is fundamentally different than the scattering from a single rough surface. The multilayer scattering is characterized by strong interference effects, due to the cor-

^{a)}Current address: OS Associates, 1174 Castro St., Suite 250, Mountain View, CA 94040; electronic mail: healthst@ricochet.net

^{b)}Current address: Ultratech Stepper, 3050 Zanker Rd., San Jose, CA 95134.

relation of the roughness of the different interfaces. Resonances in the scattering were theoretically predicted^{3,4} and have been experimentally observed.^{4,7-10} Dynamical effects arising from the multiple specular reflection and extinction of the scattered radiation can also be important,⁵ particularly in the vicinity of a specular Bragg peak. We will show that these unique characteristics of the scattering from multilayer coatings have important consequences in an imaging system.

There have been previous attempts to address the problem of nonspecular x-ray scattering in an imaging system. Church and Takacs¹¹ have considered the scattering in a simple imaging system consisting of a single reflecting surface operating near normal incidence. Here the multilayer coating is treated as a single rough surface. Harvey¹² has discussed scattering in a distributed imaging system, and has proposed an *ad hoc* method for incorporating the effects of multilayer coatings. More recently, Singh *et al.*¹³ have applied a Monte Carlo ray tracing technique to simulate nonspecular scattering in a Schwarzschild imaging system. In spite of this previous work, we believe that the current understanding of scattering in a soft x-ray imaging system is incomplete. In particular, these important issues have yet to be adequately addressed:

(1) Owing to the high spatial frequencies characteristic of roughness there is significant diffraction of the scattered field as it propagates between the optical surfaces that produce the scattering and the exit pupil. How does this diffraction affect the pupil function and the image formation process in the context of the transfer function theory of imaging?

(2) It is well known that the coherence state of the object illumination is an important parameter in the imaging process. What is the relationship between the coherence state and the effects of scattering on the image process?

(3) The scattering from a multilayer coating occurs over a large number of interfaces throughout the volume of the film. The magnitude and distribution of scattering depends on the detailed structure of the roughness of the interfaces. What is a correct description of the roughness of a multilayer coating and how is it related to the roughness of the substrate?

(4) What are the characteristics of the scattering from a multilayer coating, particularly in the vicinity of the Bragg peak, and how do they differ from that of a single rough surface? In particular, the description of the scattering process must include interference effects (from the correlation of the interfacial roughness), dynamical effects (multiple reflection of the incident and scattered fields), and extinction of the scattered radiation in the film.

To investigate these issues we present a comprehensive theoretical description of scattering in a soft x-ray imaging system, which includes rigorous treatments of the image formation process, the roughness of the multilayer coatings, and the scattering process. In the following section we derive, following Born and Wolf,¹⁴ a very general expression for the transfer function that relates the mutual intensity at the object and image planes. In Sec. III we consider the scattering in a distributed imaging system having single reflecting surfaces. We explicitly include the diffraction of the scattered field

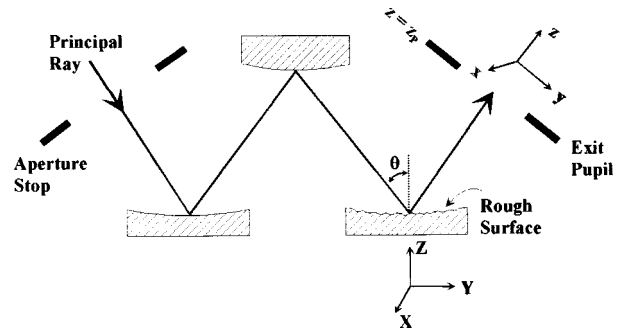


FIG. 1. Schematic diagram of a distributed imaging system showing the trajectory of the principal ray. The (X, Y, Z) coordinate system of the rough surface is related to the (x, y, z) coordinate system of the exit pupil through a rotation of angle θ . The exit pupil is located a distance $z = z_p$ from the rough surface.

and obtain an effective pupil function for the distributed imaging system. The intensity distribution at the image plane is derived in Sec. IV. We show that the effect of scattering is to convolve the image with a point spread function independent of the coherence state of the object illumination. In Sec. V we consider the case of multilayer coatings, and we relate the point spread function to the angular scattering distributions from the multilayer coatings. The calculation of these scattering distributions is the topic of the next two sections. In Sec. VI we review a thin film growth model that has been previously developed¹⁵ to describe the interfacial roughness in multilayer coatings, and we apply this model to measurements of roughness in a Mo-Si multilayer film. The multilayer scattering problem is treated in Sec. VII using an existing scattering theory extended to include dynamical effects in the scattered field. To validate the scattering theory, we compare calculations to experimental measurements of nonspecular scattering from a high-performance Mo-Si multilayer coating. In Sec. VIII we evaluate the scattering in a soft x-ray imaging system in terms of conventional performance parameters, namely the point spread function and the optical transfer function. We close our discussion by modeling the effects of scattering in a hypothetical imaging system designed for EUV lithography.

Throughout the course of the theoretical development we make several critical assumptions and approximations. It is important to observe the restrictions and constraints imposed by these approximations whenever the theory is applied to specific imaging systems. The approximations are enumerated as they appear in the text and are summarized in Appendix A.

II. DERIVATION OF THE TRANSFER FUNCTION

Consider a distributed imaging system consisting of N reflecting surfaces and having a real aperture stop as shown in Fig. 1. The Cartesian coordinates of the object plane and the image plane are S_0 and s_1 , respectively. We introduce the scale normalized coordinates for the object plane, $s_0 = MS_0$, where M is the lateral magnification of the optical system. This allows us to describe an object point and its Gaussian image point by the same coordinate values. The aperture stop of the imaging system limits the angular dis-

persion of rays through the system. For a point object, the ray that intersects the center of the aperture stop is called the principal ray. The image of the aperture stop by the part of the optical system which follows it is called the exit pupil. The exit pupil is located a distance R from the image plane. The amplitude of the radiation field at the plane of the exit pupil is called the complex pupil function, $G(\mathbf{s})$.

Let the object be illuminated by quasimonochromatic radiation of wavelength λ . The mutual intensity functions in the object and image planes are $J_0(\mathbf{s}_0, \mathbf{s}_0')$ and $J_1(\mathbf{s}_1, \mathbf{s}_1')$, respectively. Following Born and Wolf¹⁴ the Fourier transforms of the mutual intensity functions, $J_0(\mathbf{f}, \mathbf{f}')$ and $J_1(\mathbf{f}, \mathbf{f}')$, are related by

$$J_1(\mathbf{f}, \mathbf{f}') = G(\lambda R \mathbf{f}) G^*(-\lambda R \mathbf{f}') J_0(\mathbf{f}, \mathbf{f}'), \quad (1)$$

where $\mathbf{s} = \lambda R \mathbf{f}$ are the coordinates of a point in the plane of the exit pupil. This description of the transfer of the mutual intensity function through the imaging system is only valid within two important approximations. These are:

(a) The angle between the principal ray and any other ray that propagates through the imaging system is small. Specifically, if we denote the angle as φ , then the approximation is

$$\sin^2 \varphi \ll 1. \quad (2)$$

We call this the ‘‘small angle approximation.’’

(b) For a point object, the pupil function is independent of the location of the point in the object field. In this case the point spread function is independent of the position of the Gaussian image point, and the system is called ‘‘isoplanatic.’’ In practice, the assumption of isoplanacity restricts the applicability of the transfer function formalism to objects of small spatial extent.

The effect of scattering from roughness at the optical surfaces is to modify the pupil function in a simple way. Let $G_0(\mathbf{s})$ be the pupil function for the optical system without rough surfaces. Here G_0 contains all of the standard deterministic information about the imaging system such as aberrations. We will show in Sec. II that the effect of the roughness can be represented as a pure phase modulation:

$$G(\mathbf{s}) = G_0(\mathbf{s}) \exp[i\Phi(\mathbf{s})] \quad (3)$$

where $\Phi(\mathbf{s})$ is a function directly related to the structure of the rough surfaces. Then substituting (3) into (1) we obtain

$$\begin{aligned} \langle J_1(\mathbf{f}, \mathbf{f}') \rangle &= G_0(\lambda R \mathbf{f}) G_0^*(-\lambda R \mathbf{f}') \\ &\times \langle \exp[i(\Phi(\lambda R \mathbf{f}) - \Phi^*(-\lambda R \mathbf{f}'))] \rangle J_0(\mathbf{f}, \mathbf{f}'). \end{aligned} \quad (4)$$

The angular brackets denote taking an ensemble average over many configurations of the rough surface. In practice this is realized by the breaking up of the coherence of the illumination of the surface due to the finite size of the object. For a coherently illuminated object of size L and a distance D between the object plane and the optical surface, the size of the patch on the surface over which the illumination is coherent is approximately $\lambda D/2L$. For typical sources of fi-

nite size there will be many of these patches within the area illuminated on the optical surface. If the surface is sufficiently ergodic then each patch represents a different configuration of roughness, and the ensemble average can be replaced by an average over the illuminated surface area.

III. EFFECTIVE PUPIL FUNCTION

To proceed further it is necessary to derive an expression for the pupil function $G(\mathbf{s})$ that includes scattering from the optical surfaces. For the moment let the optical surfaces be single surfaces (not coated with multilayer films), and assume that all but one of the surfaces are perfectly smooth, as indicated in Fig. 1. Since our goal is to determine the effect of scattering on the pupil function, we can neglect the curvature of the incident wavefront and the optical surface (these will be included later). Then let the specular field be a plane wave, $\hat{e} e^{ik\hat{n}\cdot\mathbf{x}}$, of unit amplitude and polarization \hat{e} incident onto the rough surface with an angle θ (measured with respect to the normal). The field is reflected by the surface and propagates to the plane of the exit pupil. Choosing the plane of the exit pupil to be perpendicular to the principal ray, we find that θ is also the angle between the normal to the exit pupil and the normal to the rough surface.

An expression for the field scattered by the rough surface has been derived in a previous paper.¹⁶ The results are valid under the following approximation:

(c) The scattering is weak so that multiple scattering and shadowing effects can be neglected. This is called the ‘‘Born approximation.’’ This approximation is generally valid for x-ray wavelengths at angles of incidence away from the critical angle for total external reflection.

The component of the scattered reflected field $\mathbf{E}^R(\mathbf{x})$ having polarization \hat{a} (S or P type) can be written as:

$$\begin{aligned} \hat{a} \cdot \mathbf{E}^R(\mathbf{x}) &= \frac{\Delta}{2} (\hat{a} \cdot \hat{e}) \int \int \left(\int \int \exp(iq_X X) \exp(iq_Y Y) \right. \\ &\times \left. \frac{\exp[iq_Z H(X, Y)]}{q_Z (q_Z + k n_Z)} dX dY \right) \\ &\times \exp(ik\hat{m} \cdot \mathbf{x}) dm_X dm_Y. \end{aligned} \quad (5)$$

Here $\Delta = 1 - \epsilon$, where ϵ is the dielectric constant of the surface material, $\mathbf{q} = k(\hat{m} - \hat{n})$ is the change of momentum of the x-ray photon and $H(X, Y)$ is the surface height function describing the roughness of the surface.

The expression (5) for the scattered field has a straightforward physical interpretation: it is simply an expansion of the scattered field using the plane waves $\exp(ik\hat{m} \cdot \mathbf{x})$ as a basis set. The quantity in brackets is the scattering amplitude of the plane wave mode \hat{m} . Note that there are two different spatial coordinate systems in Eq. (5). The relationship between these coordinate systems is illustrated in Fig. 1. The coordinate system $(\hat{X}, \hat{Y}, \hat{Z})$ is defined such that \hat{Z} is normal to the plane of the rough optical surface and the Y - Z plane is the plane of incidence. The coordinate system $(\hat{x}, \hat{y}, \hat{z})$ has \hat{z} normal to the plane of the exit pupil. The transformation between the two coordinate systems is a rotation through an

angle θ about the $\hat{x}=\hat{x}'$ axis. The momentum transfer vector \mathbf{q} in the two coordinate systems is related according to

$$\begin{aligned} q_x &= q_x \\ q_y &= \cos \theta q_y + \sin \theta q_z \cong \cos \theta q_y + 2k \cos^2 \theta \sin \theta \quad (6) \\ q_z &= -\sin \theta q_y + \cos \theta q_z \cong 2k \cos \theta. \end{aligned}$$

These expressions are valid within the small angle approximation (a), which requires that q_x and q_y be small. Noting that

$$\hat{n} = \sin \theta \hat{Y} - \cos \theta \hat{Z} = \sin 2\theta \hat{y} - \cos 2\theta \hat{z} \quad (7)$$

we rearrange Eq. (5) to get

$$\begin{aligned} \hat{a} \cdot \mathbf{E}^R(\mathbf{x}) &= (1/4\pi^2) r^{\text{SP}} \cos \theta \exp(iky \sin 2\theta) \exp(-ikz \cos 2\theta) \int \int \int \int \exp(i\mathbf{q} \cdot \mathbf{x}) \exp(-iq_x X) \\ &\quad \times \exp(-i \cos \theta q_y Y) \exp(-2ik \cos^2 \theta \sin \theta Y) \exp[-2ik \cos \theta H(X, Y)] dX dY dq_x dq_y \quad (8) \end{aligned}$$

where $r^{\text{SP}} = \Delta(\hat{a} \cdot \hat{e})/4 \cos^2 \theta$ is the specular reflectance amplitude from an ideally smooth surface.

Next we propagate the reflected field to the plane of the exit pupil at position $z=z_p$. The field in this plane is the complex pupil function $G(\mathbf{s})$ where $\mathbf{s} = s_x \hat{x} + s_y \hat{y}$. Then using Eq. (8) the pupil function becomes

$$\begin{aligned} G(\mathbf{s}) &= (1/4\pi^2) r^{\text{SP}} \cos \theta \exp(ik \sin 2\theta s_y) \exp(-ik \cos 2\theta z_p) \\ &\quad \times \int \int \int \int \exp(iq_x s_x) \exp(iq_y s_y) \exp(iq_z z_p) \\ &\quad \times \exp(-iq_x X) \exp(-i \cos \theta q_y Y) \exp(-2ik \cos^2 \theta \sin \theta Y) \exp[-2ik \cos \theta H(X, Y)] dX dY dq_x dq_y. \quad (9) \end{aligned}$$

This is the correct expression for the pupil function that includes the (significant) diffraction of the scattered field on its way to the exit pupil. However, the propagation of the mutual intensity, as described in Eq. (1), requires the determination of the transfer function $\langle G(\mathbf{s})G^*(-\mathbf{s}') \rangle$. Substituting from Eq. (9) we have

$$\begin{aligned} \langle G(\mathbf{s})G^*(-\mathbf{s}') \rangle &= (1/16\pi^4) R_{\text{SP}} \cos^2 \theta \exp[ik \sin 2\theta (s_y + s'_y)] \\ &\quad \times \int \int \int \int \exp(iq_x s_x) \exp(iq_y s_y) \exp(iq_z z_p) \exp(iq'_x s'_x) \exp(iq'_y s'_y) \exp(-iq'_z z_p) \\ &\quad \times \int \int \int \int \langle \exp\{-2ik \cos \theta [H(X, Y) - H(X', Y')]\} \rangle \exp(-iq_x X) \exp(iq'_x X') \\ &\quad \times \exp[-i \cos \theta (q_y Y - q'_y Y')] \exp[-2ik \cos^2 \theta \sin \theta (Y - Y')] dX dY dX' dY' dq_x dq_y dq'_x dq'_y. \quad (10) \end{aligned}$$

We make the following assumptions about the statistical properties of the roughness:

(d) The surface height $H(X, Y)$ is a Gaussian random variable, is stationary and is ergodic in the sense that the ensemble average can be replaced by an average over the illuminated surface area.

The assumption that H is stationary leads to an important simplification: the quantity in the brackets $\langle \rangle$ depends only on the separation of the points $U = X - X'$ and $V = Y - Y'$. In particular, if we define

$$F(U, V) \equiv \langle \exp\{-2ik \cos \theta [H(X, Y) - H(X', Y')]\} \rangle \quad (11)$$

then the inner integral in Eq. (10) becomes

$$\begin{aligned} &\int \int \int \int F(U, V) \exp(-iq_x U) \exp(-i \cos \theta q_y V) \exp(-2ik \cos^2 \theta \sin \theta V) \exp[-i(q_x - q'_x)X'] \\ &\quad \times \exp[-i \cos \theta (q_y - q'_y)Y'] dX' dY' dU dV \\ &= \cos^{-1} \theta \delta(q_x - q'_x) \delta(q_y - q'_y) \int \int F(U, V) \exp(-iq_x U) \exp(-i \cos \theta q_y V) \exp(-2ik \cos^2 \theta \sin \theta V) dU dV. \quad (12) \end{aligned}$$

Substituting (12) into (10) we obtain:

$$\begin{aligned} \langle G(\mathbf{s})G^*(-\mathbf{s}') \rangle &= (1/4\pi^2)R^{SP} \cos \theta \exp[ik \sin 2\theta(s_y + s'_y)] \int \int \int \int F(U,V) \exp(-2ik \cos^2 \theta \sin \theta V) \\ &\quad \times \exp[iq_x(s_x + s'_x - U)] \exp[iq_y(s_y + s'_y - \cos \theta V)] dq_x dq_y dU dV \\ &= R^{SP} \cos \theta \int \int F(U,V) \delta(s_x + s'_x - U) \delta(s_y + s'_y - \cos \theta V) dU dV = R^{SP} F\left(s_x + s'_x, \frac{s_y + s'_y}{\cos \theta}\right). \end{aligned} \quad (13)$$

We find that the transfer function $\langle G(\mathbf{s})G^*(-\mathbf{s}') \rangle$ does not depend on z_p , the distance between the optical surface and the exit pupil. In other words, the diffraction of the scattered field between the optical surface and the exit pupil does not contribute to the image formation. This surprising conclusion is due to the process of averaging over an ensemble of configurations corresponding to a stationary distribution. Diffraction effects must cancel out in the ensemble average because all points on the optical surface are equivalent. Consequently, for the purpose of evaluating $\langle G(\mathbf{s})G^*(-\mathbf{s}') \rangle$, we can map the rough surface directly onto the exit pupil as if there was no separation ($z_p = 0$). The effect of the roughness on the pupil function can be represented as a simple phase modulation

$$G(\mathbf{s}) = G_0(\mathbf{s}) \exp\left[-2ik \cos \theta H\left(\frac{s_x}{\alpha_x}, \frac{s_y}{\alpha_y \cos \theta}\right)\right]. \quad (14)$$

Here we have reintroduced the effects of the wavefront curvature and surface figure in the factor $G_0(\mathbf{s})$, which is the pupil function in the absence of scattering. The factors $\alpha_x = s_x/X$ and $\alpha_y = s_y/(Y \cos \theta)$ account for the change of scale between the optical surface and the exit pupil, as determined, for example, by the change in separation of the extrema rays. The scaling relationship for s_y includes a factor of $\cos \theta$ to account for the angle of inclination of the optical surface with respect to the plane of the exit pupil. We emphasize that Eq. (14) is not the correct pupil function for any particular configuration of surface roughness. It can be used, however, as an *effective* pupil function, in the sense that it produces a correct result in the calculation of image formation when the quantity $\langle G(\mathbf{s})G^*(-\mathbf{s}') \rangle$ is averaged over a statistically random and *stationary* distribution of configurations.

At first glance it might appear that Eq. (14) cannot correctly account for all of the radiation scattered within the imaging system. For example, radiation scattered at large angles by the first optical surface in the distributed system will not pass through the subsequent optics and reach the exit pupil. Yet within the context of the transfer function theory, the roughness of each optical surface is mapped onto the exit pupil and all of the scattering occurs at the exit pupil. The resolution of this apparent inconsistency is to understand that any scattered radiation that in reality does not reach the exit pupil, is scattered outside of the image field in the transfer function description; the transfer function theory correctly accounts for all scattering that intersects the image field. This can be illustrated using the following argument. Consider the ideal imaging system that images a point object at \mathbf{s}_0 to a point \mathbf{s}_1 in the image plane. The scattering from a rough

optical surface into a particular nonspecular direction \hat{m} will be imaged by the subsequent optics to a different point \mathbf{s}'_1 in the image plane. Tracing rays back through the imaging system from the image point \mathbf{s}'_1 , the propagation through the imaging system of the radiation scattered into direction \hat{m} is found to be equivalent to the imaging of a point source at the conjugate position \mathbf{s}'_0 in the object field. Consequently, the propagation of the scattered radiation that intersects the image field is equivalent to the propagation of radiation from an extended object in the absence of scattering, a process that is correctly described by transfer function theory.

Thus far we have considered the scattering from a single rough surface. We next consider an imaging system where each of the N reflecting surfaces has a roughness described by a unique height function $H_n(X_n, Y_n)$. We assume that the roughness of the different surfaces each satisfies the conditions (d) for stationary and ergodic distributions, and are mutually statistically independent. The effective pupil function for the entire imaging system can be derived by imagining that we “turn on” the roughness of each surface sequentially and apply Eq. (14) iteratively. In particular, the pupil function for n rough surfaces becomes G_0 for the case of $n + 1$ rough surfaces, etc. Then the effective pupil function for the entire distributed system is

$$\begin{aligned} G(\mathbf{s}) &= G_0(\mathbf{s}) \exp[i\Phi(\mathbf{s})] \\ &= G_0(\mathbf{s}) \exp\left[-2k \sum_{n=1}^N \cos \theta_n H_n\left(\frac{s_x}{\alpha_{xn}}, \frac{s_y}{\alpha_{yn} \cos \theta_n}\right)\right]. \end{aligned} \quad (15)$$

IV. DESCRIPTION OF THE IMAGE

Having derived the effective pupil function, we now apply the transfer function formalism of Eq. (4) to obtain a description of the image. We begin by evaluating the quantity

$$\begin{aligned} &\langle \exp[i(\Phi(\mathbf{s}) - \Phi^*(-\mathbf{s}'))] \rangle \\ &= \left\langle \exp\left\{-2ik \sum_{n=1}^N \cos \theta_n \left[H_n\left(\frac{s_x}{\alpha_{xn}}, \frac{s_y}{\alpha_{yn} \cos \theta_n}\right) - H_n\left(-\frac{s'_x}{\alpha_{xn}}, -\frac{s'_y}{\alpha_{yn} \cos \theta_n}\right) \right] \right\} \right\rangle. \end{aligned} \quad (16)$$

It can be shown generally¹⁷ that for Gaussian random variables B_m the ensemble average reduces to

$$\left\langle \exp\left(\sum_n B_n\right)\right\rangle = \exp\left[\frac{1}{2} \left\langle \left(\sum_n B_n\right)^2 \right\rangle\right]. \quad (17)$$

We have assumed that the roughness of the different optical surfaces is completely uncorrelated, requiring that $\langle H_n H_m \rangle = 0$ for $n \neq m$. Then we obtain

$$\begin{aligned} &\langle \exp[i(\Phi(\mathbf{s}) - \Phi^*(-\mathbf{s}'))] \rangle \\ &= \exp \left(-4k^2 \sum_{n=1}^N \cos^2 \theta_n \langle H_n^2(X_n, Y_n) \rangle \right. \\ &\quad \left. + 4k^2 \sum_{n=1}^N \cos^2 \theta_n \langle H_n(X_n, Y_n) H_n(-X'_n, -Y'_n) \rangle \right), \end{aligned} \tag{18}$$

where $(X_n, Y_n) = [(s_x/\alpha_{xn})(s_y/\alpha_{yn} \cos \theta_n)]$ are the spatial coordinates on the n th optical surface. The assumption that H is stationary requires that the quantity $\langle H^2(X, Y) \rangle$ be independent of (X, Y) and the quantity $\langle H(X, Y)H(-X', -Y') \rangle$ depends only on the separation of the points $U = X + X'$ and $V = Y + Y'$. These statistical quantities are conventionally defined in terms of the surface height variance σ^2 , where σ is called the root-mean-square (rms) roughness, and the height-height autocorrelation function C , given by

$$\sigma^2 \equiv \frac{1}{A} \int H^2(X, Y) dXdY \tag{19}$$

and

$$C(U, V) = \frac{1}{A} \int H(X, Y)H(U+X, V+Y) dXdY. \tag{20}$$

Here we have replaced the ensemble average with an average over the area, A , of the illuminated surface. We write

$$\begin{aligned} \langle \exp[i(\Phi(\mathbf{s}) - \Phi^*(-\mathbf{s}'))] \rangle &= \exp \left(-4k^2 \sum_{n=1}^N \cos^2 \theta_n \sigma_n^2 \right. \\ &\quad \left. + 4k^2 \sum_{n=1}^N \cos^2 \theta_n C_n(\mathbf{u}_n) \right), \end{aligned} \tag{21}$$

where

$$\mathbf{u}_n \equiv \frac{s_x + s'_x}{\alpha_{xn}} \hat{x} + \frac{s_y + s'_y}{\alpha_{yn} \cos \theta_n} \hat{y}.$$

The final step for determining the intensity distribution in the image plane is to take the inverse Fourier transform of $\langle J_1(\mathbf{f}, \mathbf{f}') \rangle$. Applying the convolution theorem to Eq. (4) we obtain

$$\begin{aligned} \langle J_1(\mathbf{s}_1, \mathbf{s}'_1) \rangle &= J_1^0(\mathbf{s}_1, \mathbf{s}'_1) * \exp \left(-4k^2 \sum_n \cos^2 \theta_n \sigma_n^2 \right) \\ &\quad \times \int \int \exp \left[4k^2 \sum_n \cos^2 \theta_n C_n(\mathbf{u}_n) \right] \\ &\quad \times \exp(2\pi i \mathbf{s}_1 \cdot \mathbf{f}) \exp(2\pi i \mathbf{s}'_1 \cdot \mathbf{f}') d\mathbf{f} d\mathbf{f}'. \end{aligned} \tag{22}$$

Here

$$\begin{aligned} J_1^0(\mathbf{s}_1, \mathbf{s}'_1) &= \int \int G_0(\lambda R \mathbf{f}) G_0^*(-\lambda R \mathbf{f}') J_0(\mathbf{f}, \mathbf{f}') \\ &\quad \times \exp(2\pi i \mathbf{s}_1 \cdot \mathbf{f}) \exp(2\pi i \mathbf{s}'_1 \cdot \mathbf{f}') d\mathbf{f} d\mathbf{f}', \end{aligned} \tag{23}$$

is the mutual intensity at the image plane in the absence of roughness. Since C_n is dependent only on the difference vector \mathbf{u}_n , the double integral in (22) collapses to yield,

$$\begin{aligned} \langle J_1(\mathbf{s}_1, \mathbf{s}'_1) \rangle &= J_1^0(\mathbf{s}_1, \mathbf{s}'_1) * \delta(\mathbf{s}_1 - \mathbf{s}'_1) \\ &\quad \times \exp \left[-4k^2 \sum_n \cos^2 \theta_n \sigma_n^2 \right] \\ &\quad \times \int \int \exp \left[4k^2 \sum_n \cos^2 \theta_n C_n(\mathbf{u}_n) \right] \\ &\quad \times \exp(2\pi i \mathbf{s}_1 \cdot \mathbf{v}) d\mathbf{v}, \end{aligned} \tag{24}$$

where $\mathbf{v} \equiv \mathbf{f} + \mathbf{f}'$. The intensity distribution is obtained by setting $\mathbf{s}_1 = \mathbf{s}'_1$. Then,

$$\begin{aligned} \langle I_1(\mathbf{s}_1) \rangle &= I_1^0(\mathbf{s}_1) * \exp \left[-4k^2 \sum_n \cos^2 \theta_n \sigma_n^2 \right] \\ &\quad \times \int \int \exp \left[4k^2 \sum_n \cos^2 \theta_n C_n(\mathbf{u}_n) \right] \\ &\quad \times \exp(2\pi i \mathbf{s}_1 \cdot \mathbf{v}) d\mathbf{v}. \end{aligned} \tag{25}$$

Further simplification is possible if each surface is sufficiently smooth to satisfy the following condition:

(e) The deviations of the surface height $H_n(X_n, Y_n)$ from the ideally smooth surface are small compared to the radiation wavelength such that $2k \cos \theta_n H_n(X_n, Y_n) \ll 1$ for all X_n, Y_n . We call this the ‘‘small roughness approximation.’’ A necessary consequence of the small roughness approximation is that the power scattered into the nonspecular field is small compared to the specularly reflected power, a condition that is implicitly satisfied by high-performance optics.

For a randomly rough surface the autocorrelation function C_n will have a maximum value of σ_n^2 . Then invoking the small roughness approximation, we can expand the exponential in the integrand in Eq. (25) to obtain

$$\begin{aligned} \langle I_1(\mathbf{s}_1) \rangle &= I_1^0(\mathbf{s}_1) * \exp \left(-4k^2 \sum_n \cos^2 \theta_n \sigma_n^2 \right) \\ &\quad \times \left[\delta(\mathbf{s}_1) + \frac{4k^2}{\lambda^2 R^2} \sum_n \alpha_{xn} \alpha_{yn} \cos^3 \theta_n \right. \\ &\quad \left. \times \text{PSD}_n \left(\frac{\alpha_{xn} s_{1x}}{\lambda R}, \frac{\alpha_{yn} \cos \theta_n s_{1y}}{\lambda R} \right) \right]. \end{aligned} \tag{26}$$

Here PSD_n is the (power spectral density) of the n th surface, which is the Fourier transform of the autocorrelation function.

The result shown in Eq. (26) has a simple physical interpretation. The effect of the surface roughness on the formation of an image is to convolve the image that would exist in the absence of scattering, I_1^0 , with a point spread function due to scattering

$$\langle I_1(\mathbf{s}_1) \rangle = I_1^0(\mathbf{s}_1) * \kappa \text{PSF}^{\text{sc}}(\mathbf{s}_1). \tag{27}$$

The point spread function, PSF^{sc} , consists of two parts:

$$\text{PSF}^{\text{sc}}(\mathbf{s}_1) = \frac{1}{\kappa} \left[S \delta(\mathbf{s}_1) + \sum_n \frac{dP_n(\mathbf{s}_1)}{ds_1} \right]. \quad (28)$$

The first term is the contribution from specular reflection. It is simply a delta function reduced by the Strehl factor, S , where:

$$S = \prod_n S_n = \prod_n \exp(-4k^2 \cos^2 \theta_n \sigma_n^2). \quad (29)$$

The Strehl factor represents the power removed from the specular field due to nonspecular scattering. The second term in the PSF corresponds to the power per unit area scattered into the image plane given a point source in the object plane, where

$$\begin{aligned} \frac{dP_n(\mathbf{s}_1)}{ds_1} &= \frac{4k^2 S}{\lambda^2 R^2} \alpha_{xn} \alpha_{yn} \cos^3 \theta_n \\ &\times \text{PSD}_n \left(\frac{\alpha_{xn} s_{1x}}{\lambda R}, \frac{\alpha_{yn} \cos \theta_n s_{1y}}{\lambda R} \right). \end{aligned} \quad (30)$$

The factor κ accounts for any loss of integrated image intensity due to, for instance, scattering outside of the image field or absorption in the multilayer coating. It is defined by

$$\kappa \equiv \int \int \left[S \delta(\mathbf{s}_1) + \sum_n \frac{dP_n(\mathbf{s}_1)}{ds_1} \right] ds_1 \quad (31)$$

which ensures that the PSF integrates to unity.

We note that the effect of scattering on the image formation is *independent* of the coherence of the illumination of the object. All of the coherence effects in Eq. (29) are contained in the image $I_1^0(\mathbf{s}_1)$ formed in the absence of scattering. The effect of scattering is to convolve this image with a PSF^{sc} that is independent of the coherence state. This interesting result is due to the process of taking an ensemble average over the statistical distribution of configurations of surface roughness. The coherence state of the source determines the specific illumination of the rough surface. However, taking the ensemble average makes each surface point equivalent in terms of its contribution to scattering, which means that the specific illumination pattern cannot effect the scattering distribution.

V. EXTENSION TO MULTILAYER COATINGS

Thus far we have assumed that the optical surfaces are single reflecting surfaces. In fact, these surfaces are coated with multilayer films to produce efficient reflectivity at soft x-ray wavelengths. Although the reflectance from a single surface is small at these wavelengths, the reflections from each interface in the multilayer coating add constructively to produce a large total specular reflectance. For example, for a single Mo surface the normal incidence reflectance of soft x rays at a wavelength of 13 nm is $\sim 0.15\%$; the reflectance from a Mo-Si multilayer coating consisting of 40 bilayers of period 6.8 nm is $\sim 70\%$ (see Sec. VII).

Multilayer coatings typically have roughness at the layer boundaries, due to both replication of the substrate roughness and roughness introduced during the film growth process.

The incident specular field scatters at each of the multilayer interfaces, and these contributions add coherently to produce a total scattered field. Hence, in principal, the calculation of the scattered field from a multilayer coating requires knowledge of the PSD of each of the interfaces, as well as the correlation of the roughness between every pair of interfaces. It is intractable to measure the roughness of each interface in each coating of an imaging system. We have found that an effective approach to this very complicated problem is to describe the multilayer interface structure in terms of a simple multilayer growth model.¹⁵ The model provides a straightforward method for describing all of the detailed structural information required by the scattering theory in terms of a small set of fundamental parameters. A description of the multilayer growth model is presented in the next section.

The nonspecular scattering from a multilayer film is fundamentally different than the scattering from a single surface. This is because the scattered field is the coherent superposition of the fields scattered by each of the interfaces. Just as the specular reflectance is a resonance property of the coating, the nonspecular scattering exhibits resonance behavior that is absent in the case of a single surface. The phenomenon of resonant nonspecular scattering has been discussed previously.^{3,5} The scattering is enhanced whenever the momentum change normal to the film is equal to a reciprocal lattice vector *and* when the structure of the interfaces is correlated from layer to layer (i.e., is at least partially conformal). This has important implications for the scattering in an imaging system. Since the specular field is near the center of the Bragg peak, the scattering at small angles will necessarily satisfy the conditions for resonant scattering. To the extent that the interfacial roughness is purely conformal, the multilayer film will behave like a single surface having the roughness of the substrate. However, we will see that realistic multilayer films have intrinsic interfacial roughness that modifies the substrate roughness and reduces the conformality of the interface structure. These ‘‘multilayer effects’’ tend to enhance the resonant scattering at small angles and suppress the scattering at large angles. To accurately describe the scattering from realistic multilayer film we must account for the variation of the interface structure through the film, and the interaction of the radiation field with each interface.

Once the scattered field is outside of the multilayer coating, its propagation through the distributed optical system to the image plane is described by the transfer function formalism derived in the previous section. In particular, the effect of scattering is to convolve the image with a PSF^{sc} as described by Eq. (28), where now the quantities S_n and dP_n/ds_1 correspond to the contribution from the n th multilayer-coated optical surface. The roughness of the n th coating reduces the specular field by a factor of S_n ; the power per unit area scattered by n th coating into the image plane (for a point source) is dP_n/ds_1 .

To derive an expression for dP_n/ds_1 , we relate this quantity to the angular distribution of power scattered from the n th coating. The power incident at the point \mathbf{s}_1 in the image plane corresponds to radiation that is scattered by the n th coating into the direction \hat{m} , given by

$$\begin{aligned}
m_X &= \frac{\alpha_{nx} s_{1x}}{R} \\
m_Y &\cong \frac{\alpha_{ny} s_{1y} \cos \theta_n}{R} + \sin \theta_n \\
m_Z &\cong -\frac{\alpha_{ny} \sin \theta_n}{R} s_{1y} + \cos \theta_n.
\end{aligned} \tag{32}$$

Note that \hat{m} is projected onto the (X, Y, Z) coordinate system of the rough coating. The power distribution in the image plane is related to the power scattered per unit solid angle by the n th coating according to

$$\frac{dP_n(\mathbf{s}_1)}{ds_1} = \frac{\alpha_{nx} \alpha_{ny}}{R_n^{\text{SP}} R^2} \sum_{\hat{a}} \frac{dP_n(\hat{m}, \hat{a}; \hat{n}, \hat{e})}{d\Omega}, \tag{33}$$

where R_n^{SP} is the specular reflectivity of the coating, \hat{n} and \hat{e} are the direction of propagation and the polarization of the incident field, respectively, and we must sum over both polarization states \hat{a} of the scattered field. In essence, Eqs. (32) and (33) represent two mappings: first the n th rough coating is mapped onto the exit pupil and second the angular distribution of scattering from the rough coating is mapped to the spatial coordinates of the image plane. Our task then reduces to finding the angular distribution of scattering, $dP_n/d\Omega$, and the Strehl factor S_n for a multilayer-coated surface given an incident plane wave propagating in direction \hat{n} with polarization \hat{e} . This problem is addressed in Sec. VII. However, before we can calculate the scattering from a multilayer coating, we must obtain a realistic description of the roughness of the multilayer interfaces, which is the subject of the next section.

VI. GROWTH MODEL FOR MULTILAYER FILMS

Much attention has been given to the problem of the roughening of the surface of a thin film by growth and erosion. Stochastic theories of the evolution of the surface have been developed using two generally different approaches. In the first approach,¹⁸ the phenomenological observation that randomly rough surfaces are self-affine is used to derive simple scaling laws describing the width of the interface as a function of film thickness and the amount of surface area sampled. One consequence of the scaling theory is that the autocorrelation function for the rough surface is approximately described by:¹⁹

$$C(r) = \begin{cases} \sigma^2 \left[1 - \frac{\alpha+1}{2} \left(\frac{r}{\xi} \right)^{2\alpha} \right], & \text{for } r \leq \xi \\ 0, & \text{for } r > \xi \end{cases} \tag{34}$$

where ξ is the correlation length and α is an independent scaling parameter called the ‘‘roughness exponent.’’ The corresponding PSD of the rough surface is given by

$$\text{PSD}(f) = \begin{cases} \frac{\alpha}{\pi} \sigma^2 \xi^2, & \text{for } q < 1/\xi \\ \frac{\alpha}{\pi} \frac{\sigma^2}{\xi^{2\alpha}} f^{-2(\alpha+1)}, & \text{for } q \geq 1/\xi \end{cases}. \tag{35}$$

The rms roughness σ and correlation length ξ of the surface change with the thickness of the growing (or eroding) film. The scaling laws predict that $\sigma \sim \tau^\beta$ and $\xi \sim \tau^{\beta/\alpha}$, where τ is the thickness of the film and β is a second independent scaling parameter.

The second approach¹⁹ of describing the roughening of a surface is through the use of a kinetic continuum equation for the evolution of the surface height $H(\mathbf{r})$. The linear version of such a continuum equation (to lowest order in H) has the form:

$$\frac{\partial H(\mathbf{r})}{\partial \tau} = -\nu |\nabla^n H(\mathbf{r})| + \frac{\partial \eta}{\partial \tau}. \tag{36}$$

In this approach the evolution of the surface roughness is viewed to be a competition between relaxation of the surface, where ν is an independent growth parameter that characterizes the relaxation process, and the stochastic roughening due to the random shot noise η of the deposition (or removal) process. When ν is positive, the first term in Eq. (36) tends to dampen the surface roughness while the second term increases the roughness with film thickness. The exponent n in the relaxation term varies according to the kinetic mechanism that dominates the smoothing process. Edwards and Wilkinson²⁰ first applied Eq. (36) with $n=2$ to describe the settling of a granular layer under the influence of the gravitational potential. Herring²¹ has identified several relaxation mechanisms relevant to film growth corresponding to viscous flow ($n=1$), evaporation and condensation ($n=2$), bulk diffusion ($n=3$) and surface diffusion ($n=4$). It has been pointed out by Salditt *et al.*²² that, for high-energy deposition processes such as sputtering at low pressures, the case of $n=2$ will more likely correspond to the sputter and redeposition of adatoms via atomic bombardment of the surface. Tong and Williams¹⁹ have suggested that by using a negative value of ν the first term in Eq. (36) can also describe roughening of the surface due to three-dimensional island growth. In this case $n=1$ corresponds to island growth via deposition onto the surfaces of existing islands, and $n=3$ represents the growth of islands via the diffusion of atoms on the surface.

Taking the Fourier transform of Eq. (36) readily yields a solution for the PSD of the growing surface:¹⁵

$$\text{PSD}(\mathbf{f}) = \Omega \frac{1 - \exp[-2\nu |2\pi\mathbf{f}|^n \tau]}{2\nu |2\pi\mathbf{f}|^n}. \tag{37}$$

Here Ω is the volume of a constituent element of the film (e.g., atom, molecule, cluster). It is surprising to find that the scaling and kinetic continuum models predict essentially the same form for the PSD of the surface! A comparison of Eqs. (35) and (37) shows that the scaling parameters are related to the exponent n according to

$$\alpha = (n-2)/2, \quad \beta = (n-2)/2n. \tag{38}$$

The kinetic model (36) predicts a characteristic shape for the PSD of a single layer grown on a smooth substrate given by Eq. (37). An example is shown in Fig. 2 for several different film thicknesses and reasonable parameter values of $\Omega = 0.02 \text{ nm}^3$, $\nu = 2.5 \text{ nm}^3$, and $n=4$. The PSD is flat at low frequencies and rolls over to asymptotically approach a

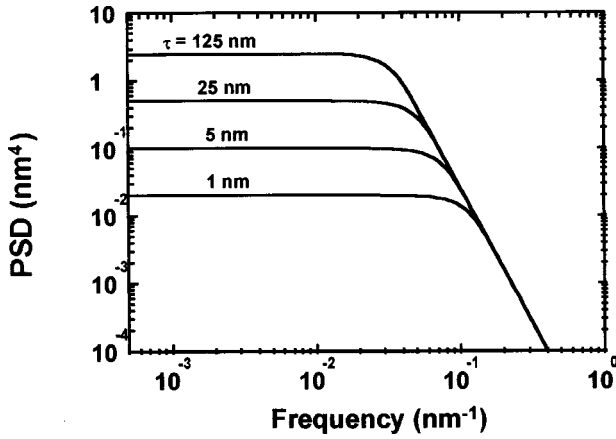


FIG. 2. The theoretical PSD of the top surface of a film grown on a perfectly smooth substrate at different values of the film thickness. The growth parameters are $\Omega = 0.02 \text{ nm}^3$, $\nu = 2.5 \text{ nm}^3$, and $n = 4$.

power law dependence of $\sim f^{-n}$ at high frequencies. The transition point moves to lower frequency as the film thickness increases. In the limit of infinite film thickness the PSD of the surface becomes a pure power law, which is the signature of a self-affine (fractal) surface, and explains in part the similarity between the kinetic continuum and scaling models. The behavior of the PSDs shown in Fig. 2 has a straightforward physical explanation. The low frequency (large wavelength) components of roughness have a flat response characteristic of white noise, which is simply the shot noise of the random deposition process. At high frequency (small wavelength) the PSD rolls off due to local relaxation of the growing surface. In particular, surface features having a size less than $(\nu t)^{1/n}$ are unstable and are damped out.

It should be emphasized that Eq. (36) is the simplest possible kinetic model for roughening. It is a linear and local description of the roughening process, and is expected to be valid only when the surface heights and slopes are small. The first nonlinear correction, corresponding to a term $\sim (\nabla H)^2$, has been considered by Kardar *et al.*²³ Physically, this term represents growth along the local normal to the film surface as might be expected under the conditions of isotropic deposition characteristic of, for example, chemical vapor deposition. The assumption that the roughening is a local process breaks down when the distribution of deposition angles is large and the surface slopes are large. In this case the deposition at a point on the surface depends on the topology of the surrounding surface due to shadowing effects. Karunasiri *et al.*²⁴ and later Tang *et al.*²⁵ have proposed growth models that explicitly include a nonlocal growth mechanism (shadowing). It is found that when the nonlinear and nonlocal effects dominate the roughening process, the film surface rapidly develops discontinuities in the form of cusps and columns. These features have often been observed in thin film morphology, particularly for films grown using low-energy deposition processes.^{26–28} In contrast, the high-performance multilayer optical coatings which we are considering in this paper have small roughness by design. This is achieved by using a high-energy growth process, such as sputtering at low pressure, that incorporates a significant re-

laxation mechanism (large ν) to compensate the natural roughening due to the stochastic nature of the deposition. By balancing the roughening and smoothing mechanisms, the roughness is never allowed to become large enough to trigger the nonlinear and nonlocal growth modes. We believe that under these conditions the continuum model of Eq. (36) is an appropriate description of the thin film growth. This view is supported by recent experimental studies⁷ of roughness in multilayer films.

Thus far we have considered the growth of a single layer. We next extend the kinetic model to describe the evolution of interfacial roughness in a multilayer film. This is achieved by considering the growth of a multilayer film to be a sequence of single layers, each growing upon a “substrate” corresponding to the underlying layer. Then the roughness of an interface naturally separates into two components: (1) the “intrinsic” roughness due to the growth of the i th layer, as would occur if the underlying layer was perfectly smooth, and (2) the “extrinsic” roughness due to the replication of the roughness of the underlying layer. To represent the growth of such a sequence of layers, we recast Eq. (36) as a finite difference equation¹⁵

$$h_i(\mathbf{f}) = \gamma_i(\mathbf{f}) + a_i(\mathbf{f})h_{i-1}(\mathbf{f}), \quad (39)$$

where $h_i(\mathbf{f})$ is the frequency spectrum of the roughness of the i th interface, $H_i(\mathbf{r})$, and

$$a_i(\mathbf{f}) = \exp[-\nu_i |2\pi f|^n \tau_i], \quad (40)$$

is the replication factor that describes the fraction of the frequency component \mathbf{f} in the $(i-1)$ th interface that is replicated in the i th interface. The first and second terms on the right-hand side of Eq. (39) correspond to the intrinsic and extrinsic roughness components of the i th interface, respectively.

The growth theory is typically applied to measurements of surface or interfacial roughness using a statistical description of the roughness in terms of the power spectral density

$$\text{PSD}_i(\mathbf{f}) = \frac{1}{A} \langle h_i(\mathbf{f})h_i^*(\mathbf{f}) \rangle, \quad (41)$$

or the autocorrelation function

$$C_i(\mathbf{r}) = \langle H_i(\mathbf{x})H_i(\mathbf{x} + \mathbf{r}) \rangle, \quad (42)$$

where the expectation value denotes an average over an ensemble of interface structures having statistically equivalent random roughness. These quantities are related by a simple Fourier transform, and in principal are equivalent descriptions of the structure of the rough surface. In practice, however, all measurements of surface roughness are limited to a finite instrumental bandwidth, and the PSD has the distinct advantage of being accurately measurable within the instrumental bandwidth.²⁹ We consider the case where the multilayer film is grown by alternately depositing N pairs of high-index (H) and low-index (L) layers onto a substrate (S) having an isotropic surface roughness described by a power spectral density PSD_{sub} . The PSD of the top surface of the multilayer film is found by successive iteration of Eq. (39) to be

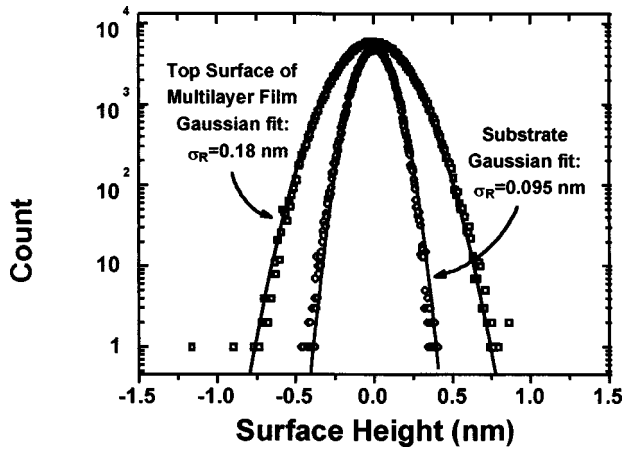


FIG. 3. Surface height distributions of a fused silica substrate and a Mo-Si multilayer film grown on the substrate, measured using atomic force microscopy. The structure of the multilayer film is [Mo(2.1 nm)/Si(4.75 nm)] \times 40. The solid lines are Gaussian fits to the data.

$$\text{PSD}_N = \frac{1 - (a_H^2 a_L^2)^N}{1 - a_H^2 a_L^2} (\text{PSD}_{\text{int}}^L + a_L^2 \text{PSD}_{\text{int}}^H) + (a_H^2 a_L^2)^N \text{PSD}_{\text{sub}}, \quad (43)$$

where $a_{H,L}$ is the replication factor of the high- or low-index layer and

$$\text{PSD}_{\text{int}}^i(f) = \frac{1}{A} \langle \gamma_i \gamma_i^* \rangle = \Omega_i \frac{1 - \exp[-2\nu_i |2\pi f|^n \tau_i]}{2\nu_i |2\pi f|^n}, \quad (44)$$

is the PSD of the intrinsic roughness of the layer. Here we have used the fact that the intrinsic roughness of each interface is statistically independent so that $\langle \gamma_i \gamma_j^* \rangle = 0$ when $i \neq j$.

Our measurements of the roughness of high-performance multilayer optical coatings are generally in good agreement with the predictions of Eqs. (43) and (44). As an example, we show in Figs. 3 and 4 results of surface metrology measurements on a superpolished fused silica substrate and the top surface of a Mo-Si multilayer film grown on the substrate, which we will refer to as our “canonical” multilayer sample throughout this paper. The multilayer film was deposited using magnetron sputter deposition in an Ar plasma of 1.75 mTorr pressure as described in detail elsewhere.³⁰ The film consisted of 40.5 layer pairs with individual layer thicknesses of 2.1 nm for Mo and 4.75 nm for Si. The first and last layers deposited were Si. Images of the surface height were measured using a Digital Instruments Dimension 5000 atomic force microscope operating in the tapping mode. The lateral resolution was ~ 10 nm, due to the width of the tip of the single-crystal Si probe, resulting in a bandwidth limit at high frequency of $\sim 0.1 \text{ nm}^{-1}$. The height resolution of the microscope was ~ 0.01 nm and the surface area sampled was a square region of width $5 \mu\text{m}$. To obtain images of these ultrasoft surfaces it was necessary to operate the microscope inside an environmental chamber that significantly reduced noise from vibrations and air currents. The surface height distributions for the two surfaces are shown in Fig. 3. The data are seen to be well described by

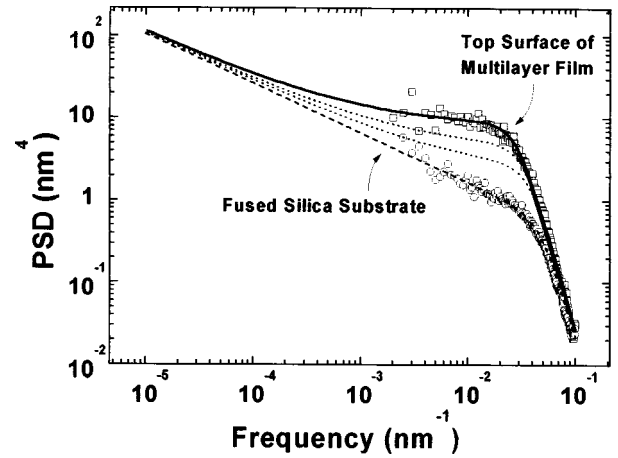


FIG. 4. The PSDs of a fused silica substrate and the top surface of a Mo-Si multilayer film grown on the substrate, measured using atomic force microscopy. The PSD of the substrate is empirically described by $\text{PSD}_{\text{SUB}}(f) = (1.4 \times 10^{-6}/f^{4.2})[1 - \exp(-7.5 \times 10^4 f^{3.6})]$ in nm^4 (dashed line). The solid line is a best fit to the PSD of the top surface of the multilayer film using the growth model discussed. The dotted lines are the calculated PSDs for the interfaces at the 10th and 20th bilayer period as measured from the substrate.

Gaussian distributions. The PSDs of the surfaces were obtained directly from the surface images through Fourier transform. The two-dimensional PSDs were found to be isotropic and were averaged over all directions to generate the radial PSDs shown in Fig. 4.

A complete description of the interfacial roughness in the multilayer film can be inferred by fitting the data shown in Fig. 4 to the model of Eqs. (43) and (44). To limit the degrees of freedom of the fitting process, we place the following constraints on the values of the growth parameters:

(1) We set the growth unit volume Ω for Si to the atomic volume of 0.020 nm^3 . The Si layers in the multilayer film are deposited in an amorphous phase. The choice of the atomic volume assumes that the final position of the adatoms on the amorphous growth surface are random and uncorrelated.

(2) We set the relaxation parameters for the Mo and Si layers to be equal, $\nu = \nu_{\text{Si}} = \nu_{\text{Mo}}$. This is an arbitrary and unrealistic constraint, which is likely to produce a result that is a weighted average of the true values.

The solid line in Fig. 4 represents the best fit using values of $\nu = 2.5 \text{ nm}^3$, $\Omega_{\text{Mo}} = 0.050 \text{ nm}^3$, and $n = 4$ for the remaining free parameters. We note that the growth unit volume for Mo is approximately three times the atomic volume. This suggests that the final position of the atoms on the growth surface are partially correlated. Indeed, the Mo layers in this film have a polycrystalline bcc phase with a strong $\langle 110 \rangle$ texture,³¹ and the ordering due to crystal growth is expected to increase the size of the growth unit. Within the context of the growth theory, the growth parameters Ω , ν , and n , along with the PSD of the substrate, provide a comprehensive description of the roughness of the multilayer film. From these parameters we can determine the PSD of any interface in the multilayer. For example, the dotted lines in Fig. 4 show the PSDs calculated for the interfaces corresponding to the tenth and twentieth bilayer periods as measured from the substrate.

The value of $n=4$ indicates that the dominant relaxation mechanism in these Mo–Si multilayer films grown by sputter deposition is surface diffusion. The importance of surface diffusion in Mo–Si multilayer growth has been previously noted³² in a study where films were grown using electron beam evaporation onto substrates at elevated temperatures. It was found that the roughness of the interfaces decreased dramatically as the temperature of the growing film was increased, up to a point where interdiffusion caused broadening of the interfaces. The decrease in roughness was accompanied by an increase in the size and texture of the crystallites in the polycrystalline Mo layers. Smooth and abrupt interfaces, comparable to the best sputtered multilayer films, were obtained in a rather narrow temperature range around 525 K. This result was interpreted to indicate that the formation of smooth interfaces required sufficient energy at the growth surface to allow adequate surface mobility without activating bulk diffusion. A similar result of $n=4$ has been found for sputtered Ni_{0.81}Fe_{0.19}–Au multilayer films.⁹ In contrast, Salditt *et al.*²² have observed $n=2$ behavior in sputtered W–Si multilayer films, indicating that sputtering and redeposition might be another important smoothing mechanism for specific material systems. It is interesting to note that in these experiments both the W and Si layers were amorphous, whereas in the case of the Mo–Si and Ni_{0.81}Fe_{0.19}–Au multilayer films at least one of the layers was polycrystalline. Hence it is possible that surface diffusion is the dominant smoothing mechanism when the major source of interfacial roughness is polycrystalline faceting.

For the case of relaxation via surface diffusion, it is shown in Appendix B that the parameter ν can be related to other standard growth parameters according to

$$\nu = \frac{\xi D V_0^{A/3}}{r_D k T}. \quad (45)$$

Here ξ is the surface energy, D is the surface diffusion coefficient, V_0 is the atomic volume, r_D is the deposition rate, k is Boltzmann’s constant, and T is the local temperature of the growth surface. Based on our measurement of the relaxation parameter ν we can infer from Eq. (45) an estimate of the surface diffusion coefficient for the Mo–Si multilayer film growth. Using values³³ for Mo of $\xi=2250$ erg/cm², $V_0=0.016$ nm³, $r_D=0.2$ nm/s, and $T=525$ K we obtain a surface diffusion coefficient of $D=4 \times 10^{-15}$ cm²/s. Then the range of an adatom on the surface before it is “frozen” by the deposition of the next monolayer would be approximately given by $\sqrt{Dt}=0.9$ nm. This suggests that the adatom has the opportunity to relax to a energetically favorable position within a radius of several atomic sites. Monte Carlo simulations³⁴ of thin film growth have indicated that such a relaxation mechanism is sufficient to produce low defect films of near bulk density.

It is evident in Figs. 3 and 4 that the roughness of the top surface of the multilayer film is significantly greater than the substrate. The kinetic growth theory predicts three distinct regimes:

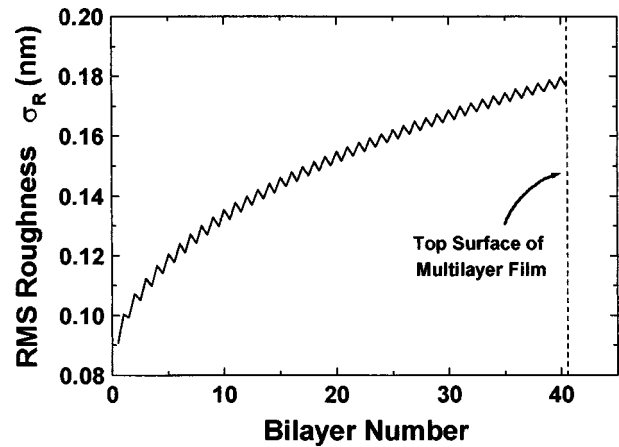


FIG. 5. The variation of the rms roughness of the interfaces within the Mo–Si multilayer film, obtained by integrating the PSDs over the frequency range of 10^{-4} – 10^{-1} nm⁻¹.

- (1) At low spatial frequencies (less than $\sim 10^{-4}$ nm⁻¹ in Fig. 4) the interfacial roughness replicates the substrate roughness and is purely conformal.
- (2) There is an intermediate frequency range (10^{-4} – 10^{-1} nm⁻¹ in Fig. 4) in which the top surface of the multilayer film is significantly rougher than the substrate due to the additional intrinsic roughness associated with the growth of the film.
- (3) At high frequencies (greater than $\sim 10^{-1}$ nm⁻¹ in Fig. 4) the multilayer film growth process has a smoothing effect and can actually result in a damping of the roughness of the substrate.

In general, the transition points between these frequency regimes are not unique; they can vary with both the multilayer growth parameters and the PSD of the substrate.

The increase in the multilayer film roughness in the frequency range of 10^{-4} – 10^{-1} nm⁻¹ is a particular concern for soft x-ray imaging, as it represents in some sense the limit of smoothness that can be obtained for a multilayer-coated surface. For 13 nm radiation near normal incidence these frequency components will produce scattering at angles ranging from ~ 0.1 to 90 degrees. The integrated power scattered over this angular range is proportional to the variance of the surface height, σ^2 , which is the second moment of the surface height distribution shown in Fig. 3, and can also be obtained from the PSD according to

$$\sigma^2 = 2\pi \int_{f_{\min}}^{f_{\max}} \text{PSD}(f) f df. \quad (46)$$

The rms roughness, σ , determined by integrating the PSD over the frequency range of 10^{-4} – 10^{-1} nm⁻¹, is plotted in Fig. 5 for all of the interfaces in the multilayer film. The rms roughness is observed to double throughout the thickness of the film, increasing from a value of $\sigma=0.09$ nm at the substrate to $\sigma=0.18$ nm at the top surface. From this example it is evident that the intrinsic roughness associated with the growth of the multilayer film can be a significant part of the

total roughness, and should be included to obtain an accurate description of nonspecular scattering from multilayer-coated optical surfaces.

VII. THEORY OF NONSPECULAR SCATTERING FROM A MULTILAYER FILM

The last decade has seen considerable progress towards developing a rigorous theory of the scattering of x rays from multilayer films. The existing theoretical framework exploits the fact that the interaction between x rays and matter is typically weak, and treats the nonspecular scattering from interfacial roughness using first- or at most second-order perturbation theory. Consequently the theory is limited to the case where the scattered power is small compared to the incident power. Within the context of perturbation theory there are basically two different formulations, each valid in a different regime. Stearns³ has presented a theory of scattering from multilayer structures based upon previous work¹⁶ describing the scattering from a single interface within the Born approximation. In this treatment, the incident field at each interface consists of plane waves incoming from both sides, corresponding to the exact eigenstate of the ideal multilayer structure (no roughness). The rough interface is considered to be the perturbation, and a solution of Maxwell's equations is found for the scattered vector field, which includes the polarization dependence. The total scattered field, consisting of outgoing plane waves from each of the interfaces, is treated kinematically. The Born approximation neglects the refraction of the incident field, which becomes important near the critical angle for total internal reflection, and hence this scattering theory is only valid for angles greater than the critical angle (as measured from the surface).

In an alternate approach, Holy *et al.*⁵ have developed a scattering theory using the distorted-wave Born approximation (DWBA), based upon the description of scattering from a single rough surface presented by Sinha *et al.*³⁵ The theory has been extended to second order by de Boer.³⁶ In this approach the incident field is an eigenstate of the ideal multilayer structure (in the absence of roughness, although the interfaces need not be abrupt³⁶) having a wave vector \mathbf{k}_0 , including both the incoming and outgoing waves, and the scattered field is a time-reversed version of an incident field having a different wave vector \mathbf{k} . The perturbation is just the change of the multilayer structure upon introducing the roughness. At first glance the DWBA formulation appears to be unphysical since the scattered field includes incoming plane waves. This paradox is resolved by realizing that the final state only needs to be a reasonable approximation of the scattered field within the interaction region, that is, the regions where the roughness exists. When the reflectivity is large, such as near the critical angle, the "outgoing" scattered plane wave will experience multiple reflections within the interaction region, thereby creating a strong "incoming" plane wave component, and this state is well-represented by the DWBA final state. Hence this theory is valid at angles near the critical angle, but is generally not applicable at larger angles. Another limitation of the DWBA approach is that it is based on the Helmholtz equation for the scalar field

and neglects polarization effects, which is strictly only valid at grazing incidence.

An important practical issue in the formulation of the scattering theory is the way in which the roughness of the interfaces is incorporated. It is easily shown³⁵ that the scattering from a single surface is proportional to the Fourier transform of the quantity $\exp[q_z^2 C(\mathbf{r})/2]$. Consequently, there has been a tendency to describe and model surface roughness in terms of the autocorrelation function. However, in the limit where $q_z^2 \sigma^2 \ll 1$, which we call the "small roughness approximation," the exponential can be expanded to obtain the well-known result that the scattering cross section is proportional to the PSD of the surface roughness. The formulation of the scattering theory in terms of the PSD has several distinct advantages:

- (1) The PSD is directly measurable by instruments having finite bandwidths, as mentioned previously.
- (2) Knowledge of the PSD within a limited bandwidth is sufficient to model scattering for a given angular range. In contrast, the complete autocorrelation function is required to describe the scattering within any angular range.
- (3) The scattering problem can be inverted to determine the PSD of a surface from the angular distribution of the scattering.

In the case of scattering from multilayer films the situation gets more complicated; the scattering is proportional to a sum of Fourier transforms of exponential terms containing cross-correlation functions between every pair of interfaces. Specific models of the correlation functions are typically introduced in an *ad hoc* fashion. In contrast, applying the small roughness approximation (when valid) provides the important simplification of linearizing the dependence of the scattering amplitude on the interface roughness $h(\mathbf{f})$. It then becomes possible to directly integrate into the scattering theory the linear growth model described in the previous section.

In this paper we are interested in modeling the scattering from high-performance multilayer optical coatings in configurations near normal incidence. Under these conditions it is appropriate to apply the scattering theory of Stearns based on the Born approximation and linearized using the small roughness approximation. It is necessary, however, to extend the previous theory to account for two effects which are important in modeling the performance of realistic imaging systems. These new developments are:

- (1) The scattered field is treated dynamically, that is, we take into account the multiple specular reflection of the scattered field within the multilayer structure. The dynamical treatment of the scattered field is important when the scattering angle is within a Bragg resonance condition, as will generally be the case for small angle scattering in an imaging system.
- (2) The description of the unperturbed multilayer structure (without roughness) is allowed to include interfacial diffuseness. The diffuseness, corresponding to a broadened composition profile across the interface, arises from interdiffusion and reaction at the layer boundaries. For example, high performance Mo-Si multilayer coatings exhibit inter-

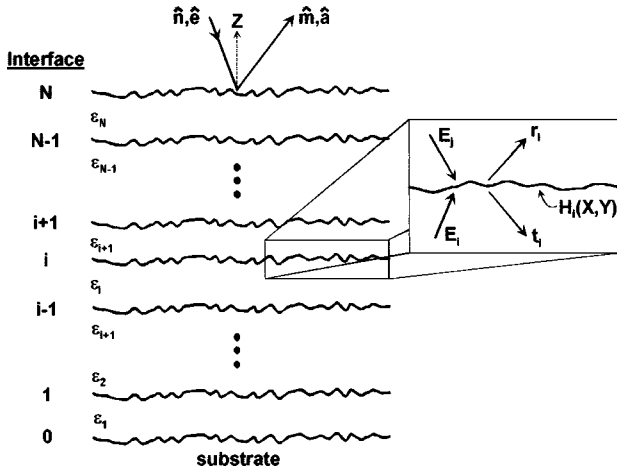


FIG. 6. Schematic diagram of a multilayer film having rough and diffuse interfaces. The inset shows the scattering process at the i th interface. The specular fields E_i and E_j are incident on either side of the interface. The nonspecular scattering into mode (\hat{m}, \hat{a}) consists of two parts, the field r_i that is scattered towards the top of the film and the field t_i that is scattered towards the substrate.

diffusion zones of ~ 1 nm at the Mo-on-Si interface and ~ 0.5 nm at the Si-on-Mo interface.³⁷ The relative effects of roughness and diffuseness on x-ray scattering are discussed in Ref. 16. In general, diffuseness of the interfaces reduces the specular reflectivity of each interface, and thereby redistributes the specular field within the multilayer structure. In this way diffuseness can have an important effect on the nonspecular scattering without producing any scattering *per se*.

We begin by considering a multilayer film having a series of rough and diffuse interfaces as shown schematically in Fig. 6. Let the incident field be a plane wave with wavevector $k\hat{n}$ and polarization \hat{e} , corresponding to either S or P type. Multiple specular reflection within the multilayer film produces counterpropagating plane waves in each layer and refraction modifies the wave vectors and polarization vectors. The wave vectors in the i th layer, $k_i\hat{n}_i^\pm$, for the fields propagating towards the top of the film (+) and towards the substrate (-) are related to the incident field according to

$$\begin{aligned} k_i n_{iX}^\pm &= k n_X \\ k_i n_{iY}^\pm &= k n_Y \\ k_i n_{iZ}^\pm &= \pm k \sqrt{\epsilon_i - n_X^2 - n_Y^2}. \end{aligned} \quad (47)$$

Here the wavenumber $k_i = \epsilon_i^{1/2} k$ becomes a complex quantity for the case of an absorbing medium. The polarization vectors within the i th layer are given by

$$\begin{aligned} S \text{ type: } e_{iX}^\pm &= \frac{n_{iY}}{\sqrt{(n_{iX})^2 + (n_{iY})^2}}, \\ e_{iY}^\pm &= -\frac{n_{iX}}{\sqrt{(n_{iX})^2 + (n_{iY})^2}}, \quad e_{iZ}^\pm = 0 \end{aligned}$$

$$\begin{aligned} P \text{ type: } e_{iX}^\pm &= \frac{n_{iX} n_{iZ}^\pm}{\sqrt{(n_{iX})^2 + (n_{iY})^2}}, \\ e_{iY}^\pm &= \frac{n_{iY} n_{iZ}^\pm}{\sqrt{(n_{iX})^2 + (n_{iY})^2}}, \quad e_{iZ}^\pm = \mp \sqrt{(n_{iX})^2 + (n_{iY})^2}. \end{aligned} \quad (48)$$

We define interface i to be located between layers i and $j = i + 1$. Then there are two plane waves, $E_j^- \hat{e}_j^- \exp(ik_j \hat{n}_j^- \cdot \mathbf{x})$ and $E_i^+ \hat{e}_i^+ \exp(ik_i \hat{n}_i^+ \cdot \mathbf{x})$, incident on the i th interface from above and below, respectively. Within the spirit of perturbation theory, the incident plane waves correspond to the specular field in the multilayer film in the absence of roughness.

Let us consider the field scattered by the multilayer film into direction \hat{m} with polarization \hat{a} . As before, the scattered field undergoes multiple specular reflections within the film which produces counterpropagating waves in each layer having wave vectors $k_j \hat{m}_j^\pm$ and polarizations \hat{a}_j^\pm . Following the formalism of Ref. 3, the amplitude of the field scattered by the i th interface towards the top of the multilayer film is given by

$$\begin{aligned} r_i(\hat{m}_j^+, \hat{a}_j^+) &= \frac{\Delta_{ji} k_j^3}{8\pi^2 \epsilon_j m_{jZ}^+} \left(E_j^- (\hat{a}_j^- \cdot \hat{e}_j^-) \frac{g_i(\mathbf{q}_r)}{q_{rZ}} \right. \\ &\quad \left. + E_i^+ (\hat{a}_j^+ \cdot \hat{e}_i^+) \frac{\tilde{g}_i(\mathbf{q}'_r)}{q'_{rZ}} \right). \end{aligned} \quad (49)$$

Here $\mathbf{q}_r = k_j \hat{m}_j^+ - k_i \hat{n}_i^-$ and $\mathbf{q}'_r = k_j \hat{m}_j^+ - k_i \hat{n}_i^+$ are the momentum transfer vectors, $\Delta_{ji} = \epsilon_j - \epsilon_i$ is the change in the dielectric function across the interface, $g_i(\mathbf{q})$ is the Fourier transform of the normalized gradient of the dielectric function given by

$$g_i(\mathbf{X}) \equiv \frac{1}{\Delta} \frac{\partial \epsilon(\mathbf{X})}{\partial Z}, \quad (50)$$

and $\tilde{g}_i(q_X, q_Y, q_Z) = g_i(q_X, q_Y, -q_Z)$. Since we are treating the scattered field dynamically, we must also include the scattering that is initially directed towards the substrate, as this radiation can be reflected back out of the film by underlying interfaces. The field scattered by the i th interface towards the substrate is given by

$$\begin{aligned} t_i(\hat{m}_i^-, \hat{a}_i^-) &= \frac{\Delta_{ij} k_i^3}{8\pi^2 \epsilon_i m_{iZ}^-} \left(E_i^+ (\hat{a}_i^- \cdot \hat{e}_i^+) \frac{\tilde{g}_i(\mathbf{q}_t)}{q_{tZ}} \right. \\ &\quad \left. - E_j^- (\hat{a}_i^- \cdot \hat{e}_j^-) \frac{g_i(\mathbf{q}'_t)}{q'_{tZ}} \right), \end{aligned} \quad (51)$$

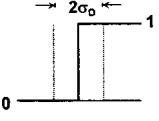
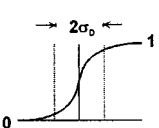
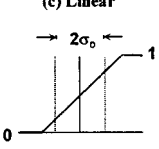
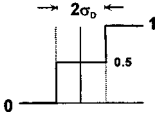
where $\mathbf{q}_t = k_j \hat{m}_i^- - k_i \hat{n}_i^+$ and $\mathbf{q}'_t = k_j \hat{m}_i^- - k_j \hat{n}_j^-$.

All of the information about the structure of the interface is contained in the quantity g , which can be thought of as a structure factor for the interface in the terms of x-ray diffraction theory. We choose to describe the interface using a model

$$g(\mathbf{X}) = W^D[Z - H(X, Y)]. \quad (52)$$

Here the function $W^D(Z)$ represents the gradient of the dielectric function across the interface due to the diffuseness; the position of this diffuse interface is modulated by the

TABLE I. Several examples of the gradient function $W^D(Z)$ for a diffuse interface and its Fourier transform $w^D(q_Z)$.

Description of interface	$W^D(Z)$	$w^D(q_Z)$
(a) Ideal 	$\delta(Z)$	1
(b) Error Function 	$\frac{1}{\sqrt{2\pi\sigma_D^2}} \exp(-Z^2/2\sigma_D^2)$	$\exp(-\sigma_D^2 q_Z^2/2)$
(c) Linear 	$\begin{cases} 0, & Z > \sqrt{3}\sigma_D \\ \frac{1}{2\sqrt{3}\sigma_D}, & Z < \sqrt{3}\sigma_D \end{cases}$	$\frac{\sin(\sqrt{3}\sigma_D q_Z)}{\sqrt{3}\sigma_D q_Z}$
(d) Step 	$\frac{1}{2} [\delta(Z+\sigma_D) + \delta(Z-\sigma_D)]$	$\cos(\sigma_D q_Z)$

roughness function $H(X, Y)$. The key underlying assumption of this model is that the diffuseness is constant over the interface. We would expect this model to be valid when the physical mechanisms causing the roughness and diffuseness are essentially independent. This would be the case, for example, when the interface roughness is predominantly due to the replication of roughness of the underlying layer and the diffuseness is due to the local interdiffusion or reaction of the layers. One example where our model would be inappropriate is the case where the interface roughness is produced by nonuniform interdiffusion or reaction at the layer boundary.

Several important examples of a diffuse interface are listed in Table I, along with the gradient function $W^D(Z)$ and its Fourier transform $w^D(q_Z)$. In case (a) we show an ideal interface, where the dielectric function changes abruptly between layers. In this case the gradient is a delta function with a Fourier transform of unity. Classical interdiffusion is represented by case (b), where the dielectric function across the interface is described by an error function, and both the gradient and its Fourier transform are Gaussian. When a compound is formed at the interface, and the growth of the interlayer is rate limited by diffusion through the interlayer, then the dielectric function should have a linear profile as shown in case (c). However, if the growth of the interlayer is limited by the reaction rate at the interlayer boundary, then the dielectric function has a step profile as shown in case (d). In Table I we normalize the width of the different interface

models to the second moment of the gradient function, σ_D , defined as

$$\sigma_D^2 \equiv \int Z^2 W^D(Z) dZ. \quad (53)$$

Choosing the appropriate model requires a detailed knowledge of the microstructure of the interface. This information is accessible from high-resolution imaging techniques such as transmission electron microscopy of cross-section specimens.³¹ Advances in new scanning techniques such as high-angle annular dark-field microscopy³⁸ make it possible to map the composition gradient at interfaces with nanometer resolution.

Taking the Fourier transform of Eq. (52) we obtain for the nonspecular case ($q_X, q_Y \neq 0$):

$$\begin{aligned} g(\mathbf{q}) &= w^D(q_Z) \int \exp(-iq_X X) \exp(-iq_Y Y) \\ &\quad \times \exp[-iq_Z H(X, Y)] dX dY \\ &\equiv -iq_Z h(q_X, q_Y) w^D(q_Z) \end{aligned} \quad (54)$$

where we have used the small roughness approximation (e) to expand the exponential. Substituting into Eqs. (49) and (51) yields

$$\begin{aligned} r_i(\hat{m}_j^+, \hat{a}_j^+) &= -\frac{i\Delta_{ji} k_j^3 h_i(q_X, q_Y)}{8\pi^2 \epsilon_j m_{jZ}^+} [E_j^-(\hat{a}_j^+ \cdot \hat{e}_j^-) w^D(q_{rZ}) \\ &\quad + E_i^+(\hat{a}_j^+ \cdot \hat{e}_i^+) w^D(-q'_{rZ})] \\ t_i(\hat{m}_i^-, \hat{a}_i^-) &= \frac{i\Delta_{ij} k_i^3 h_i(q_X, q_Y)}{8\pi^2 \epsilon_i m_{iZ}^-} [E_i^+(\hat{a}_i^- \cdot \hat{e}_i^+) w^D(-q_{tZ}) \\ &\quad + E_j^-(\hat{a}_i^- \cdot \hat{e}_j^-) w^D(q'_{tZ})]. \end{aligned} \quad (55)$$

The power per unit solid angle scattered by all of the interfaces in the multilayer film is

$$\frac{dP(\hat{m}, \hat{a})}{d\Omega} = \frac{4\pi^2 m_Z^2}{k^2 A |n_Z|} \left| \sum_i (\phi_i^r r_i + \phi_i^t t_i) \right|^2, \quad (56)$$

where A is the area of the film illuminated by the incident field. The propagation factors ϕ_i^r and ϕ_i^t account for the phase shift and attenuation of the field scattered from the i th interface as it propagates to the top surface of the multilayer film. We rearrange Eq. (56) to show explicitly the dependence on the interface structure:

$$\frac{dP(\hat{m}, \hat{a})}{d\Omega} = \frac{m_Z^2}{16\pi^2 k^2 A |n_Z|} \sum_{ik} (\Gamma_i \Gamma_k^* h_i h_k^*), \quad (57)$$

where

$$\begin{aligned} \Gamma_i &= \frac{\Delta_{ji} k_j^3 \phi_i^r}{\epsilon_j m_{jZ}^+} [E_j^-(\hat{a}_j^+ \cdot \hat{e}_j^-) w^D(q_{rZ}) \\ &\quad + E_i^+(\hat{a}_j^+ \cdot \hat{e}_i^+) w^D(-q'_{rZ})] \\ &\quad - \frac{\Delta_{ji} k_i^3 \phi_i^t}{\epsilon_i m_{iZ}^-} [E_i^+(\hat{a}_i^- \cdot \hat{e}_i^+) w^D(-q_{tZ}) \\ &\quad + E_j^-(\hat{a}_i^- \cdot \hat{e}_j^-) w^D(q'_{tZ})]. \end{aligned} \quad (58)$$

The next step is to incorporate the multilayer growth model to describe the roughness of the interfaces, including the correlation of roughness between interfaces. In particular, iteration of Eq. (39) shows that the roughness h_i of the i th interface is a superposition of the intrinsic roughness γ_i of each of the underlying layers (and the substrate). The roughness h_i can be written as

$$h_i = \sum_{n=0}^i c_{in} \gamma_n. \tag{59}$$

The factor c_{in} represents the amount of intrinsic roughness of the n th layer that propagates to the i th interface. It is explicitly related to the replication factors, a_m , of the intervening interfaces according to

$$c_{in} = \frac{\prod_{m=0}^i a_m}{\prod_{m=0}^n a_m}. \tag{60}$$

Assuming that the intrinsic roughness γ_i of each interface is statistically independent, we have

$$h_i h_k^* \xrightarrow{\text{for } k < i} \sum_{n=0}^k c_{in} c_{kn} \gamma_n \gamma_n^* = A \sum_{n=0}^k c_{in} c_{kn} \text{PSD}_{\text{int}}^n. \tag{61}$$

Substituting into Eq. (57) yields

$$\begin{aligned} \frac{dP(\hat{m}, \hat{a})}{d\Omega} &= \frac{m_z^2}{16\pi^2 k^2 |n_z|} \\ &\times \sum_{i=0}^N \left[\left(\sum_{n=0}^i c_{in}^2 \text{PSD}_{\text{int}}^n \right) \Gamma_i \Gamma_i^* \right. \\ &\left. + \sum_{k=0}^{i-1} \left(\sum_{n=0}^k c_{in} c_{kn} \text{PSD}_{\text{int}}^n \right) (\Gamma_i \Gamma_k^* + \Gamma_k \Gamma_i^*) \right]. \end{aligned} \tag{62}$$

This expression is the central result of the multilayer scattering theory. The angular distribution of the scattering power is directly related to the detailed structure of the interfaces through the PSD_{int} of the intrinsic roughness (including the substrate) and the factors c_{in} which describe the replication of roughness between interfaces. These quantities are in turn defined, within the context of our growth model, by the growth parameters Ω , ν , and n , which are characteristic of the film media and deposition conditions. It is evident in Eq. (62) that the scattering separates naturally into two terms. The first term corresponds to the uncorrelated scattering, and is simply the sum of the intensities scattered by each interface independently. The second term corresponds to the correlated scattering. This contribution represents the interference of the radiation fields scattered by interfaces that are correlated due to the replication of roughness from layer to layer.

We note that Eq. (62) is only applicable under the conditions for which the multilayer growth model is expected to be valid, that is, when the roughness is sufficiently small so that the growth kinetics are local and linear. This limit is consistent with the ‘‘small roughness approximation’’ (e) that was invoked previously, and is expected to be satisfied

by high performance multilayer optical coatings, where the roughness is minimized by design. Equation (62) should not be valid when the roughness is large and the film growth is dominated by nonlinear and nonlocal effects such as shadowing and columnar growth.

Although the formulation of the scattering theory is complete, its implementation requires a method of calculating the incident field amplitudes, E_i^+ and E_j^- , and the propagation factors ϕ_i^r and ϕ_i^t . These quantities are to be determined in the absence of roughness, since we are considering the scattering process as a first-order perturbation (the Born approximation). This is accomplished using a well-known matrix approach to analyze the propagation of the specular fields within the multilayer film. The matrix method is described in detail in Appendix C.

The description of the image formation in the presence of scattering (Eq. [29]) also requires the calculation of the Strehl factor, S . This factor accounts for the total decrease in the specular intensity due to scattering and, for the case of a multilayer film, includes losses due to the absorption of the scattered field within the film. In practice, the accurate calculation of the Strehl factor is problematic when there is a strong reflected field. This is because the scattering from the roughness significantly alters the configuration of the incident specular field. In particular, the roughness redistributes the power between the reflected and transmitted specular fields, which generates loss through increased absorption. This is a purely dynamical effect, requiring second-order perturbation theory to correctly describe the lowest-order change in the specular field due to the interfacial roughness. Unfortunately, a general second-order theory of scattering from rough multilayer structures has not yet been developed. An alternative approach for estimating the Strehl factor, based on an *ad hoc* treatment of these interference effects, is presented at the end of this section.

As an example of the application of the multilayer scattering theory, we have modeled the specular reflectivity and nonspecular scattering from the canonical Mo–Si multilayer film described in Sec. VI, and we compare these results to experimental measurements. The x-ray scattering measurements were performed using synchrotron radiation (S polarization) provided by Beamline 6.3.2 of the Advanced Light Source at Lawrence Berkeley Laboratory. A detailed description of the beamline and reflectometer is presented elsewhere.³⁹ A unique feature of this experimental facility, which is particularly important for performing scattering measurements on high-quality multilayer films, is the combination of high photon flux ($\sim 10^{12}$ photons/s in 0.1% bandwidth) and excellent collimation of the incident beam. An example of the profile of the incident beam is shown in Fig. 7. At angles greater than four degrees the wings of the incident beam are suppressed by over nine orders of magnitude, making it possible to measure very low levels of scattering.

The measured specular reflectivity of the Mo–Si multilayer as a function of x-ray wavelength is shown in Fig. 8 for angles of incidence ranging from 5 to 20 degrees as measured from the film normal. The reflectivity was modeled using the matrix method described in Appendix C, with optical constants provided by the CXRO World Wide Web

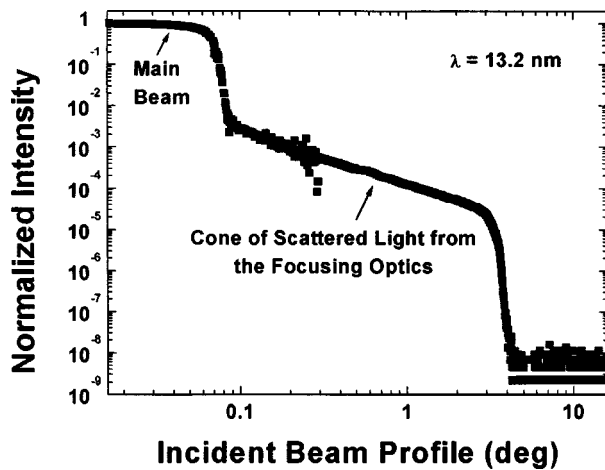


FIG. 7. The measured angular profile of the incident beam for the experimental configuration used to obtain the scattering data. The intensity of the incident beam is reduced by nine orders of magnitude within four degrees of the center of the beam. The high spatial purity is achieved using a combination of focusing optics and apertures.

site.⁴⁰ Modeling the position and width of the Bragg peaks provides an accurate and unique determination of the individual layer thicknesses. The interfaces have been modeled as asymmetric zones of intermixing having linear composition profiles, based upon previous detailed studies of the microstructure of similar Mo–Si multilayer films.⁴¹ The width, σ_D , of these zones is 0.3 nm for the Mo-on-Si interfaces and 0.15 nm for the Si-on-Mo interfaces. The best fits are shown as the solid lines in Fig. 8, and correspond to a layer structure of [Mo(2.1 nm)/Si(4.75 nm)] \times 40. The amplitude of the reflectivity (i.e., the Strehl factor) is not accurately modeled by the matrix method, as discussed above, and has been treated as a free fitting parameter.

The nonspecular scattering measured at normal incidence ($\theta=0$ deg) and at wavelengths of 12.8 and 13.2 nm is shown in Fig. 9 as a function of the scattering angle. We also show the calculated specular reflectivity for comparison

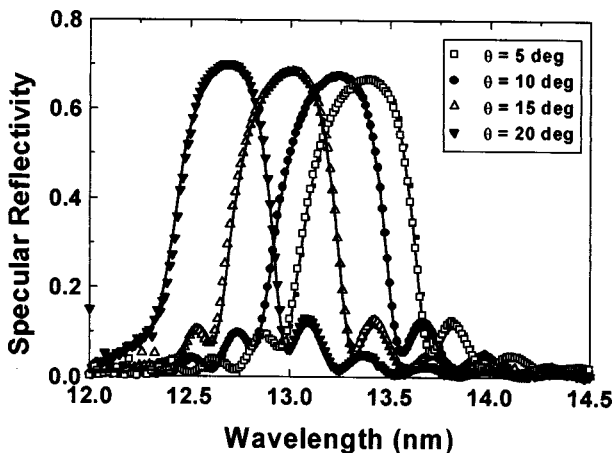


FIG. 8. Measured specular reflectivity of the canonical Mo–Si multilayer film as a function of soft x-ray wavelength for several different angles of incidence. The peak reflectivity varies from 66% at five degrees and 13.4 nm to 70% at 20 degrees and 12.6 nm (just above the Si *L* edge). The solid lines are best fits using a multilayer structure of [Mo(2.1 nm)/Si(4.75 nm)] \times 40.

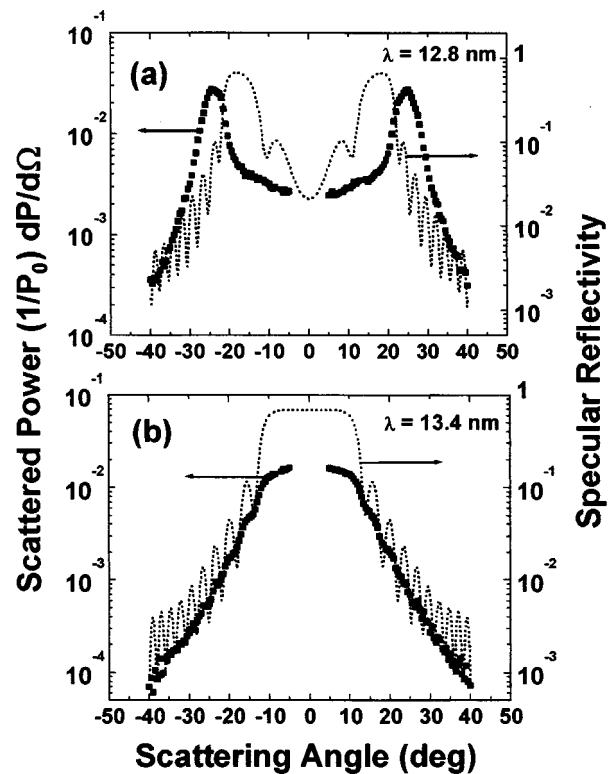


FIG. 9. Nonspecular scattering measured from the canonical Mo–Si multilayer film for normal incidence radiation at a wavelength of (a) 12.8 nm and (b) 13.4 nm. The dotted lines are the calculated specular reflectivity of the film as a function of incident angle.

(dotted lines). The measurements correspond to the scattered power per unit solid angle, normalized to the incident power. These data were obtained using a channeltron detector operating in pulse counting mode. The solid angle subtended by the detector was defined by a 2.0-mm-diameter pinhole positioned 225 mm from the multilayer sample. The scattering was measured by scanning the detector in the plane of incidence while keeping the incident beam fixed. The scattering could be measured to within approximately 4 degrees of the angle of specular reflection, at which point the background level overwhelmed the scattering signal.

The angular dependence of the nonspecular scattering exhibits several characteristic features. In both cases there is a broad peak that mimics the specular Bragg peak. At 12.8 nm [Fig. 9(a)] the scattering peak is shifted to a larger angle than the specular Bragg peak. At 13.4 nm [Fig. 9(b)] the scattering and specular peaks appear to coincide. Furthermore, the nonspecular scattering exhibits a small oscillation, more easily observed in the 13.4 nm data [Fig. 9(b)], which dies out at larger scattering angles.

The origin of the broad peak in the nonspecular scattering is the same as the Bragg peak in specular reflection: the interference of the fields scattered from the different interfaces. This phenomenon has been called “quasi-Bragg scattering”³ or “resonant diffuse scattering”⁵ in the literature. We will refer to it as resonant nonspecular scattering (RNS) in this paper. Two conditions are required to observe a peak in RNS. First there must be correlation between the roughness of the interfaces in the multilayer. Second, the

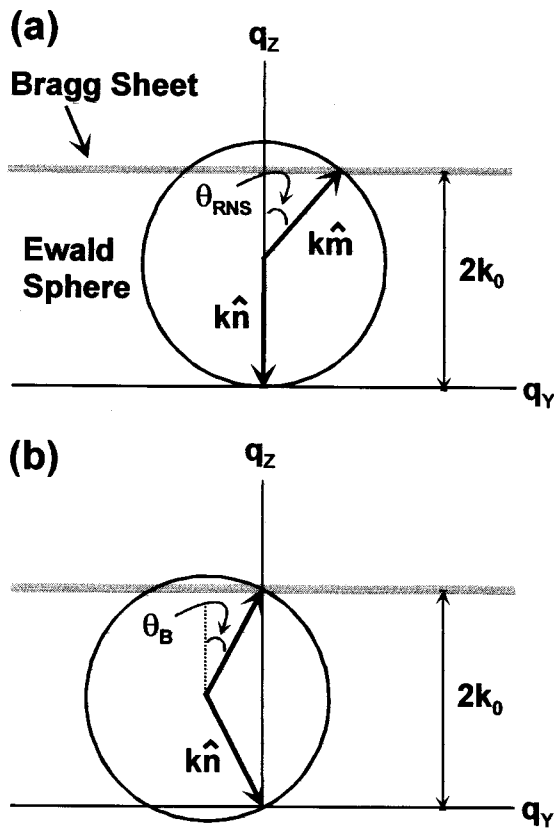


FIG. 10. (a) An Ewald construction showing the nonspecular scattering process in reciprocal space. The Bragg sheet is located at $q_z = 2k_0$ and the incident radiation, of momentum $k\hat{n}$, is normal to the film. The nonspecular scattered field, of momentum $k\hat{m}$, is constrained to the surface of the Ewald sphere. A peak in the resonant nonspecular scattering (RNS) occurs when the Ewald sphere intersects the Bragg sheet. (b) An Ewald construction illustrating the conditions for specular reflectivity.

fields scattered from the different interfaces must add in phase constructively. These requirements are best illustrated using an Ewald construction in reciprocal space, as shown in Fig. 10. Here the Bragg reflection at $q_z = 2k_0$ is spread out into a sheet parallel to the $q_x - q_y$ plane due to the correlated roughness of the multilayer interfaces, which produces coherent scattering with finite momentum transfer in the X-Y plane. Figure 10(a) shows the configuration for scattering at normal incidence with an x-ray momentum $k > k_0$ [as is the case in Fig. 9(a)]. The allowed (elastic) values of momentum transfer are constrained to be on the surface of the Ewald sphere. The peak in the RNS, θ_{RNS} , is given by the angle at which the scattering vector $k\hat{m}$ intersects the Bragg sheet. The RNS peak generally occurs at a larger angle than the specular Bragg peak. This can be seen in Fig. 10(b), where we show an Ewald construction for specular reflection from the multilayer at the same value of x-ray momentum k . Here the angle of incidence and reflection is θ_B . Inspection of the two diagrams in Fig. 10 shows that the relationship between the angular positions of the RNS and Bragg peaks is

$$2k \cos \theta_B = k + k \cos \theta_{RNS}, \tag{63}$$

which reduces to $\theta_{RNS} \cong \sqrt{2}\theta_B$ in the limit of small angles. This predicted behavior is consistent with the data of Fig. 9(a), where the RNS and Bragg peaks are at ~ 25 and 18

degrees, respectively. The two peaks only coincide when the wavelength and angle of the incident field satisfy the condition for Bragg reflection ($k = k_0$), as is the case in Fig. 9(b).

An important consequence of the relationship between the position of the RNS and Bragg peaks is that the total integrated scattering increases significantly as k exceeds k_0 . The total integrated scattering (TIS) corresponds to the total power nonspecularly scattered into all angles for a given incident angle and wavelength. The TIS obtained by integrating the scattering shown in Fig. 9 is found to be 0.98% and 0.30% at the wavelengths of 12.8 and 13.4 nm, respectively. The increase in TIS at the shorter wavelength (larger k) is due to a significant increase in the transmission of the multilayer film as the RNS peak shifts away from the specular Bragg peak. Within the Bragg peak, scattered radiation is trapped inside the film in a standing wave similar to the specular field, which reflects much of the radiation back into the film. However, when the RNS is outside of the Bragg peak, as occurs at shorter wavelengths [Fig. 9(a)]. The radiation scattered at interfaces within the film propagates to the top surface with little loss. This purely dynamical effect causes the extinction of the RNS to vary dramatically with scattering angle.

In Fig. 9 the RNS exhibits a small oscillation having the same period as the high frequency oscillation of the specular reflectivity (sometimes called ‘‘Kiessig fringes’’). The oscillation in the RNS has the same origin as that in the specular reflectivity, namely the interference of the radiation scattered from the front and back surfaces of the multilayer film. This can occur in scattering whenever there is a correlation between the roughness of the substrate and the roughness of the top surface. Indeed, the existence of a finite thickness oscillation in the scattering intensity is an unequivocal indicator of conformality in the roughness of the multilayer film. The amplitude of the oscillation indicates the degree to which the roughness of the substrate is replicated at the top surface. The growth theory of Sec. VI asserts that the degree of replication is a strong function of frequency, decreasing at higher frequency. Hence we expect that the RNS at small scattering angles, corresponding to lower frequency roughness, should exhibit larger finite thickness oscillations than the RNS at large scattering angles. This is consistent with the data shown in Fig. 9, where the amplitude of the oscillation is observed to dampen with increasing scattering angle, and is essentially absent at angles greater than ~ 25 degrees.

In Fig. 11 we present additional measurements of nonspecular scattering from the canonical Mo-Si multilayer film for normal incidence and wavelengths of 12.8, 13.0, 13.2, and 13.4 nm. The solid lines are calculations of the scattering intensity using the parameters summarized in Table II. The growth parameters that characterize the multilayer roughness are based on the measured PSDs of the substrate and top surface of the multilayer film, shown in Fig. 4. The layer thicknesses are derived from measurements of the specular reflectivity, shown in Fig. 8. We emphasize that all of the input parameters are obtained from independent measurements and the calculations of the nonspecular scattering have no adjustable parameters. The good agreement between the measured scattering and the calculations based on the mea-

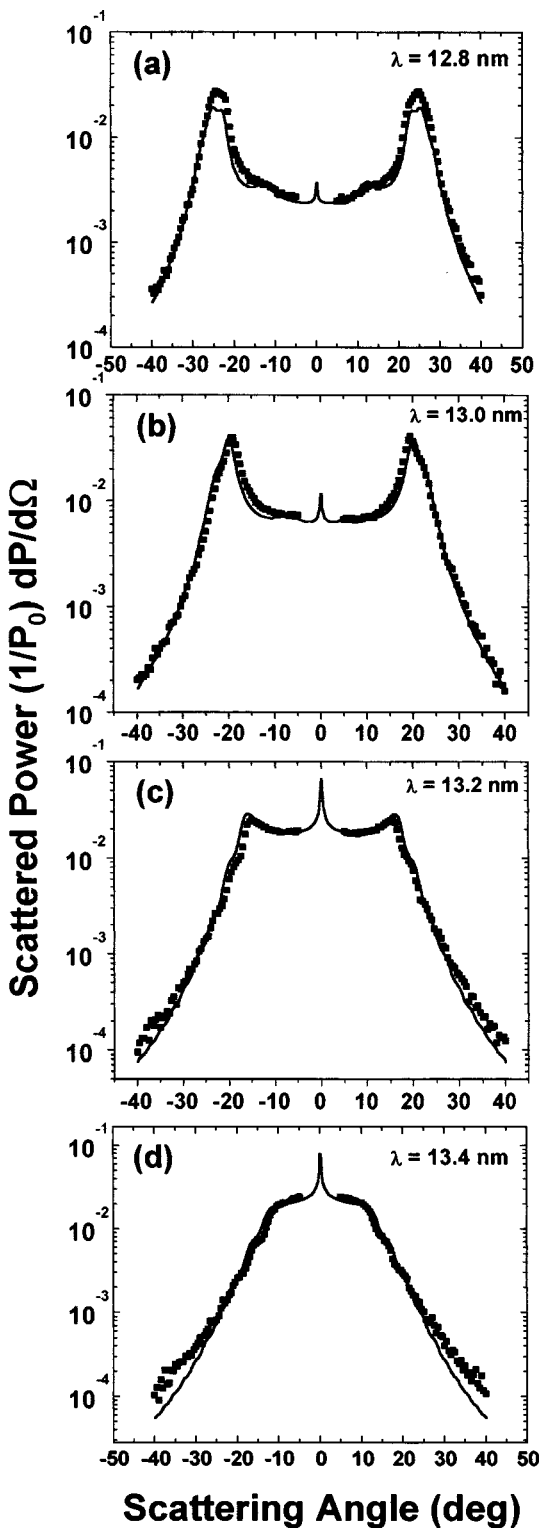


FIG. 11. Nonspecular scattering measured from the canonical Mo-Si multilayer film at normal incidence and for several different wavelengths. Data within four degrees of the specular direction is obscured by the wings of the specularly reflected beam. The solid lines are the scattering distributions predicted by the theory, based on the measured roughness of the multilayer film.

sured roughness provides an important validation of the multilayer growth model and scattering theory.

Finally we address an issue that is central to the appli-

cation of multilayer coatings in imaging systems: how does the scattering from a multilayer coating compare to the scattering from a single reflecting surface? The unique characteristics of scattering from a multilayer film are illustrated in Fig. 12(a) where we show calculations of the nonspecular scattering *normalized to the specular reflectivity* for three configurations of the surface. In each case the incidence field is unpolarized, has a wavelength of 13.4 nm and is incident normal to the surface. The dotted line corresponds to scattering from a single surface having the roughness of the fused silica substrate shown in Fig. 4. The scattering is featureless and decreases relatively slowly with increasing scattering angle. The rolloff is mostly due to the frequency dependence of the PSD. In contrast, the dashed line represents the scattering from our canonical Mo-Si multilayer film having completely conformal interfaces, that is, the roughness at each interface is identical to the substrate. Here the scattering is characterized by strong interference effects (RNS). The RNS from the conformal multilayer is comparable to the scattering from the single surface at angles less than ~ 12 degrees. (The scattering from the multilayer is slightly reduced due to an increase of the x-ray wavelength within the film.) Beyond 12 degrees the scattering intensity drops precipitously, as the radiation fields scattered by the different interface interfere destructively. Hence the conformal multilayer scatters like a single surface within the RNS peak, and strongly suppresses scattering at larger angles.

The solid line in Fig. 12(a) shows the scattering calculated for the canonical Mo-Si multilayer film (Fig. 9), where the interfacial roughness is due to both the replication of the substrate and the intrinsic roughness of the film growth process. The scattering exhibits an angular dependence similar to the case of the purely conformal multilayer, but has a nearly sixfold increase in scattering at all angles greater than ~ 1 degree. The scattering is increased because the multilayer interfaces are rougher than the substrate, particularly towards the top of the film where most of the scattering originates (see Fig. 5). It is also apparent that the finite thickness oscillation is smaller and the decrease in scattering at large angles is less rapid than for the case of the purely conformal multilayer film, behavior which is consistent with the partial correlation of the interfacial roughness. Comparing the realistic multilayer film to the single surface, we find that the scattering is equivalent only at very small angles of < 1 degree, where the interfacial roughness in the multilayer film is purely conformal. The scattering from the multilayer is enhanced in the region of 1–20 degrees due to the intrinsic roughness of the film, and is suppressed at angles greater than 20 degrees due to the interference effects characteristic of RNS.

The total integrated scatter (TIS) within a cone of half-width θ centered about the film normal is plotted as a function of θ in Fig. 12(b). The TIS is normalized to the specular reflectivity, R^{SP} . We observe that, compared to the single surface, the scattering from the multilayer coatings is concentrated in the relatively small annular region within ~ 14 degrees from the normal, corresponding to the peak in RNS. This suggests a simple *ad hoc* method for estimating the Strehl factor for the multilayer film in the condition

TABLE II. A list of the parameters used to model the nonspecular scattering from the canonical Mo–Si multilayer film. The multilayer growth parameters Ω , ν , and n are described in Sec. VI. These together with the substrate PSD (shown in Fig. 4) define the roughness of the multilayer interfaces. The diffuseness of the interfaces is described by a linear profile of width σ_D (case [c] in Table I). The thickness of the individual layers is τ . The atomic scattering factors are f_1 and f_2 , the ρ is the mass density, and W is the atomic weight.

	Growth parameters			Structural parameters		Optical parameters				
	Ω (nm ³)	ν (nm ³)	n	τ (nm)	σ_D (nm)	λ (nm)	f_1	f_2	ρ (g/cm ³)	W (g/mole)
Mo	0.05	2.5	4	2.1	0.3 (Mo-on-Si)	12.8	14.34	1.270	10.2	95.94
						13.0	14.52	1.320		
						13.2	14.67	1.372		
						13.4	14.82	1.424		
Si	0.02	2.5	4	4.75	0.15 (Si-on-Mo)	12.8	-1.397	0.487	2.33	28.086
						13.0	-0.763	0.475		
						13.2	-0.321	0.464		
						13.4	0.023	0.452		

where the RNS and Bragg peaks effectively coincide. Our main assertion is that the effect of roughness can be divided into two regimes, corresponding to the frequencies that scatter within and without the RNS peak. Defining θ_C as the scattering angle at the edge of the RNS peak, we divide the rms roughness into two parts: the low frequency roughness, σ_L , obtained by integrating the PSD over the spatial frequencies less than the value $f_C = \sin \theta_C / \lambda$, and the high frequency roughness σ_H obtained by integrating the PSD over the spatial frequencies greater than f_C . The low-frequency roughness produces scattering within the RNS peak. Since the roughness is conformal at these frequencies, the scattering from the different interfaces is coherent and interferes constructively. Then the reduction in the specular reflectivity due to these low frequencies can be estimated by a simple factor of the Debye–Waller type, $\exp(-16\pi^2\sigma_L^2 \cos^2 \theta / \lambda^2)$. For the frequencies of the roughness that scatter outside of the RNS peak, the situation is very different. Here the loss due to scattering is significantly reduced for two reasons: (1) the interference of the fields scattered by the different interfaces becomes destructive, and (2) the coherence of the scattering is reduced due to the decreased correlation of the interfacial roughness. Thus in the high-frequency range the primary effect of roughness is not to produce scattering, but instead to increase the transmission of the interfaces, thereby resulting in a larger penetration depth for the incident specular field and correspondingly greater absorption. This is in fact the same loss mechanism as the case of a diffuse interface broadened by intermixing or chemical reaction, and can be treated in a similar way. Specifically, we estimate the reduction of the specular reflectivity due to the high-frequency roughness by including a contribution from the high-frequency roughness in the interface width $\sigma_D \rightarrow \sqrt{\sigma_D^2 + \sigma_H^2}$. This modified value of σ can be applied in the matrix method described in Appendix C to calculate the specular reflectivity $R^{SP}(\sigma)$ of the multilayer coating reduced by both diffuseness and high-frequency roughness. Then the Strehl factor describing the reduction in the specular reflectivity due to interfacial roughness is estimated as

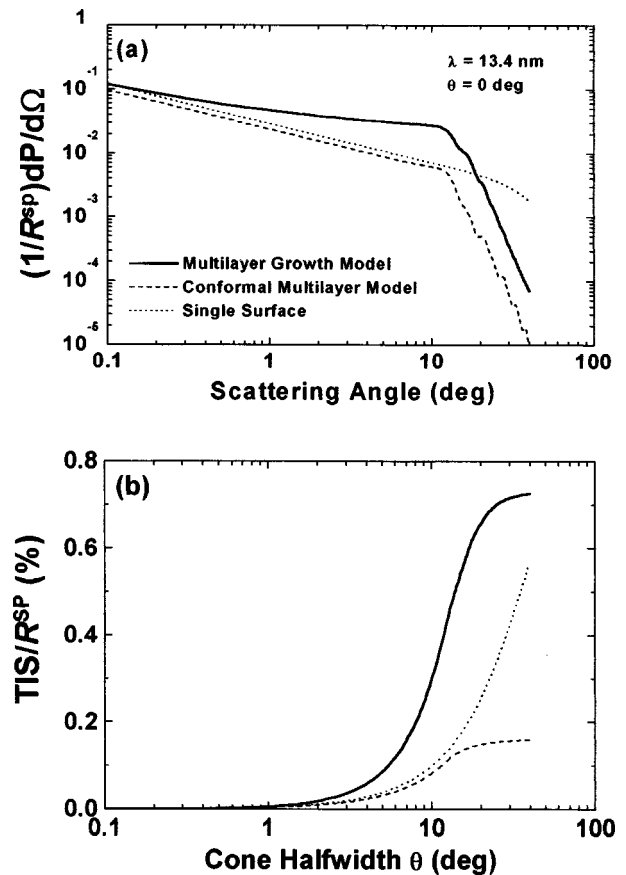


FIG. 12. (a) Calculations of nonspecular scattering from three different surfaces, normalized to the specular reflectivity. The dotted line is a single surface having the roughness of the fused silica substrate shown in Fig. 4. The dashed line corresponds to an ideally conformal Mo–Si multilayer film where the roughness of each interface is identical to the roughness of the single surface. The solid line is a realistic Mo–Si multilayer film having interfacial roughness due to both replication of the substrate roughness and the intrinsic roughness of the growth process. (b) The total integrated scattering (TIS) within a cone of halfwidth θ , calculated for the three surfaces and normalized to the specular reflectivity. Nearly all of the scattering from the multilayer films is within 20 degrees of the specular direction.

$$S = \frac{R^{\text{SP}}(\sigma = \sqrt{\sigma_D^2 + \sigma_H^2})}{R^{\text{SP}}(\sigma = \sigma_D)} \exp\left(-\frac{16\pi^2\sigma_L^2 \cos^2 \theta}{\lambda^2}\right). \quad (64)$$

As an example, consider the scattering from the canonical multilayer coating calculated from the PSDs of Fig. 4 and shown as the solid line in Fig. 12(a). The separation of the low- and high-frequency ranges is found by inspection to be at a scattering angle of $\theta_C \cong 14$ deg, corresponding to a frequency of $f_C = 0.02 \text{ nm}^{-1}$. We integrate the PSD of the top surface of the multilayer coating as prescribed in Eq. (46) over the low- and high-frequency ranges to obtain $\sigma_L = 0.09 \text{ nm}$ and $\sigma_H = 0.15 \text{ nm}$, respectively. Using these values in Eq. (64) in conjunction with the structural parameters of Table II, we obtain a Strehl factor of 0.988 for normal incidence and $\lambda = 13.4 \text{ nm}$.

We emphasize that the method described by Eq. (64) for estimating the Strehl factor is only necessary when there is a strong reflected field, such that dynamical effects associated with the interference of the fields scattered by the different interfaces are important. When the incident field is not near the Bragg peak, or if the specular reflectivity is small (< 0.1) then the scattering process is well approximated by kinematical theory, that is, the scattering does not significantly alter the configuration of the incident field. In this case, the Strehl factor can be estimated from either the Debye–Waller factor of Eq. (29) or the matrix method of Appendix C with modified Fresnel coefficients, using a rms roughness σ obtained by integrating the PSD over all frequencies.

VIII. MODELING THE PERFORMANCE OF A SOFT X-RAY IMAGING SYSTEM

We now turn our attention back to the problem of modeling the nonspecular scattering in a distributed optical system consisting of multilayer coated optics. The conventional method for characterizing the performance of an imaging system is to measure the optical transfer function (OTF). The OTF is the ratio of the image intensity to the object intensity at a particular spatial frequency, and is also the Fourier transform of the point spread function. It is only defined for the case of incoherent illumination, where there is a purely linear relationship between the Fourier transforms of the intensities in the image and object planes. However, we have shown that the effect of scattering is to produce a point spread function, PSF^{sc} , that is independent of the coherence of the illumination. Then the Fourier transform of PSF^{sc} yields an OTF^{sc} that describes the modulation of the image intensity due to scattering under any illumination conditions. In particular, collecting the results of Secs. II and III, the intensity at the image plane is given by

$$\langle I_1(\mathbf{s}_1) \rangle = I_1^0(\mathbf{s}_1) * \kappa \text{PSF}^{\text{sc}}(\mathbf{s}_1), \quad (65)$$

where I_1^0 is the image produced by the optical system in the absence of scattering and

$$\begin{aligned} \text{PSF}^{\text{sc}}(\mathbf{s}_1) &= \frac{1}{\kappa} \left(\prod_n S_n \delta(\mathbf{s}_1) + \sum_n \frac{\alpha_{nx} \alpha_{ny}}{R_n^{\text{SP}} R^2} \sum_{\hat{a}} \frac{dP_n(\hat{m}, \hat{a}; \hat{n}, \hat{e})}{d\Omega} \right), \end{aligned} \quad (66)$$

is the point spread function due to scattering. The quantity in brackets is calculated using the scattering theory presented in the previous section; the angular scattering distributions $dP_n/d\Omega$ are obtained from Eq. (62), where the scattering vector is related to the point \mathbf{s}_1 in the image field through Eq. (32). The Strehl factor S_n , corresponding to the ratio between the specular reflectivity of the n th surface with and without roughness, can be estimated from the PSD of the top surface of the multilayer coating using Eq. (64). The normalizing factor κ is

$$\begin{aligned} \kappa &= \int \int \left(\prod_n S_n \delta(\mathbf{s}_1) \right. \\ &\quad \left. + \sum_n \frac{\alpha_{nx} \alpha_{ny}}{R_n^{\text{SP}} R^2} \sum_{\hat{a}} \frac{dP_n(\hat{m}, \hat{a}; \hat{n}, \hat{e})}{d\Omega} \right) d\mathbf{s}_1, \end{aligned} \quad (67)$$

where the integration is over the image field. This factor accounts for the loss of image intensity due to the scattering outside of the image field and the increased absorption arising from the high-frequency interfacial roughness.

Taking the Fourier transform of (65) we obtain

$$I_1(\mathbf{f})/I_1^0(\mathbf{f}) = \text{OTF}^{\text{sc}}(\mathbf{f}), \quad (68)$$

where $I_1(\mathbf{f})$ is the Fourier transform of the image intensity, and

$$\begin{aligned} \text{OTF}^{\text{sc}}(\mathbf{f}) &= \frac{1}{\kappa} \prod_n S_n + \frac{1}{\kappa} \int \int \sum_n \frac{\alpha_{nx} \alpha_{ny}}{R_n^{\text{SP}} R^2} \\ &\quad \times \sum_{\hat{a}} \frac{dP_n(\hat{m}, \hat{a}; \hat{n}, \hat{e})}{d\Omega} \exp(-2\pi i \mathbf{s}_1 \cdot \mathbf{f}) d\mathbf{s}_1. \end{aligned} \quad (69)$$

Equations (68) and (69) provide the basis for relating the optical performance in the presence of scattering, as characterized by the OTF^{sc} , to the key structural parameters of the optical surfaces, including the surface finish of the substrates and the roughness of the multilayer coatings. This allows us to determine specifications for the roughness of the substrates and coatings, given certain performance requirements. The operational procedure for deriving such specifications consists of first defining a minimally acceptable $\text{OTF}^{\text{sc}}(\mathbf{f})$ that will allow the production of useful images. Then, taking into account the intrinsic roughness of the multilayer coating, we determine the limits of substrate roughness required to satisfy the specified value of OTF^{sc} at each frequency.

A significant simplification is possible in the limit of very smooth substrates, where the scattering is dominated by the intrinsic roughness of the multilayer coatings. In this case the scattering is uniform out to fairly large angles (~ 10 degrees) because the PSD of the intrinsic roughness is flat for frequencies less than $\sim 10^{-1} \text{ nm}^{-1}$ (see Fig. 2). When the scattered light is uniformly distributed throughout

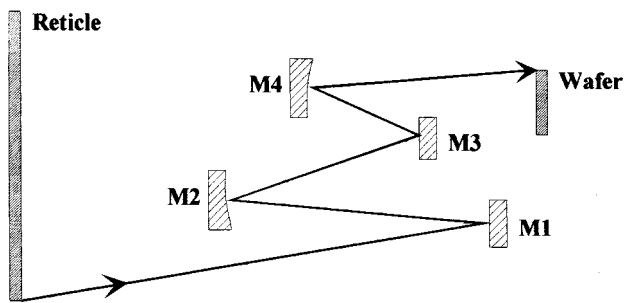


FIG. 13. Schematic diagram of a hypothetical soft x-ray imaging system for EUV lithography. The optical system, consisting of four multilayer-coated mirrors, projects an image of the reticle onto the wafer.

the image field it is called “veiling glare.” Under these conditions the second term in Eq. (69) is negligible and the OTF^{sc} can be approximated as having a constant value of S/κ , that is, the image contrast is reduced by a constant amount at all but the lowest frequencies.

As an example, we model the nonspecular scattering in the distributed optical system shown schematically in Fig. 13. The imaging system is purely hypothetical, but is based on generic designs being considered for applications in EUV lithography.^{42,43} It consists of four reflecting surfaces and, although designed to be used as a ring field, we will consider for the purpose of modeling scattering that the image field is a square of width 2.5 cm. A requirement for lithography applications is that the imaging system be telecentric at the wafer, that is, the principal ray is parallel to the optical axis for all points in the image field. A consequence of telecentricity is that the exit pupil is infinitely large and is located an infinite distance from the image plane. However, we showed in Sec. III that the effects of scattering on the transfer function are independent of the position of the actual exit pupil. We can choose to evaluate the transfer function at any position on the image side of the last optical surface, provided that we apply the correct scaling factors. In this case we evaluate the transfer function at the position of the last mirror (M4), located 23 cm from the image plane. The scaling factors and angles of incidence of the principal ray, as determined by ray tracing calculations, are listed in Table III. We assume that the optical surfaces are coated with Mo–Si multilayer films designed for an operating wavelength of 13.2 nm. Since the dispersion of the angles of incidence on any given optical surface is small, the multilayer coatings will have uniform bilayer spacing. The multilayer structure

TABLE III. Design parameters for a hypothetical soft x-ray imaging system consisting of four mirrors. The scaling factors, α_x and α_y , are set equal and θ is the angle of incidence of the principal ray as measured from the normal to the optical surface. Also listed are the Strehl factors S_n for the multilayer coatings calculated at an x-ray wavelength of 13.2 nm.

Mirror	$\alpha_x = \alpha_y$	θ (deg)	Multilayer structure	S_n
M1	1.7	3.0	[Mo(2.8 nm)/Si(4.0 nm)] \times 40	0.985
M2	0.9	7.0	[Mo(2.8 nm)/Si(4.0 nm)] \times 40	0.985
M3	1.8	12.0	[Mo(2.8 nm)/Si(4.1 nm)] \times 40	0.985
M4	1.0	6.0	[Mo(2.8 nm)/Si(4.0 nm)] \times 40	0.986

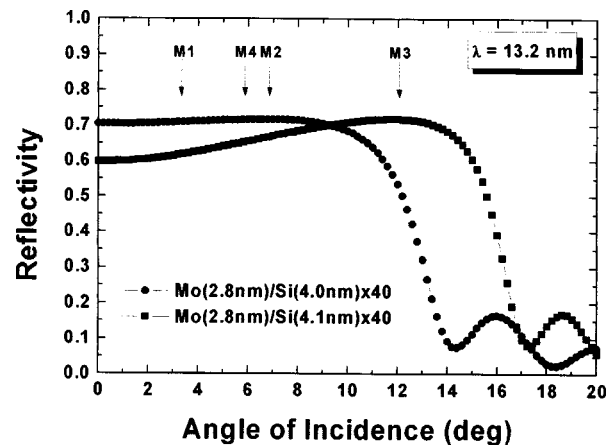


FIG. 14. Calculated reflectivity of the two Mo–Si multilayer coatings used in the hypothetical imaging system. The arrows indicate the angles of incidence of the principal ray on each of the optical surfaces.

that optimizes the reflectivity for the first, second, and fourth surfaces is [Mo(2.80 nm)/Si(4.00 nm)] \times 40. The third surface requires a slightly different design of [Mo(2.80 nm)/Si(4.10 nm)] \times 40, due to the larger angle of incidence. The calculated reflectivity of these designs at a wavelength of 13.2 nm is shown in Fig. 14. These calculations include interdiffusion at the interfaces of $\sigma_D=0.3$ nm for the Mo-on-Si interface and $\sigma_D=0.15$ nm for the Si-on-Mo interface. All roughness and oxidation is neglected, and hence the reflectivity values are slightly overestimated.

The PSF^{sc} is calculated using the methodology described above. The plane of incidence of the principal ray is the $y-z$ plane for all optical surfaces, and the radiation incident on each surface is assumed to be unpolarized. We assume that the roughness of the substrates is the same as the superpolished fused silica flat having the PSD shown in Fig. 4. Furthermore, we assume that the roughness of the Mo–Si multilayer coatings is equivalent to the “canonical” film discussed in the previous sections, and that the roughness is described by the thin film growth model and the corresponding growth parameters listed in Table II. Consequently, the multilayer coating contributes roughness to the optical surfaces, causing the rms roughness to increase from the substrate to a final value of $\sigma=0.18$ nm at the top surface. The Strehl factors S_n for the coatings are determined from Eq. (64), where the rms roughness is divided into low- and high-frequency components of $\sigma_L=0.09$ nm and $\sigma_H=0.15$ nm, corresponding to those frequencies that scatter within and out of the RNS peak, respectively. The calculated values of the Strehl factors are listed in Table III.

The PSF^{sc} calculated over a 2.5×2.5 -cm image field is shown in Fig. 15. The delta function corresponding to the specular field [the first term in Eq. (66)] has been omitted from the plot. The PSF^{sc} exhibits a peak at the optical axis which drops off to a relatively constant level of scattering at distances beyond ~ 0.5 cm from the optical axis. The edge of the image field corresponds to a scattering angle of only ~ 3 degrees. Since the strong resonant scattering (RNS) from the multilayer coatings exists out to an angle of ~ 14 degrees, it is evident that the image field intercepts only

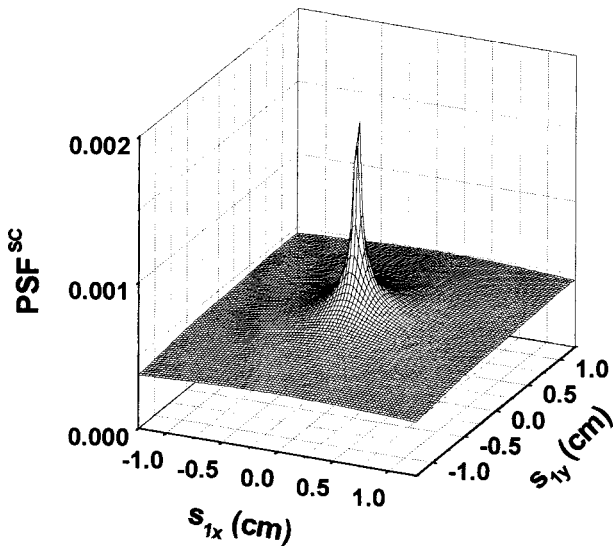


FIG. 15. The point spread function due to scattering (PSF^{sc}) of the hypothetical imaging system, calculated assuming that the roughness of the Mo-Si multilayer coatings is equivalent to the canonical film shown in Fig. 4. The delta-function component of PSF^{sc} is not shown.

a small fraction of the total scattered radiation. In this case the Strehl factor S for the imaging system is 0.94, corresponding to a 6% decrease in the specular image intensity. However the fraction of the specular intensity scattered into the image field is only 0.3% ($S/\kappa=0.997$). The OTF^{sc} obtained by taking the Fourier transform of the PSF^{sc} is shown in Fig. 16. The OTF^{sc} drops rapidly to a constant value of $S/\kappa=0.997$ for frequencies greater than $\sim 2.5 \text{ cm}^{-1}$. This behavior is characteristic of veiling glare and illustrates the dominant effect of the intrinsic roughness of the multilayer coatings in this example; the scattering is fairly uniformly distributed throughout the image field and hence reduces the

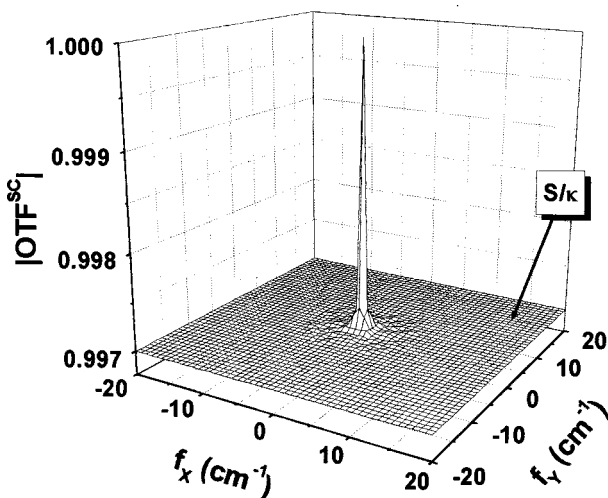


FIG. 16. The optical transfer function due to scattering (OTF^{sc}) of the hypothetical imaging system. The nonspecular scattering reduces the OTF of the imaging system by a factor $S/\kappa=0.997$ at all but the lowest frequencies.

image contrast by a constant amount at all but the lowest frequencies.

At the risk of oversimplification, we can use our example to make some general comments regarding the effect of scattering in the performance of multilayer-coated imaging systems. High performance imaging systems for soft x rays require a numerical aperture of ~ 0.1 or less in order to have a reasonable depth of focus ($\geq 1 \mu\text{m}$). Consequently the range of scattering angles subtended by the image field will be limited to a few degrees, and all of this scattering will be within the RNS peak of the multilayer coatings. The components of roughness that scatter into the image field are in the midspatial frequency range of $\sim 10^{-5}/\lambda - 10^{-1}/\lambda \text{ nm}^{-1}$; it is this range of frequencies that is responsible for the decrease in image resolution and contrast. In this range the roughness of the multilayer coatings is dominated by the replication of the substrate roughness and includes (at the higher end of the frequency range) some intrinsic roughness of the multilayer film. Consequently, the scattering within the image field for a multilayer-coated imaging system is expected to be comparable to, and slightly greater than, an equivalent system having single reflecting surfaces. Most of the intrinsic roughness of the multilayer-coatings occurs at higher frequencies ($10^{-3} - 10^{-1} \text{ nm}^{-1}$) that will scatter outside of the image field. Hence the main detrimental effect of the intrinsic roughness of the coatings is to reduce the throughput of the imaging system.

IX. CONCLUSION

In summary, we have presented a theoretical framework for modeling nonspecular scattering in a soft x-ray imaging system consisting of multilayer-coated reflecting optics. The theory directly relates the image degradation due to scattering to the statistical properties of the interfacial roughness of the multilayer coatings. Consequently, the theory can be a versatile tool for tasks such as modeling the performance of optical components of known roughness, deriving specifications for the roughness of optical substrates and coatings, and comparing the performance of different optical designs. When applying the theory in practice, it is important to recall the numerous approximations that were invoked, and to observe the restrictions imposed by these approximations. We summarize the key approximations of the theory in Appendix A.

Throughout the course of this presentation we have attempted to illustrate the theoretical formalism with realistic examples and analysis of experimental data whenever possible. In particular, the good agreement between the measured scattering from Mo-Si multilayer films and the calculations based on the measured roughness of the films serves to validate our treatment of the scattering problem. The ultimate test of the theory will require the complete characterization of a distributed imaging system, corresponding to independent measurements of the PSF and the roughness of the multilayer-coated optics. This will be the goal of future work.

In addition to its practical importance, our theoretical investigation has broadened the fundamental understanding

of scattering in a distributed imaging system and, in particular, the effects of multilayer coatings. The most important results are summarized below:

(1) Image formation in a distributed optical system can be described as a convolution of the image formed in the absence of scattering with a PSF^{sc} due to scattering.

(2) The PSF^{sc} is independent of the coherence state of the object.

(3) The roughness of a multilayer coating originates from both the intrinsic roughness of the growth process and the replication of the roughness of the substrate. At the lowest spatial frequencies the multilayer film exactly replicates the substrate roughness. In the range $\sim 10^{-3} - 10^{-1} \text{ nm}^{-1}$ the roughness increases from the substrate to the top surface of the multilayer, and the roughness of the different interfaces is partially correlated. At higher spatial frequencies the multilayer film tends to smooth the substrate roughness.

(4) The nonspecular scattering from a multilayer coating exhibits strong interference effects due to the partial correlation of the roughness of the interfaces. This produces a resonance in the nonspecular scattering (RNS) in the vicinity of the specular Bragg peak. In particular, the RNS peak and the Bragg peak are coincident when the incident field satisfies the Bragg condition for specular reflection.

(5) In a soft x-ray imaging system, the roughness in the midspatial frequency range of $\sim 10^{-5}/\lambda - 10^{-1}/\lambda \text{ nm}^{-1}$ produces the scattering that reaches the image field. In this frequency range the roughness of the multilayer coatings is due to replication of the substrate roughness and, to a small extent, the intrinsic roughness of the multilayer film. Hence the scattering within the image field for a multilayer-coated imaging system is expected to be slightly greater than an equivalent system having single reflecting surfaces, and depends predominantly on the roughness of the optical substrates.

(6) The main detrimental effect of the intrinsic roughness of the multilayer coatings is to scatter radiation outside the image field, thereby reducing the throughput of the optical system.

We conclude with a comment regarding the impact of scattering on the performance of soft x-ray imaging systems. The example that we have presented using a hypothetical imaging system designed for EUV lithography shows a very minor degradation of performance due to scattering; the OTF is reduced by only 0.3% and the throughput is decreased by 6%. One might be tempted to infer that scattering is not a significant problem in such an imaging system. In fact, our example demonstrates that scattering can be limited to acceptably low levels in a soft x-ray imaging system *if the optical substrates can be fabricated with roughness equivalent to the best superpolished flats measured to date*. Our analysis indicates that, once these ultrasoft substrates are available, the existing multilayer-coating technology is capable of producing soft x-ray imaging systems that have acceptably low levels of scattering. This conclusion is supported by experiments performed⁴⁴ on a soft x-ray telescope designed for normal incidence operation at $\lambda = 6.35 \text{ nm}$. The optical components were coated with Co-C multilayer films, and were measured to have roughness similar to the PSDs

shown in Fig. 4. Analysis of the images obtained with the telescope showed no measurable scattering. Although these results are encouraging, they must be considered a best case scenario. We anticipate that fabricating sufficiently smooth figured optics will be a significant technical challenge, particularly as the size of the optical components increases and the figures become aspherical. In practice the effect of scattering on the performance of the soft x-ray imaging system will define the acceptable limits of roughness for these optics.

ACKNOWLEDGMENTS

We thank F. Weber for fabricating the Mo-Si multilayer films. The atomic force microscopy measurements were performed by S. L. Baker. We are grateful to J. H. Underwood for his assistance in designing and performing the scattering measurements on Beamline 6.3.2 at the Advanced Light Source. This work was supported by the Department of Energy under Contract DE-AC03-76SF00098 and CRADA TC-0191/0192-92.

APPENDIX A: SUMMARY OF APPROXIMATIONS

We summarize below the key assumptions and approximations underlying the theoretical development presented in this paper.

(a) The angle between the principal ray and any other ray that propagates through the imaging system is small. Specifically, if we denote the angle as φ , then the approximation is

$$\sin^2 \varphi \ll 1. \quad (2)$$

We call this the “small angle approximation.”

(b) For a point object, the pupil function is independent of the location of the point in the object field. In this case the point spread function is independent of the position of the Gaussian image point, and the system is called “isoplanatic.” In practice, the assumption of isoplanacity restricts the applicability of the transfer function formalism to objects of small spatial extent.

(c) The scattering is weak so that multiple scattering and shadowing effects can be neglected. This is called the “Born approximation.” This approximation is generally valid for x-ray wavelengths at angles of incidence away from the critical angle for total external reflection.

(d) The surface height $H(X, Y)$ is a Gaussian random variable, is stationary and is ergodic in the sense that the ensemble average can be replaced by an average over the illuminated surface area.

(e) The deviations of the surface height $H_n(X_n, Y_n)$ from the ideally smooth surface are small compared to the radiation wavelength such that $2k \cos \theta_n H_n(X_n, Y_n) \ll 1$ for all X_n, Y_n . We call this the “small roughness approximation.” A necessary consequence of the small roughness approximation is that the power scattered into the nonspecular field is small compared to the specularly reflected power, a condition that is implicitly satisfied by high-performance optics.

APPENDIX B: RELAXATION OF A ROUGH SURFACE BY SURFACE DIFFUSION

Consider a rough surface $H(X, Y)$ where the growth units (e.g., atoms) have mobility to move between sites on the surface. The chemical potential at each point on the surface depends on the curvature at that point. The gradient of the chemical potential is the driving force for the surface diffusion that causes the smoothing of the surface. To express these concepts quantitatively let us model the local curvature of the surface at a particular point as a sphere of radius R . Then the curvature at that point is

$$\nabla^2 H(X, Y) = -\frac{2}{R}. \quad (\text{B1})$$

The chemical potential of the point $H(X, Y)$ is found by letting the radius of the spherical feature change by an infinitesimal amount ΔR . The chemical potential is given by

$$\mu = \frac{\Delta E_s}{\Delta N}, \quad (\text{B2})$$

where ΔE_s is the change in the surface energy and ΔN is the change in the number of atoms within the sphere. The change in the surface energy is just proportional to the change in the surface area

$$\Delta E_s = 8\pi R \xi \Delta R, \quad (\text{B3})$$

where ξ is the surface energy per unit area. The change in the number of atoms in the sphere is

$$\Delta N = \frac{4\pi R^2 \Delta R}{V_0}, \quad (\text{B4})$$

where V_0 is the atomic volume. Combining Eqs. (B1)–(B4) we obtain

$$\mu = \frac{2\xi V_0}{R} = -\xi V_0 \nabla^2 H(X, Y). \quad (\text{B5})$$

This shows explicitly that the chemical potential is proportional to the local curvature of the surface.

The driving force, F , for surface diffusion is the gradient of the chemical potential

$$F = -\nabla \mu. \quad (\text{B6})$$

From the Nernst–Einstein relation⁴⁵ the mean velocity of an atom on the surface is given by

$$\langle v \rangle = \frac{FD_s}{kT} = -\frac{D_s \nabla \mu}{kT} \quad (\text{B7})$$

where D_s is the surface diffusion coefficient, k is Boltzmann's constant, and T is the surface temperature. The flux of atoms, J , on the surface is

$$J = \frac{\langle v \rangle}{V_0^{2/3}}. \quad (\text{B8})$$

The surface flux is the mechanism of mass transport through which the smoothing of the surface takes place. However, the surface height at a given point can change only if there is a divergence of flux. Then the change in the surface height per unit time is given by

$$\frac{dH(X, Y)}{dt} = -V_0 \nabla \cdot J. \quad (\text{B9})$$

Combining Eqs. (B5)–(B9) we obtain

$$\frac{dH(X, Y)}{dt} = -\frac{\xi D_s V_0^{4/3}}{kT} \nabla^4 H(X, Y). \quad (\text{B10})$$

In the thin film growth model the evolution of the surface is measured as a function of film thickness, τ , and not time. However, time and thickness are simply related through the deposition rate $r_D = d\tau/dt$. Then we can rewrite Eq. (B10) as

$$\frac{dH(X, Y)}{d\tau} = -\frac{\xi D_s V_0^{4/3}}{r_D kT} \nabla^4 H(X, Y). \quad (\text{B11})$$

Comparing this result to Eq. (36) we identify the relaxation parameter for the thin film growth model

$$\nu = \frac{\xi D_s V_0^{4/3}}{r_D kT}. \quad (\text{B12})$$

Not surprisingly, the rate at which the smoothing occurs is proportional to the surface diffusion coefficient. The temperature dependence of the relaxation parameter is dominated by the surface diffusion coefficient which is proportional to $\exp(-E_A/kT)$, where E_A is the activation energy. In general the relaxation of the surface will be enhanced at higher temperature and lower deposition rate.

APPENDIX C: MATRIX METHOD FOR PROPAGATING SPECULAR FIELDS IN A MULTILAYER FILM

The multilayer scattering theory requires as input parameters the incident field amplitudes, E_i^+ and E_j^- , and the propagation factors ϕ_i^r and ϕ_i^t for each interface of the multilayer film in the absence of roughness. These are most easily calculated using a well-known matrix approach⁴⁶ to analyze the propagation of the specular fields within the multilayer film. First we define a scattering matrix, \mathbf{T}_i , that relates the specular fields across the i th interface according to

$$\begin{pmatrix} E_j^- \\ E_j^+ \end{pmatrix} = \mathbf{T}_i \begin{pmatrix} E_i^- \\ E_i^+ \end{pmatrix}. \quad (\text{C1})$$

It is easily shown that

$$\mathbf{T}_i = \frac{1}{t_{ji}} \begin{pmatrix} 1 & r_{ji} \\ r_{ij} & t_{ji}t_{ij} + r_{ji}^2 \end{pmatrix}, \quad (\text{C2})$$

where t_{ji} and r_{ji} are the specular transmission and reflection amplitudes, respectively, for the i th interface. For a compositionally abrupt interface the transmission and reflection amplitudes are given by the Fresnel equations

$$S \text{ polarization: } t_{ji}^0 = \frac{2\chi_j}{\chi_j + \chi_i}, \quad r_{ji}^0 = \frac{\chi_j - \chi_i}{\chi_j + \chi_i} \quad (\text{C3})$$

$$P \text{ polarization: } t_{ji}^0 = \frac{2\sqrt{\epsilon_j \epsilon_i} \chi_j}{\epsilon_i \chi_j + \epsilon_j \chi_i}, \quad r_{ji}^0 = \frac{\epsilon_i \chi_j - \epsilon_j \chi_i}{\epsilon_i \chi_j + \epsilon_j \chi_i}$$

where

$$\chi_i = k \sqrt{\epsilon_i - n_X^2 - n_Y^2}. \quad (\text{C4})$$

Diffuseness at the interface, characterized by a composition gradient $W^D(Z)$, modifies the transmission and reflection amplitudes according to the well-known formulas first derived by Nevot and Croce⁴⁷

$$t_{ji} = t_{ji}^0 \frac{1}{w^D(k_j n_{jz}^+ - k_i n_{iz}^+)}, \quad (\text{C5})$$

$$r_{ji} = r_{ji}^0 \frac{w^D(k_j n_{jz}^+ + k_i n_{iz}^+)}{w^D(k_j n_{jz}^+ - k_i n_{iz}^+)}.$$

Specific examples of the function $w^D(q_z)$, corresponding to several simple interface profiles, are listed in Table I.

The scattering matrix describes the propagation of the specular field across an interface. To propagate the field through the i th layer of thickness τ_i we define the propagation matrix \mathbf{P}_i

$$\mathbf{P}_i = \begin{pmatrix} \exp(-i\varphi_i) & 0 \\ 0 & \exp(i\varphi_i) \end{pmatrix}, \quad (\text{C6})$$

where

$$\varphi_i = k \tau_i \sqrt{\epsilon_i - n_X^2 - n_Y^2}. \quad (\text{C7})$$

The propagation of the specular field from layer to layer in the multilayer film is represented by a series of matrix multiplications. In particular, the field above interface i is related to the field below the underlying interface m through a matrix $\mathbf{A}^{i,m}$ according to

$$\begin{pmatrix} E_{i+1}^- \\ E_{i+1}^+ \end{pmatrix} = \mathbf{A}^{i,m} \begin{pmatrix} E_m^- \\ E_m^+ \end{pmatrix}, \quad (\text{C8})$$

where

$$\mathbf{A}^{i,m} = \begin{pmatrix} A_{11}^{i,m} & A_{21}^{i,m} \\ A_{12}^{i,m} & A_{22}^{i,m} \end{pmatrix} = \mathbf{T}_i \mathbf{P}_i \mathbf{T}_{i-1} \cdots \mathbf{T}_{m+1} \mathbf{P}_{m+1} \mathbf{T}_m. \quad (\text{C9})$$

The transmission and reflection amplitudes for the entire multilayer film, t_{ML} and r_{ML} , are obtained from $\mathbf{A}^{N,0}$, corresponding to propagation through all N interfaces. In particular,

$$t_{\text{ML}} = \frac{1}{A_{11}^{N,0}}, \quad r_{\text{ML}} = \frac{A_{21}^{N,0}}{A_{11}^{N,0}}, \quad (\text{C10})$$

and the specular transmission and reflectance are correspondingly,

$$T^{\text{SP}} = |t_{\text{ML}}|^2, \quad R^{\text{SP}} = |r_{\text{ML}}|^2. \quad (\text{C11})$$

Knowledge of the transmitted amplitude allows us to determine the specular fields above and below each interface using the relations

$$\begin{pmatrix} E_{i+1}^- \\ E_{i+1}^+ \end{pmatrix} = \mathbf{A}^{i,0} \begin{pmatrix} t_{\text{ML}} \\ 0 \end{pmatrix}, \quad \begin{pmatrix} E_i^- \\ E_i^+ \end{pmatrix} = \mathbf{P}_i \mathbf{A}^{i-1,0} \begin{pmatrix} t_{\text{ML}} \\ 0 \end{pmatrix}.$$

We introduced the factors ϕ_i^r and ϕ_i^t in the scattering theory to account for the propagation of the scattered field from the i th interface to the top surface of the multilayer film. Consider a field of unit amplitude initially scattered at the i th interface towards the top of the film. This produces a

field exiting the front surface of the film of amplitude ϕ_i^r and a field exiting the bottom surface into the substrate of amplitude E_s . Then the matrix equation that describes the propagation of this scattered radiation through the system of layers is given by

$$\begin{pmatrix} 0 \\ \phi_i^r \end{pmatrix} = \mathbf{A}^{N,i+1} \mathbf{P}_{i+1} \begin{bmatrix} 0 \\ 1 \end{bmatrix} + \mathbf{A}^{i,0} \begin{pmatrix} E_s \\ 0 \end{pmatrix}, \quad (\text{C12})$$

where the matrices \mathbf{A} and \mathbf{P} now correspond to a scattered plane wave mode. Similarly, for a field of unit amplitude initially scattered towards the bottom of the multilayer film we can write a matrix equation:

$$\begin{pmatrix} 0 \\ \phi_i^t \end{pmatrix} = \mathbf{A}^{N,i} \begin{bmatrix} 1 \\ 0 \end{bmatrix} + \mathbf{P}_i \mathbf{A}^{i-1,0} \begin{pmatrix} E_s \\ 0 \end{pmatrix}. \quad (\text{C13})$$

Solving these matrix equations for ϕ_i^r and ϕ_i^t we obtain

$$\phi_i^r = e^{i\varphi_i} (A_{22}^{N,i+1} - r_{\text{ML}} A_{12}^{N,i+1})$$

$$\phi_i^t = A_{21}^{N,i} - r_{\text{ML}} A_{11}^{N,i}. \quad (\text{C14})$$

- ¹G. D. Kubiak and D. R. Kania, OSA Trends in Optics and Photonics Vol. 4, *Extreme Ultraviolet Lithography* (Optical Society of America, Washington, DC, 1996).
- ²E. Spiller, in *Soft X-Ray Optics* (SPIE, Bellingham, 1994), p. 235.
- ³D. G. Stearns, J. Appl. Phys. **71**, 4286 (1992).
- ⁴D. E. Savage, J. Kleiner, N. Schimke, Y.-H. Phang, T. Jankowski, J. Jacobs, R. Kariotis, and M. G. Lagally, J. Appl. Phys. **69**, 1411 (1991).
- ⁵V. Holy and T. Baumbach, Phys. Rev. B **49**, 668 (1994); V. Holy *et al.*, *ibid.* **47**, 896 (1993).
- ⁶A. P. Payne and B. M. Clemens, Phys. Rev. B **47**, 2289 (1993).
- ⁷T. Salditt, D. Lott, T. H. Metzger, J. Peisl, G. Vignaud, P. Hoghoj, O. Scharpf, P. Hinze, and R. Lauer, Phys. Rev. B **54**, 5860 (1996); T. Salditt, T. H. Metzger, and J. Peisl, Phys. Rev. Lett. **73**, 2228 (1994).
- ⁸J. B. Kortright, J. Appl. Phys. **70**, 3620 (1991).
- ⁹R. Paniago, H. Homma, P. C. Chow, S. C. Moss, Z. Barnea, S. S. P. Parkin, and D. Cookson, Phys. Rev. B **52**, 52 (1995).
- ¹⁰D. R. Lee, Y. J. Park, D. Kim, Y. H. Jeong, and K. B. Lee, Phys. Rev. B. (submitted for publication).
- ¹¹E. L. Church and P. Z. Takacs, Opt. Eng. (Bellingham) **34**, 353 (1995); E. L. Church and P. Z. Takacs, Appl. Opt. **32**, 3344 (1993).
- ¹²J. E. Harvey, Appl. Opt. **34**, 3715 (1995); J. E. Harvey, K. L. Lewotsky, and A. Kotha, Opt. Eng. (Bellingham) **35**, 2423 (1996).
- ¹³S. Singh, H. Solak, and F. Cerrina, Rev. Sci. Instrum. **67**, 3355 (1996).
- ¹⁴M. Born and E. Wolf, in *Principles of Optics*, 6th ed. (Pergamon, New York, 1987), p. 480.
- ¹⁵D. G. Stearns, Appl. Phys. Lett. **62**, 1745 (1993).
- ¹⁶D. G. Stearns, J. Appl. Phys. **65**, 491 (1989).
- ¹⁷B. R. Frieden, in *Probability, Statistical Optics, and Data Testing*, 2nd ed. (Springer, New York, 1991), p. 75.
- ¹⁸For a review see, A. L. Barabasi and H. E. Stanley, in *Fractal Concepts in Surface Growth* (Cambridge University Press, Cambridge, 1995), p. 19.
- ¹⁹W. M. Tong and R. S. Williams, Annu. Rev. Phys. Chem. **45**, 401 (1994).
- ²⁰S. F. Edwards and D. R. Wilkinson, Proc. R. Soc. London, Ser. A **381**, 17 (1982).
- ²¹C. Herring, J. Appl. Phys. **21**, 301 (1959).
- ²²T. Salditt, D. Lott, T. H. Metzger, J. Peisl, R. Fischer, J. Zweck, P. Hoghoj, O. Scharpf, and G. Vignaud, Europhys. Lett. **36**, 565 (1996).
- ²³M. Kardar, G. Parisi, and Y.-C. Zhang, Phys. Rev. Lett. **56**, 889 (1986).
- ²⁴R. P. U. Karunasiri, R. Bruinsma, and J. Rudnick, Phys. Rev. Lett. **62**, 788 (1989).
- ²⁵C. Tang, S. Alexander, and R. Bruinsma, Phys. Rev. Lett. **64**, 772 (1990).
- ²⁶J. A. Thornton, Thin Solid Films **45**, 387 (1977).
- ²⁷R. Messier and J. E. Yehoda, J. Appl. Phys. **58**, 3739 (1985).
- ²⁸D. J. Miller, K. E. Gray, R. T. Kampwirth, and J. M. Murduck, Europhys. Lett. **19**, 27 (1992).
- ²⁹E. L. Church, Appl. Opt. **27**, 1518 (1988).

- ³⁰D. G. Stearns, R. S. Rosen, and S. P. Vernon, *J. Vac. Sci. Technol. A* **9**, 2662 (1991).
- ³¹Y. Cheng, D. J. Smith, M. B. Stearns, and D. G. Stearns, *J. Appl. Phys.* **72**, 5165 (1992).
- ³²M. B. Stearns, C.-H. Chang, and D. G. Stearns, *J. Appl. Phys.* **71**, 187 (1992).
- ³³E. S. Machlin, in *An Introduction to Thermodynamics and Kinetics Relevant to Materials Science* (Giro, Croton-on-Hudson, 1991), p. 115.
- ³⁴K. H. Muller, *Surf. Sci.* **184**, L375 (1987); *Phys. Rev. B* **35**, 7906 (1987).
- ³⁵S. K. Sinha, E. B. Sirota, S. Garoff, and H. B. Stanley, *Phys. Rev. B* **38**, 2297 (1988).
- ³⁶D. K. G. de Boer, *Phys. Rev. B* **53**, 6048 (1996).
- ³⁷D. G. Stearns, M. B. Stearns, Y. Cheng, J. H. Stith, and N. M. Ceglio, *J. Appl. Phys.* **67**, 2415 (1990).
- ³⁸Y. Cheng, J. Liu, M. B. Stearns, and D. G. Stearns, *Proc. SPIE* **1547**, 167 (1992).
- ³⁹J. H. Underwood, E. M. Gullikson, M. Koike, P. J. Batson, P. E. Denham, K. D. Franck, R. E. Tackaberry, and W. F. Steele, *Rev. Sci. Instrum.* **67**, 3372 (1996), CD-ROM only.
- ⁴⁰URL: www-cxro.lbl.gov; B. L. Henke, E. M. Gullikson, and J. C. Davis, *Atomic Data Nucl. Data Tables* **54**, 181 (1993).
- ⁴¹R. S. Rosen, D. G. Stearns, and S. P. Vernon, *Appl. Opt.* **32**, 6975 (1993).
- ⁴²W. C. Sweatt, *OSA Trends in Optics and Photonics Vol. 4, Extreme Ultraviolet Lithography*, edited by G. D. Kubiak and D. Kania (Optical Society of America, Washington, DC, 1996), p. 178.
- ⁴³G. E. Sommargren and L. Seppala, *Appl. Opt.* **32**, 6938 (1993).
- ⁴⁴E. Spiller, D. Stearns, and M. Krumrey, *J. Appl. Phys.* **74**, 107 (1993).
- ⁴⁵*Physical Metallurgy*, edited by R. W. Cahn and P. Haasen, 3rd ed. (Elsevier, Amsterdam, 1983), p. 398.
- ⁴⁶M. Born and E. Wolf, in *Principles of Optics*, 6th ed. (Pergamon, New York, 1987), p. 51; O. S. Heavens, *Optical Properties of Thin Films* (Dover, New York, 1966).
- ⁴⁷L. Nevot and P. Croce, *Rev. Phys. Appl.* **15**, 761 (1980).

IMD - Software for modeling the optical properties of multilayer films

David L. Windt

Bell Laboratories

Room 1D-456, 600 Mountain Ave.

Murray Hill, NJ 07974

windt@bell-labs.com

www.bell-labs.com/user/windt

To be published in

Computers In Physics

Jul/Aug 1998

IMD - Software for modeling the optical properties of multilayer films

David L. Windt

Bell Laboratories

Room 1D-456, 600 Mountain Ave.

Murray Hill, NJ 07974

windt@bell-labs.com

www.bell-labs.com/user/windt

Abstract

A computer program called IMD is described. IMD is used for modeling the optical properties (reflectance, transmittance, electric field intensities, etc.) of multilayer films, i.e., films consisting of any number of layers of any thickness. IMD includes a full graphical user interface, and affords modeling with up to eight simultaneous independent variables, as well as parameter estimation (including confidence interval generation) using non-linear, least-squares curve fitting to user-supplied experimental optical data. The computation methods and user interface are described, and a number of examples are presented which illustrate some of IMD's unique modeling, fitting and visualization capabilities.

Keywords: multilayer films, optical modeling, parameter estimation.

1. Introduction

IMD is a computer program for modeling the optical properties — reflectance, transmittance, absorptance, phase shifts and electric field intensities — of multilayer films, i.e., films consisting of any number of layers of any thickness. Estimating the optical properties of multilayer films is integral to instrument design and modeling in many fields of science and technology, such as astronomy, lithography, plasma diagnostics, synchrotron instrumentation, etc. Also, fitting the calculated reflectance of a multilayer stack to experimental data is the basis of X-Ray Reflectance (XRR) analysis of thin films, where one uses the measured reflectance to determine film thicknesses, densities, and roughnesses, and to optical constant determination from reflectance vs. incidence angle data, a technique utilized in many spectral regions.¹ IMD was designed, therefore, as a completely general modeling and parameter estimation tool, intended to be used for these and other applications, in order to meet the needs of a broad range of researchers. Furthermore, IMD's flexibility enables many new and unique types of computations. IMD is available for free via the Internet.²

In IMD, a layer can be composed of any material for which the optical constants are known or can be estimated. Any number of such layers can be designated and optionally grouped together to define periodic multilayers; 'groups of groups' of layers can be defined, in fact, with no limit on nesting depth. The IMD distribution includes an optical constant database for over 150 materials, spanning the X-ray to the far infrared region of the spectrum. User-defined optical constants can be used as well, and in the 30 eV to 30 keV region in particular, optical constants can be generated by the user for arbitrary compounds using the CXRO atomic scattering factors.³ Imperfections at an interface, i.e., roughness and/or diffuseness, can be easily included; the effect of such imperfections, namely, to reduce the specular reflectance at the interface, becomes especially important at shorter wavelengths (i.e., below ~30 nm), where the length scale of these imperfections is comparable to the wavelength of light.

The optical functions (reflectance, transmittance, etc.) can be computed not just versus wavelength and/or incidence angle, but also as a function of any of the parameters that describe the multilayer stack (e.g., layer thicknesses, roughnesses, etc.) or the incident beam (polarization,

angular/spectral resolution.) An interactive visualization tool, IMDXPLOT, is used to display the results of such multiple-variable computations; with this visualization tool one can vary a given parameter and see the resulting effect on the optical functions (in one or two dimensions) in real time. This last feature is especially helpful in discerning the relative sensitivities of the optical functions to the parameters that describe the multilayer structure.

Parameter estimation is afforded by fitting an optical function to user-supplied experimental data: non-linear, least-squares curve fitting based on the χ^2 test of fit is utilized. The precision of the best-fit parameters can be estimated as well, by computing multi-dimensional confidence intervals. The ability to simultaneously vary multiple parameters ‘manually’, as mentioned above, prior to performing least-squares fitting, is particularly useful in selecting initial parameter values; indeed choosing initial fit parameter values that are reasonably close to the best-fit values is generally the most difficult aspect of multi-parameter non-linear fitting.

IMD is written in the IDL language,⁴ and makes extensive use of IDL’s built-in ‘widgets’ to provide a full graphical user interface (GUI.) As such, IMD can be run on most (currently) popular platforms, including MacOS, MS Windows, and most flavors of Unix.

In the following sections, I will describe first the physics and algorithms used for modeling and parameter estimation, followed by a description of the IMD user interface. Finally, I present several illustrative examples, demonstrating IMD’s unique modeling and fitting capabilities.

2. Computation Methods

2.1 Optical Functions

Computations of the optical functions of a multilayer film in IMD are based on application of the Fresnel equations, modified to account for interface imperfections, which describe the reflection and transmission of an electromagnetic plane wave incident at an interface between two optically dissimilar materials.

2.1.1 Reflection and Transmission at an Ideal Interface

We consider first the behavior of a plane electromagnetic wave at an idealized interface, i.e., the abrupt interface between two semi-infinite media, as shown in Figure 1. The complex index of refraction $\mathbf{n} = n + ik$ (where n is the refractive index and k is the extinction coefficient) is given in the two regions as \mathbf{n}_i and \mathbf{n}_j . The incident wave vector, with electric field amplitude \mathbf{E}_i , makes an angle θ_i with respect to the interface normal (the z axis). The amplitude of the reflected and transmitted electric fields, \mathbf{E}'_i and \mathbf{E}_j , respectively, are given by the well-known Fresnel equations:⁵

$$\frac{|\mathbf{E}'_i|}{|\mathbf{E}_i|} = \frac{\mathbf{n}_i \cos \theta_i - \mathbf{n}_j \cos \theta_j}{\mathbf{n}_i \cos \theta_i + \mathbf{n}_j \cos \theta_j} \equiv r_{ij}^s \quad (1a)$$

and

$$\frac{|\mathbf{E}_j|}{|\mathbf{E}_i|} = \frac{2\mathbf{n}_i \cos \theta_i}{\mathbf{n}_i \cos \theta_i + \mathbf{n}_j \cos \theta_j} \equiv t_{ij}^s \quad (1b)$$

for s -polarization (i.e., \mathbf{E} perpendicular to the plane of incidence); and

$$\frac{|\mathbf{E}'_i|}{|\mathbf{E}_i|} = \frac{\mathbf{n}_i \cos \theta_j - \mathbf{n}_j \cos \theta_i}{\mathbf{n}_i \cos \theta_j + \mathbf{n}_j \cos \theta_i} \equiv r_{ij}^p \quad (1c)$$

and

$$\frac{|\mathbf{E}_j|}{|\mathbf{E}_i|} = \frac{2\mathbf{n}_i \cos \theta_i}{\mathbf{n}_i \cos \theta_j + \mathbf{n}_j \cos \theta_i} \equiv t_{ij}^p \quad (1d)$$

for p -polarization (i.e., \mathbf{E} parallel to the plane of incidence), where θ_j is the angle of refraction, determined from Snell's law: $\mathbf{n}_i \sin \theta_i = \mathbf{n}_j \sin \theta_j$. In equation (1) we have introduced the Fresnel reflection and transmission coefficients, r_{ij} and t_{ij} , respectively.⁶

2.1.2 Interface Imperfections

In order to account for the loss in specular reflectance due to interface imperfections (i.e., interfacial roughness and/or diffuseness), we now consider the case where the change in index across the interface is not abrupt, but can be described instead by an interface profile function $p(z)$. (See Figure 2.) That is, following the formalism developed by Stearns,⁷ we define $p(z)$ as the normalized, average value along the z direction of the dielectric function, $\epsilon(\mathbf{x})$ (with $\mathbf{n} = \sqrt{\epsilon}$):

$$p(z) = \frac{\iint \epsilon(\mathbf{x}) dx dy}{(\epsilon_i - \epsilon_j) \iint dx dy}, \quad (2)$$

where

$$\epsilon(\mathbf{x}) = \begin{cases} \epsilon_i, & z \rightarrow +\infty \\ \epsilon_j, & z \rightarrow -\infty \end{cases} \quad (3)$$

Stearns has shown that in the case of non-abrupt interfaces, the resultant loss in specular reflectance can be approximated by multiplying the Fresnel reflection coefficients (equations 1a and 1c) by the function $\tilde{w}(s)$, the Fourier transform of $w(z) = dp/dz$. That is, the modified Fresnel reflection coefficients are given by

$$r'_{ij} = r_{ij} \tilde{w}(s_i) \quad (4)$$

where $s_i = 4\pi \cos\theta_i / \lambda$, and λ is the wavelength of light. Note that the loss in specular reflectance depends only on the *average* variation (over x and y) in index across the interface. Consequently, the reflectance can be reduced equally well by either a rough interface, in which the transition between the two materials is abrupt at any point (x,y) , or a diffuse interface, in which the index varies smoothly along the z direction (or by an interface that can be described as some combination of the two cases.)

Stearns presents four particularly useful interface profiles, all of which are available for use in IMD; these interface profile functions and the associated $\tilde{w}(s)$ functions are listed Table 1. Also available in IMD are modified $\tilde{w}(s)$ functions, where s_i has been replaced with $s_{ij} = 4\pi\sqrt{\cos\theta_i \cos\theta_j} / \lambda$, in accord with the formalism developed by Névot and Croce⁸ to properly account for the effect of roughness on the specular reflectance below the critical angle of total external reflection in the X-ray region.

The width of each interface profile function presented in Table 1 is characterized by the parameter σ (see Figure 2), which is a measure of either an rms interfacial roughness, in the case of a purely rough interface, an interface width, in the case of a purely a diffuse interface, or some combination of the two properties in the case of an interface that is both rough and diffuse; it is the parameter σ (along with the choice of interface profile function) that is specified in IMD to account for the effects of interface imperfections using the modified Fresnel coefficient approach just described.

2.1.3 Optical Functions of a Multilayer Stack

We now consider a plane wave incident on a multilayer stack, that is, a series of N layers (and $N+1$ interfaces), where the i^{th} layer has thickness d_i , interfacial roughness/diffuseness σ_i , and optical constants \mathbf{n}_i , as shown in Figure 3. The region above the multilayer stack — the ambient — has optical constants \mathbf{n}_a , and the region below the film — the substrate — has optical constants \mathbf{n}_s . (Note that the case of a free-standing film refers to the condition $\mathbf{n}_s = \mathbf{n}_a$.) Under these circumstances, the net reflection (r_i) and transmission (t_i) coefficients of the i^{th} layer are given by:⁹

$$r_i = \frac{r_{ij} + r_j e^{2i\beta_i}}{1 + r_{ij} r_j e^{2i\beta_i}} \quad (5a)$$

and

$$t_i = \frac{t_{ij} t_j e^{2i\beta_i}}{1 + r_{ij} r_j e^{2i\beta_i}} \quad (5b)$$

where $\beta_i = 2\pi d_i \mathbf{n}_i \cos \theta_i / \lambda$; the reflection coefficients r_{ij} are computed from equation (4), the transmission coefficients t_{ij} from equations (1b) and (1d), and r_j and t_j are the net reflection and transmission coefficients of the j^{th} interface. Thus, the procedure to compute the net reflection (r) and transmission (t) coefficients for the multilayer stack is to apply equation (5) recursively, starting at the bottom-most layer, i.e., $i = N, j = s$. (The coefficients r and t for s - and p -polarization are computed separately, using the appropriate Fresnel coefficients.) The reflectance, R and transmittance, T , which measure the energy reflected from or transmitted through the film, respectively, are then given by

$$R = |r|^2 \quad (6a)$$

and

$$T = \text{Re} \left\{ \frac{\mathbf{n}_s \cos \theta_s}{\mathbf{n}_a \cos \theta_a} \right\} |t|^2 \quad (6b)$$

(again, computing separately the values for s - and p -polarization, i.e., R^s, R^p, T^s , and T^p .) The absorptance, A , which measures the amount of energy absorbed by the film, is approximated by

$$A = 1 - R - T \quad (6c)$$

(Note that equation (6c) is inaccurate when light is removed from the specular direction, i.e., and scattered into non-specular directions, due to interfacial or surface roughness.) Finally, the phases of the reflected and transmitted waves are given by:

$$\phi_r = \tan^{-1}(\text{Im}\{r\} / \text{Re}\{r\}) \quad (7a)$$

and

$$\phi_t = \tan^{-1}(\text{Im}\{t\} / \text{Re}\{t\}) \quad (7b)$$

2.1.4 Electric Field Intensity in a Multilayer Stack

In order to compute, in addition to the optical functions, the electric field intensity as a function of depth in a multilayer stack, a slightly different formalism from that described in the previous section must be used. (The previous, more efficient, formalism is used in IMD when electric field intensities are not required.) Consider the interface between the i^{th} and the j^{th} layers in a multilayer stack, where we now have both positive-going and negative-going electromagnetic plane waves in both layers. Solving Maxwell's equations in this case, it can be shown that the positive-going and negative-going field amplitudes at a distance z_i above the interface are given by

$$E_i^+(z_i) = \frac{1}{t_{ij}} e^{-i\beta_i(z_i)} E_j^+(0) + \frac{r_{ij}}{t_{ij}} e^{-i\beta_i(z_i)} E_j^-(0) \quad (8a)$$

and

$$E_i^-(z_i) = \frac{r_{ij}}{t_{ij}} e^{i\beta_i(z_i)} E_j^+(0) + \frac{1}{t_{ij}} e^{i\beta_i(z_i)} E_j^-(0) \quad (8b)$$

respectively, where $\beta_i(z_i) = 2\pi z_i \mathbf{n}_i \cos \theta_i / \lambda$, and $E_j^+(0)$ and $E_j^-(0)$ are the field amplitudes at the top of the j^{th} layer. Again, a recursive approach can be used to compute the field amplitudes throughout the stack, starting at the bottom-most layer ($i = N, j = s$) with the field amplitudes in the substrate given as $E_s^+(0) = 1$ and $E_s^-(0) = 0$. The net reflection and transmission coefficients of the film can then be computed from the field amplitudes in the ambient:

$$r = \frac{E_a^-(0)}{E_a^+(0)} \quad (9a)$$

and

$$t = \frac{1}{E_a^+(0)} \quad (9b)$$

Once the transmission coefficient is computed from equation (9b), the field amplitudes versus depth are then re-scaled using

$$E^\pm(z) \rightarrow tE^\pm(z), \quad (10)$$

(i.e., taking the incident electric field to have unit amplitude) and the field intensities for s - and p -polarization computed from

$$I(z) = |E^+(z) + E^-(z)|^2 \quad (11)$$

2.1.5 Polarization

In the case of an incident beam that consists of a mixture of s - and p -polarization, it is often necessary to compute the ‘average’ values of the optical functions R , T , and A , and the electric field intensity I , i.e., the values of these quantities for ‘average’ polarization. We thus define the incident polarization factor f as

$$f = \frac{I^s - I^p}{I^s + I^p}, \quad (11)$$

where I^s and I^p are the incident intensities for s - and p -polarization (e.g., unpolarized radiation corresponds to $f = 0$.) Furthermore, we define the polarization analyzer sensitivity, q , as the sensitivity to s -polarization divided by the sensitivity to p -polarization; specifying a value of q other than 1.0 could be used to simulate, for example, the reflectance one would measure using a detector that (for whatever reason) was more or less sensitive to s -polarization than to p -polarization. It can be shown that the average reflectance is then given by

$$R^a = \frac{R^s q(1+f) + R^p(1-f)}{f(q-1) + (q+1)}, \quad (12)$$

with equivalent expressions for T^a , A^a and I^a .

2.1.6 Instrumental Resolution

In general, the experimental determination of an optical function such as R , T or A is made with instrumentation that is limited in angular and/or spectral resolution. As such, it is desirable to estimate resolution-limited values of the calculated optical functions. This is achieved in IMD by convolving the calculated optical functions with a Gaussian of width $\delta\theta$, in the case of finite angular resolution, or with a

Gaussian of width $\delta\lambda$ in the case of finite spectral resolution, using the convolution algorithm built into IDL.

2.1.7 Graded Interfaces

In addition to the option of using the modified Fresnel coefficients to account for interfacial roughness and diffuseness, as described in Section 2.1.2, in IMD it's also possible to model the effects of a diffuse interface on the optical functions and electric field intensities by specifying a 'graded' interface. That is, an abrupt interface can be replaced by one or more layers whose optical constants vary gradually between the values for the pure materials on either side of the interface.

In IMD, a graded interface is described by three parameters, as shown in Figure 4: the interface width, w_g , the number of layers comprising the graded interface, N_g , and the distribution factor, X_g , which determines where the graded interface region resides relative to the original abrupt interface (as will be described below.)

The optical constants in each of the N_g layers of a graded interface are computed as follows. Consider the graded interface between the i^{th} and j^{th} layers in a multilayer stack. The thickness of each of the N_g graded interface layers is equal to w_g / N_g . The optical constants in the ℓ^{th} graded interface layer are thus given by

$$n_\ell = \frac{(N_g + 1 - \ell)n_i + \ell n_j}{(N_g + 1)} \quad (13a)$$

and

$$k_\ell = \frac{(N_g + 1 - \ell)k_i + \ell k_j}{(N_g + 1)} \quad (13b)$$

with $\ell = 1, \dots, N_g$. The resulting layer thicknesses, d'_i and d'_j , of the pure materials in the i^{th} and j^{th} layers, respectively, after including the graded interface layers, are given by

$$d'_i = d_i - w_g(1 - X_g) \quad (14a)$$

and

$$d'_j = d_j - w_g X_g \quad (14b)$$

with $0 < X_g < 1$. (Note that the total thickness of the two layers — including all the graded interface layers — is constant, i.e., $d'_i + d'_j + w_g = d_i + d_j$.) As an example, a distribution factor of 50% ($X_g = 0.5$) would result in equal reductions of the i^{th} and j^{th} layer thicknesses.

2.2 Parameter Estimation

As will be described in section 3.2, it is possible in IMD to designate simultaneously up to eight independent variables when computing optical functions and electric field intensities. When attempting to model experimental optical data, however, it is often desirable to estimate parameter values automatically, using nonlinear, least-squares curve-fitting. To this end, parameter estimation based on the χ^2 test of fit can be used in IMD to determine any number of parameters that describe the multilayer stack (or the incident beam polarization and/or instrumental resolution), as will now be described.

2.2.1 Fitting Algorithm

Consider a one-dimensional optical function $Y(X)$ for a multilayer stack, where Y may be any one of R^a , T^a or A^a , and X is some independent variable (e.g., λ , θ , etc.) The values for $Y(X)$ depend on the values of all of the parameters that describe the multilayer stack (optical constants, layer thicknesses, etc.) and the incident beam (polarization, instrumental resolution, etc.). The problem we wish

to solve is the following: determine the values for some fixed number p of these adjustable parameters, such that the calculated optical function $Y(X)$ most closely fits a particular set of experimentally-determined optical data, $Y_m \pm \delta Y_m$, measured as a function of the independent variable X_m , where X_m takes on $i = 1, \dots, N_m$ discrete values.

To solve this problem, IMD makes use of the so-called Marquardt gradient-expansion algorithm,¹⁰ based on the χ^2 test,¹¹ in which we minimize the value of the statistic S , defined as

$$S \equiv \sum_{i=1}^{N_m} \frac{(Y[i] - Y_m[i])^2}{w[i]^2}, \quad (15)$$

where $w[i]$ are the weighting factors for each point. IMD uses the CURVEFIT procedure,¹¹ an adaptation of the Marquardt algorithm included in the IDL library. The user designates adjustable parameters, and initial values for each. (In IMD, a constraint on the range of acceptable parameter values can be specified as well.) Iterations are then performed until the change in S is less than a specified amount, or until a maximum number of iterations have been performed. The user can choose to use for $w[i]$ either (a) ‘instrumental weighting,’ using the experimental uncertainties, $w[i] = \delta Y_m[i]$, (b) ‘statistical weighting,’ with $w[i] = \sqrt{Y_m[i]}$, or (c) ‘uniform weighting,’ with $w[i] = 1$. Additionally, logarithmic fitting can be used, in which the numerator in equation (15) is replaced by $(\ln Y[i] - \ln Y_m[i])^2$.

2.2.2 Confidence Interval Computation

In addition to a point estimate determination of the ‘best-fit’ parameter values, using the fitting technique just described, for example, it is generally necessary to estimate also the *range* of acceptable parameter values that are consistent with the experimental data. To this end, in IMD it is possible to compute multi-dimensional confidence intervals associated with the best-fit values of the adjustable parameters, using the formalism described in references 12 and 13.

It can be shown that when using the χ^2 test of fit, the minimum value of the S statistic, S_{\min} , associated with the best-fit parameter values, is distributed as the χ^2 probability function with $N_m - p$ degrees of freedom:

$$S_{\min} = \chi_{N_m - p}^2(\alpha), \quad (16)$$

where α is the significance of fit. That is, if we find, for example, that $S_{\min} = \chi_{N_m - p}^2(0.68)$, then we can conclude that there is a 68% probability that the model (using the p best-fit parameter values) correctly describes the data.

The confidence region, with significance α' , is then defined as the p -dimensional region of parameter space for which the value of S is less than or equal to some value S_L , where

$$S_L = S_{\min} + \Delta S(\alpha'), \quad (17)$$

with $\Delta S(\alpha')$ equal to the value of the χ^2 probability function with p degrees of freedom and significance α' ; the confidence region so defined would enclose the true values of the p parameters in $1 - \alpha'$ of all experiments.

In IMD, a multi-dimensional confidence region can be determined for up to eight adjustable (i.e., fit) parameters simultaneously. In this case a grid-search algorithm is utilized, wherein the user specifies the extent and resolution of the grid along each parameter axis. At each point in the grid, the value of the statistic S is computed using one of two methods, depending on the dimensionality of the confidence region being determined. That is, suppose the best-fit parameters were determined by varying p adjustable parameters, as described above, and of these p parameters we are interested in the confidence region associated with some subset of parameters q , where $q \leq p$. In the case that $q = p$, the value of S at each point on the grid is determined directly from equation (15). On the other hand, in the case that $q < p$, the value of S at each point on the grid is determined in IMD using the minimization algorithm described in

the previous section, but with only $(p - q)$ adjustable parameters, i.e., q of the parameters are now fixed. In this case, we note that the correct value of $\Delta S(\alpha')$ to be used in equation (17) is equal to the value of the χ^2 probability function with q (not p) degrees of freedom and significance α' . As an example of a situation for which $q < p$, consider the case of making a determination of thin film optical constants from reflectance vs. incidence angle data, where three adjustable parameters have been used, say — the optical constants n and k , and the film thickness, d — but of these three parameters, we are interested only in the uncertainty on the derived values of n and k , and so we must compute the associated 2-dimensional confidence region in n - k space. A specific example of a confidence interval computation which illustrates the concepts described here will be presented in Section 4.4.

3. User Interface

I now describe the IMD graphical user interface (GUI). This interface, which is created from the widgets tool kit built into IDL, is used to specify all parameters and variables, and to visualize the results of all calculations.

Shown in Figure 5 is the main IMD widget as it might look after a periodic multilayer and associated independent and dependent variables have been specified. In addition to the menu bar at the top of the widget, there are three regions of this widget of particular interest to us now: the STRUCTURE region, and the INDEPENDENT and DEPENDENT VARIABLES regions.

3.1 Structure Specification

The first step in performing a calculation in IMD is defining the ‘structure’, i.e., the parameters that define the ambient material, the multilayer stack, and (optionally) a substrate. There are a number of parameters that can be assigned to each structure element, i.e., layer thicknesses, interface roughness/diffuseness parameters, etc. But common to all structure elements is the material designation, which determines which optical constants are used for the calculation, as described in the next section.

3.1.1 Material Designation

Each structure element - the ambient, the substrate, and each multilayer stack layer element - is composed of some material. There are two different methods available to the user to designate materials in IMD: in the first method, the designated material name refers to an optical constants file contained in the IMD optical constant database; in the second method, which is applicable only in the X-ray region for energies between 30 eV and 30 keV, the material is specified by its composition and density, and the optical constants are computed directly from the atomic scattering factors.

The IMD optical constants database is a directory of ASCII files, where each optical constants file contains three columns of optical data (λ , n and k) associated with a single material. To designate a material by reference to an optical constants file, the user need only specify a valid file name contained in the optical constants directory. For example, shown in Figure 6(a) is a typical IMD layer widget where the material has been designated as amorphous Al_2O_3 , i.e., corresponding to a file called 'a-Al2O3.nk'.

The IMD optical constants database contains data for over 150 materials, compiled from a variety of published sources, with wavelength coverage extending from the X-ray to the far infrared region of the spectrum. In order to use additional optical constants, a user need only create an ASCII file containing the optical constants for the desired material, in accord with a simple format specified in the IMD documentation. For many materials, the user can choose from among several data sets already available in the database. The contents of any of the files contained in the database can be displayed graphically using an interactive plot widget, available through a pull-down menu option from the main IMD widget.

The basis for the second method of material designation — by composition and density — is that in the X-ray region, the complex index of refraction for a compound of density ρ is related to the atomic scattering factors f_1 and f_2 by ³

$$\mathbf{n} \cong 1 - \frac{e^2 N_a}{2\pi m_e c^2} \lambda^2 \rho \frac{\sum_j x_j (f_{1,j} + i f_{2,j})}{\sum_j x_j A_j}, \quad (18)$$

where the sums range over each of the chemical elements that comprise the compound, the x_j are the relative concentrations of each element, and the A_j are the associated atomic densities; e , m_e , c , and N_a are the electron charge, the electron mass, the speed of light, and Avogadro's number, respectively. To utilize this method of material designation, the user must specify the atomic composition (i.e., the x_j) and the density of the material, as illustrated in Figure 6(b), for example, showing the layer widget for a layer composed of Cr_3C_2 having a density of 6.68 gm/cm^3 .

3.1.2 Layer and Group Parameters

To create an IMD structure, the user adds layers, periodic multilayers,¹⁴ and optionally a substrate as desired. Accomplishing these tasks is simply a matter of pushing the appropriate buttons on the main IMD widget (i.e., on the right side of the STRUCTURE area of the widget shown in Figure 5.) Layers and periodic multilayers can be subsequently grouped together to form higher level periodic multilayers (with no limit on nesting depth), and can be moved up or down in the stack, again by pushing the appropriate buttons. The structure components are listed on the main IMD widget (on the left side); by double-clicking on a structure element, the associated ambient, layer, multilayer, or substrate widget is created, allowing the user to specify adjustable parameters (e.g., materials, layer thicknesses, interface parameters, multilayer repeat periods, etc.), as well as the preferred units (i.e., Å, nm, μm, etc.), and the displayed precision of parameter values. Thus, rather complicated structures can be defined or changed quickly and with relative ease.

3.2 Variable Designation

For all calculations, at least one wavelength (or energy) and incidence angle must be specified; multiple wavelengths and/or angles can be specified as well, if desired. (In the case of electric field intensity calculations, a third independent variable — depth, i.e., the position in the structure, measured from the top of the first layer — must also be defined.) In addition to these variables, any of the parameters that describe the multilayer stack (i.e., layer thicknesses, interface σ values, graded interface parameters, multilayer parameters, etc.) or the incident beam (i.e., polarization parameters f and q , and

angular and spectral resolution) can be designated as independent variables; up to eight independent variables can be designated simultaneously, and the dimensionality of the resulting optical functions will be equal to the number of independent variables specified.

For every independent variable so designated, the user must define the extent and resolution of the grid of points over which the optical functions are to be computed. The resolution of the grid can be designated either by specifying the size of the increment between points, or by the total number of parameter values that comprise the independent variable; Logarithmically spaced grids can also be designated. The user can again specify the preferred precision and units, and in the case of wavelengths (or energies) the instrumental resolution and polarization parameters; the angular instrumental resolution is likewise specified using the incidence angle independent variable widget.

Once the structure and independent variables are defined, any or all of the optical functions R , T , and A , and the electric field intensity I , can be computed, by selecting these functions in the DEPENDENT VARIABLES area of the main IMD widget (see Figure 5.) By then choosing the appropriate menu option, the computation is performed and the results displayed using another GUI tool, IMDXPLOT. Specific examples illustrating the functionality of IMDXPLOT will be presented in Section 4.

3.3 Fit Parameter Designation

As described in section 2.2, parameter estimation using non-linear, least-squares fitting can be performed, utilizing user-supplied experimental data. The experimental data is read by accessing a menu option from the main IMD widget, and the Parameter Estimation and Confidence Interval widget, shown in Figure 7(a), allows the user to add and remove adjustable (fit) parameters, and to specify the parameters that control how the fitting is performed (i.e., number of iterations, weighting, etc.) Shown in Figure 7(b) is a typical Fit Parameter widget, wherein the user specifies the initial parameter value (and optionally constraints on the fit parameter), as well as the parameters associated with confidence interval computations, as described above in Section 2.2.2.

4. Examples

4.1 Multi-Dimensional Optical Functions of a Thin Film

The first example demonstrates how IMD can be used to visualize multi-dimensional optical functions: I present the results of a computation of the reflectance and transmittance of an amorphous carbon film¹⁵ on an amorphous SiO₂ substrate, determined as a function of three independent variables: wavelength, for $150 \text{ nm} < \lambda < 2.0 \text{ }\mu\text{m}$, i.e., from the UV to the infrared; incidence angle, for $0^\circ < \theta < 90^\circ$; and film thickness, for $0 \text{ \AA} < d < 1000 \text{ \AA}$.

To visualize the results of this computation, one might imagine displaying one-dimensional graphs of R and T , for example, as a continuous function of one variable, θ , say, and for discrete values of λ and d . Or, perhaps it would be more useful to display a plot in two dimensions, as a continuous function of two variables, and for discrete values of the remaining independent variable. The IMDXPLOT widget, which is the interactive visualization tool in IMD, indeed allows the user to display such ‘slices’ of the optical functions, in either one or two dimensions. For example, presented in Figure 8 are some of the results of the computation just described. Figure 8(a) shows superposed 2-dimensional surface plots of $R(\theta, \lambda)$ and $T(\theta, \lambda)$, for two discrete values of the film thickness, 100 \AA and 350 \AA . In Figure 8(b), on the other hand, are 1-dimensional plots of $R(d)$ and $T(d)$, as well as the transmitted phase, $\phi_T(d)$, at normal incidence, for two discrete wavelengths, 193 nm and 248 nm (i.e., the wavelengths used for DUV lithography.) Using the buttons, sliders, and menu options available on the IMDXPLOT interface, the user can easily display such slices through parameter space, and customize the graphs according to their preference: multiple optical functions can be superposed, the appearance (i.e., colors, line-styles, plotting symbols, etc.) of the different functions can be adjusted, and various legends and plot-labels can be generated. Additionally, the sliders associated with each of the independent variables (shown in the INDEPENDENT VARIABLES region of the IMDXPLOT widgets in Figure 8, for example) can be used to vary in real time one or more independent variables and view the resulting effect on the optical

functions. A variety of standard graphics file formats (i.e., PostScript, PCL, HPGL, and CGM) are available for output.

4.2 Reflectance and Electric Field Intensity for an X-Ray Multilayer Film

The second example shows how IMD can be used to adjust, for optimal performance, design parameter values of a periodic multilayer. A determination of the electric field intensity in a periodic multilayer film is presented as well. Shown in Figure 9(a) is an IMD-generated plot, showing the normal incidence soft X-ray reflectance of a Y/Al periodic multilayer film ($d=90 \text{ \AA}$, $N=40$), as a function of one particular design parameter, the film thickness ratio, Γ (where $\Gamma \equiv d_Y / (d_Y + d_{Al})$). By using IMD to compute $R(\Gamma)$, the optimal value of Γ (i.e., giving the highest peak reflectance) is immediately evident. Optimized values of other design parameters can be similarly obtained.

Displayed in Figure 9(b) is an IMDXPLOT widget showing the electric field intensity as a function of depth for the $\Gamma = 0.5$ Y/Al multilayer, for two values of λ . An observation of the position of the local maxima of the electric field intensity in the standing-wave pattern at $\lambda=192 \text{ \AA}$ (i.e., the wavelength corresponding to the peak reflectance) suggests, for example, that any interface imperfections at the Al-on-Y interfaces, where the electric field intensity is strongest, might have a much different effect on the peak reflectance than interface imperfections at the Y-on-Al interfaces, where the electric field intensity is much weaker.

4.3 XRR Analysis of a W/Cr Bilayer

The third example demonstrates how the unique ability in IMD to interactively vary model parameters ‘manually’ can be used, in conjunction with the non-linear, least-squares fitting capability, to accurately determine a large number of film parameters from experimental data.

Shown in Figure 10 are the measured and calculated grazing incidence X-ray reflectance-vs.-incidence-angle curves for a W/Cr bilayer thin film. These particular films are currently being used as the electron scattering layers in masks for a projection electron-beam lithography tool currently being developed¹⁶ (SCALPEL®) in which the image contrast achieved at the focal plane of the tool depends

critically on the W and Cr layer thicknesses and densities. A precise measurement of these parameters is thus required, and such a measurement can be obtained through the use of XRR analysis, using the curve-fitting techniques described in Section 2.2. However, even for these relatively simple bilayer films, there are a number of additional parameters in the model that must be varied in order to fit the data with sufficient accuracy. For example, the best-fit curve shown in Figure 10 (labeled ' $\sigma=3.5 \text{ \AA}$ ') was obtained by fitting eight adjustable parameters: the densities, layer thicknesses, and interface roughnesses of both the W and Cr layers, as well as the thickness and roughness of a top layer oxide (WO_3) that forms on these films.

In order to utilize non-linear, least-squares curve-fitting to determine fit parameters, the choice of initial parameter values must be relatively close to the final, 'best-fit' values, or else the fitting algorithm will be unable to locate the global minimum in parameter space corresponding to the minimum value of the χ^2 statistic. This point is especially true in this particular example, where the fitting was performed with so many adjustable parameters. The ability in IMD to first vary parameters 'manually' (as described in Section 3.2) and to visualize in real-time the resulting effect on the optical functions (reflectance, in this case), greatly facilitates the task of determining initial fit parameter values.

To illustrate, in order to fit the data shown in Figure 10, one might start (using bulk densities) by manually varying the W and Cr layer thicknesses, until both the high-frequency and low-frequency modulations in the calculated reflectance are reasonably coincident with those in the measured data. These two superposed modulations (seen in Figure 10 as having periods of $\sim 0.18^\circ$ and $\sim 1.0^\circ$), correspond to interference due to the total film thickness (i.e., $\text{WO}_3 + \text{W} + \text{Cr}$ layer thicknesses) and the Cr layer thickness, respectively. Therefore, it's especially useful to be able to manually vary two (or more) layer thicknesses in a single calculation, and to view the results interactively using IMDXPLOT, in order to match both modulations simultaneously. Nonetheless, the W and Cr layer thicknesses will generally need significant refinement once other parameters are varied as well, as the effect on the reflectance of other adjustable parameters are effectively coupled to the layer thicknesses. An example of such a coupling can be seen in Figure 10, where reflectance curves are shown for several values of the W layer roughness: it

can be seen that the thickness modulations shift significantly with roughness (σ), an effect that cannot be completely de-coupled from the effect of the individual layer thicknesses.

4.4 Optical Constants Determination for a Thin Film

The final example illustrates the ability in IMD to compute confidence intervals, in order to estimate the precision of fit parameters determined from non-linear, least-squares curve-fitting. Shown in Figure 11(a) are the results of non-linear, least-squares curve-fitting to determine, from reflectance vs. incidence angle measurements, the optical constants (n and k) for a thin film. Once the best-fit parameters were found (as indicated in Figure 11(a)), the value of the χ^2 statistic S was computed over a grid of points in parameter space, as described above in Section 2.2.2. The result of this computation are displayed in the IMDXPLOT widget shown in Figure 11(b), where the contours-of-constant- S are shown in two-dimensions, corresponding to the 68% (i.e., '1- σ ') and 95% ('2- σ ') joint confidence regions. The IMDXPLOT sliders in this case can be used to vary the value of $\Delta S(\alpha')$ (see equation 17), or to vary the parameter values when displaying contours-of-constant- S in one dimension (not shown.)

5. Summary

I have described the physics and algorithms on which the IMD computer program is based, and have presented a number of examples that illustrate some of IMD's unique capabilities. Future enhancements to IMD's capabilities will include the ability to compute the non-specular (diffuse) scattered intensity due to interfacial roughness, the ability to define depth-graded thicknesses and interface parameters, and tools to allow the user to further analyze interactively the computed optical functions (e.g., minimum and maximum values, feature widths, averages, integrals, etc.) The software is available for free, and can be downloaded from the website listed in reference (2).

References

-
- ¹ See, for example, *Handbook of Optical Constants of Solids*, edited by E. D. Palik, Academic Press, Inc., 1985.
- ² IMD can be downloaded from <http://www.bell-labs.com/user/windt/idl>.
- ³ B. L. Henke, E. M. Gullikson, and J. C. Davis, 'X-ray Interactions: photoabsorption, scattering, transmission, and reflection at E=50-30,000 eV, Z=1-92', *Atomic Data and Nuclear Data Tables*, Vol. **54**, No. 2, July 1993. In addition to the data contained therein, the Center For X-Ray Optics (CXRO), Lawrence Berkeley Laboratory, maintains an active database of atomic scattering factors; these data are available at <http://www-cxro.lbl.gov>, and have been included in IMD, courtesy of E. M. Gullikson.
- ⁴ IDL is available from Research System, Inc., Boulder, Colorado, <http://www.rsinc.com>.
- ⁵ See, for example, J. D. Jackson, *Classical Electrodynamics*, 2nd edition, John Wiley and Sons, New York, pp. 281-282, 1975.
- ⁶ Note that in our definition of the Fresnel coefficients we have assumed that (a) each material is optically isotropic, and (b) the magnetic permeability is the same in both regions.
- ⁷ D. G. Stearns, 'The scattering of X-rays from non-ideal multilayer structures', *J. Appl. Phys.* **65**, 491-506 (1989).
- ⁸ L. Nénot and P. Croce, 'Caractérisation des surfaces par réflexion rasante de rayons X. Application à l'étude du polissage de quelques verres silicates.', *Revue. Phys. Appl.* **15**, 761-779 (1980).
- ⁹ M. Born and E. Wolf, *Principles of Optics*, sixth edition, Pergamon Press, Oxford, 1980.
- ¹⁰ D. W. Marquardt, 'An algorithm for least-squares estimation of nonlinear parameters', *J. Soc. Ind. Appl. Math.*, **11**, 2, pp. 431-441, June (1963).
- ¹¹ P. R. Bevington, *Data Reduction and Error Analysis for the Physical Sciences*, McGraw-Hill, New York, 1969.
- ¹² M. Lampton, B. Margon, and S. Bowyer, 'Parameter estimation in X-ray astronomy', *Ap. J.*, **208**, 177 (1976).

¹³ W. Cash, 'Generation of confidence intervals for model parameters in X-ray astronomy', *Astron. & Astrophys.*, **52**, 307 (1976).

¹⁴ A periodic multilayer is defined here as a group of m layers that is repeated N times to make a stack consisting of a total of $m \times N$ layers.

¹⁵ Due to the particular optical properties of amorphous carbon films, namely the 180° phase change for transmittance values near 10% at certain deep UV wavelengths that are used in photolithography for the manufacture of integrated circuits, phase-shift masks (used to compensate for the effects of diffraction in order to print features smaller than the exposure wavelength) made from such films are currently being developed. Such films are also being developed for use as variable transmission apertures, which can be used to greatly enhance the process latitude of DUV lithography tools. See, for example, R. A. Cirelli, M. Mkrтчyn, G. P. Watson, L. E. Trimble, G. R. Weber, D. L. Windt, and O. Nalamasu, 'A new variable transmission illumination technique optimized with design rule criteria', *Proc. SPIE*, **3334** (1998).

¹⁶ See <<http://www.lucnet.com/SCALPEL>> for a complete bibliography of papers describing SCALPEL technology.

Tables

	$p(z)$	$\tilde{w}(s)$
Error Function	$\frac{1}{\sqrt{\pi}} \int_{-\infty}^z e^{-t^2/2\sigma^2} dt$	$e^{-s^2\sigma^2/2}$
Exponential	$\begin{cases} \frac{1}{2}e^{\sqrt{2}z/\sigma}, & z \leq 0 \\ 1 - \frac{1}{2}e^{\sqrt{2}z/\sigma}, & z > 0 \end{cases}$	$\frac{1}{1 + s^2\sigma^2/2}$
Linear	$\begin{cases} 0, & z < -\sqrt{3}\sigma \\ \frac{1}{2} + \frac{z}{2\sqrt{3}\sigma}, & z \leq \sqrt{3}\sigma \\ 1, & z > \sqrt{3}\sigma \end{cases}$	$\frac{\sin(\sqrt{3}\sigma s)}{\sqrt{3}\sigma s}$
Sinusoidal	$\begin{cases} 0, & z < -a\sigma \\ \frac{1}{2} + \frac{1}{2}\sin\left(\frac{\pi z}{2a\sigma}\right), & z \leq a\sigma \\ 1, & z > a\sigma \end{cases}$ $a = \pi / \sqrt{\pi^2 - 8}$	$\frac{\pi}{4} \left(\frac{\sin(a\sigma s - \pi/2)}{a\sigma s - \pi/2} + \frac{\sin(a\sigma s + \pi/2)}{a\sigma s + \pi/2} \right)$

Table 1. Interface profile functions, $p(z)$, and the associated Fresnel reflection coefficient modification factors $\tilde{w}(s)$ (from reference 7) available for use in IMD.

Figure Captions

Figure 1. Diagram of a plane wave incident at the interface between two optically dissimilar materials.

Figure 2. Sketch of the interface profile function $p(z)$, which describes a rough or diffuse interface.

Figure 3. Diagram of a multilayer stack containing N layers, where the optical constants, thickness, propagation angle, and interface roughness/diffuseness parameter of the i^{th} layer are \mathbf{n}_i , d_i , θ_i and σ_i , respectively. The ambient (i.e., the region above the film) has optical constants \mathbf{n}_a , and the substrate has optical constants \mathbf{n}_s .

Figure 4. Diagram of a graded interface of width w_g , consisting of $N_g = 3$ layers. In this case, the distribution parameter X_g is slightly less than 0.5, approximately.

Figure 5. The main IMD widget, as configured to compute the normal incidence reflectance of a Y/Al multilayer as a function of wavelength and layer thickness parameter Γ . (The results of this particular computation are presented in Section 4.2)

Figure 6. A typical IMD layer widget, with material designation (a) by reference to an optical constants file, and (b) by specification of material composition and density.

Figure 7. (a) The IMD Parameter Estimation and Confidence Interval widget (configured for the curve-fitting example in Section 4.3,) and (b) a typical Fit Parameter widget (configured for the confidence interval computation example in Section 4.4.)

Figure 8. Results of the computation of reflectance and transmittance of an amorphous carbon film on an amorphous SiO_2 substrate, as described in the text. (a) The IMDXPLOT widget showing two-dimensional surface plots of reflectance and transmittance versus incidence angle and wavelength, for discrete values of the carbon film thickness. (b) One-dimensional plots of reflectance, transmittance, and transmitted phase versus film thickness, at normal incidence, and for two discrete wavelengths.

Figure 9. (a) Reflectance of a Y/Al periodic multilayer film as a function of the film thickness ratio, Γ . (b) Electric field intensity as a function of depth into the film, for two wavelengths.

Figure 10. Measured grazing incidence X-ray reflectance for a W/Cr bilayer film (filled circles) and calculated reflectance curves for different values of the W layer interfacial roughness (as indicated.)

Figure 11. (a) Results of non-linear, least-squares curve-fitting to determine, from reflectance vs. incidence angle measurements, the optical constants (n and k) for a gold film. (b) An IMDXPLOT widget showing joint confidence intervals associated with the best-fit values of the optical constants.

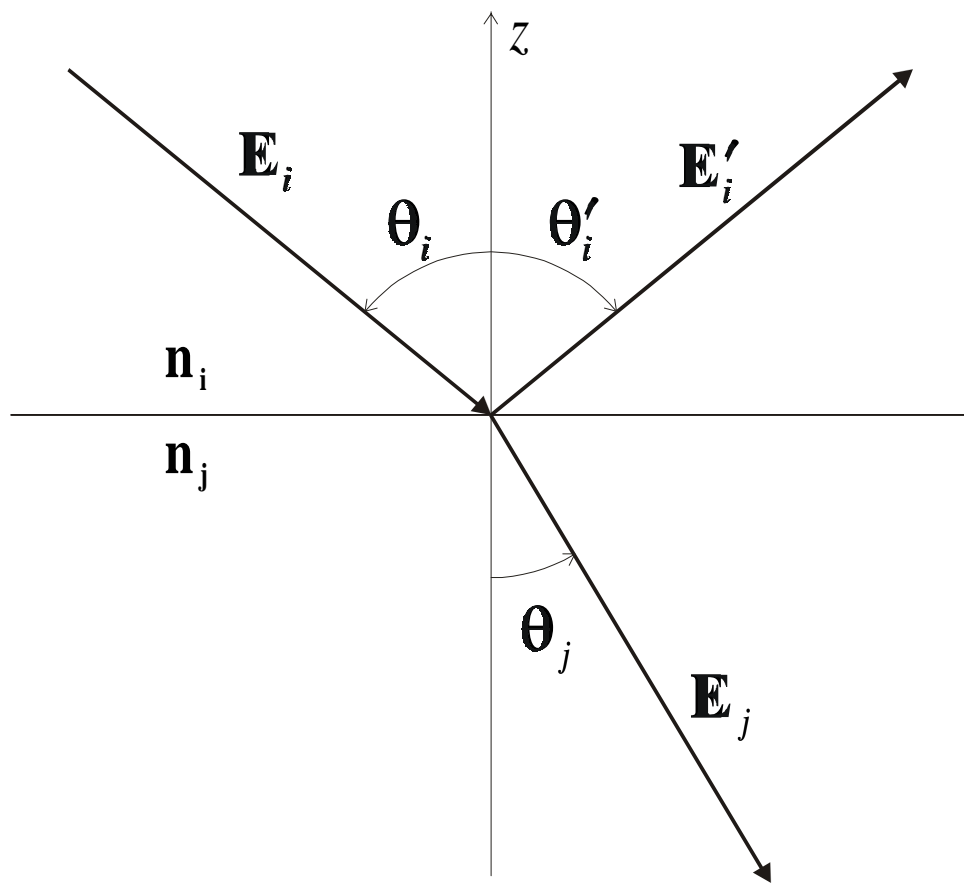


Figure 1.

D. L. Windt

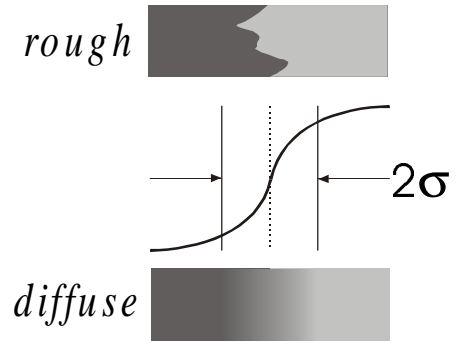


Figure 2.

D. L. Windt

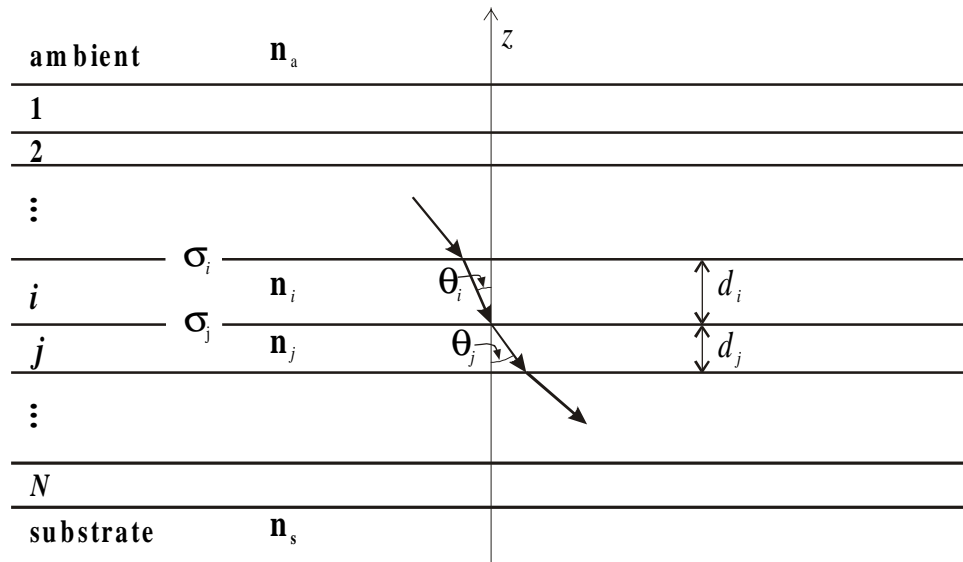


Figure 3.

D. L. Windt

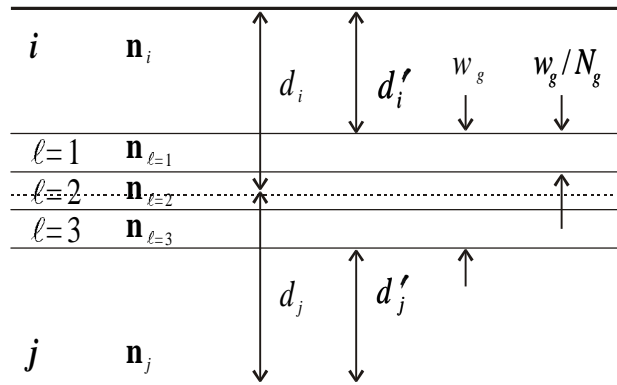


Figure 4.

D. L. Windt

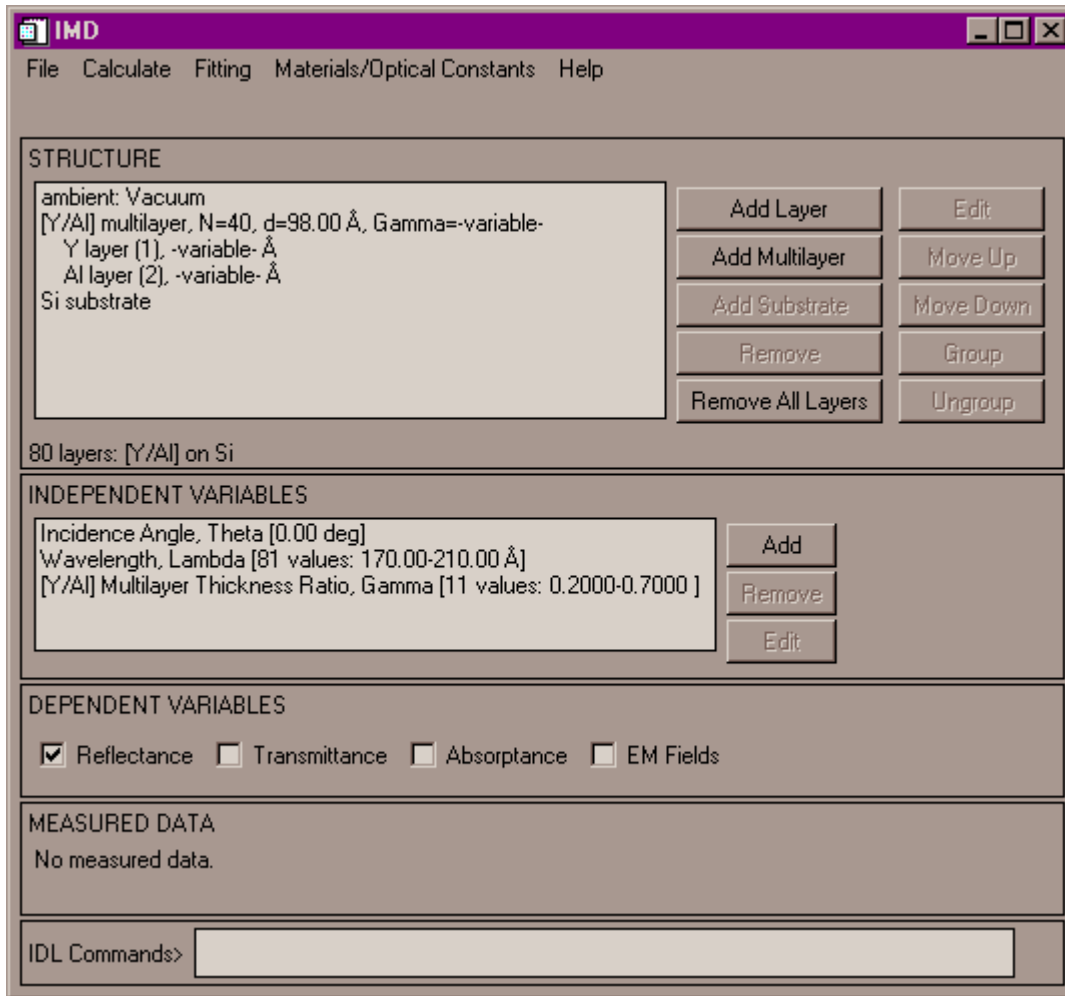


Figure 5.

D. L. Windt

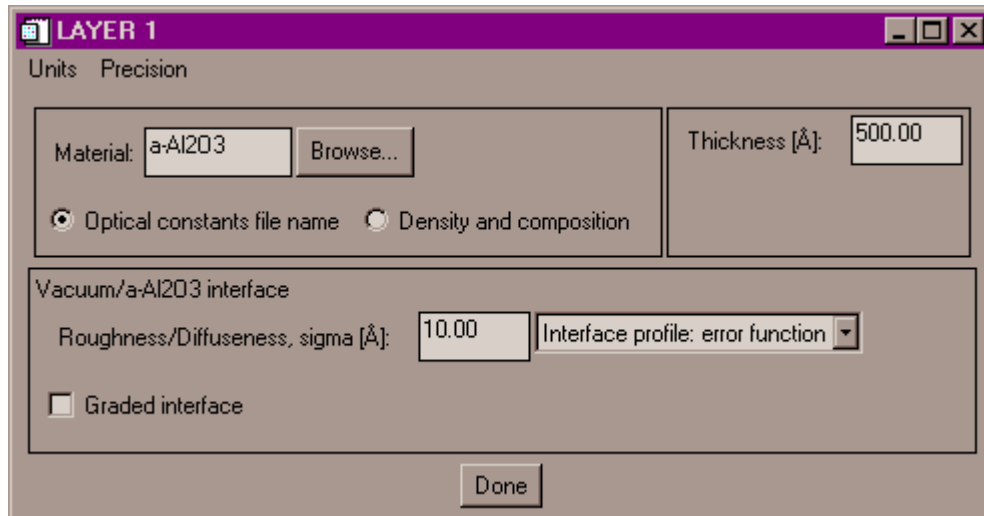


Figure 6(a).

D. L. Windt

LAYER 2 [min] [max] [close]

Units Precision

Material: Density [g/cm3]:

Thickness [Å]:

Composition:

atoms of (At. Wt.=51.9960)

atoms of (At. Wt.=12.0110)

Optical constants file name Density and composition

a-Al2O3/Cr3C2 interface

Roughness/Diffuseness, sigma [Å]: Interface profile: error function ▾

Graded interface Width [Å]: Layers: Distribution [%]:

Figure 6(b).

D. L. Windt

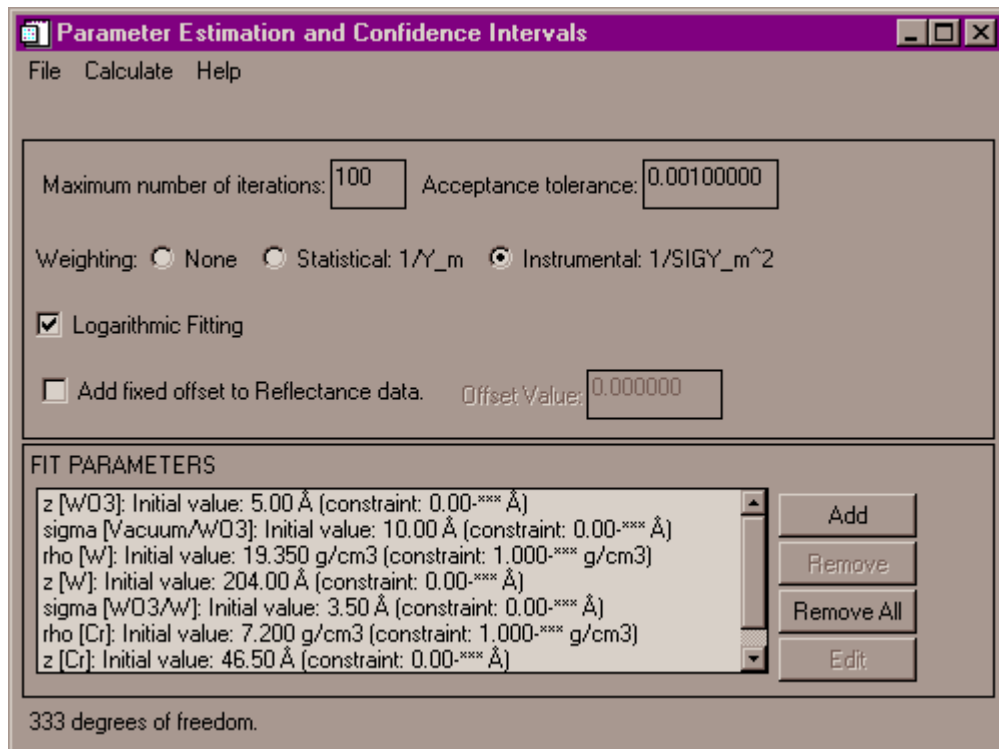


Figure 7(a).

D. L. Windt

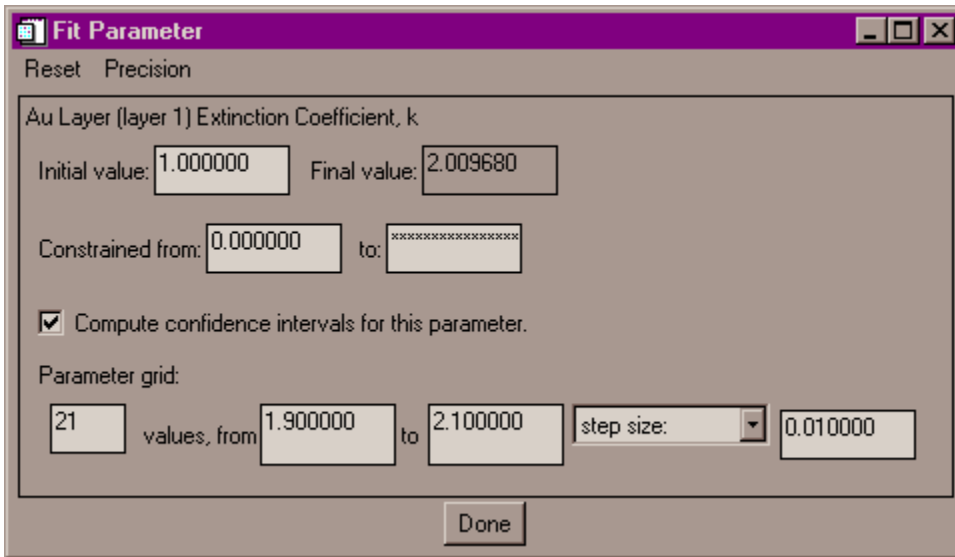


Figure 7(b).

D. L. Windt

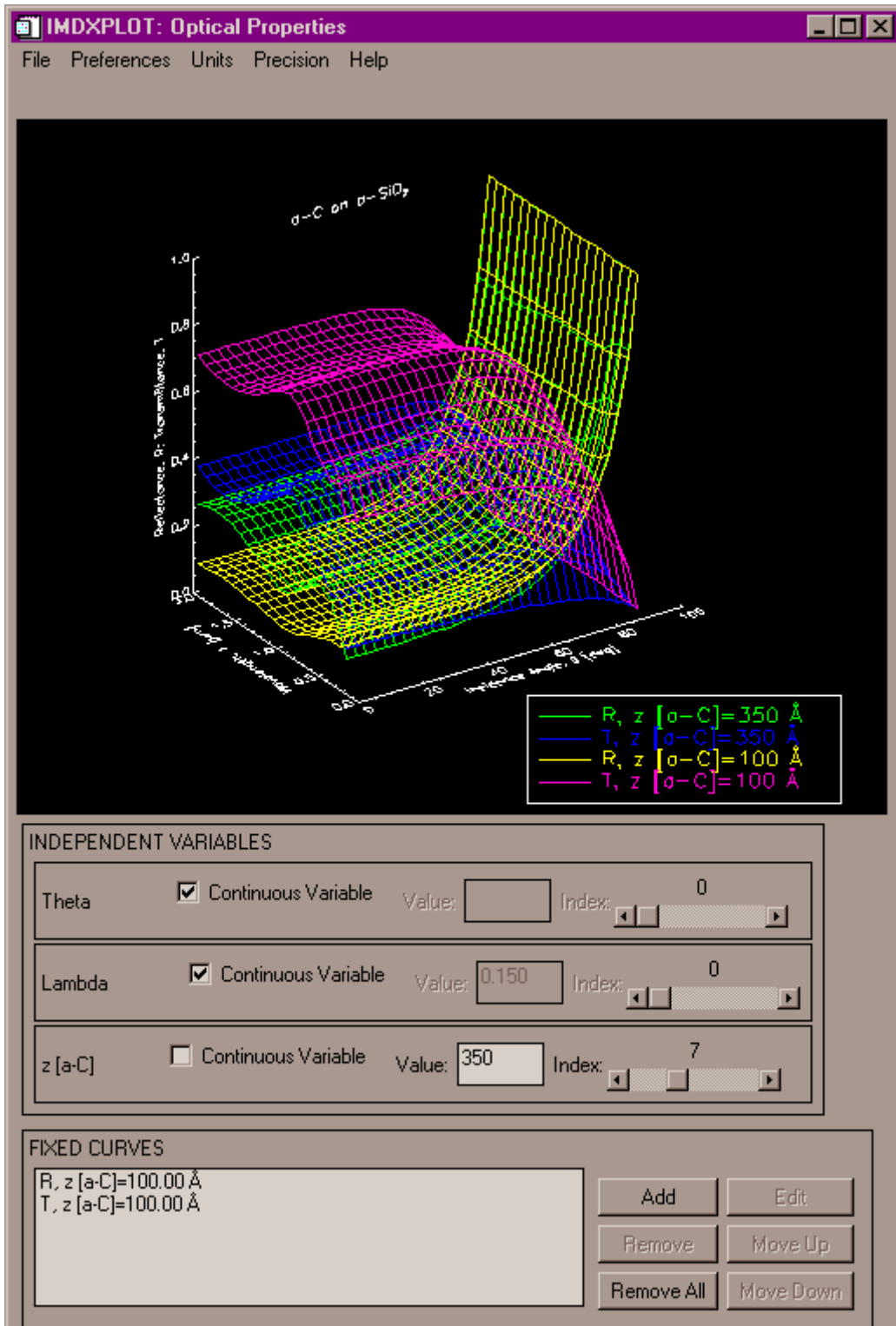


Figure 8(a).

D. L. Windt

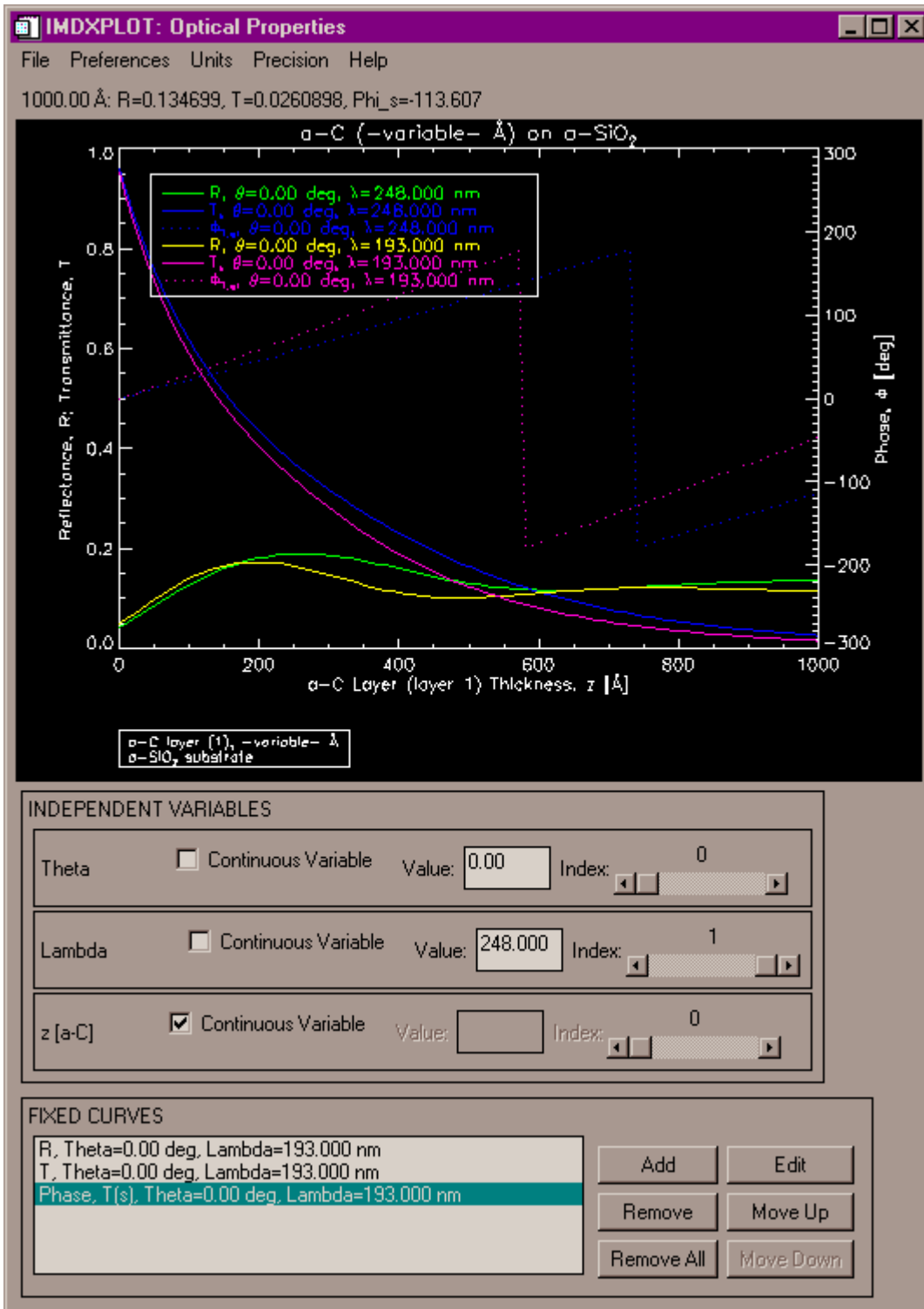


Figure 8(b).

D. L. Windt

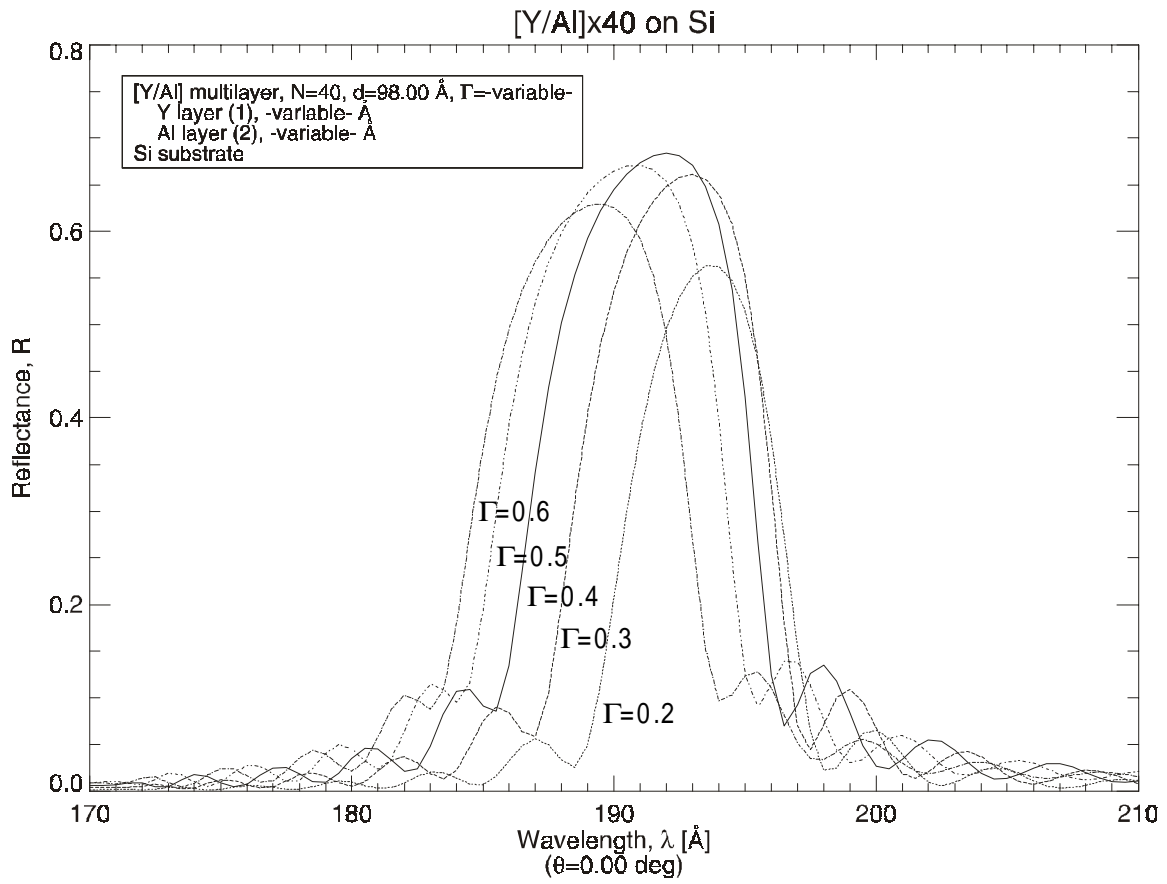


Figure 9(a).

D. L. Windt

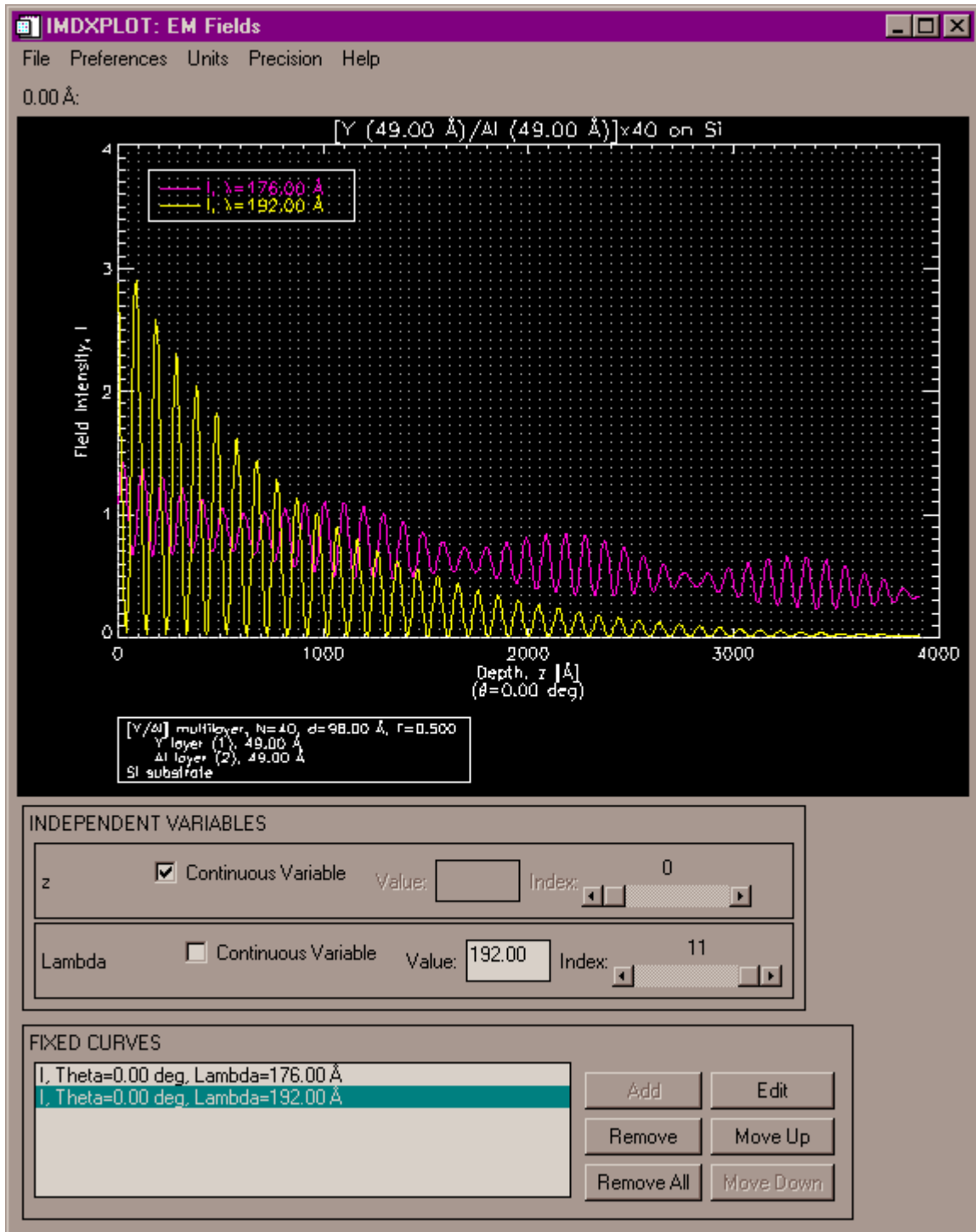


Figure 9(b).

D. L. Windt

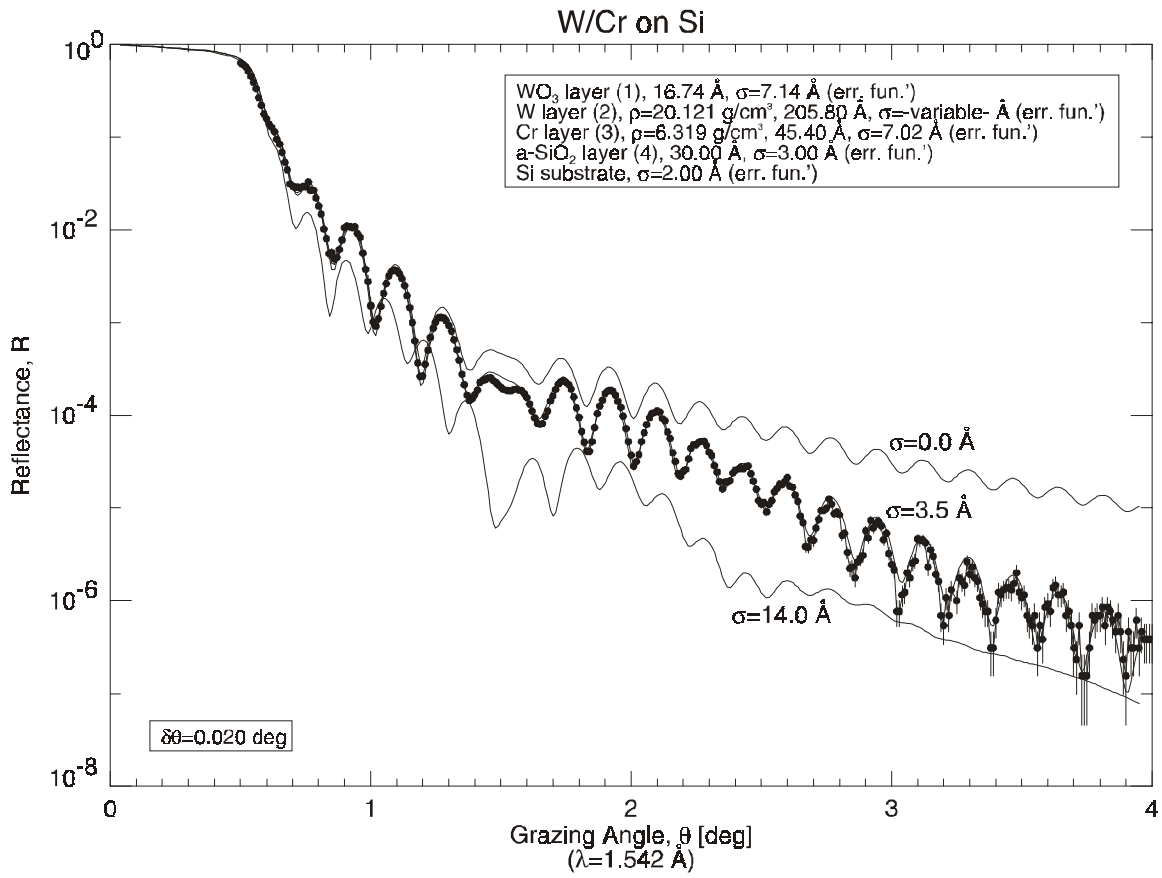


Figure 10.

D. L. Windt

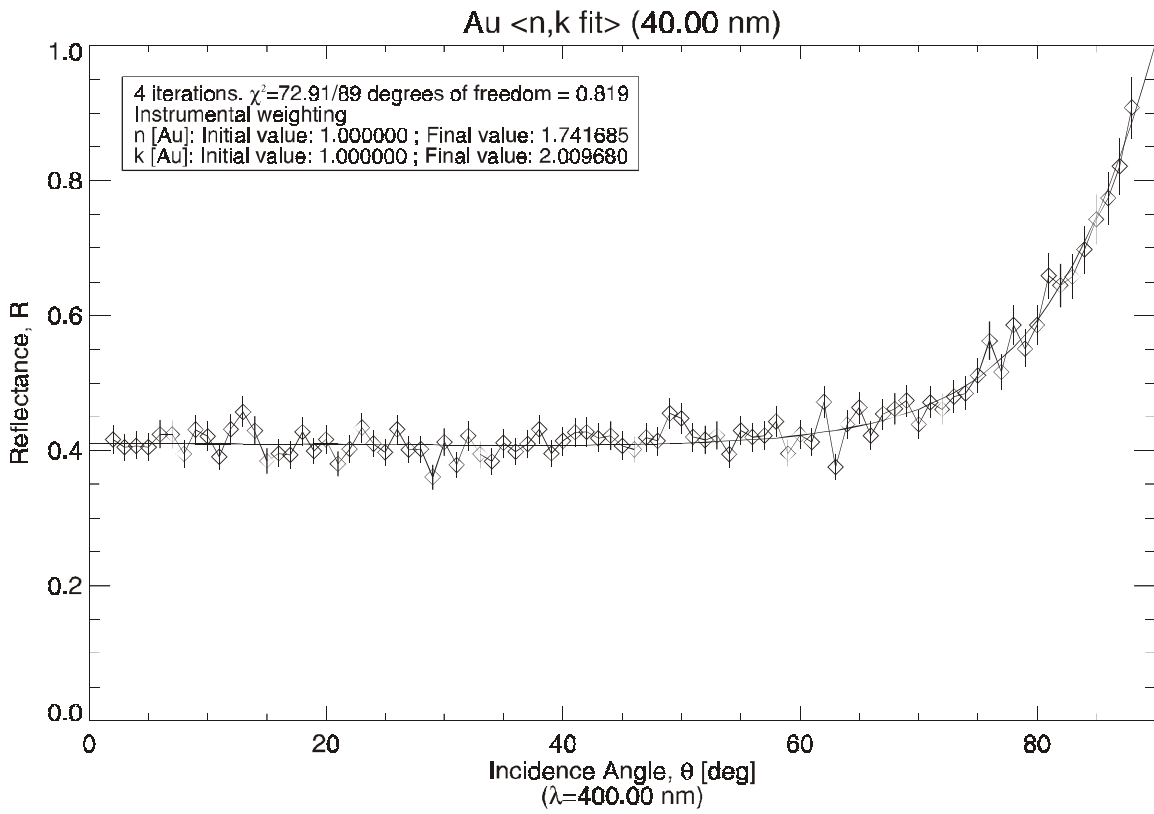


Figure 11(a).

D. L. Windt

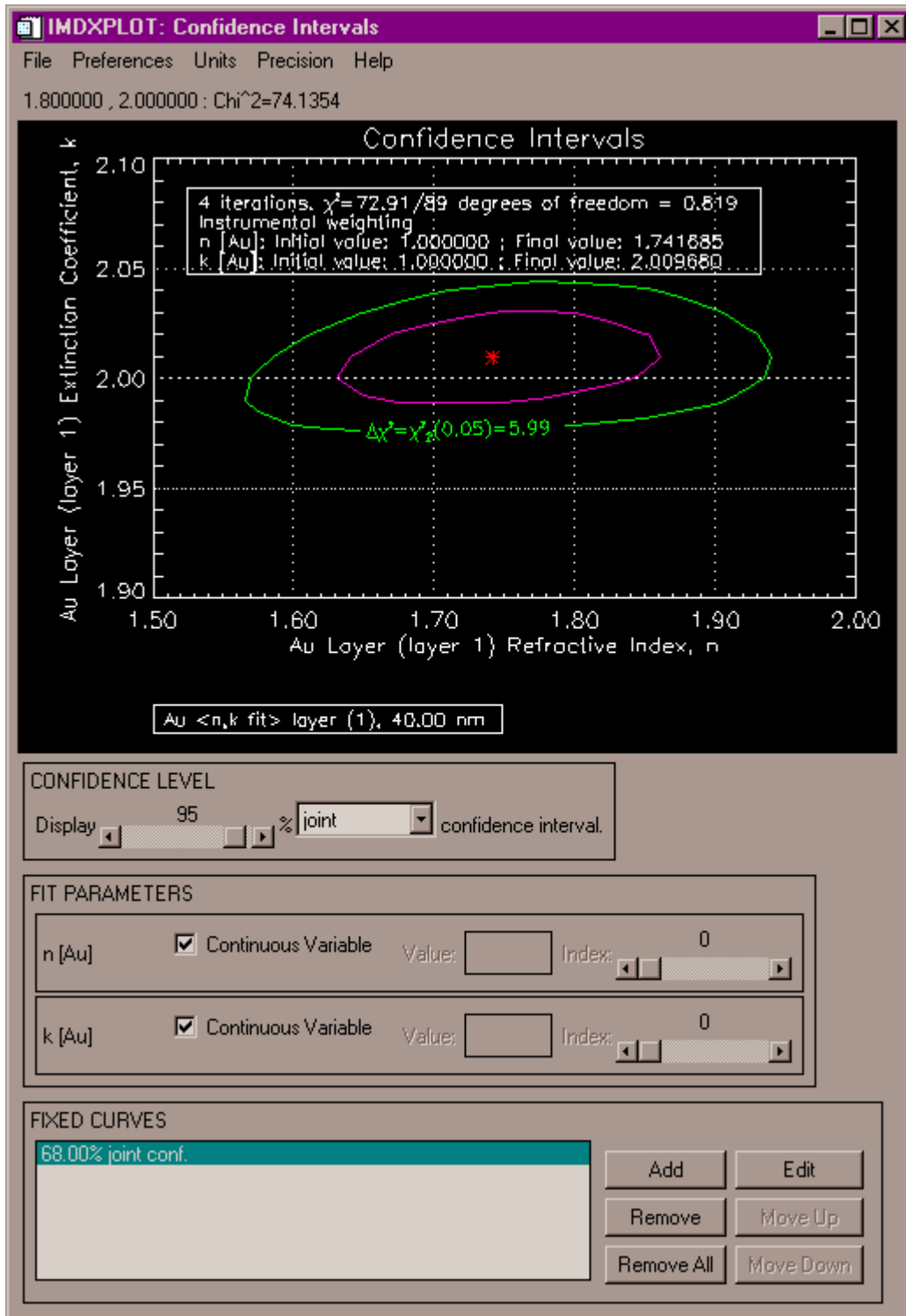


Figure 11(b).

D. L. Windt

[IMD Overview](#)

[What's New in Version 4](#)

[Chapter 1. Getting Started](#)

[1.1 System requirements](#)

[1.2 Downloading IMD](#)

[1.3 Installing IMD](#)

[1.4 Starting IMD](#)

[Chapter 2. Modeling](#)

[2.1 Designating materials and optical constants](#)

- [Browsing the IMD optical constants database](#)
- [Material designation method 1: *by reference to an optical constants file*](#)
- [Material designation method 2: *by specification of density and composition*](#)

[2.2 Defining a structure: specifying parameters](#)

- [Ambient](#)
- [Multilayer stack](#)
 - [Layers](#)
 - [Periodic multilayers](#)
 - [Depth-graded multilayers](#)
 - [Nested multilayers](#)
 - [Layer-data files](#)
- [Substrate](#)
- [Interfaces](#)
 - [Modified Fresnel coefficients: interface widths and interface profile functions](#)
 - [Power-Spectral-Density functions](#)

- [Graded interfaces](#)

2.3 Specifying variables and coupled parameters

- [Dependent variables](#)
 - [Specular optical functions / Electric fields](#)
 - [User-defined specular optical functions](#)
 - [Non-specular optical functions](#)
- [Independent variables](#)
 - [Independent variables specific to electric field calculations](#)
 - [Independent variables specific to non-specular optical functions](#)
- [Coupled parameters](#)

2.4 Performing the computation

2.5 Viewing, printing and saving the results

- [Saving the Results](#)
 - [Viewing and Printing the Results - IMDXPLOT](#)
 - [Fixed Curves](#)
 - [Statistics: estimating film thicknesses, feature widgets, etc.](#)
 - [Examples](#)
 - [Reflectance and transmittance contours of a Y/Al multilayer](#)
 - [Electric field intensity contours of a Mo/Si multilayer](#)
 - [Reflectance of a depth-graded C/Ni multilayer, using coupled parameters](#)
 - [Normal incidence non-specular scattering for a Mo/Si multilayer using the BA](#)
 - [Grazing incidence non-specular scattering for a W/Si multilayer using the DWBA](#)
-

Chapter 3. Measured Data and Parameter Estimation

3.1 Using your measured data

3.2 Specifying fit parameters

3.3 Curve-fitting

3.4 Confidence intervals

[Chapter 4. Problem Solving, and Reporting Bugs](#)

[Appendix A - Optical Constants](#)

[A.1 The IMD optical constants database](#)

[A.2 Using your own optical constants](#)

[A.3 Creating new X-ray optical constants](#)

[Appendix B- Notes for IDL programmers](#)

[B.1 Customizing the installation](#)

[B.2 Some IMD functions and procedure](#)

[B.3 Reading measured data files](#)

[B.4 IMD COMMON block variables](#)

[References](#)

[Preprint of *Computers in Physics* article on IMD](#)

What's New in Version 4.0

IMD Version 4.0 includes several major new features:

- **Non-specular reflected intensity calculations**

Computations are performed using either a dynamical Born approximation vector theory [4], or the so-called 'Distorted-Wave Born Approximation' formalism [5-8], a scalar theory which is nonetheless valid below the critical angle of total external reflection in the X-ray region.

Two power-spectral-density (PSD) function models are available: a PSD function based on the stochastic model of film growth and erosion developed by D. Stearns (see below), and a more conventional PSD function parameterized by roughness, correlation length, and jaggedness parameters.

- **A stochastic model of thin film growth and erosion**

The model can be used to account for the evolution of interfacial roughness through the film stack [9], and can be applied to both specular and non-specular optical function calculations.

- **Depth-graded multilayers**

A choice of depth-grading profiles is available to model aperiodic multilayer films. When using the conventional PSD function (see above,) depth graded roughness and correlation length parameters can be defined as well.

- **Coupled parameters**

An unlimited number of structure parameters (optical constants, compositions, densities, layer thicknesses, PSD parameters, etc..) can be coupled to one another. Thus, a single independent variable or fit parameter can be used to adjust multiple parameters simultaneously.

- **High-energy optical constants and atomic scattering factors**

Atomic scattering factors and optical constants now extend to 100 keV.

- **New specular optical functions**

Ellipsometric psi and delta functions, and user-defined specular optical functions (for example, R_s/R_p , T^3/R , or whatever) can be computed.

- **Enhanced graphics**

Several new features have been added to the IMDXPLOT visualization tool:

- There are now four ways to display 2D optical functions: surface plots, contour plots, filled color contour plots, and superimposed contour/color image plots.
- Interactive zoom and window resizing is now available.
- A new IMDXPLOT Tools menu allows for (a) live cross-hair display on 1D and 2D contour plots (with live 1D-slices), and (b) region-of-interest analysis: periodicities, min and max, average, integral, full-width-half-max, and full-width-half-min.

What's New in Version 4.1

- **Parameter Estimation**

In addition to the Marquardt (CURVEFIT) algorithm, IMD now includes C. W. Markwardt's implementation of the (more robust) Levenburg-Marquardt (MINPACK-1) fitting algorithm.

Fit parameter values - as well as a 'live' plot - are now displayed during curve-fitting, showing the progress of the fit with each iteration.

Offsets and/or Scale Factors can be added to your measured data. In addition, Offsets and/or Scale Factors can be designated as fit parameters.

In addition to these changes, users may wish to consult the [RELEASE NOTES](#).

[Back](#) | [Contents](#) | [Next](#)

Chapter 1. Getting Started

[1.1 System Requirements](#)

[1.2 Downloading IMD](#)

[1.3 Installing IMD](#)

[1.4 Starting IMD](#)

[Contents](#) | [Next](#)

1.1 System Requirements

IMD is written in the IDL language, and will run on any platform supported by IDL. Little or no IDL expertise is required to use IMD.

You will need a valid, licensed copy of IDL to run IMD. IDL version 5.0, 5.1 or 5.2 is required; **Version 5.1/5.2 is strongly recommended, especially for Windows and Macintosh platforms.** IDL is available from Research Systems, Inc, <<http://www.rsinc.com>>

Note: IMD will not run with the Student Version of IDL.

Note: It is possible to run IMD as an 'extension' to the XOP program, which is available for Unix and Windows platforms, free of charge to research institutes and non-profit organizations. Information on XOP can be found at <<http://www.esrf.fr/computing/expg/subgroups/theory/idl/xop/xop.html>>. Please consult the instructions in Section 7 of the IMD [README](#) file for further details on using IMD as a XOP extension.

[Back](#) | [Contents](#) | [Next](#)

IMD

Version 4.1, December 1998

David L. Windt

windt@bell-labs.com

www.bell-labs.com/user/windt/idl

Copyright (c) 1997-1998, David L. Windt
Bell Laboratories, Lucent Technologies.
All rights reserved

This file contains instructions for downloading, unpacking and installing IMD.

Contents of this file:

1. System requirements
 2. Downloading IMD
 3. Unpacking IMD
 4. Installing IMD
 5. Starting IMD
 6. Getting help
 7. Using IMD as a XOP extension
-

1. SYSTEM REQUIREMENTS

IMD is written in the IDL language, and will run on any platform supported by IDL. Little or no IDL expertise is required to use IMD.

You will need a valid, licensed copy of IDL to run IMD. IDL version 5.0, 5.1 or 5.2 is required; Version 5.1/5.2 is *strongly* recommended, especially for Windows and Macintosh platforms. IDL is available from Research Systems, Inc, <<http://www.rsinc.com>>

NOTE: IMD will not run with the Student Version of IDL.

NOTE: It is possible to run IMD as an 'extension' to the XOP program, which is available for Unix and Windows platforms, free of charge to research institutes and non-profit organizations. Information on XOP can be found at
<<http://www.esrf.fr/computing/expg/subgroups/theory/idl/xop/xop.html>>.
Please see section 7 of this document for further instructions.

2. DOWNLOADING IMD

There is only one IMD distribution, and it should run on any platform supported by IDL. For your convenience, however, I have created several different download files, making it easier for you to unpack IMD on your particular platform. (The contents of the three download files are virtually identical, however.) Choose whichever one you like.

Download files:

Unix: imd.tar.Z

Windows: imd.zip

MacOS: imd.hqx

(Note that you may need to explicitly configure your browser to save the download file directly to disk.)

3. UNPACKING IMD

To unpack the file you downloaded, follow the instructions below for your specific platform. When you have finished unpacking the distribution, you will find two directories: "imd" and "windt". The total distribution requires approximately 38 MB of disk space, including approximately 15 MB for the IMD optical constants and atomic scattering factors databases, ~3 MB for the hypertext documentation, and ~12 MB for the examples files. (The examples files are optional and can be deleted if necessary; consult Appendix B.1 of the IMD documentation for additional help on conserving disk space.)

Unix

o Unpack the imd.tar.Z file, using the Unix uncompress and tar commands:

```
$ uncompress -c imd.tar.Z | tar -xvf -
```

Windows

o Use the (32-bit) WinZip shareware program to unpack the imd.zip file.

MacOS

o Use the Stuffit Expander freeware program to unpack the imd.hqx file; the "imd" and "windt" folders will be located in the newly-created "imd.sea Folder".

4. INSTALLING IMD

The IMD distribution is contained entirely in the directory (or folder, if you prefer) called imd. Within this directory are the IMD programs, and the subdirectories containing optical constants, atomic scattering factors, documentation, and examples.

The main IMD program is distributed as an IDL SAVE file, and all the required IDL procedures and functions are already loaded, so you will not need to include any other directories in your IDL path. However, included along with the imd directory is the directory called windt, which contains a variety of IDL programs for general use, many of which are used by IMD. (But again, these files are not needed by IMD as they are already compiled into the IMD SAVE file.) When you unpack the file you downloaded from the web, you will find both the imd and windt directories.

The imd directory should nominally be installed in a directory that you must create called user_contrib, inside the main IDL directory. That is, you should end up with a directory called

.../idl/user_contrib/imd (using Unix "notation".) You can also install the windt directory in the user_contrib directory if you choose.

Consult Appendix B.1 of the IMD documentation if you need to install IMD someplace else, and for instructions on other IMD customization options.

5. STARTING IMD

Before you attempt to start IMD, make sure that the imd directory is included in your IDL Path. Consult the IDL manuals for instructions on how to do this.

To start IMD, at the IDL prompt type:

```
IDL> .run imdstart
```

This will load IMD and launch the main IMD program. If you exit IMD and wish to run it again during the same IDL session, at the IDL prompt type:

```
IMD> imd
```

Note: You can define NORUN=1 before executing '.run imdstart', to inhibit automatic execution of the imd procedure.

Note: On Unix platforms, the IDL_DEVICE environment variable must be set to 'X'.

6. GETTING HELP

A complete hypertext manual explaining how to use IMD is included with the IMD distribution. Users are *strongly* encouraged to have a look at this material in order to fully appreciate the many unique capabilities of IMD. Point your browser to the file .../imd/docs.dir/index.html.

In addition, there are several IMD files in the examples.dir directory that illustrate some of the features of IMD, so you might want to have a look there.

7. USING IMD AS A XOP EXTENSION

(If you will use IMD with a licensed copy of IDL, you can skip the following instructions.)

A. To install IMD as a XOP extension, perform the following four steps:

i. Download and install the XOP program, as described at the XOP website: <<http://www.esrf.fr/computing/expg/subgroups/theory/idl/xop/xop.html>>.

ii. Download and unpack the IMD distribution, following the instructions given above in section 2 and 3. Install the imd directory in the XOP extensions directory. When you complete this step, you should end up with a directory called .../xop/extensions/imd.

iii. Copy and rename the appropriate imd4xop.sav_V file - where V=50

for the version of XOP built from IDL version 5.0, V=51 for the version of XOP built from IDL version 5.1, and V=52 for the version of XOP built from IDL version 5.2 - from the imd directory to the XOP extensions directory. When you complete this step, you should end up with a file called ../xop/extensions/imd4xop.sav. That is:

for XOP / IDL V5.0:

```
copy ../extensions/imd/extras.dir/imd4xop.sav_50
to ../extensions/imd4xop.sav
```

for XOP / IDL V5.1:

```
copy ../extensions/imd/extras.dir/imd4xop.sav_51
to ../extensions/imd4xop.sav
```

for XOP / IDL V5.2:

```
copy ../extensions/imd/extras.dir/imd4xop.sav_52
to ../extensions/imd4xop.sav
```

iv. Using a text editor, edit the xop_extensions.lis file and add the single line:

```
imd4xop.sav
```

Consult Appendix B.1 of the IMD documentation for instructions on other IMD customization options.

B. Starting IMD as a XOP extension:

There are two (platform-specific) ways to run IMD as a XOP extension:

For Unix platforms:

At the unix system prompt, type:

```
xop imd4xop
```

-or-

From the main XOP window:

- a. Select Tools -> IDL Macro
- b. Clear the window and type imd4xop
- c. Select File -> Quit and accept changes

For Windows platforms:

Assuming your XOP installation directory is c:\xop, double-click on the file:

```
c:\xop\extensions\imd\extras.dir\imd4xop.bat
```

Note: If your XOP installation is different from c:\xop, you will need to edit the imd4xop.bat file accordingly.

-or-

From the main XOP window:

- a. Select Tools -> IDL Macro

b. Clear the window and type imd4xop

c. Select File -> Quit and accept changes

1.2 Downloading IMD

The latest version of IMD can be downloaded starting from the following URL:

<<http://www.bell-labs.com/user/windt/idl>>

(To unpack the download file, follow the instructions in the IMD [README](#) file.)

[Back](#) | [Contents](#) | [Next](#)

1.3 Installing IMD

The IMD distribution is contained entirely in the directory (or folder, if you prefer) called `imd`. Within this directory are the IMD programs, and the subdirectories containing optical constants, atomic scattering factors, documentation, and examples.

The main IMD program is distributed as an IDL SAVE file, and all the required IDL procedures and functions are already loaded, so you will not need to include any other directories in your IDL path. However, included along with the `imd` directory is the directory called `windt`, which contains a variety of IDL programs for general use, many of which are used by IMD. (But again, these files are not needed by IMD as they are already compiled into the IMD SAVE file.) When you unpack the file you downloaded from the web, you will find both the `imd` and `windt` directories.

The `imd` directory should nominally be installed in a directory that you must create called `user_contrib`, inside the main IDL directory. That is, you should end up with a directory called `.../idl/user_contrib/imd` (using Unix "notation".) You can also install the `windt` directory in the `user_contrib` directory if you choose.

Consult [Appendix B.1](#) if you need to install IMD someplace else, and for instructions on other IMD customization options.

[Back](#) | [Contents](#) | [Next](#)

B.1 Customizing the installation

If you will use IMD with a licensed copy of IDL, and you choose not to install the `imd` directory inside of the `user_contrib` directory in the main IDL directory, then you **must** edit the file `imdsiteconfig.pro`, located in the `imd` directory. The file `imdsiteconfig.pro` contains executable IDL code (although the program itself will not run if you just type `.run imdsiteconfig.pro` at the IDL prompt.) You must change the value of the **`imdhome`** variable in this file so that it refers to the actual IMD installation directory.

There are several other parameters you can adjust in this file:

- You can specify default widget fonts to be used by IDL, as per your preference: set the value of the **`font_w`** variable to the name of a valid IDL widget font for your site. In addition, you can tell IMD how to display the angstrom symbol and the greek "mu" symbol for the font you specify.
- You can add additional optical constant directories to the default IMD optical constants search path (so that you don't have to add them using the IMD menu option described in [Section A.2.](#)) The variable **`imd_nkpath`** in `imdsiteconfig.pro` is a string array containing the list of optical constant directories to be searched by IMD.
- The **`sp_max_array_size`** and **`ns_max_array_size`** parameters can be adjusted according to the memory limitations of your computer. That is, you might be able to avoid the 'Not enough memory to make array' error message when trying to calculate large arrays, under certain conditions:

For specular optical functions, the largest arrays that IMD will attempt to create to perform the actual computation are proportional to (number of wavelengths) x (number of angles) x (number of layers). So if you get the 'Not enough memory' message when computing specular optical functions *as a function of multiple wavelengths*, you can try *DECREASING* the **`sp_max_array_size`** parameter.

For non-specular reflected intensities, the 'Not enough memory' error is most likely to occur when using the Omega/Nu/N PSD model, if you have defined large Nu values or Omega values equal to zero. In this case, IMD will need to create arrays that are proportional to (number of angles) x (number of layers) x (number of layers), where (number of angles) is equal to the number of incidence angles for Rocking and Offset scans, and the number of scattering angles for Detector scans. So if you get the 'Not enough memory' message when computing non-specular reflected intensities *as a function of multiple angles* using the Omega/Nu/N PSD model under the circumstances just

mentioned, you can try *DECREASING* the `ns_max_array_size` parameter.

Also, these parameters can be decreased if you find that your computer is using a lot of virtual memory (i.e., spending a lot of time swapping to disk). Note, however, that decreasing `sp_max_array_size` or `ns_max_array_size` too low will result in a large speed penalty.

CONSERVING DISK SPACE

If you need to conserve disk space, there are a number of files that are included in the imd distribution that are optional, and can be safely deleted. Specifically, the `examples.dir` directory contains many examples files, all of which can be deleted. Also, three versions of the IMD binary file are shipped: one to be used with IDL version 5.0, called `imd_50`, another to be used with IDL version 5.1, called `imd_51`, and another to be used with IDL version 5.2, called `imd_52`. If you are sure you will only use one version of IDL (V5.0, V5.1, or V5.2), then you can delete whichever IMD binary files are not going to be used. Finally, this hypertext documentation is non-essential, and so the entire `docs.dir` directory can also be removed.

[Back](#) | [Contents](#) | [Next](#)

A.2 Using your own optical constants

If you wish, you can use your own optical constants with IMD. To add you own optical constants, you must follow these two steps:

1) Create an nk file, according to these conventions: the file must consist of three columns of data (lambda [in angstroms], n, k). You can include comments (preceded by semicolons in the first column) at the beginning of the file, but there can be no comments or blank lines anywhere else in the file. (Make sure there are no blank lines at the end of the file!) You should also follow the file-naming convention described in the previous section. When creating plots, IMD can display the reference portion of the file name as a subscript. (See the **File->Global Plot Preferences->Material Names** option.) Also, any numbers in the Material name are displayed as subscripts, e.g., the "2" in SiO₂ will be displayed as a subscript.

2) Tell IMD where to find the file you've created. This is done by selecting **Materials/Optical Constants->Optical Constants Search Path** from the IMD menu bar. A widget will appear that allows you to add and subtract directories to the IMD optical constants search path; you can also adjust the order of directories searched, as IMD will search the directories in the order listed, and will use the first file found that matches the material name you specify. Note that the default optical constants search path can be changed as desired by editing the `imdsiteconfig.pro` file. See [Appendix B.1](#) for details.

If you wish, you can also create a file called `AAACATALOG.TXT`, to be kept in your personal optical constants directory, so that you will be able to use the **Materials/Optical Constants -> Browse Optical Constants Database** option to view the contents of your files using **XNKPLOT** directly from IMD. Follow the same format that's used in the `AAACATALOG.TXT` file in `nk.dir`,

[Back](#) | [Contents](#) | [Next](#)

A.1 The IMD optical constant database

The IMD optical constant database is located in the directory called `nk.dir`, in the `imd` directory. Optical constant files are designated by a `.nk` extension, and are ASCII files containing three columns of numbers: wavelength (in angstroms), n , and k . Comment lines (beginning with a semicolon) may precede the data.

Each `.nk` file in `nk.dir` corresponds to one material, although there is usually more than one `.nk` file for any given material. The naming convention I have adopted for `.nk` files is `Material_reference.nk`. For example, the file `Si_palik.nk` corresponds to the optical constants for silicon, taken from the optical constant handbook by Palik [18]; the file `Si_llnl_cxro.nk` corresponds to other data for silicon, in this case data in the X-ray region compiled from the LLNL and CXRO atomic scattering factors (see [section A.3](#) below.) Source reference information is usually included as a comment at the beginning of the file. In addition to these source-specific files, for every material I have created compilation files that cover as wide a range in wavelength as possible. The compilation files include no reference in the name. For example, the file `Si.nk` is a compilation of the data from `Si_llnl_cxro.nk` and `Si_palik.nk`, and spans the range from 0.124 angstroms to 3.33e6 angstroms.

To use a specific file for a given material, enter the full name of the file (excluding the `.nk` extension) in the Material fields in the relevant **ambient**, **layer**, or **substrate** widgets (be sure that the **Optical constants file name** button is checked, rather than the **Composition and density** button.). For example, to use the data for silver published by Hagemann, et al, specify `Ag_hagemann`, instead of just plain `Ag`.

The `.nk` files contained in the `nk.dir` directory are listed in the file called `AAACATALOG.TXT`, which is also located in `nk.dir`. This file is displayed when you select **Materials/Optical Constants - > Browse Optical Constants Database** from the IMD menu bar.

[Back](#) | [Contents](#) | [Next](#)

A.3 Creating new X-ray optical constants

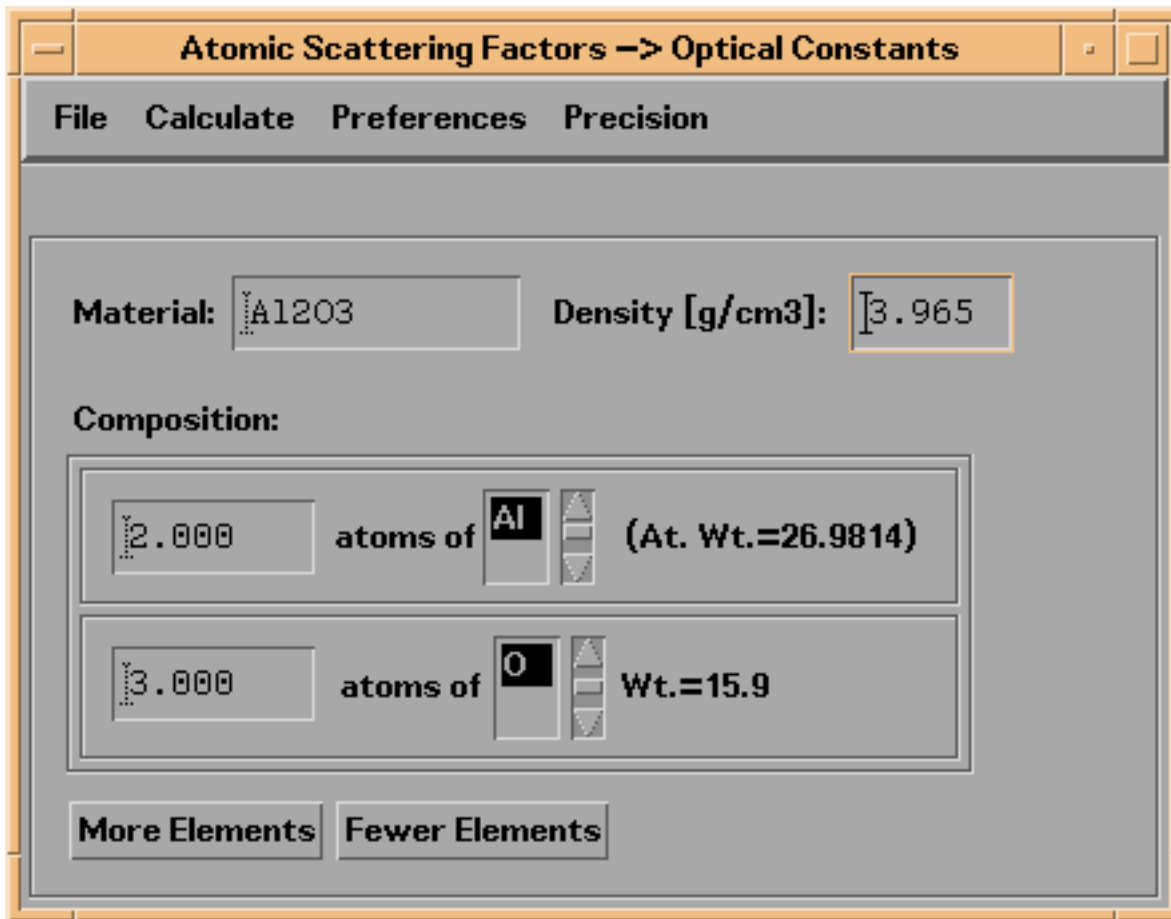
If there is a material that you wish to model using IMD in the X-ray region that is not included in the IMD optical constants database, as an alternative to designating that material by composition and density as described in [Section 2.1](#), you can generate a file of optical constants over the entire 30 eV to 100 keV photon energy range using the program [IMD_F1F2TONK](#). You can then designate IMD structure element materials by reference to this file. (Many of the files in the IMD optical constants database were, in fact, created using this program.)

The `IMD_F1F2TONK` program can be run independently of IMD, by typing `imd_f1f2tonk` at the IDL prompt, or it can be accessed from within IMD by selecting the **Materials/Optical Constants->Create New X-Ray Optical Constants** option from the main IMD menu.

The program computes the optical constants for a compound (specified by its composition and density) using the atomic scattering factors, f_1 and f_2 , as described in reference [\[12\]](#). A combination of atomic scattering factors from two sources are used: from 30 eV to 30 keV, the program uses atomic scattering factors compiled by Eric Gullikson at the Center for X-Ray Optics, Lawrence Berkeley Laboratory, as described in reference [\[12\]](#); from 30 keV to 100 keV, atomic scattering factors from the Lawrence Livermore National Laboratory are used, as described in reference [\[13\]](#). The composite atomic scattering factors files are located in the directory called `f1f2.dir` in the `imd` directory.

The `IMD_F1F2TONK` widget is shown in figure A.3.1:

Figure A.3.1 `IMD_F1F2TONK` widget, in this example set to calculate the optical constants for Al_2O_3 .



To create the optical constants for a compound, you must first specify how many different elements comprise the compound (using the **More Elements** and **Fewer Elements** buttons), the names of the elements (by selecting from the list of the 92 available elements,) the relative numbers of each element, and the density (in grams/cm³) of the compound. The **Precision** menu allows you to adjust the number of decimal spaces displayed for both density and composition values. By selecting the **Calculate->Optical Constants** menu item, the program will read the f_1 and f_2 values for each element specified, compute the values of n and k , and plot the results. You can then save these results to an IMD optical constant file by selecting the **File->Save** menu item.

[Back](#) | [Contents](#) | [Next](#)

2.1 Designating Materials and Optical Constants

The first step in performing a calculation is defining the structure. At the highest level, a structure consists of three components: the ambient material, the multilayer stack, and (optionally) a substrate. Although the different structure components are specified in somewhat different ways, as described in [section 2.2](#), common to all structure elements is the material designation, which determines what optical constants are used for the calculation. This section discusses material designation and optical constants.

Each structure element - the ambient, the substrate, and each multilayer stack layer element - is composed of some material. There are two different methods you can use to designate materials:

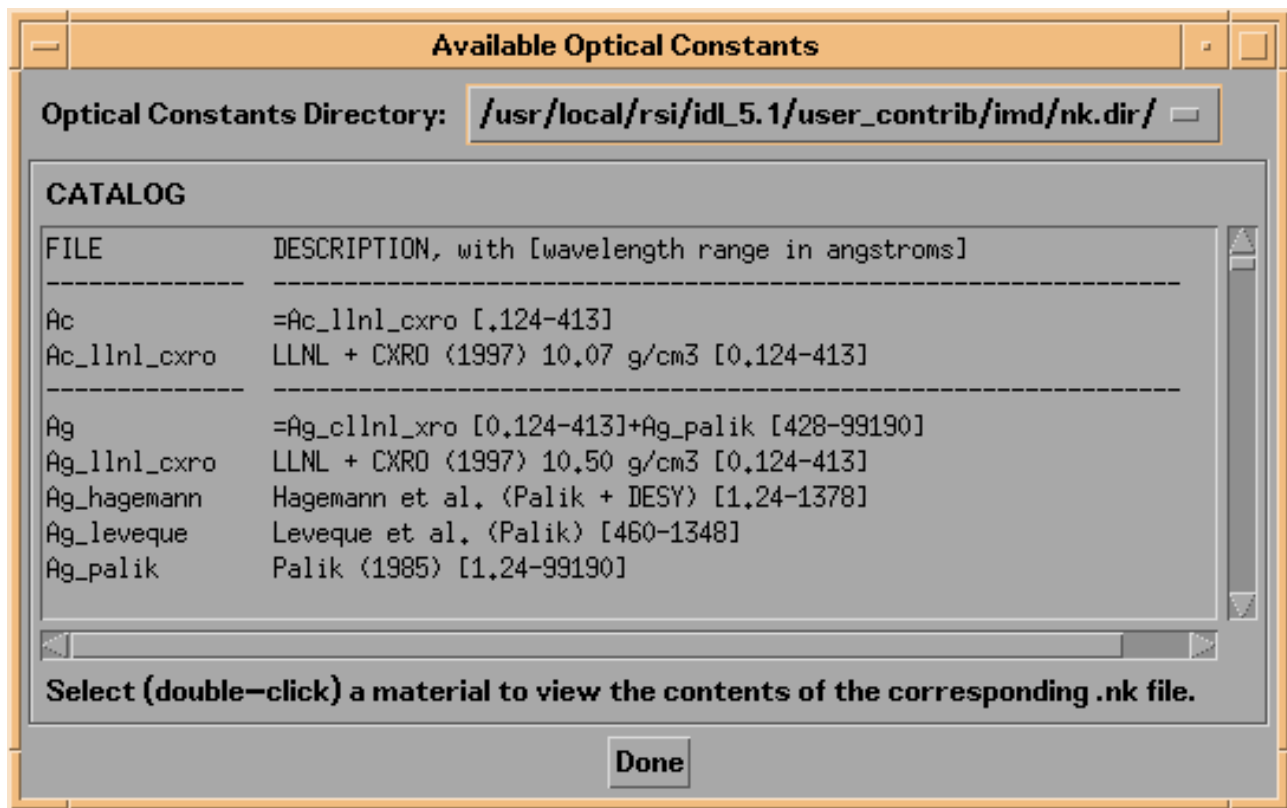
- In the first method, the designated material name refers to an optical constants file contained in the IMD optical constant database.
- In the second method, which is applicable only in the X-ray region for energies between 30 eV and 100 keV, the material is specified by its composition and density, and the optical constants are computed directly from the atomic scattering factors.

The use of the two methods for material designation is best illustrated by example. But before illustrating the techniques for material specification, I will describe in the next section the IMD optical constants database.

BROWSING THE IMD OPTICAL CONSTANTS DATABASE

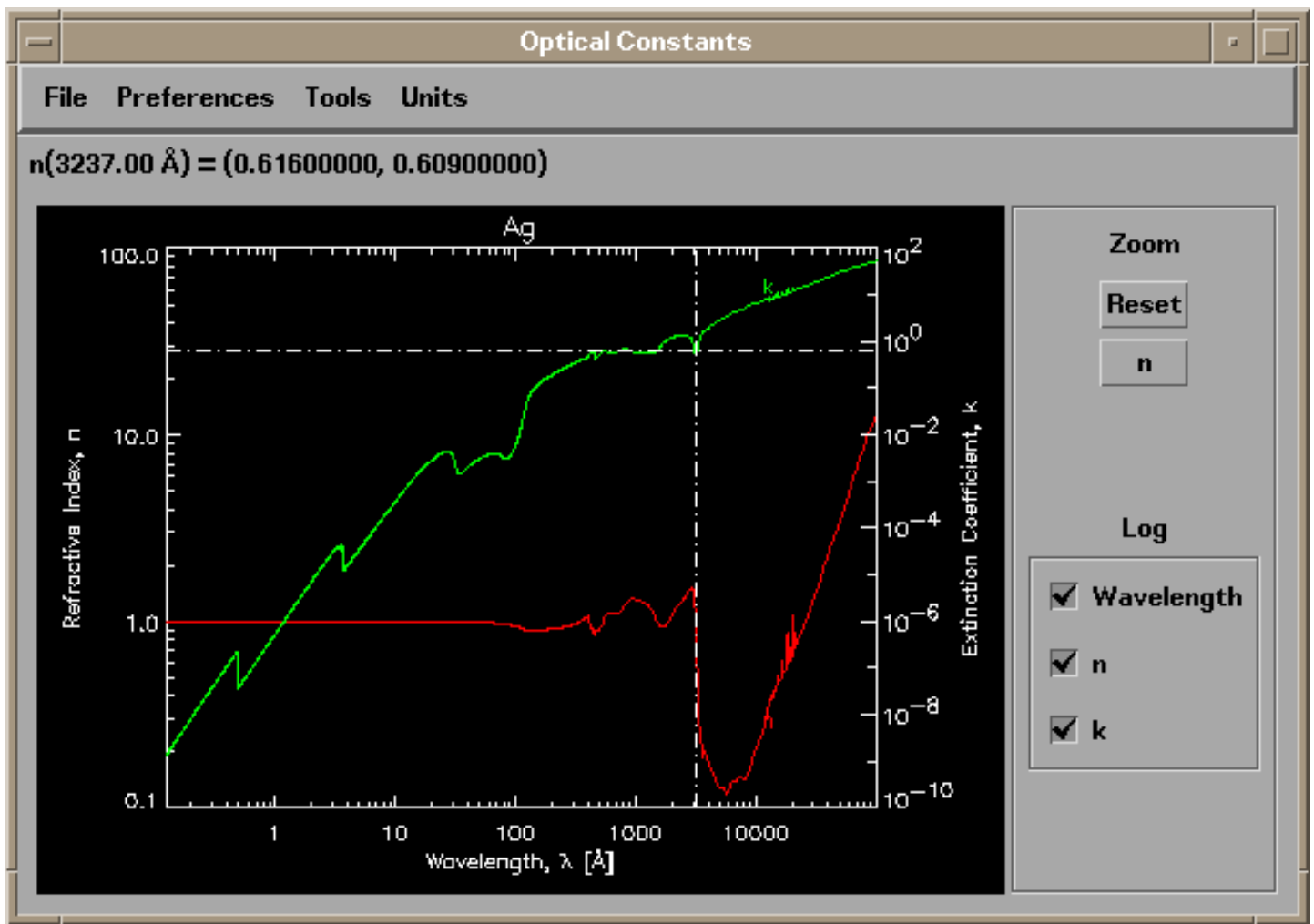
To see which materials are available (and over which wavelengths) in the IMD optical constant database, i.e., the materials available for use by the first method of material specification above, select **Materials/Optical Constants -> Browse Optical Constants Database** from the menu bar. Doing so will bring up the catalog of available optical constants, as shown in Figure 2.1.1:

Figure 2.1.1 IMD Available Optical Constants widget



Each available optical constant file is listed, along with abbreviated source reference and wavelength coverage information. By selecting an item from the catalog, two new widgets will appear: one displaying a text listing of the optical constants contained in the file you selected, and another (an [XNKPLOT](#) widget) showing a plot of the optical constants (n and k) versus wavelength. For example, shown in Figure 2.1.2 are the optical constants for silver:

Figure 2.1.2 XNKPLOT of the optical constants of Ag



You can use the XNKPLOT **Prefences** menu items to adjust the appearance of the optical constants plot, and you can print the plot using the **File->Print** menu option (as if you couldn't have figured that one out.)

Consult [Appendix A](#) for more details on optical constants, including how to use your own optical constants, and how to create new X-ray optical constants.

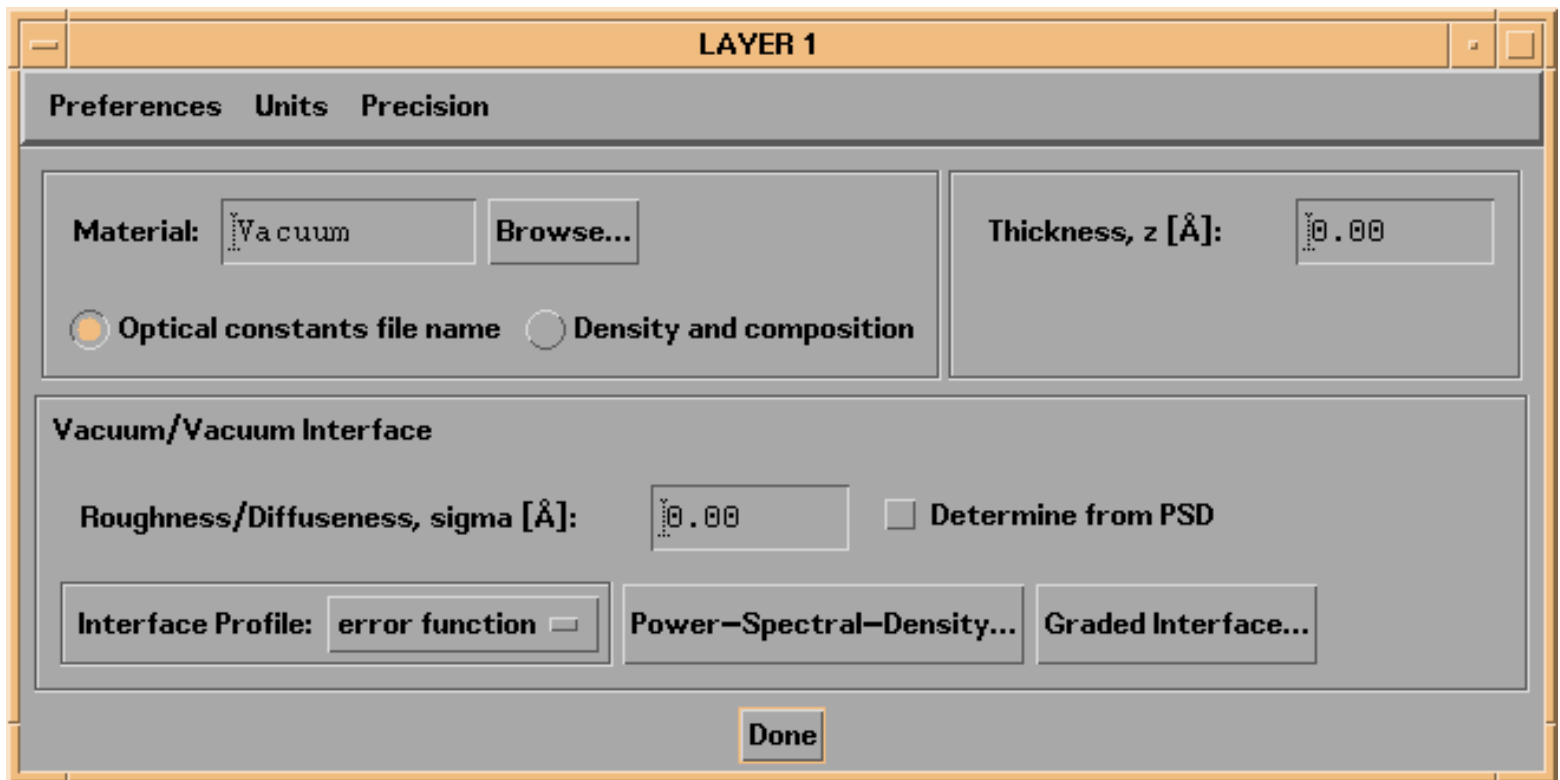
MATERIAL DESIGNATION

As mentioned above, there are two different methods available for material designation in IMD. These two methods will now be described in more detail. Although the material designation techniques described here apply to all structure elements - ambient, substrate and layers - I will show how to specify the material in a layer element as a specific example.

METHOD 1: Material designation by reference to an optical constants file

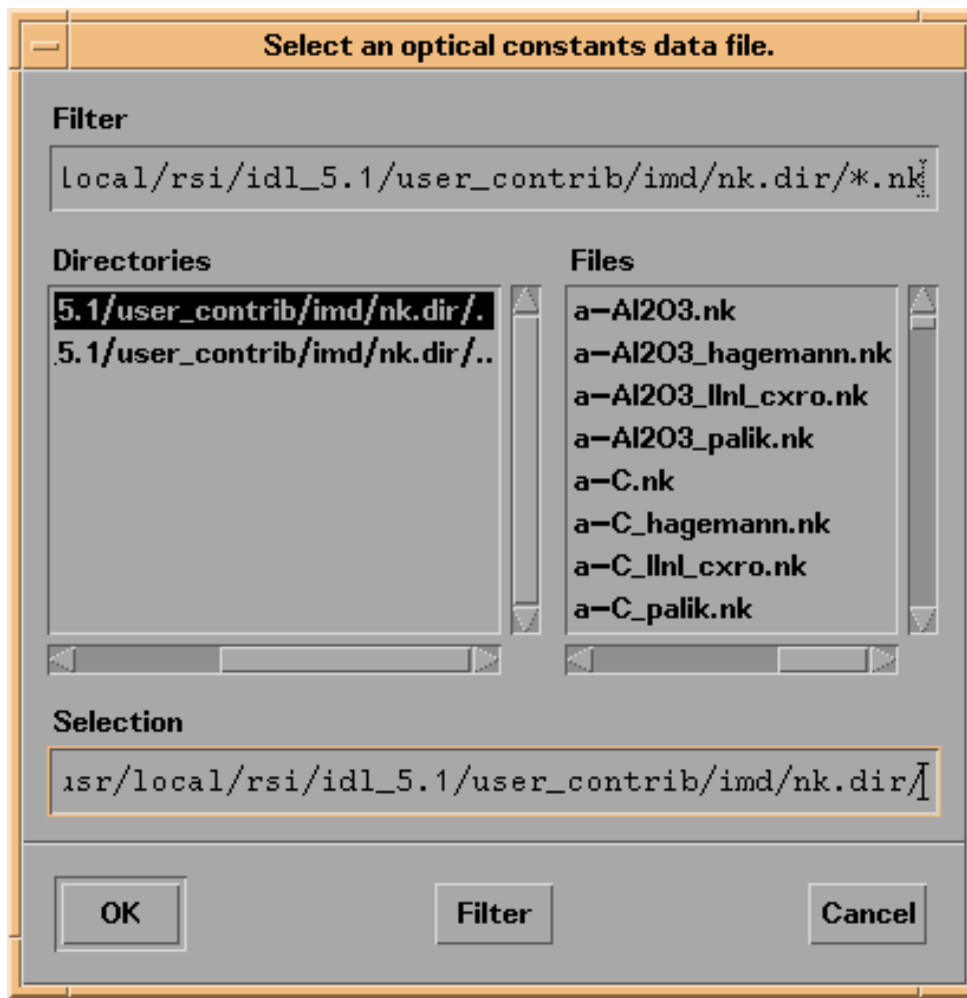
Shown in Figure 2.1.3 is the layer widget associated with a new layer. (i.e., the widget that appears when you press the **Add Layer** button; the techniques for adding a new layer to the multilayer stack are described fully in [section 2.2.](#))

Figure 2.1.3 An IMD *Layer* widget, as it appears when a new layer is added to the multilayer stack.



The **Optical constants file name** button is selected by default, indicating that material designation is by reference to a valid optical constants file. The default layer material is "Vacuum", which means that the optical constants (n,k) have the value of (1.,0.) for all wavelengths. (Indeed, "Vacuum" is the default material for all new structure elements.) To change the material, you can enter a (valid) material name in the material field, or else press the **Browse...** button to display a choice of all available materials, as show in the next figure (entering an invalid material name has the same effect as pressing the **Browse...** button):

Figure 2.1.4 Pressing the **Browse...** button: the IMD material selection widget

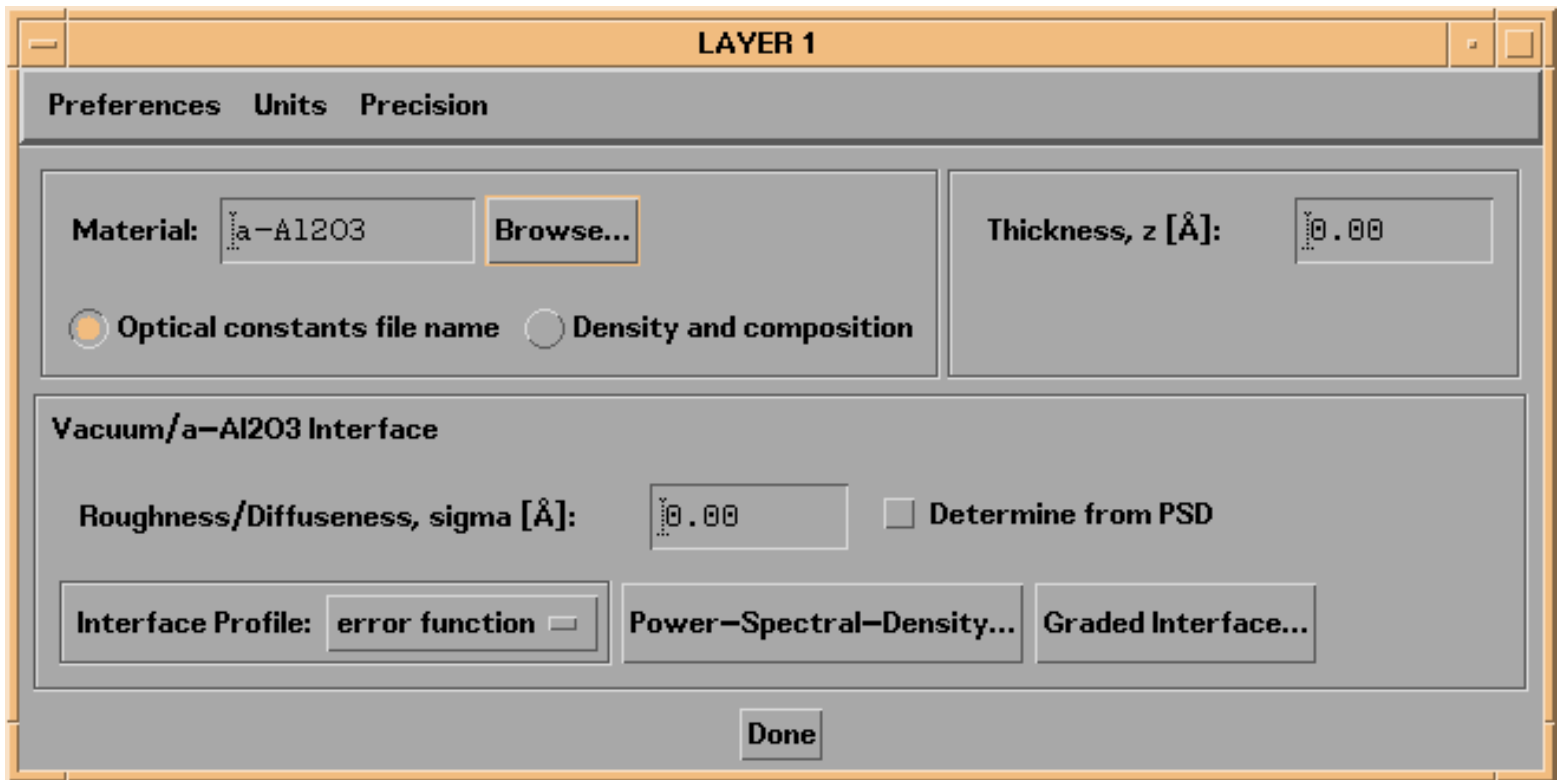


The material selection widget lists all available optical constant files (.nk files). You can scroll through the list of available files and select the material you like by clicking on the file name, and pressing the **OK** button.

Note: you'll see that there are no files named 'Vacuum' available. To designate Vacuum as a material, you must either type 'Vacuum' in the material field (or leave it blank) and hit return.

As an example, shown in Figure 2.1.5 is the Layer widget after selecting amorphous aluminum oxide - the first choice in the list of available optical constants show in Figure 2.1.4.

Figure 2.1.5: IMD **Layer** widget corresponding to an amorphous aluminum oxide layer.



METHOD 2: Material designation by density and composition specification

To utilize the second method for material specification, click on the **Density and composition** button. Doing so will cause the **Layer** widget to appear as in Figure 2.1.6.

Figure 2.1.6: An IMD **Layer** widget with the **Density and composition** button selected.

LAYER 1

Preferences Units Precision

Material: Density [g/cm³]:

Thickness, z [Å]:

Composition:

atom of wt.=227.0

Optical constants file name Density and composition

Vacuum/Ac Interface

Roughness/Diffuseness, sigma [Å]: Determine from PSD

Interface Profile:

When specifying a material by density and composition, you must specify how many different elements comprise the compound (using the **More Elements** and **Fewer Elements** buttons), the names of the elements (by selecting from the list of the 92 available elements,) the relative numbers of each element, and the density (in grams/cm³) of the compound. The **Precision** menu allows you to adjust the number of decimal spaces displayed for both density and composition values. As an example, shown in Figure 2.1.7 is a **Layer** widget configured to use a material consisting of 3 parts Cr and 2 parts C, having a density of 6.68 gm/cm³.

Figure 2.1.7: An IMD **Layer** widget corresponding to a layer of Cr₃C₂, having a density of 6.68 gm/cm³.

LAYER 1

Preferences Units Precision

Material: Density [g/cm3]:

Thickness, z [Å]:

Composition:

atoms of Wt.=51.9

atoms of Wt.=12.0

Optical constants file name Density and composition

Vacuum/Cr3C2 Interface

Roughness/Diffuseness, sigma [Å]: Determine from PSD

Interface Profile:

Note: material specification by density and composition is applicable only in the photon energy range from 30 eV to 100 keV (i.e., wavelengths between 413 and 0.124 angstroms.) See [Appendix A.3](#) for more details.

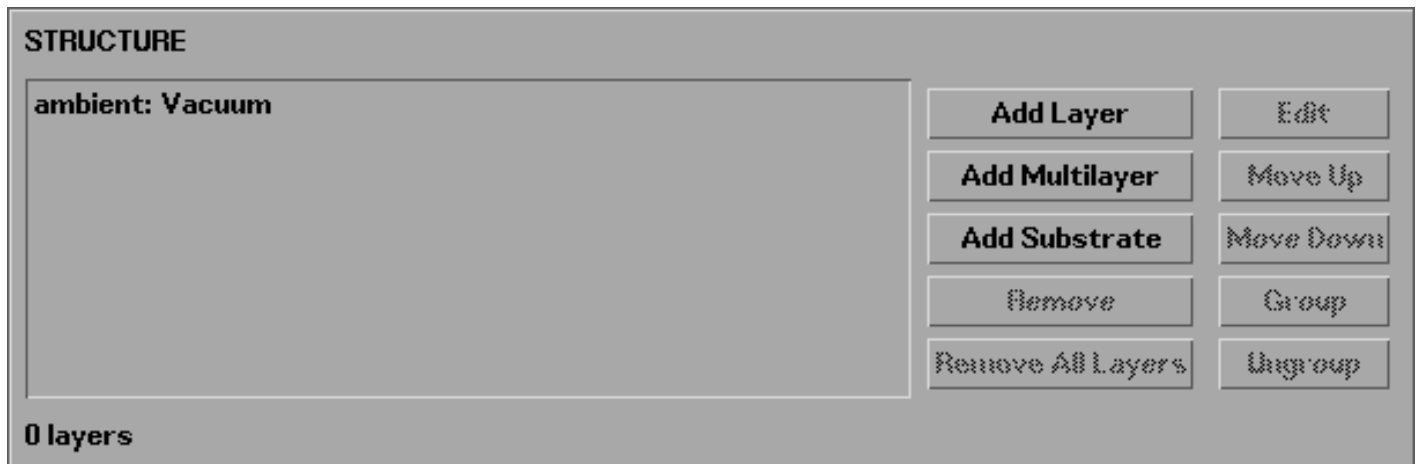
Regardless of which method you use to specify a material, the results of your material selection will be listed in the *Structure List*. For example, if you have chosen water as the ambient material, the *Structure List* will indicate 'ambient: H2O'.

[Back](#) | [Contents](#) | [Next](#)

2.2 Defining a Structure: Specifying Parameters

The STRUCTURE area of the main IMD widget (shown in Figure 2.1.1) consists of the *Structure List*, which lists the current structure elements, the buttons to the right of the *Structure List*, which are used to add, remove, and modify structure elements, and the *Layer Count* indicator below the *Structure List*, which indicates the total number of layers that comprise the structure.

Figure 2.2.1 The STRUCTURE area of the main IMD widget.

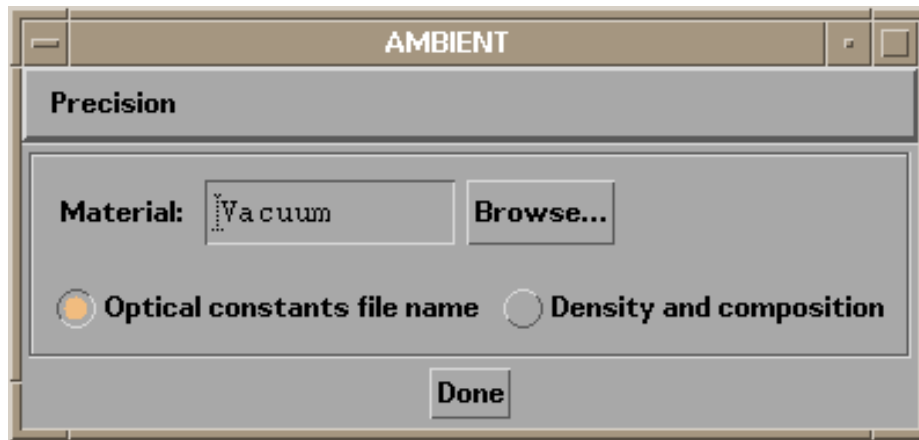


The techniques for defining each type of structure element - ambient, layers, and the substrate - will be described in turn below.

AMBIENT

When IMD first starts up cold, the only structure component listed in the STRUCTURE area of the main widget is the ambient (as in Figure 2.2.1). To edit the ambient parameters, double-click on the "ambient" line in the *Structure List*, or select (highlight) this line and press the **Edit** button (to the right of the *Structure List*.) This brings up the **Ambient** widget, as shown in Figure 2.2.2.

Figure 2.2.2 IMD **Ambient** widget



The material is the only parameter that can be specified for the ambient. (In contrast, there are many layer and substrate parameters, e.g., thicknesses, roughnesses, etc., as described below.) The default ambient material is "Vacuum". Use the techniques described in [section 2.1](#), to change the ambient material.

MULTILAYER STACK

In IMD, a 'multilayer structure' consists of individual layers, which can optionally be grouped together to define periodic (or aperiodic, i.e., depth-graded) multilayers. You define each layer by specifying the material comprising the layer, the layer thickness, and the interface properties: interfacial roughness, diffuseness, power-spectral-density parameters, etc.

Interface parameters are discussed in detail [below](#).

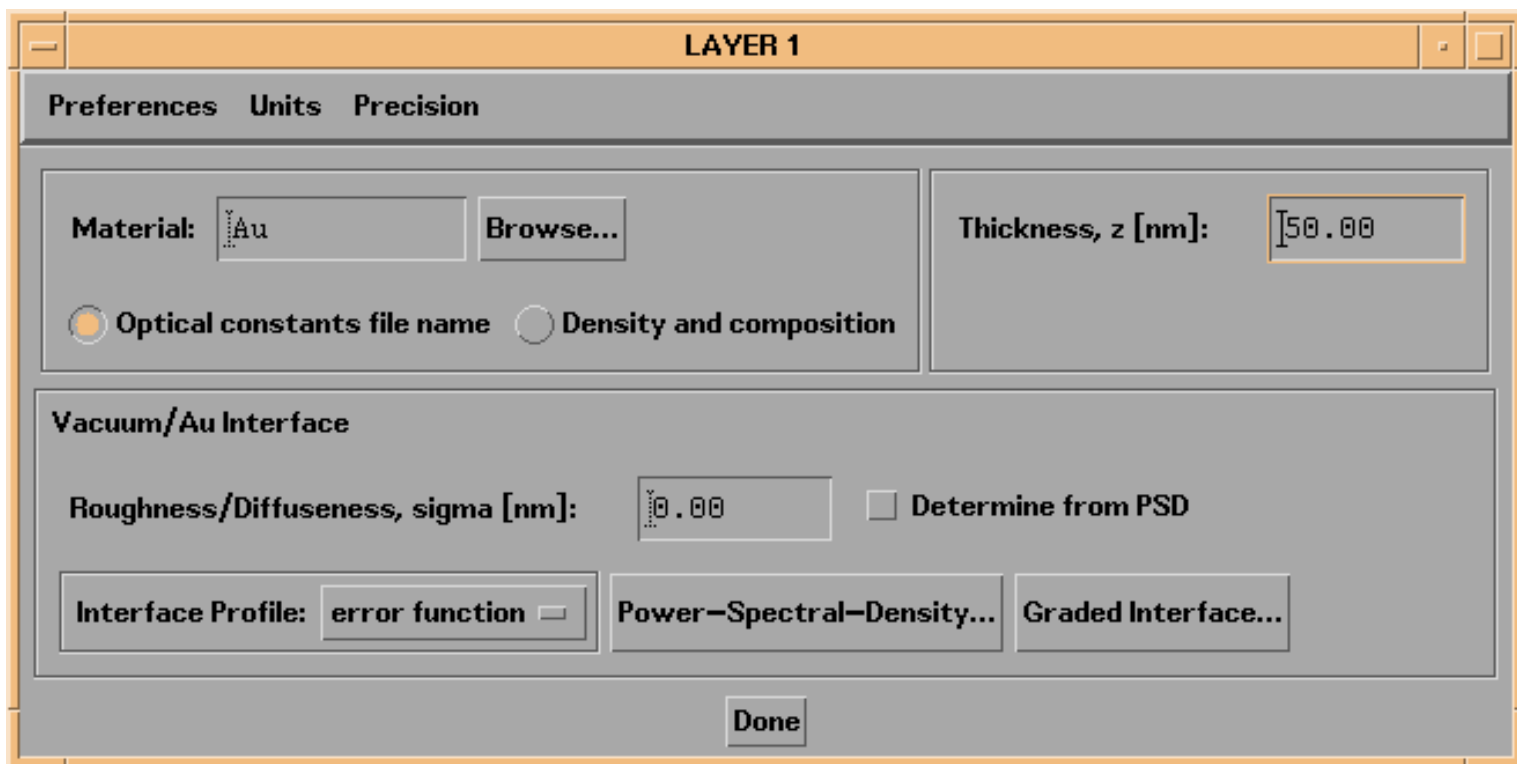
LAYERS

To add a layer to the multilayer stack, press the **Add Layer** button to the right of the *Structure List*. Doing so brings up a **Layer** widget like the one shown in [Figure 2.1.3](#) in the previous section. Use the techniques described in that section to specify the layer material.

For every layer, you must also specify the layer thickness, by entering the desired thickness value in thickness entry area. You can specify the desired length units (i.e., angstroms, nanometers, or microns) and precision using the **Units** and **Precision** menus.

Note: length units and precision - which affect layer thicknesses and interface parameters - are *global*, i.e., all layers are described by the same length units and precision, so any changes made in one **layer** widget will affect all others.

As an example, shown in the next figure is the layer widget associated with a layer of gold, 50 nm thick.

Figure 2.2.3 IMD **Layer** widget corresponding to a 50-nm-thick layer of gold.

To add more layers to the structure, continue to press the **Add Layer** button (to the right of the *Structure List*.) Each new layer will be inserted into the stack just below the currently selected (highlighted) layer. Use the **Move Up** and **Move Down** buttons to change the position of layers in the stack, and use the **Remove** and **Remove All Layers** buttons to delete selected layers.

The layers you create are listed in the *Structure List*, and are numbered consecutively (starting with layer number 1) from the top down (towards the substrate.) Layers can be edited either by double-clicking on the corresponding element listed in the *Structure List*, or by selecting a layer from the *Structure List* and then pressing the **Edit** button.

PERIODIC MULTILAYERS

Any number of layers can be grouped together to create periodic multilayers. There are two ways to define such multilayers:

A. Layers that have already been added to the structure can be grouped by pressing the **Group** button (to the right of the *Structure List*), once you have selected (highlighted) the layer that you want to designate as the top of the group in the *Structure List*. You will then be asked to choose which layer to designate as the bottom of the group; you must choose from a list of available layers (or multilayers) that will be presented. You can then edit the periodic multilayer by double-clicking on the corresponding element in the *Structure List*, or by selecting the periodic multilayer in the *Structure List* and then pressing the **Edit** button.

or

B. Press the **Add Multilayer** button (to the right of the *Structure List*). You will be prompted to enter the

number of different layer elements (NOT the total number of layers!) to be contained in the new periodic multilayer. Once you have entered the desired number of layer elements (and pressed the **OK** button), a widget appears that allows you to specify the periodic multilayer parameters.

Once layers have been grouped to form a periodic multilayer, these layers will be indented in the *Structure List*, and an additional line describing the multilayer parameters will be added to the list. For example, Figure 2.2.4 shows the STRUCTURE area of the main IMD widget after defining a periodic multilayer consisting of two layers. An example of the corresponding **Multilayer** widget is shown in Figure 2.2.5:

Figure 2.2.4 The STRUCTURE area of the main IMD widget after defining a 2-element periodic multilayer.

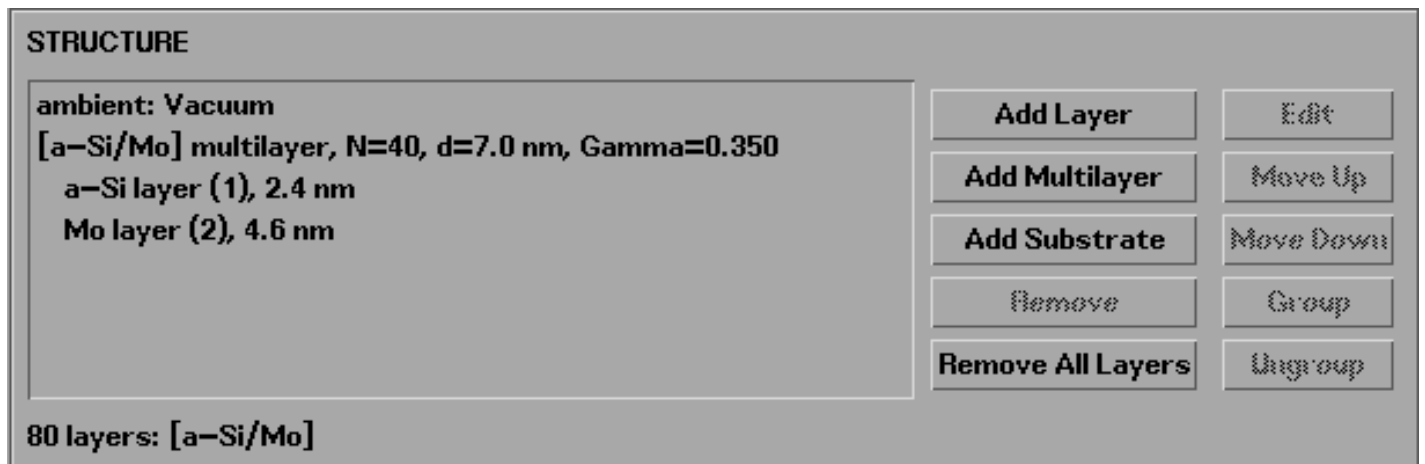
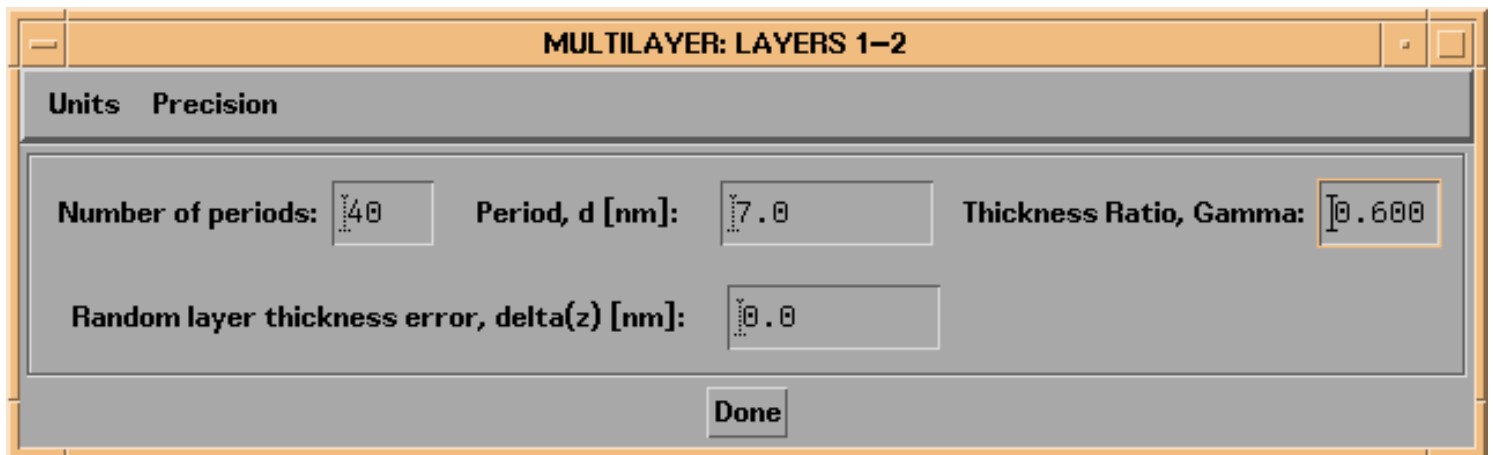


Figure 2.2.5 IMD *Multilayer* widget.



The **Multilayer** widget includes an area to enter parameters specific to the multilayer.

For a periodic multilayer, you must specify the **Number of Periods, N**, i.e., the number of repetitions of the individual layers that comprise the periodic multilayer. For example, a multilayer consisting of three different layers - A, B, and C - with $N=2$ periods, would contain a total of 6 layers: A/B/C/A/B/C.

The **Period, d** of the multilayer is determined by the thickness of the individual layers that comprise the periodic multilayer. For example, if the A, B, and C layers just described had thickness of 1, 2, and 3 nm, respectively, then the multilayer period would be $d=(1 + 2 + 3)= 6$ nm. (The total thickness of the periodic multilayer is $N \times d$, or 12 nm in this example.)

The multilayer period is indicated in both the *Structure List* and on the **Multilayer** widget. *The period can be specified directly only in the case of periodic multilayers consisting of just two layers*, in which case the **Layer Thickness Ratio, Gamma** (which is defined as the thickness of the top layer divided by the multilayer period) is also indicated and available for direct specification.

If desired, you can also specify a **Random layer thickness error, $\delta(z)$** , in order to simulate, for example, the thickness errors that might actually occur during the growth of a multilayer film. Doing so will result in each individual layer thickness differing from the specified value by a random amount; the errors follow a Gaussian distribution with width **$\delta(z)$** . For example, again using the A, B, C layers with thicknesses 1, 2, and 3 nm, with **N=2**, choosing **$\delta(z)$** =.1 nm might result in the following thicknesses: A(.997 nm)/B(2.05 nm)/C(3.01 nm)/A(1.05 nm)/B(2.01 nm)/C(3.05 nm). Note that an error will occur if you specify a random thickness error large enough to cause negative layer thicknesses.

Once you have defined a periodic multilayer, you can use the **Move Up** and **Move Down** buttons to rearrange the order of the layers (or multilayers) within the multilayer. You can remove multilayer elements (i.e., layers or multilayers) using the **Remove** button (once you have selected the element you wish to remove), and you can use the **Add Layer** and **Add Multilayer** buttons to insert more layers or multilayers inside of an existing multilayer.

Note: To add layers or multilayers *after* an existing multilayer, highlight the top line of the existing multilayer in the *Structure List* before pressing the **Add Layer** or **Add Multilayer** button.

You can edit layers or multilayers by double-clicking in the *Structure List*, or by using the **Edit** button after selecting the layer or multilayer you wish to edit.

DEPTH-GRADED MULTILAYERS

It's possible in IMD to vary with depth the layer thicknesses of any or all of the individual layers that comprise a periodic multilayer. Figure 2.2.6 shows the layer widget for a layer element that is part of a periodic multilayer containing 200 periods: note the button labelled '**Depth Grading...**'. Figure 2.2.7 shows the **Layer Thickness Depth Grading** widget that appears when the **Depth Grading...** button is pressed.

Figure 2.2.6 IMD **Layer** widget for a layer that is part of a periodic multilayer consisting of 200 bilayers.

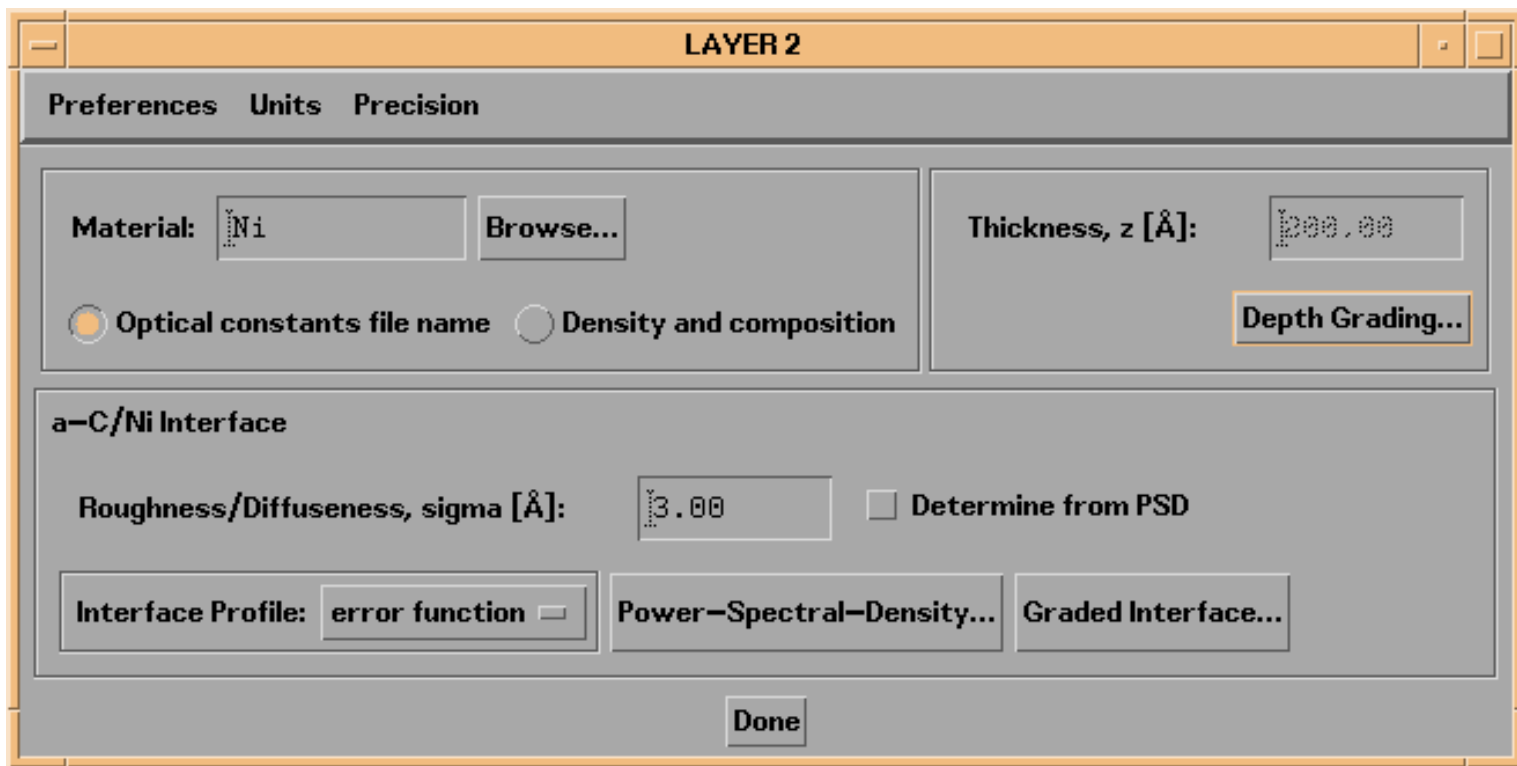
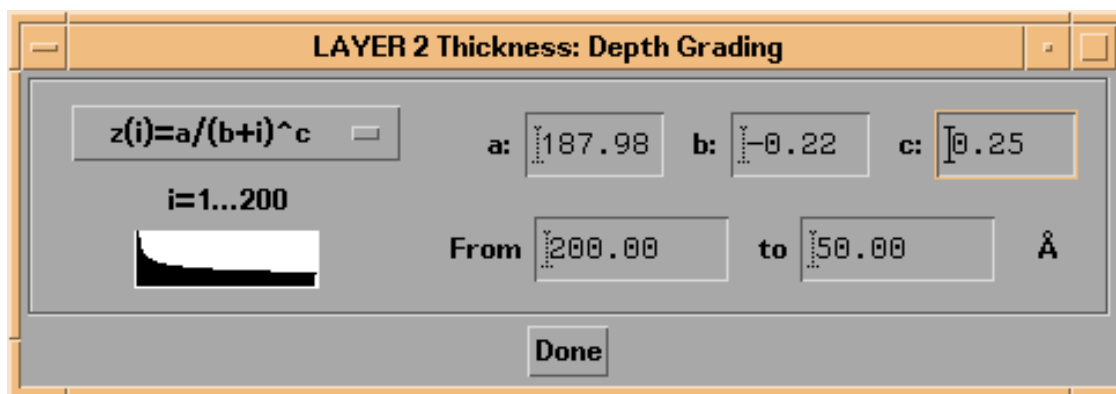


Figure 2.2.7 IMD Layer Thickness Depth Grading widget for the layer shown in Figure 2.2.6.



Four different depth grading profiles are available:

Parabolic: $z(i)=a+b*i+c*i^2$

Exponential: $z(i)=a+b*\exp(c*i)$

Logarithmic: $z(i)=a+b*\ln(c*i)$

Power-Law: $z(i)=a/(b+i)^c$

where i is the layer index (starting with the top-most layer in the group), $z(i)$ is the thickness of layer i , and a , b , and c are parameters you specify. In Figure 2.2.7, a power-law depth-grading profile is shown: for the a , b , and c parameters indicated in the figure, the resultant top layer ($i=1$) thickness is 200 angstroms and the bottom layer ($i=200$) thickness is 50 angstroms. A plot of the layer thickness variation is shown in the widget as well.

Note: when you enter values for the **a** and **b** parameters, the resultant top- and bottom-layer thicknesses are computed (using the currently defined **c** parameter); alternatively, you can specify the top- and bottom-layer thicknesses, and the resultant **a** and **b** parameters are computed. Specifying the **c** parameter will result in the computation of new **a** and **b** parameters based on the current top- and bottom-layer thicknesses. (Got that?)

Each layer in a multilayer can have its own depth grading profile (or no depth grading at all, of course). However, if you wish to grade every layer element in a multilayer by the same relative amount, you can either specify identical profiles and proportional depth grading parameters for each layer, or else make use of Coupled Parameters, as described in [Section 2.3](#) (the latter method is much simpler.) See [Section 2.5](#) for a graded multilayer example.

NESTED MULTILAYERS

Periodic multilayers can be nested inside one another if so desired. For example, suppose you wish to create a multilayer stack consisting of five different materials (A, B, C, D, E), arranged as follows:

A/B/C/D/E/D/E/A/B/C/D/E/D/E/A/B/C/D/E/D/E.

A shorthand notation for this 21-layer structure is [A/B/C/[D/E]x2]x3

One way to create such a structure would be as follows: (a) Use the **Add Multilayer** button to create a periodic multilayer consisting of 2 periods of the D and E layers; (b) Use the **Add Layer** button three times to insert the A, B, and C layers on top of the [D/E] multilayer, and then (c) use the **Group** button to define the A/B/C/[D/E] multilayer, by selecting the A layer as the top element of the group, and the [D/E] multilayer as the bottom element.

LAYER-DATA FILES

In some cases, for example when you wish to model a structure consisting of a very large number of unique layers, rather than using the **Add Layer** button repeatedly, it is more convenient to read in a text file containing the required layer information (i.e., materials, thicknesses, etc.). To do this, use the **File->Open Layer-Data File** option from the menu bar. You will find instructions on how to create such a file in the `sample_layerfile.txt` file (or in the `.xcl`, `.wkz`, and `.slk` spreadsheet versions of this file) located in the directory called `examples.dir` in the `imd` directory. Also, once you have created a layer structure in IMD, you can save the layer information to a Layer-Data file using the **File->Save to Layer-Data File** option from the menu bar.

Note: when saving to a layer-data file, all layer-group information is lost.

Note: layer-data files can only use materials specified by reference to optical constant data files; materials specification by density and composition is not possible with layer-data files.

SUBSTRATE

The final component of an IMD structure is the substrate. Use the **Add Substrate** and **Remove** buttons to add and remove a substrate. A substrate is specified in a way entirely analogous to the way a layer is specified, except that a substrate has no thickness, i.e., a substrate is a semi-infinite slab of material. If no substrate is selected, the ambient material is used on both sides of the multilayer stack.

Note: a structure consisting of just the ambient and a substrate is valid, allowing you to simulate the optical properties of a front-surface mirror.

INTERFACES

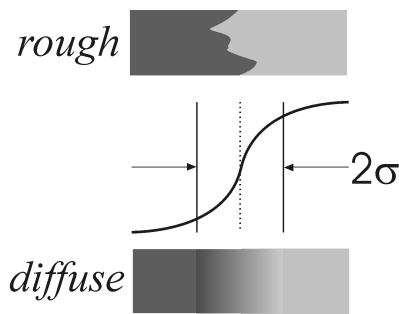
Interface imperfections, i.e., interfacial roughness and diffuseness, have the effect of reducing the specular reflectance of an interface either by scattering light into non-specular directions, in the case of interfacial roughness, or by increasing the transmittance of the interface, in the case of interfacial diffuseness. A number of options are available in IMD to account for the effects of imperfect interfaces on the specular and non-specular optical functions. These options are described below.

Note: Each interface in the IMD structure is described by its own set of interface parameters. Specifically, you can specify the interface parameters for the top surface of the substrate and the top surface of every layer element. In the case of periodic multilayers, note that there are two types of interfaces associated with the top layer in the stack. Thus, for example, in the case of a periodic multilayer containing A and B layers, with A on top of B, there are three different types of interfaces: A-on-B, B-on-A, and ambient-on-A. (Assuming there are no other layers on top of the A/B periodic multilayer.)

MODIFIED FRESNEL COEFFICIENTS: INTERFACE WIDTHS AND INTERFACE PROFILE FUNCTIONS

For the calculation of specular optical functions in IMD, the modified Fresnel coefficient formalism is used, as described in reference [2]. In the case of specular optical functions, the effects of interfacial roughness and interfacial diffuseness are indistinguishable: both types of imperfections reduce the reflectance of the interface. Thus, the interface can be characterized simply in terms of an interface profile function, $p(z)$ (described below) and the interfacial width, σ , as shown in Figure 2.2.8.

Figure 2.2.8. Imperfect interfaces: roughness and diffuseness.



In the case of a purely rough interface, the value of σ refers to the rms interfacial roughness, σ_r . In the case of a purely diffuse interface, σ refers to the interfacial diffuseness, σ_d . In the general case of an interface that is both rough and diffuse, $\sigma = \sqrt{\sigma_r^2 + \sigma_d^2}$.

The interface profile function, $p(z)$, is defined as the normalized, average value along the z direction of the dielectric functions, $\epsilon(\mathbf{x})$:

$$p(z) = \frac{\iint \epsilon(\mathbf{x}) dx dy}{(\epsilon_i - \epsilon_j) \iint dx dy}$$

where

$$\epsilon(\mathbf{x}) = \begin{cases} \epsilon_i, & z \rightarrow +\infty \\ \epsilon_j, & z \rightarrow -\infty \end{cases}$$

The resultant loss in reflectance due to interface imperfections is approximated in IMD by multiplying the Fresnel reflection and transmission coefficients by the functions $w(s)$, the Fourier transform of $w(z)=dp/dz$, as described below. Five types of interface profile functions are available in IMD. These functions, and their Fourier transforms, are summarized in Table 2.2.1.

Table 2.2.1. Interface profile functions and Fresnel coefficient modification factors available in IMD.

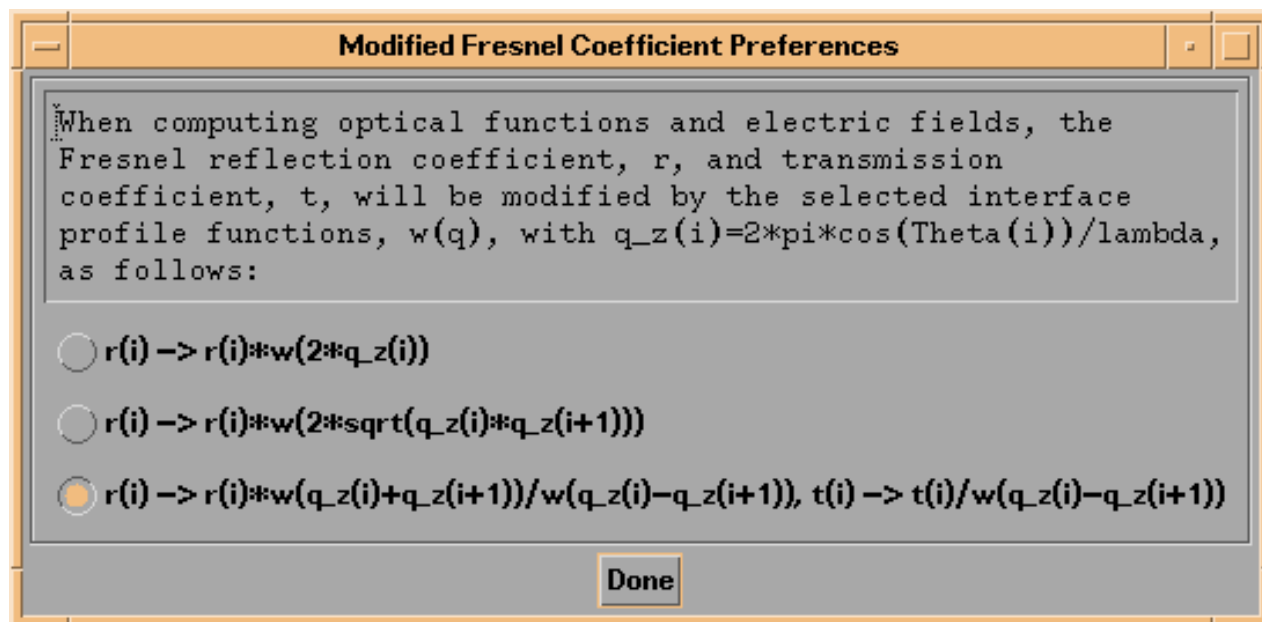
	$p(z)$	$\tilde{w}(s)$
Error Function	$\frac{1}{\sqrt{\pi}} \int_{-\infty}^z e^{-t^2/2\sigma^2} dt$	$e^{-s^2\sigma^2/2}$
Exponential	$\begin{cases} \frac{1}{2} e^{-\sqrt{2}z/\sigma}, & z \leq 0 \\ 1 - \frac{1}{2} e^{-\sqrt{2}z/\sigma}, & z > 0 \end{cases}$	$\frac{1}{1 + s^2\sigma^2/2}$
Linear	$\begin{cases} 0, & z < -\sqrt{3}\sigma \\ \frac{1}{2} + \frac{z}{2\sqrt{3}\sigma}, & z \leq \sqrt{3}\sigma \\ 1, & z > \sqrt{3}\sigma \end{cases}$	$\frac{\sin(\sqrt{3}\sigma s)}{\sqrt{3}\sigma s}$
Sinusoidal	$\begin{cases} 0, & z < -a\sigma \\ \frac{1}{2} + \frac{1}{2} \sin\left(\frac{\pi z}{2a\sigma}\right), & z \leq a\sigma \\ 1, & z > a\sigma \end{cases}$ $a = \pi / \sqrt{\pi^2 - 8}$	$\frac{\pi}{4} \left(\frac{\sin(a\sigma s - \pi/2)}{a\sigma s - \pi/2} + \frac{\sin(a\sigma s + \pi/2)}{a\sigma s + \pi/2} \right)$
Step	$\frac{1}{2} [\delta(z + \sigma) + \delta(z - \sigma)]$	$\cos(\sigma s)$

As can be seen in Figures [2.2.3](#) and [2.2.6](#) above, a droplist on the **Layer** widget is used to select an interface profile function. The sigma value can be entered on the **Layer** widget as well, or, as will be described below, when you select the **Determine from PSD** button, the sigma value can be computed directly from the power-spectral-density function.

You can also specify precisely how you wish to modify the Fresnel coefficients used to compute specular optical functions, specular electric field, and the electric fields used to compute non-specular optical functions. The **Modified**

Fresnel Coefficient Preferences widget, shown in Figure 2.2.9, is available from either the **File->Preferences** menu option on the main IMD widget, or from the **Preferences** menu option available on all **Layer** and **Substrate** widgets. As shown in Figure 2.2.9, there are three options available:

Figure 2.2.9. Fresnel coefficient modification options.



In the first option, the Fresnel reflection coefficient at the top surface of layer i is multiplied by $w(2q_z(i))$, where $q_z(i) = 2\pi \cos(\Theta(i))/\lambda$, $\Theta(i)$ is the propagation angle in the layer (determined from the incidence angle through Snell's law,) and λ is the wavelength of light. The function w corresponds to the interface profile function you specify, as in Table 2.2.1.

In the second option, the reflection coefficient is multiplied by $w(2\sqrt{q_z(i)q_z(i+1)})$, (the so-called Nevot-Croce factor,) in accord with the formalism described in reference [3] which is valid below the critical angle of total external reflection in the X-ray region.

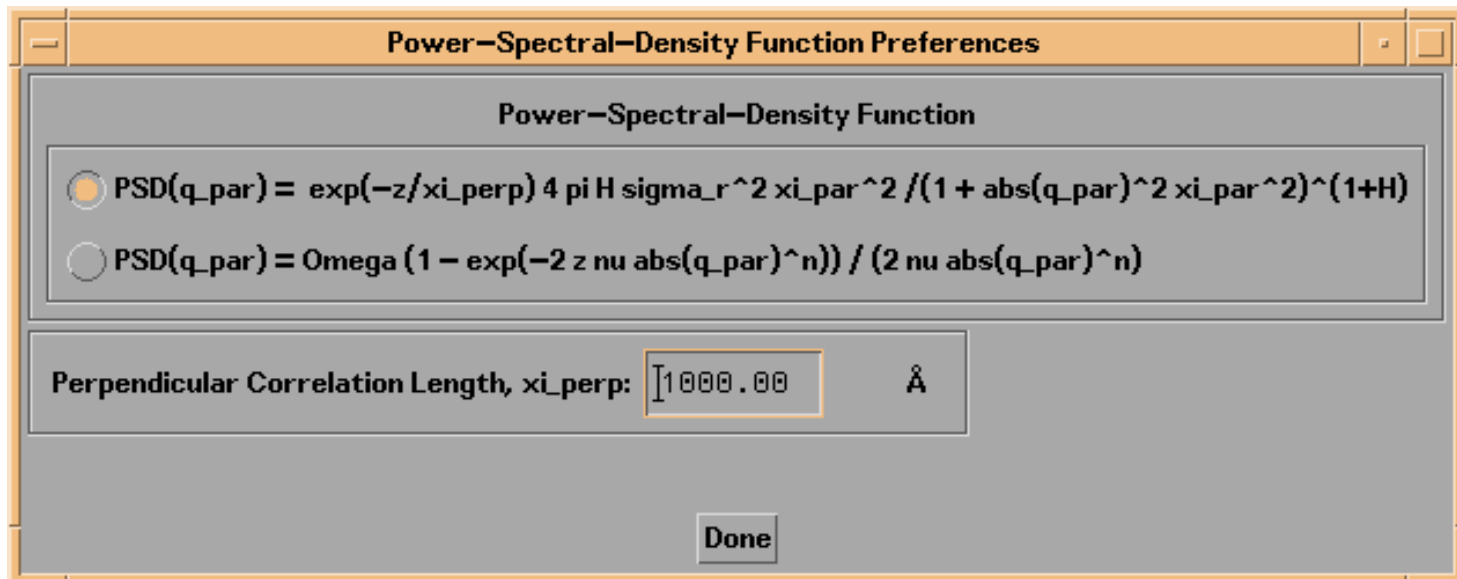
In the third option, both the reflection and the transmission coefficients are modified, as indicated in the Figure, in accord with the formalism described in reference [4].

POWER-SPECTRAL-DENSITY FUNCTIONS

For the calculation of non-specular optical functions, it is necessary to specify the power-spectral-density (PSD) function of each interface in the structure. The PSD function can also be used to compute the sigma values used in specular optical functions computations, by selecting the **Determine from PSD** button on the associated **Layer** or **Substrate** widget.

Two power-spectral-density functional forms are available in IMD, as indicated in the **Power-Spectral-Density Function Preferences** widget shown in Figure 2.2.10. This widget is accessible either from the **File->Preferences** menu option, or from the **Preferences** menu available on all **Layer** and **Substrate** widgets.

Figure 2.2.10. The **Power-Spectral-Density Function Preferences** widget.



In the case of the first PSD function shown in Figure 2.2.10 (described in reference [10],) each interface is characterized by three parameters: the interfacial roughness, σ_r , the in-plane, or parallel correlation length, ξ_{par} , and the so-called jaggedness factor, H . In addition, a (global) vertical or perpendicular correlation length parameter, ξ_{perp} , can be specified as well, in order to account for correlated roughness in a multilayer. Following the formalism described in reference [8], the vertical correlation function describing the correlation between two interfaces i and j is given by

$$c_{ji}^{\perp} = \exp\left(-\sum_{n=j_{\leftarrow}}^{j_{\rightarrow}-1} d_n / \xi_{\perp}\right)$$

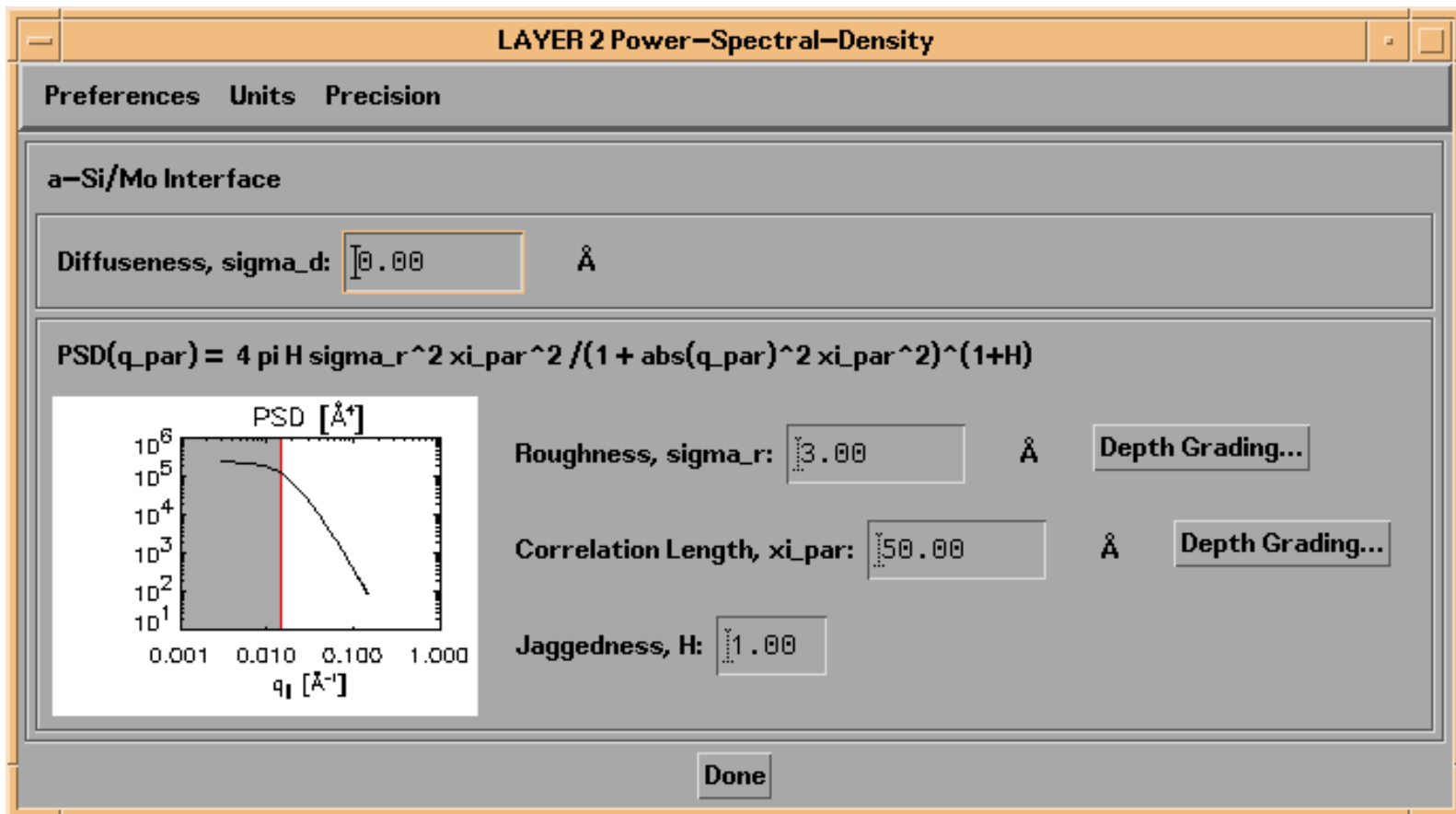
where $j_{\leftarrow} = \min(j, i)$, and d_n is the thickness of layer n . The perpendicular correlation length, ξ_{perp} , is specified on the **Power-Spectral-Density Function Preferences** widget.

The second PSD function available is based on the stochastic model of thin film growth and erosion described in reference [9]. In this case, the (intrinsic) PSD at each interface is characterized by the three parameters Ω , the volume element growth parameter, ν , the relaxation coefficient, and the exponent n ; the intrinsic PSD also depends on the layer thickness z . (In the case of the substrate PSD, z does not necessarily refer to the substrate thickness, but is just another parameter that you must specify.) Note that in accord with this model of film growth, the total PSD at a given interface is equal to the intrinsic PSD at that interface (as specified by the $\Omega/\nu/n/z$ parameters for that interface) plus the contribution of the PSD's of all the underlying interfaces; the amount of roughness that is replicated from layer to layer depends on the PSD parameters of each of the interfaces involved. Thus, this PSD model can be used to account for the evolution of roughness throughout a multilayer stack.

Note: The PSD function you select in the **Power-Spectral-Density Function Preferences** widget will apply to all interfaces in the structure you define.

Shown in Figure 2.2.11 is the **Power-Spectral-Density Function** widget associated with a layer that is part of a periodic multilayer, for the case of the $\sigma_r/xi_par/H$ PSD model. This type of widget appears when you press the **Power-Spectral-Density...** button of a **Layer** or **Substrate** widget.

Figure 2.2.11. A **Power-Spectral-Density Function** widget, for the case of the $\sigma_r/xi_par/H$ PSD model.

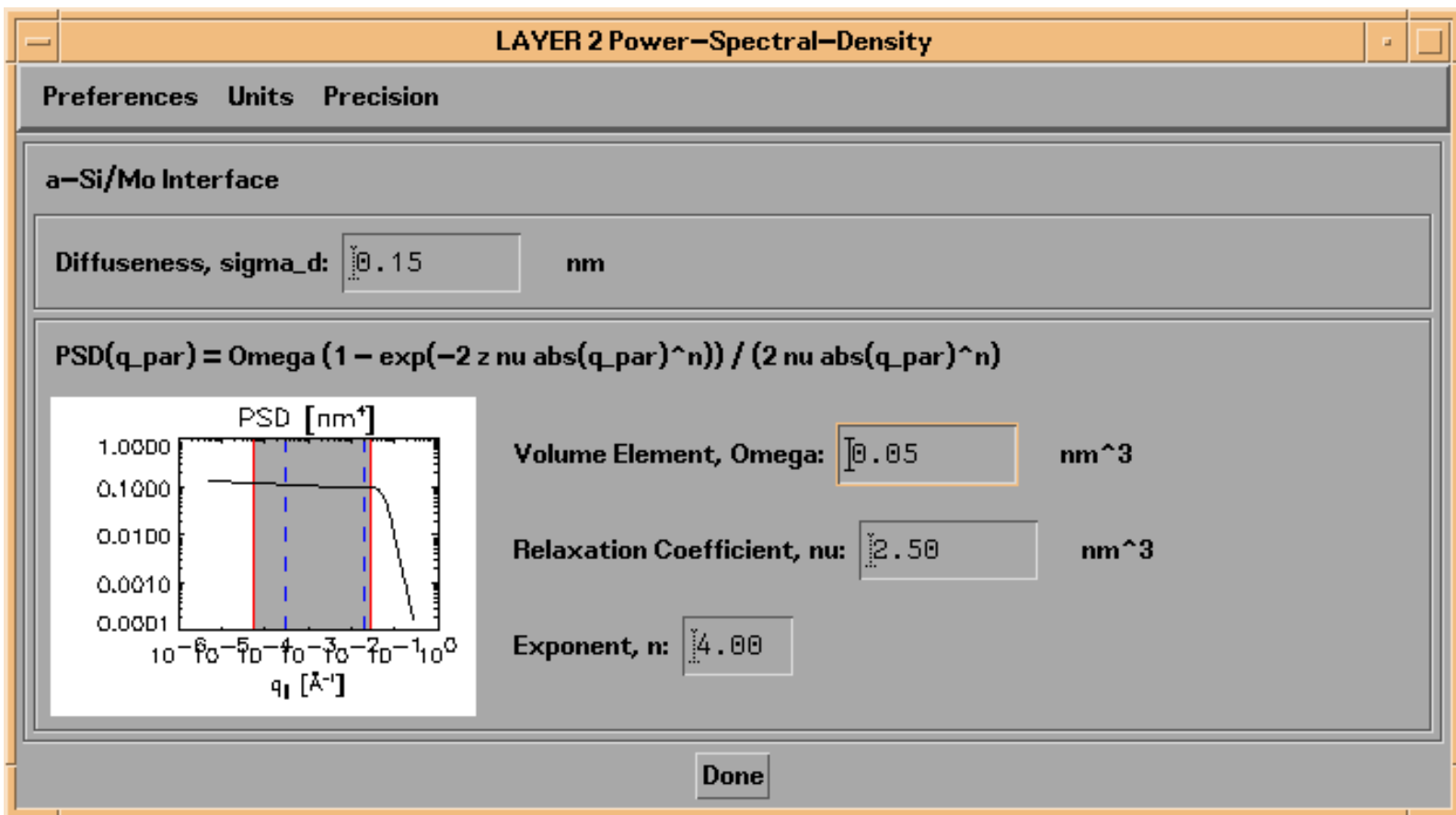


Note that a graph of the PSD function is displayed in the widget, over the range of transverse momentum values, q_{par} associated with the incidence and scattering angles you define, as described in [Section 2.3](#) (The range of q_{par} values associated with the non-specular scattering parameters you define are indicated by the grey region in the plot.)

Note: In the case of layers that are part of periodic multilayers, as in Figure 2.2.11, it is possible to define depth-graded σ_r and xi_par parameters as well, by pressing the **Depth Grading...** buttons shown in the widget. You will then be presented with a **Depth Grading** widget completely analagous to the graded-thickness widgets described above.

Similarly, shown in Figure 2.2.12 is the **Power-Spectral-Density Function** widget for the case of the $\Omega/\nu/n$ PSD model.

Figure 2.2.12. A **Power-Spectral-Density Function** widget, for the case of the $\Omega/\nu/n$ PSD model.



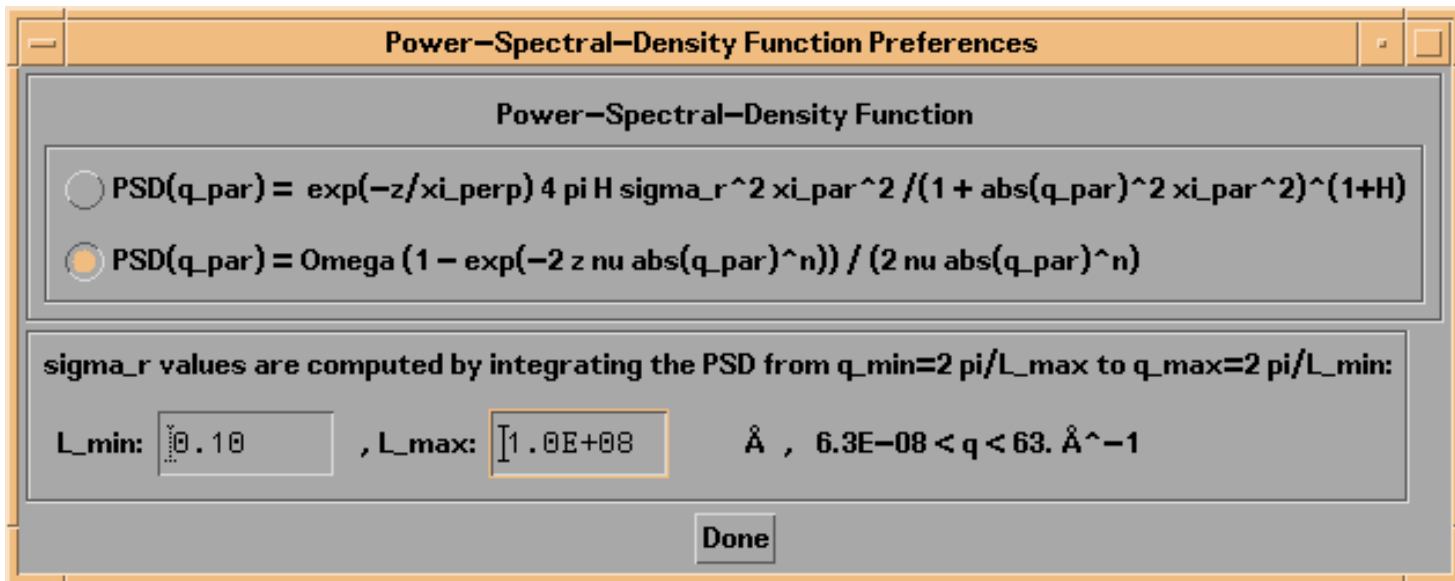
As can be seen in Figures 2.2.11 and 2.2.12, in addition to specifying the PSD parameter values for the interface, you can also specify a value of the interface diffuseness, σ_d . The value of σ_d will be used (along with the interface profile function you select) to compute the modified Fresnel coefficients (using the specified form of the Fresnel coefficient modification factors (Figure 2.2.9)) when computing the electric fields needed for non-specular reflected intensity calculations. (See references 4-8.)

If you have selected the **Determine from PSD** button on a **Layer** or **Substrate** widget, the σ value used for that interface for computing specular optical functions via the modified Fresnel coefficient formalism described above will be equal to the value of $\sqrt{\sigma_r^2 + \sigma_d^2}$. In the case of the $\sigma_r/xi_par/H$ PSD model, the σ_r value used to compute the total σ value is just equal to the value of σ_r that you specify on the PSD parameters widget. On the other hand, in the case of the $\Omega/\nu/n$ PSD model, σ_r^2 is given by:

$$\sigma_r^2 = 2\pi \int_{f_{\min}}^{f_{\max}} \text{PSD}(f) f \, df$$

where $f_{\min} = 1/L_{\max}$, $f_{\max} = 1/L_{\min}$, and L_{\min} and L_{\max} must be specified by you, on the **Power-Spectral-Density Function Preferences** widget, as shown in Figure 2.2.13. The q values (where $q=2\pi f$), corresponding to the values of L_{\min} and L_{\max} you enter, are indicated as dashed blue lines in the PSD plots on the **Power-Spectral-Density Layer** and **Substrate** widgets, as can be seen, for example, in Figure 2.2.12.

Figure 2.2.13. The **Power-Spectral-Density Preferences** widget, showing entry areas for L_{\min} and L_{\max} available when using the $\Omega/\nu/n$ PSD model.

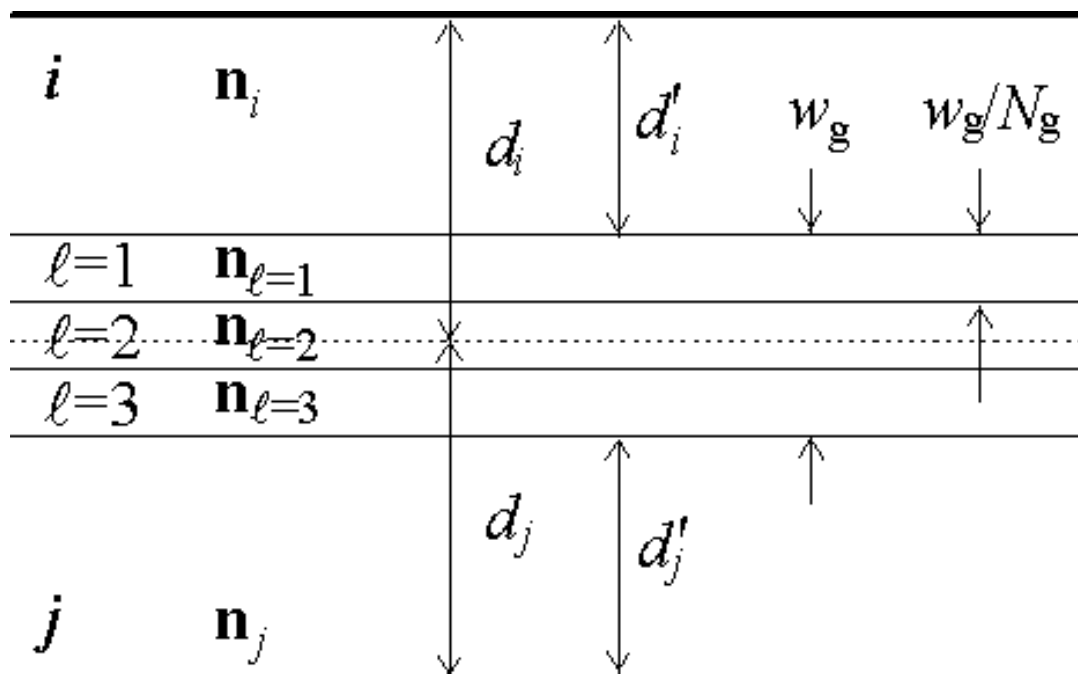


GRADED INTERFACES

Independent of the interface profile function, σ , and PSD parameters you specify for a given interface, in IMD it's also possible to model the effects of a diffuse interface on the specular and non-specular optical functions by specifying a 'graded' interface. That is, an abrupt interface can be replaced by one or more layers whose optical constants vary gradually between the values for the pure materials on either side of the interface.

In IMD, a graded interface is described by three parameters, as shown in Figure 2.2.14: the interface width, w_g , the number of layers comprising the graded interface, N_g , and the distribution factor, X_g , which determines where the graded interface region resides relative to the original abrupt interface (as will be described below.)

Figure 2.2.14. A graded interface.



The optical constants in each of the N_g layers of a graded interface are computed as follows. Consider the graded interface between the i^{th} and j^{th} layers in a multilayer stack. The thickness of each of the N_g graded interface layers is equal to w_g/N_g . The optical constants in the l^{th} graded interface layer are thus given by

$$n_\ell = \frac{(N_g + 1 - \ell)n_i + \ell n_j}{(N_g + 1)}$$

and

$$k_\ell = \frac{(N_g + 1 - \ell)k_i + \ell k_j}{(N_g + 1)}$$

with $l=1, \dots, N_g$. The resulting layer thickness, d_i' and d_j' of the pure materials in the i^{th} and j^{th} layers, respectively, after including the graded interface layers, are given by

$$d_i' = d_i - w_g(1 - X_g)$$

and

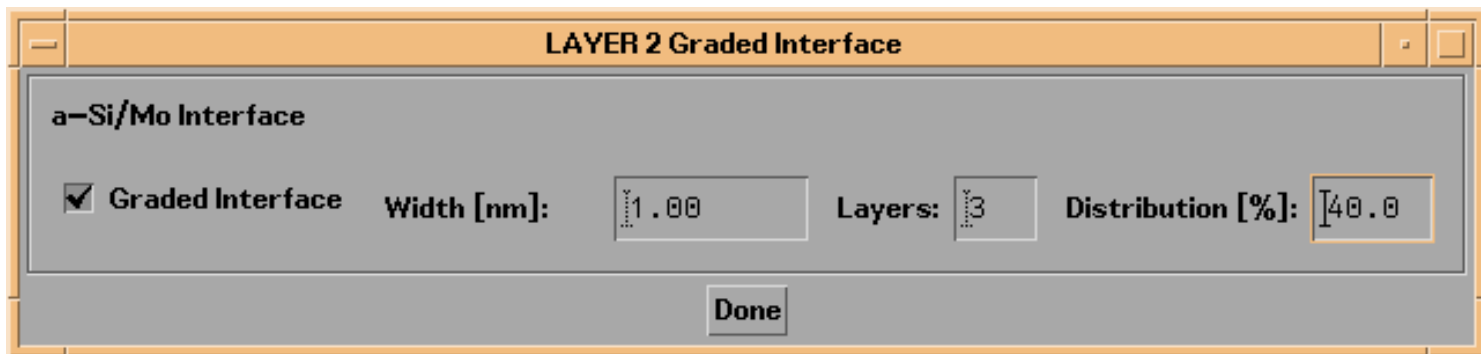
$$d_j' = d_j - w_g X_g$$

with $0 < X_g < 1$. (Note that the total thickness of the two layers - including all the graded interface layers - is constant, i.e., $d_i' + d_j' + w_g = d_i + d_j$.) As an example, a distribution factor of 50% ($X_g = 0.5$) would result in equal reductions of the i^{th} and j^{th} layer thicknesses.

To specify a graded interface in IMD, press the **Graded Interface...** button on the relevant **Layer** or **substrate** widget. Doing so will cause a **Graded Interface** widget to appear, as shown in Figure 2.2.15, in which you can specify values for the graded interface number of layers, the interface width, and the distribution factor.

Note: you must not specify graded interface parameters that result in layer thicknesses less than zero; doing so will cause the optical functions computation to be aborted.

Note: the same interface profile function, sigma, and PSD parameters are applied to every interface in a graded interface.

Figure 2.2.15. A **Graded Interface** widget.

[Back](#) | [Contents](#) | [Next](#)

2.3 Specifying Variables and Coupled Parameters

DEPENDENT VARIABLES

Specifying dependent variables - the optical functions you wish to compute - is simple: just click on the desired variables in the DEPENDENT VARIABLES area of the main IMD widget:

SPECULAR OPTICAL FUNCTIONS / ELECTRIC FIELDS

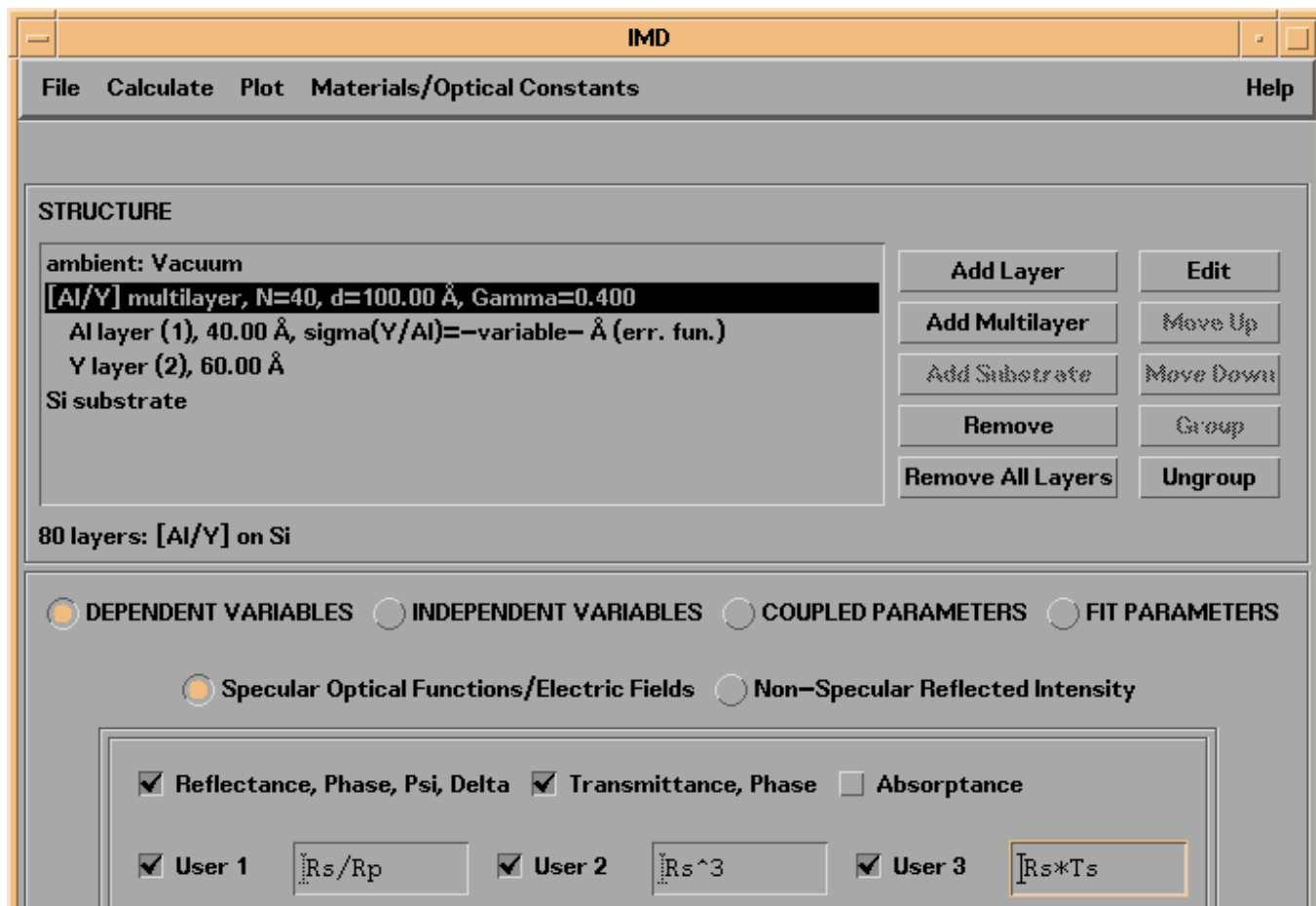
[Figure 2.1](#) shows the main IMD widget as it appears when the **DEPENDENT VARIABLES** button is selected, and the **Specular Optical Functions / Electric Fields** button is selected. Select whichever functions you wish to compute.

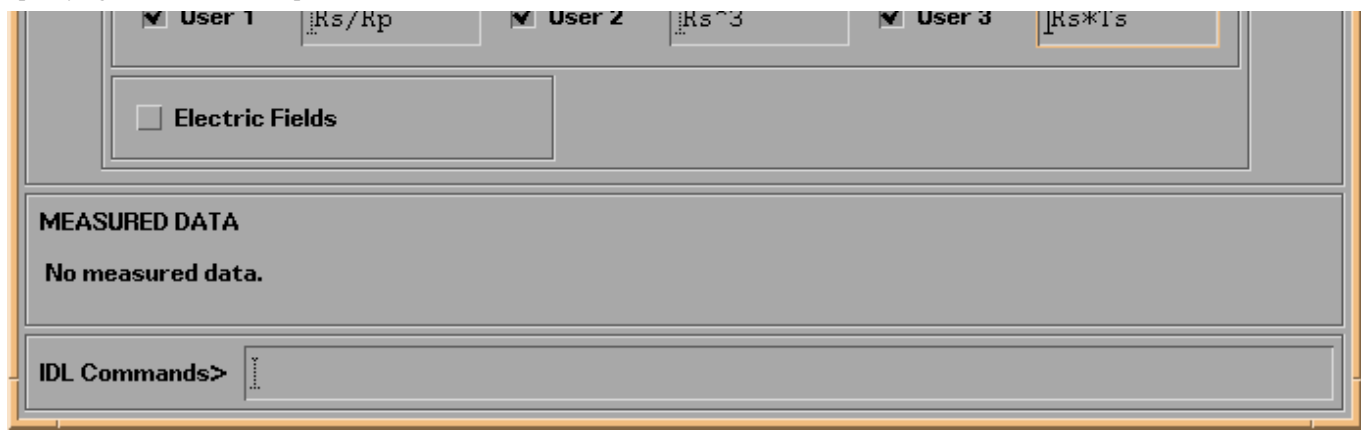
Note that for each specular optical function you select, the program will calculate the values of that property for pure s and pure p polarization, as well as the average value of the property for the specified polarization parameters **f** and **q** (described below). For instance, if you select reflectance as a dependent variable, when you actually perform the calculation the program will compute the reflectances for pure s and p polarization, $R(s)$, and $R(p)$, in addition to the average reflectance $R(f,q)$. In the case of reflectance and transmittance, the program will also compute the phases of the reflected and/or transmitted waves for pure s and pure p polarizations; the ellipsometric psi and delta functions will be computed as well if Reflectance is selected as a dependent variable. Once the calculation is performed, any or all of these variables can be displayed.

USER-DEFINED SPECULAR OPTICAL FUNCTIONS

Once you have selected any specular optical functions (reflectance, transmittance, and/or absorptance) as dependent variables, you can also choose to calculate up to three so-called 'user-defined' optical functions. These functions are completely arbitrary combinations of whatever optical functions you're interested in. For example, to compute the ratio of reflectance for pure s to pure p polarization, you can define a user-function equal to R_s/R_p , as shown in Figure 2.3.1 (i.e., the User 1 function):

Figure 2.3.1 The main IMD widget, showing some user-defined function examples.





User-functions can make use of any of the specular optical functions you wish to calculate, and can also use any other valid IDL functions. The only constraints are that (a) you must use valid IDL syntax, (b) you must use the correct variable names of any IMD optical functions you reference, and (c) the user-functions you calculate must have the same dimensionality as all the other optical functions for a given calculation (an example of an invalid user function is `total(Rs)`, which is a scalar.)

Consult [Appendix B.4](#) for a complete listing of all the IMD specular optical function variable names available for use in user-defined functions.

NON-SPECULAR OPTICAL FUNCTIONS

The non-specular (i.e., diffuse) reflected intensity from a multilayer film can be computed using either a dynamical Born approximation (BA) vector theory, described in reference [4], or the so-called 'Distorted-Wave Born Approximation' (DWBA) formalism, described in references [5-8], a scalar theory which is nonetheless valid below the critical angle of total external reflection in the X-ray region.

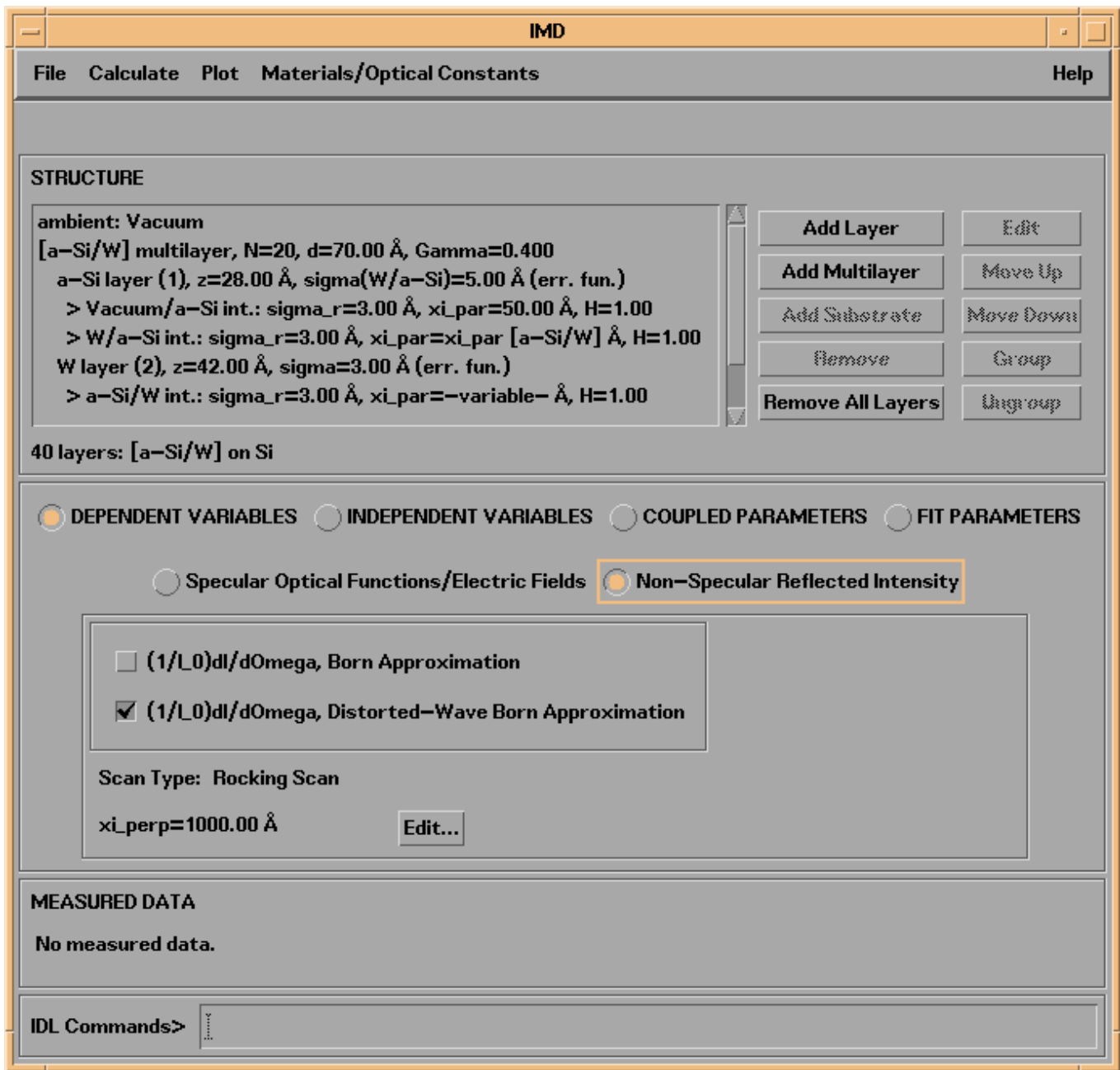
Note: In order to compute non-specular reflected intensities, you must define the power-spectral-density function of each interface in the structure. See [Section 2.2](#) for details on how to do this.

Note: IMD uses the 'small roughness' approximation when computing non-specular reflected intensities, which is to say that the amount of light scattered from any interface is proportional to the power-spectral-density function of that interface.

Note: Please refer to the references listed above in order to appreciate the range of validity of each of these theories.

Figure 2.3.2 shows the main IMD widget as it appears when the **DEPENDENT VARIABLES** button is selected, and the **Non-Specular Optical Functions** button is selected.

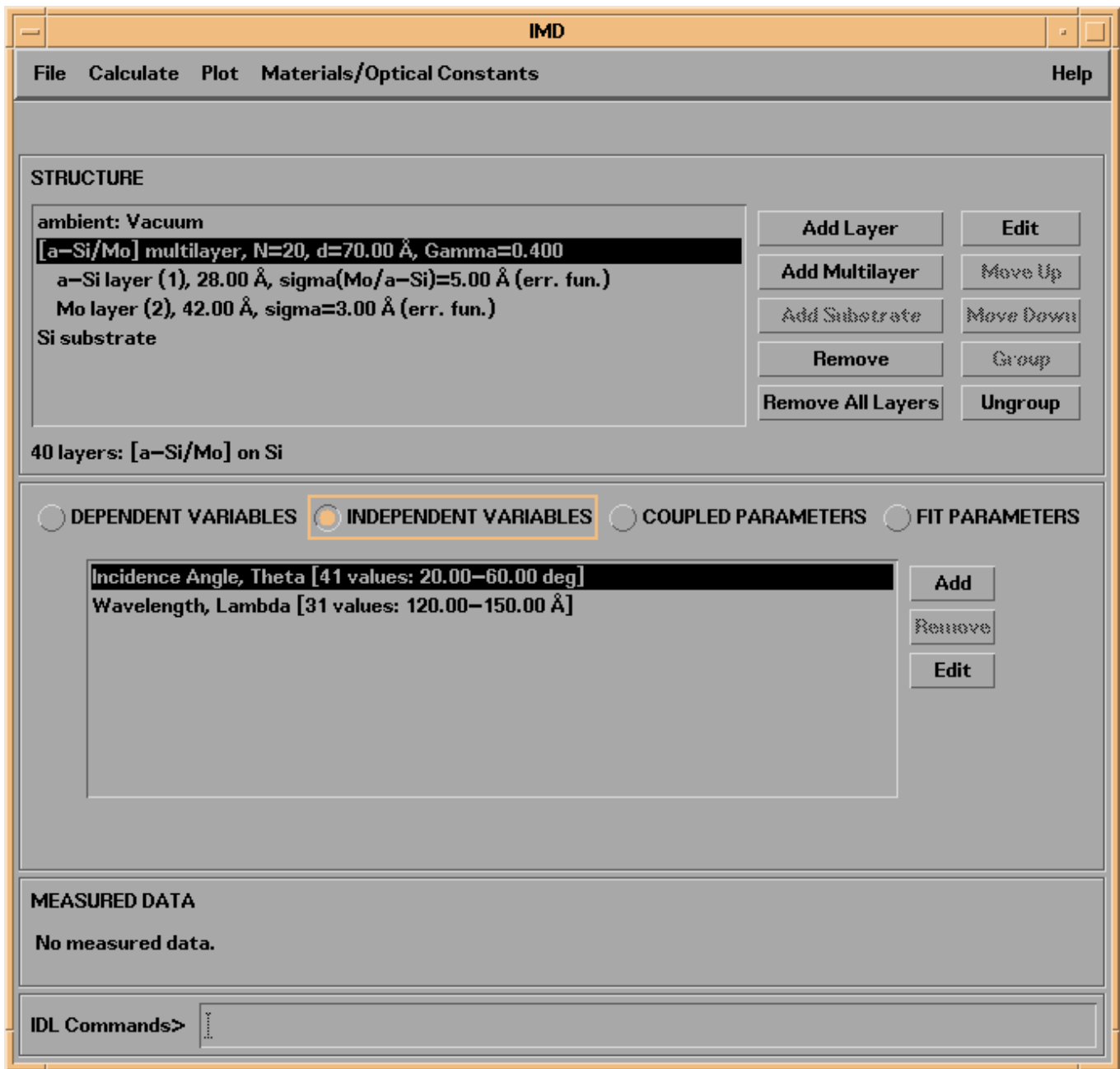
Figure 2.3.2 The DEPENDENT VARIABLES / Non-Specular Optical Functions section of the main IMD widget.



INDEPENDENT VARIABLES

For all computations, you must specify one or more incidence angles, and one or more photon wavelengths or energies. These two independent variables are always listed in the *Independent Variables List*, as shown in Figure 2.2.3

Figure 2.3.3 The main IMD widget as it appears when the **INDEPENDENT VARIABLES** button is selected.



To specify angles and wavelengths (or energies), either double-click on the corresponding *Independent Variables List* element, or use the **Edit** button (to the right of the *Independent Variables List*) after selecting the variable you wish to edit.

The **Incidence Angles** and **Wavelengths/Energies** independent variables widgets are shown in the next two figures:

Figure 2.3.4 Angles widget

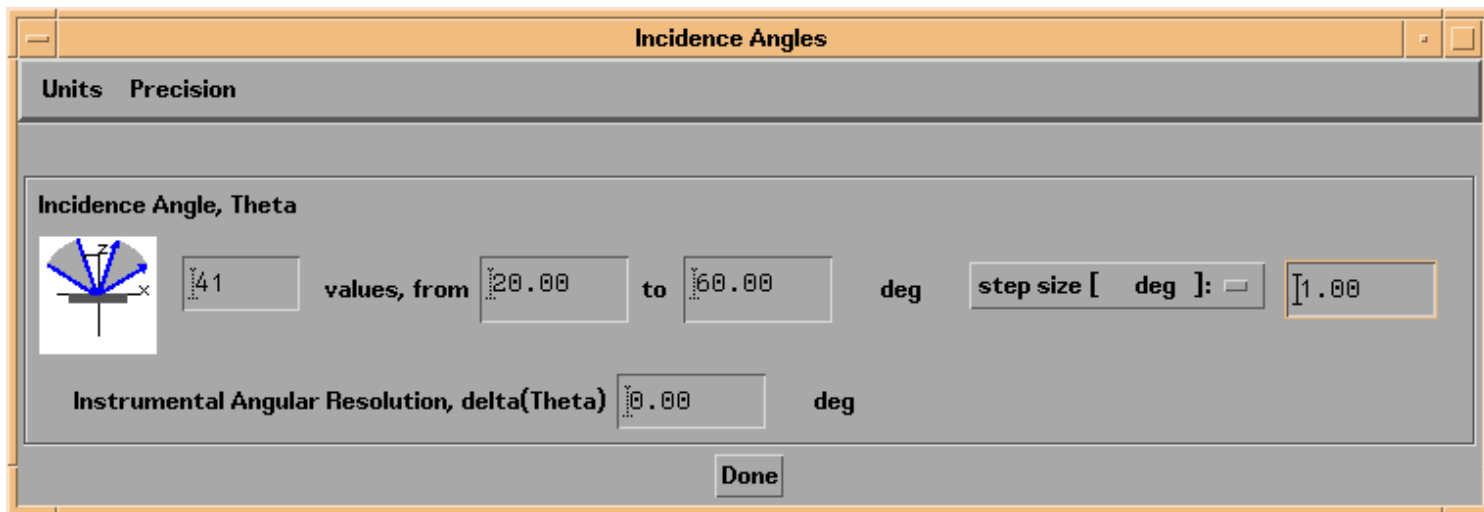
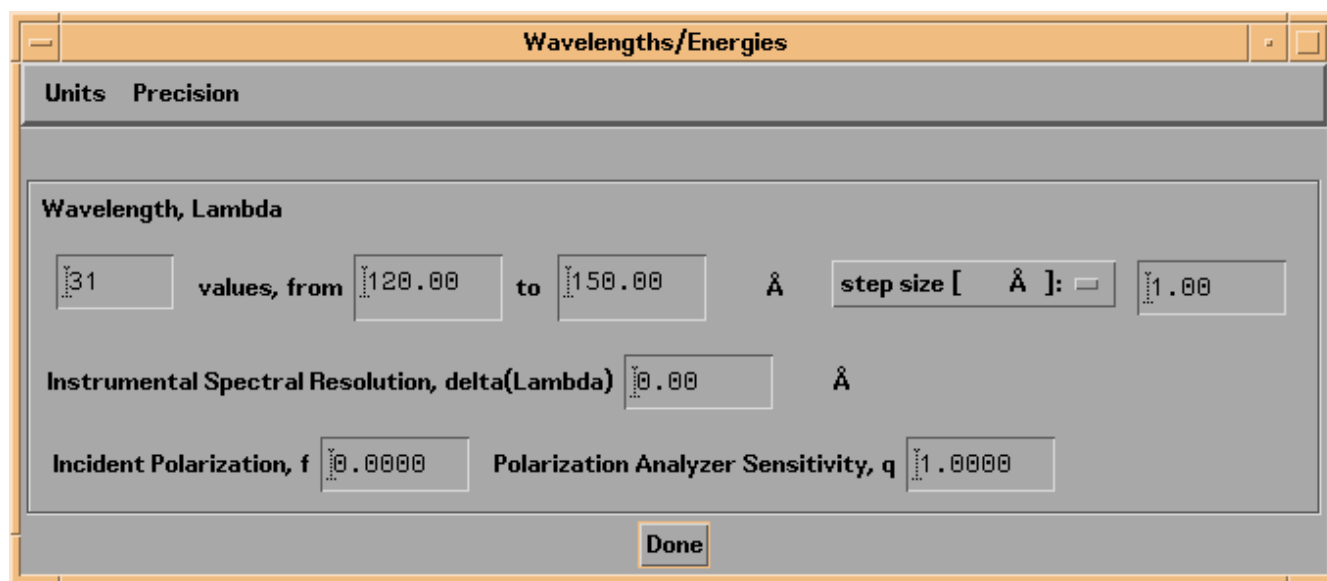


Figure 2.3.5 Wavelengths/Energies widget



As can be seen from these figures, you can specify the desired number of values, the range of values, or the step size for angles and wavelengths (or energies.) (You can also select logarithmic steps, if desired, in which case the step size entry area disappears, as the step size is no longer constant.)

Additionally, if three or more angles (wavelengths/energies) are specified, you can specify the Instrumental Angular Resolution (Instrumental Spectral Resolution), in order to simulate finite instrumental resolution. For example, if you specify an Instrumental Angular Resolution of 0.5 degrees, then the optical functions you calculate will be convolved with a 0.5-degree-wide Gaussian function.

Note: Specifying instrumental resolution has no effect on the Electric Field Intensity calculations.

In the case of wavelengths/energies, you must also specify the **Incident polarization factor, f** , and the **Polarization analyzer sensitivity, q** . The quantity f is defined as the ratio $(I(s)-I(p)) / (I(s)+I(p))$, where $I(s)$ and $I(p)$ are the incident intensities of s and p polarizations. So for pure s-polarization, specify $f=+1$; for pure p-polarization specify $f=-1$, or for unpolarized incident radiation, specify $f=0$. The quantity q is defined as the sensitivity to s-polarization divided by the sensitivity to p-polarization. Specifying a value of q other than 1.0 could be used to simulate, for example, the reflectance you would measure using a detector that (for whatever reason) was more or less sensitive to s-polarization than to p-polarization.

Note: For *specular* optical functions, the values of **f** and **q** that you specify only determine the values of the 'average' optical properties.

For example, the 'average' reflectance is given by:

$$R = (R_s * q * (1 + f) + R_p * (1 - f)) / (f * (q - 1) + (q + 1)).$$

The average transmittance, absorptance, and electric field intensities are given by equivalent expressions. As mentioned above, the optical properties for the pure polarizations are always calculated.

Note: For *non-specular reflected intensity* calculations using the Born approximation, since there is coupling between s and p polarizations (in general), things are more complicated:

For an incident beam having a polarization factor **f**, the s-polarized and p-polarized components of the non-specular reflected intensity, $(1/I_0)dI/d\Omega_s$ and $(1/I_0)dI/d\Omega_p$, respectively, are given by:

$$(1/I_0)dI/d\Omega_s = ((1/I_0)dI/d\Omega_{ss} * (1 + f) + (1/I_0)dI/d\Omega_{ps} * (1 - f)) / 2$$

$$(1/I_0)dI/d\Omega_p = ((1/I_0)dI/d\Omega_{sp} * (1 + f) + (1/I_0)dI/d\Omega_{pp} * (1 - f)) / 2$$

where

$(1/I_0)dI/d\Omega_{ss}$ = reflected intensity component having s polarization, resulting from the fraction of the incident beam having s polarization

$(1/I_0)dI/d\Omega_{sp}$ = reflected intensity component having s polarization, resulting from the fraction of the incident beam having p polarization

$(1/I_0)dI/d\Omega_{ps}$ = reflected intensity component having p polarization, resulting from the fraction of the incident beam having s polarization

$(1/I_0)dI/d\Omega_{pp}$ = reflected intensity component having p polarization, resulting from the fraction of the incident beam having p polarization

The 'average' reflected intensity, i.e., as measured with a detector having polarization sensitivity **q** (as defined above,) is then given by:

$$(1/I_0)dI/d\Omega_a = 2 * ((1/I_0)dI/d\Omega_s * q + (1/I_0)dI/d\Omega_p) / (1 + q)$$

Thus, the values of the s and p components of the scattered intensity depend on the specified value of **f**, while the 'average' scattered intensity depends on both **f** and **q**.

Use the **Units** and **Precision** menus to specify angle and photon units and precision, respectively. That is, you can choose to specify angles relative to normal incidence or relative to grazing incidence, and in degrees, arc-minutes, arc-seconds, or milliradians, and you can choose to specify photon wavelengths in angstroms, nanometers, microns, or cm^{-1} , or photon energies in eV or keV.

In addition to angles and wavelengths (or energies), **any of the (continuously variable) parameters that describe the structure can be designated as independent variables**: optical constants, densities, compositions, layer thicknesses, interface widths, PSD parameters, graded interface parameters, etc. You can also specify the instrumental resolutions and polarization factors (f and q) as independent variables. **Up to eight independent variables can be specified simultaneously.**

To specify additional independent variables, press the **Add** button to the right of the *Independent Variables List* to bring up a menu of

parameters available. Once you add a new independent variable to the *Independent Variable List*, you can edit the variable in the usual way: either by double-clicking or pressing the **Edit** button.

As an example, shown in Figure 2.3.6 is the independent variable widget that would result from specifying a multilayer period **N** to be an independent variable. In this case, I have selected 9 values of **N**, from 5 to 50. Note that in the *Structure List*, shown in Figure 2.3.7, the multilayer description line now reads **N=-variable-**, indicating that **N** is an independent variable. Other specific examples of specifying multiple independent variables will be presented in [Section 2.5](#).

Figure 2.3.6 An independent variable widget corresponding to defining multilayer period **N** as an independent variable.

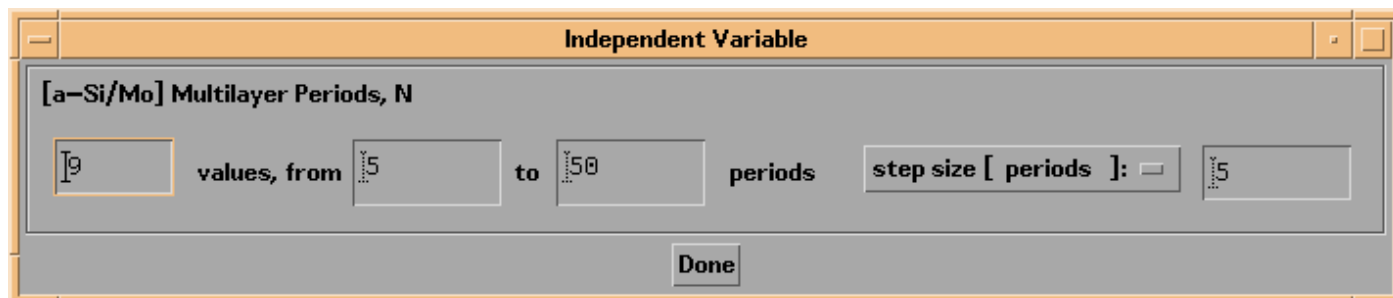
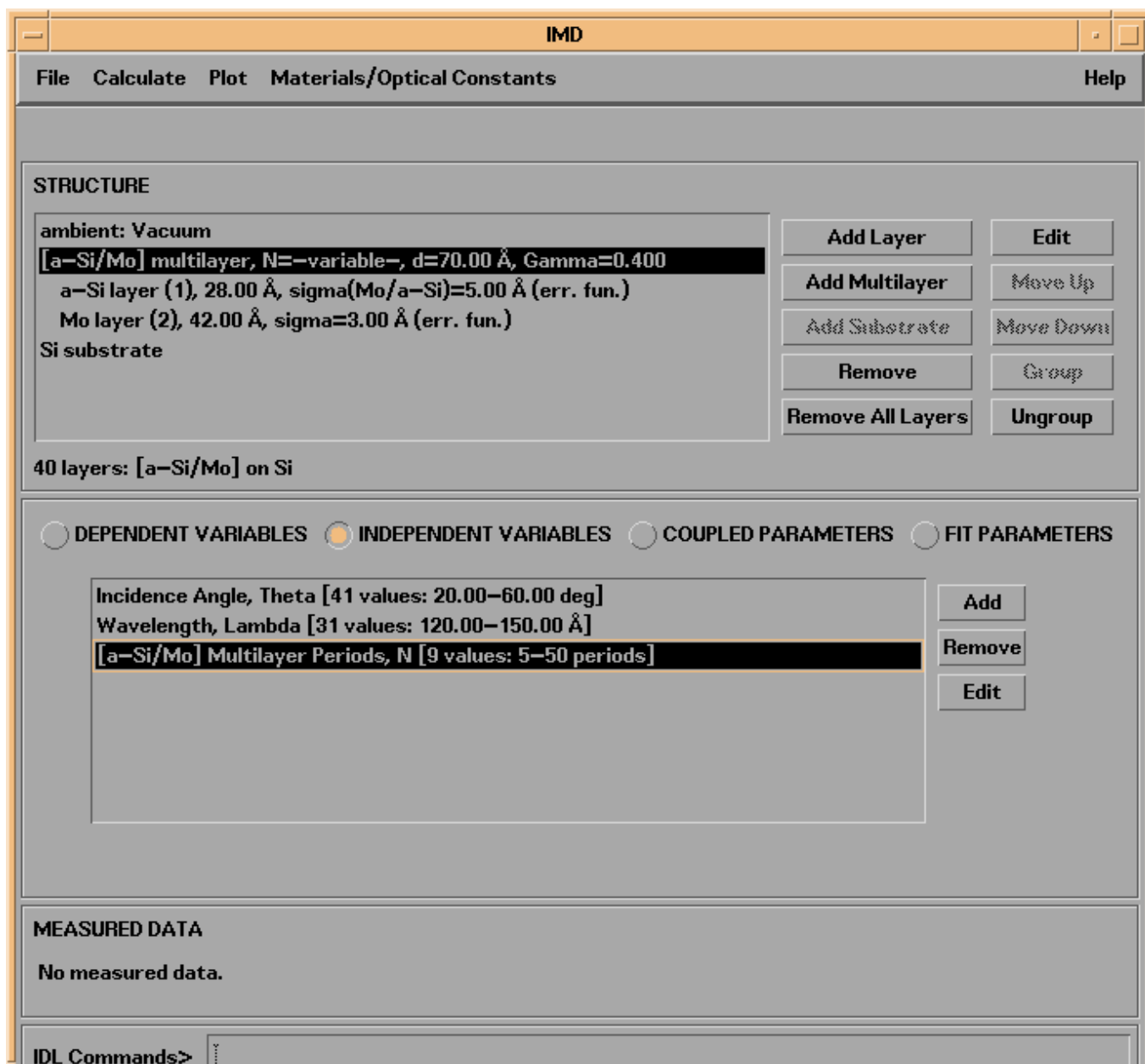
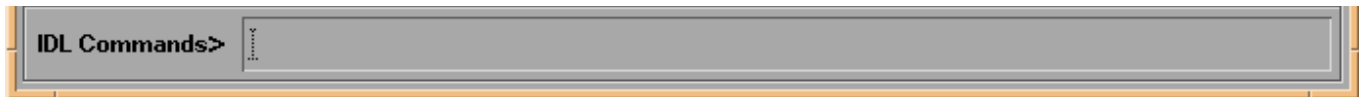


Figure 2.3.7 The main IMD widget showing the multilayer period **N** as an independent variable.

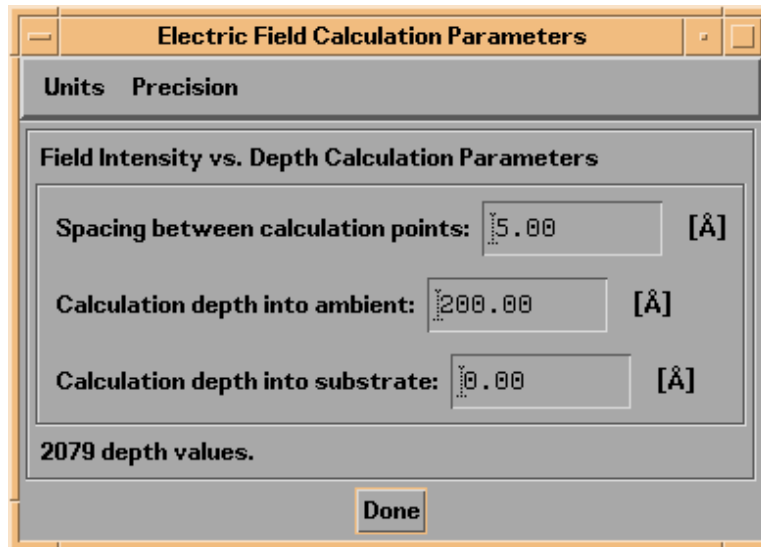




INDEPENDENT VARIABLES SPECIFIC TO ELECTRIC FIELD CALCULATIONS

In the case of electric field intensity calculations, a third independent variable - **depth**, i.e., the position in the structure, measured from the top of the first layer - is always defined as well. This independent variable is not listed in the *Independent Variables List*. It is specified by pressing the button labelled **Parameters...** that appears when you select the **Electric Fields** dependent variable button. The **depth** variable is specified by three parameters, the **spacing between calculation points**, the **calculation depth into the ambient**, and the **calculation depth into the substrate** (if the substrate is present.) Note that the **depth** values are not equally spaced, as it is necessary to calculate the field intensities precisely at the interfaces between layers. So the specified **spacing between calculation points** represents an average value.

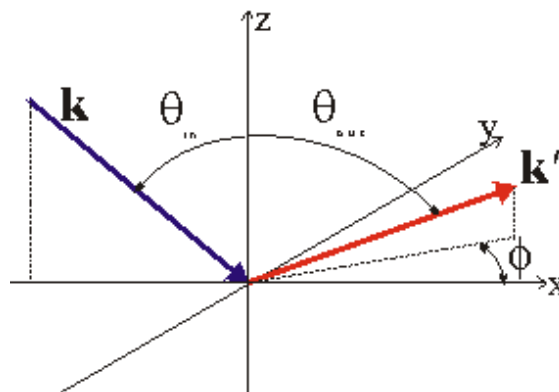
Figure 2.3.8 The **Electric Field Calculation Parameters** widget.



INDEPENDENT VARIABLES SPECIFIC TO NON-SPECULAR OPTICAL FUNCTIONS

For non-specular computations, you must also specify the **scattering angles** and the type of **'scan'** you wish to model. Thus, when you select either the BA or DWBA functions as dependent variables, two additional independent variables will be defined: the first is related to the scattering angle, θ_{out} , the second is the scattering plane azimuthal angle, ϕ . These angles are illustrated in Figure 2.3.9.

Figure 2.3.9 Scattering geometry associated with non-specular scattering.



Non-specular reflected intensity computations can be computed for any one of three different scattering geometries, or 'scans', as summarized in table 2.3.1 The three scan types - Rocking Scan, Detector Scan, and Offset Scan - are common to grazing incidence X-ray scattering measurements, but are equally valid for any wavelengths and over any range of incidence angles.

Table 2.3.1 Non-specular scattering scan types.

<i>Scan Type</i>	<i>Description</i>
Rocking Scan	Detector fixed, sample rotated
Detector Scan	Sample fixed, detector rotated
Offset Scan	Sample and detector rotated simultaneously; Detector offset from specular direction by a constant angle

- A **Rocking Scan** refers to the case of a measurement of the non-specular reflected intensity wherein the detector is held fixed relative to the incident beam, and the sample is rotated, or 'rocked', with respect to the incident beam. In this case, both the incidence angle Θ_{in} and the scattering angle Θ_{out} vary simultaneously.
- A **Detector Scan** refers to the case wherein the sample is fixed relative to the incident beam, and the detector is varied. Thus Θ_{in} is constant, while Θ_{out} is varied.
- In an **Offset Scan**, the sample and detector are both rotated, with the detector offset from the specular direction by a constant offset angle, i.e., $\Theta_{out} - \Theta_{in} = \text{constant}$

The way that you specify scattering angles in IMD depends on both the type of scan you have selected, and whether you choose to specify grazing incidence angles or normal incidence angles, as summarized in Table 2.3.2:

Table 2.3.2. Independent variable angle specification for non-specular scattering computations.

<i>Scan Type</i>	Angle specified in IMD Incidence Angles independent variable widget	Angle specified in IMD Scattering Angles independent variable widget
Rocking Scan, Normal Incidence	$\Theta = \Theta_{in}$	$\Theta_{in} + \Theta_{out}$
Rocking Scan, Grazing Incidence	$\Theta = 90 \text{ deg} - \Theta_{in}$	$2\Theta = 180 \text{ deg} - \Theta_{in} - \Theta_{out}$
Detector Scan, Normal Incidence	$\Theta = \Theta_{in}$	$\Theta_{in} + \Theta_{out}$
Detector Scan, Grazing Incidence	$\Theta = 90 \text{ deg} - \Theta_{in}$	$2\Theta = 180 \text{ deg} - \Theta_{in} - \Theta_{out}$
Offset Scan, Normal Incidence	$\Theta = \Theta_{in}$	$\Delta(\Theta_{out})$
Offset Scan, Grazing Incidence	$\Theta = 90 \text{ deg} - \Theta_{in}$	$\Delta(2\Theta)$

Shown in Figures 2.3.10 and 2.3.11 are the independent variable widgets associated with the scattering angle variable and the scattering plane azimuthal angle variable. Included on each widget is a schematic diagram illustrating the scattering geometry corresponding to the range of values you specify. In addition, the **Scattering Angles** widget includes plots of q_x vs q_z and q_y vs q_z , illustrating the corresponding scan trajectories in momentum space; the greyed regions on these plots indicate inaccessible regions of q-space, i.e., regions where either Θ_{in} or Θ_{out} are greater than 90 degrees. The relationships between scattering angles and q-vectors are shown in Figure 2.3.12.

Figure 2.3.10. The **Scattering Angles** independent variable widget. In this case, a Rocking Scan has been selected for a single value of the scattering angle 2Θ .

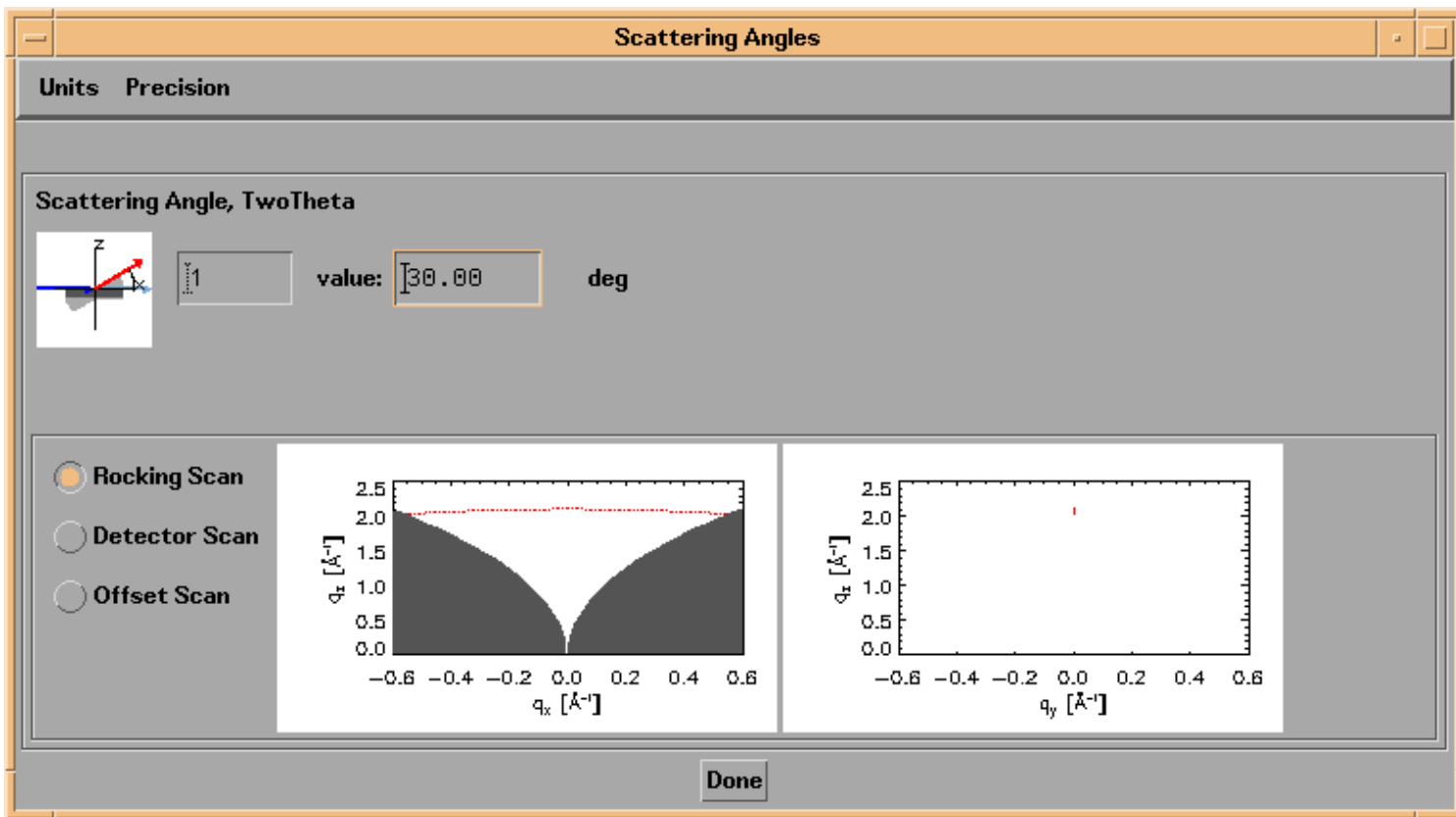
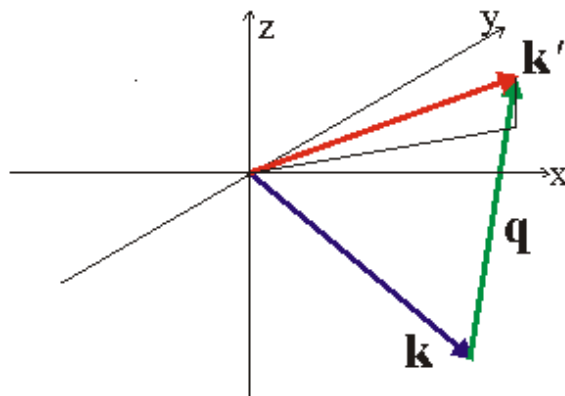


Figure 2.3.11. The Scattering Plane Azimuthal Angle independent variable widget.



Figure 2.3.12 Relationship between incidence and scattering angles and momentum vectors.



$$\mathbf{q} \equiv \mathbf{k}' - \mathbf{k} = \frac{2\pi}{\lambda} \left[(\sin \theta_{out} \cos \phi - \sin \theta_{in}) \hat{\mathbf{x}} + \sin \theta_{out} \sin \phi \hat{\mathbf{y}} + (\cos \theta_{out} + \cos \theta_{in}) \hat{\mathbf{z}} \right]$$

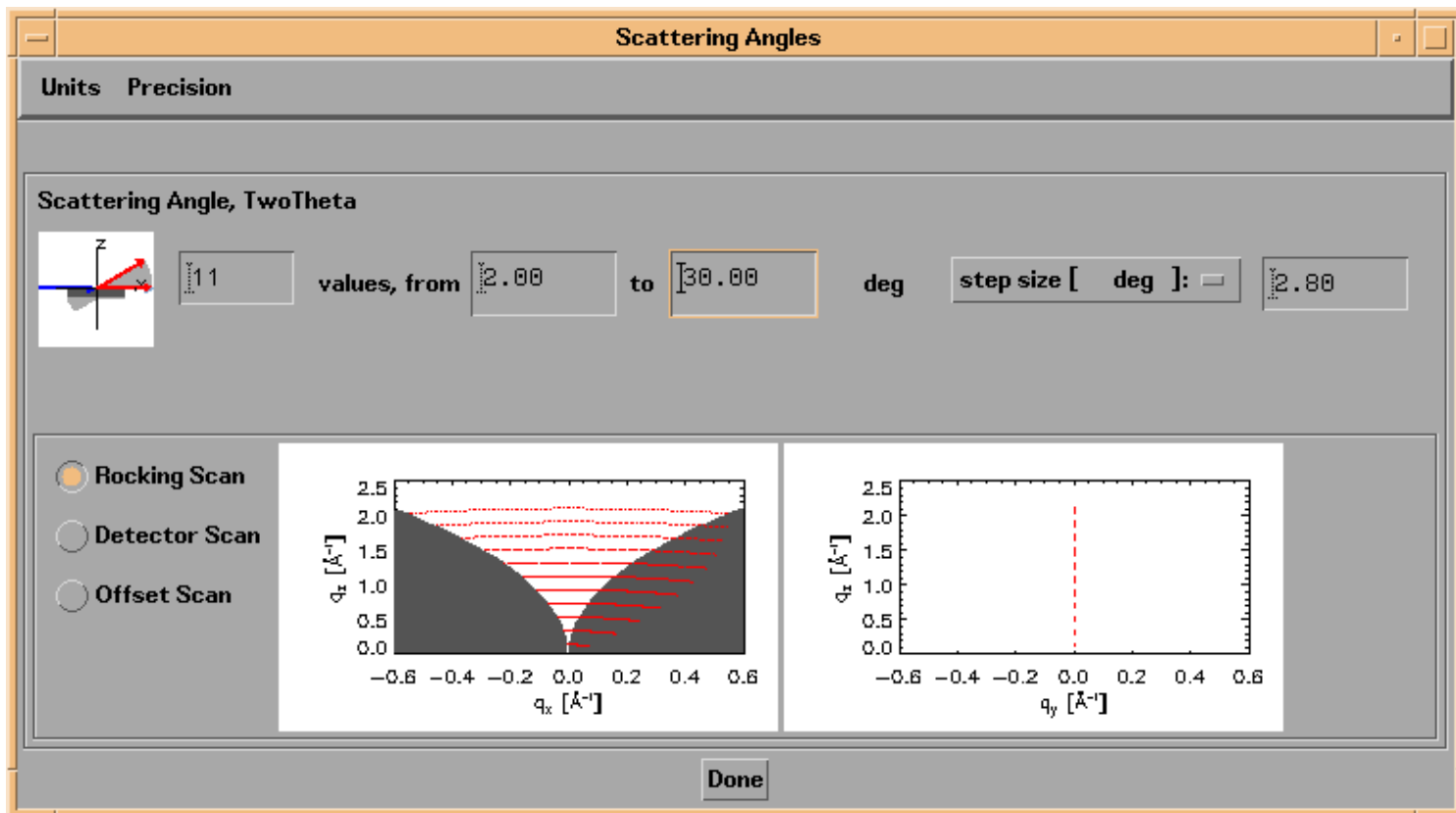
$$q_{\parallel} \equiv \sqrt{q_x^2 + q_y^2} = \frac{2\pi}{\lambda} \sqrt{\sin^2 \theta_{out} + \sin^2 \theta_{in} - 2 \sin \theta_{out} \sin \theta_{in}}$$

$$q_{\perp} = q_z = \frac{2\pi}{\lambda} (\cos \theta_{out} + \cos \theta_{in})$$

Although each of the three non-specular scan types refers to a one-dimensional scan, you are free to specify both multiple incidence angles and multiple scattering angles for any type of scan, in order to compute non-specular reflected intensity as a function of both angles. As a specific example, in the case of a Rocking Scan at grazing incidence, you can compute the non-specular reflected intensity for a range of incidence angles θ_{in} , and for a single value of $2\theta_{out}$ (as in Figure 2.3.10, for example,) or, you can compute the scattered intensity for both a range of θ_{in} values and a range of $2\theta_{out}$ values. In the latter case, the scattered intensity will be computed as a series of Rocking Scans, i.e., the scattered intensity will be computed as a function of θ_{in} , for every value of $2\theta_{out}$ you have specified. Figure 2.3.13 illustrates.

Note: The non-specular reflected intensity functions will be set to zero wherever either the incidence angle (θ_{in}) or the scattering angle (θ_{out}) exceeds 90 degrees.

Figure 2.3.13. The **Scattering Angle** independent variable widget for the case of a Rocking Scan when multiple values of the scattering angle $2\theta_{out}$ have been specified.



Note: Because of the fact that the momentum transfer vector \mathbf{q} depends on the wavelength, the incidence angle, and the two scattering angles, and because it is possible in IMD to vary any or all of these four parameters simultaneously, it is not possible to specify \mathbf{q} -vectors directly. However, the results of your computations can be displayed as plots in momentum space, as will be described in [Section 2.5](#).

COUPLED PARAMETERS

It's possible in IMD to constrain individual layer or substrate parameters to be equal or proportional to other layer or substrate parameters, through the use of so-called 'Coupled Parameters'.

As an example, suppose you define a structure containing two layers, and you wish to set the interfacial width of layer A to be twice the interfacial width of layer B. As an alternative to entering directly the interface width values for each of the two layers, you can instead define a coupled parameter, such that the interface width of the A layer will always be equal to 2 times the value of the B layer interface width. The main advantage of using a coupled parameter in this case is that if you then define the 'source' of the coupled parameter - in this case the B layer interface width - to be an independent variable (or a fit parameter, as described in [Section 3.2](#)), both parameter values can be varied simultaneously. In fact, multiple layer or structure parameters can all be coupled to the same 'source' parameter, allowing you to vary many parameters simultaneously, using only a single independent variable (or fit parameter.)

To define a coupled parameter, select the **COUPLED PARAMETERS** button on the main IMD widget, and then press the **Add** button in the Coupled Parameters region. (See [Figure 2.3.14](#).) You will be presented with a list of available parameters that can be designated as coupled parameters. Choose one of these parameters. You will then be presented with a list of available 'source' parameters. Once you select the source parameter, a new **Coupled Parameters** widget will appear, as shown in [Figure 2.3.15](#).

Figure 2.3.14. The main IMD widget as it appears when the **COUPLED PARAMETERS** button is selected.

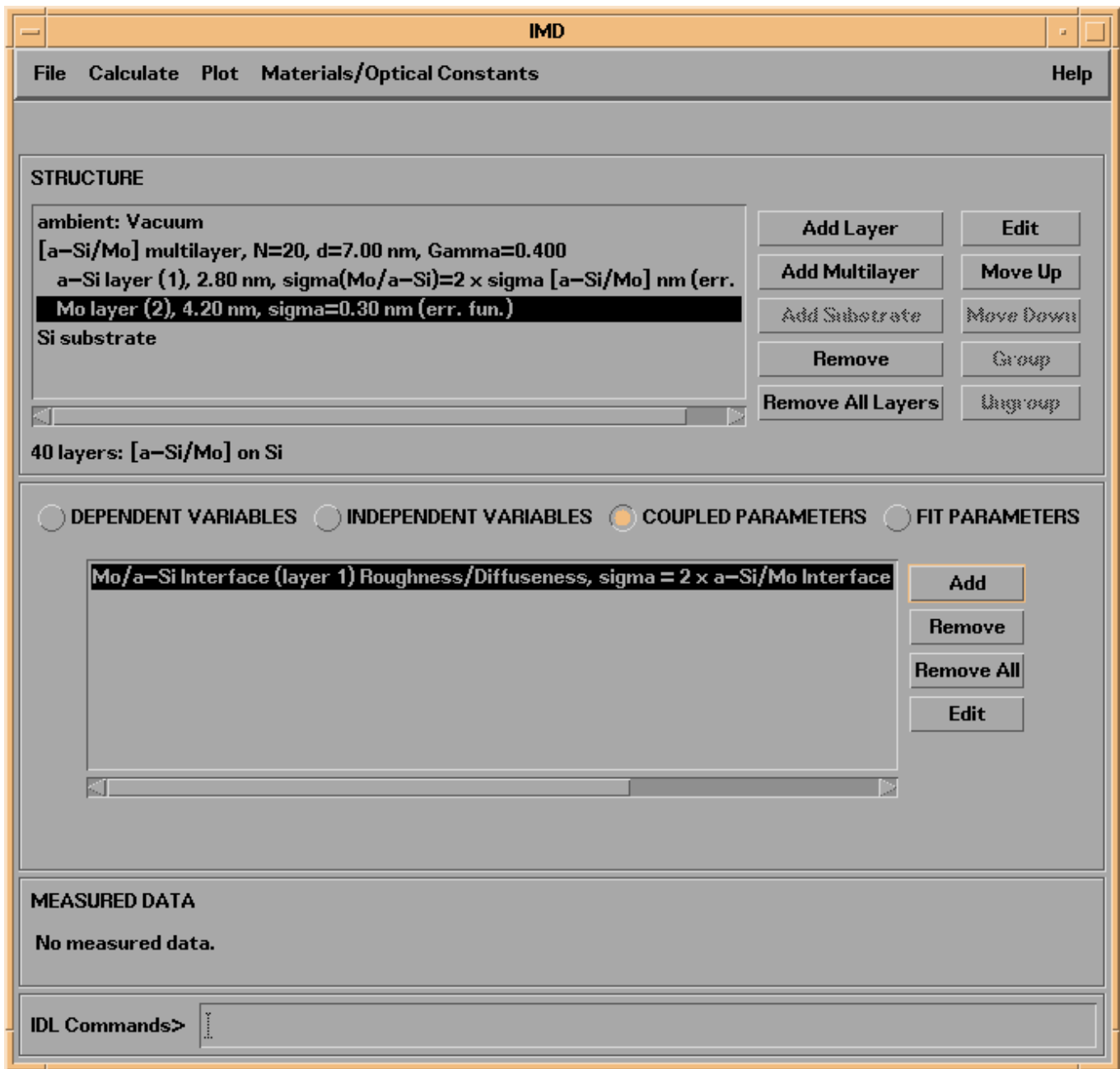
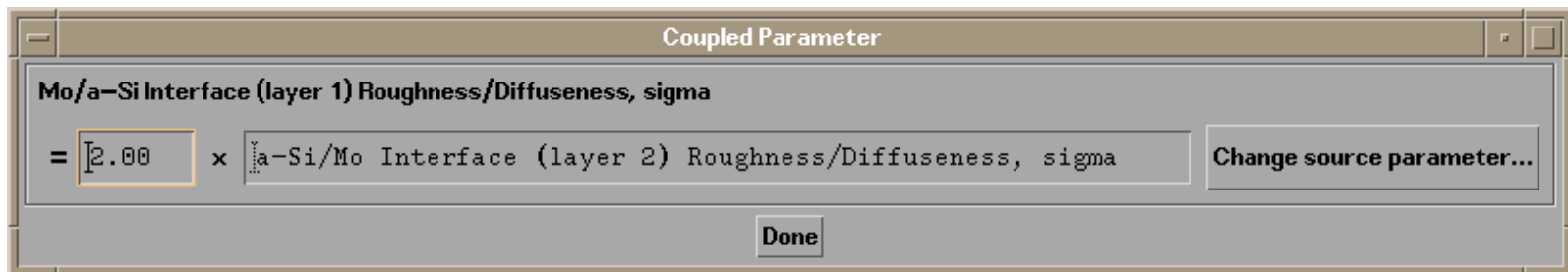


Figure 2.3.15. A Coupled Parameters widget.



On the **Coupled Parameters** widget you can enter the proportionality factor relating the source and destination parameters - a factor of 2 is shown in Figure 2.3.15 - and you can press the **Change source parameter...** button in order to (yes, you guessed it) change the source parameter.

The number of coupled parameters that can be defined is limited only by the number of layers you define in the structure.

Note: Once a parameter is defined as (the destination parameter of) a coupled parameter, it's value can no longer be specified directly, nor can that parameter be defined as an independent variable or fit parameter.

See [Section 2.5](#) for several examples illustrating the use of coupled parameters.

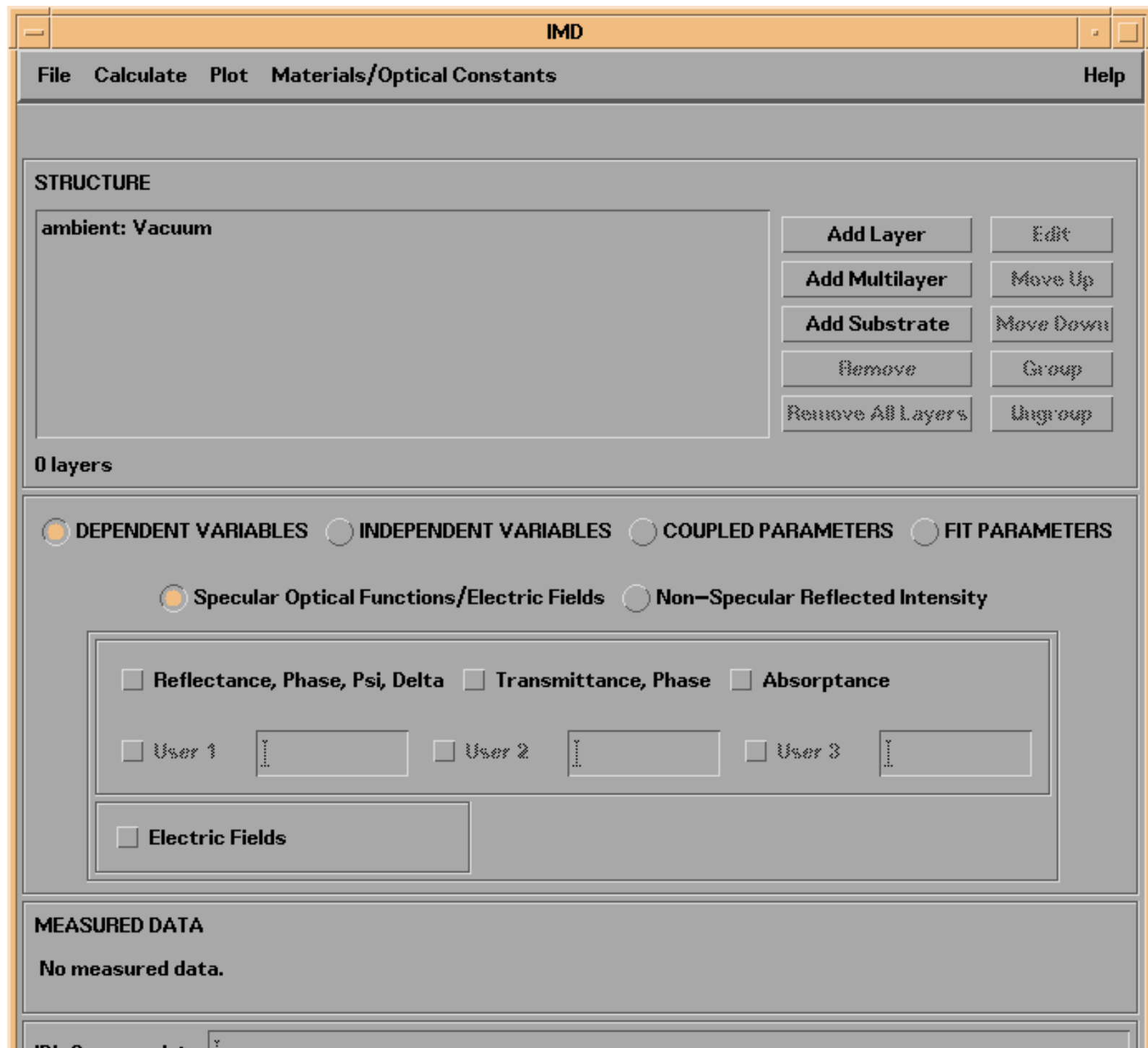
[Back](#) | [Contents](#) | [Next](#)

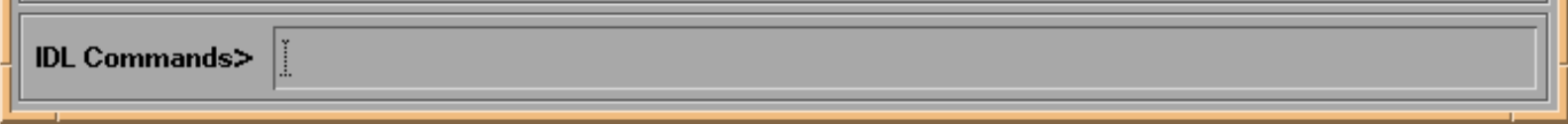
Chapter 2. Modeling

This chapter explains how to perform a calculation using IMD.

Figure 2.1 is a picture of the main IMD window, or widget, in IDL terminology, as it appears when you start IMD for the first time. This widget consists of the following components: the menu bar, the STRUCTURE area, the DEPENDENT VARIABLES / INDEPENDENT VARIABLES / COUPLED PARAMETERS / FIT PARAMETERS area, the MEASURED DATA area, and the IDL Commands area.

Figure 2.1 The main IMD widget



The image shows a graphical user interface element for an IDL (Interactive Data Language) environment. It consists of a horizontal bar with a grey background and a thin orange border. On the left side, the text "IDL Commands" is displayed in a bold, black font, followed by a right-pointing chevron symbol. To the right of this text is a large, empty rectangular area, likely intended for displaying command output or a list of commands.

IDL Commands>

The sections that follow describe how to use the main IMD widget in order to accomplish these tasks:

[2.1 Designating materials and optical constants](#)

[2.2 Defining the structure](#)

[2.3 Specifying variables and coupled parameters](#)

[2.4 Performing the computation](#)

[2.5 Viewing, printing, and saving the results](#)

[Back](#) | [Contents](#) | [Next](#)

2.4 Performing the computation

Once you have defined the structure, specified independent and dependent variables, and optionally any coupled parameters, select the appropriate menu item from the **Calculate** menu, in order to perform the actual computation.

[Back](#) | [Contents](#) | [Next](#)

2.5 Viewing, printing, and saving the results

SAVING THE RESULTS

After the calculation is completed, the results will be saved to an IMD file automatically, unless you have disabled this feature in the **File->Preferences->Auto-Save...** menu option.

Note: Unless you disable auto-save, IMD will remember exactly how you left things the last time you ran IMD, so that you can continue right where you left off.

If you wish to save the results of different calculations in different IMD files for later use, use the **File->Save as...** menu option. Saved IMD files can later be opened using the (you guessed it) **File->Open...** menu option.

You can also save the results as plain text, if you wish, by selecting **File->Save as Text...** from the menu bar. You will be presented with a widget that allows you to specify which dependent variables you wish to save, and as a function of which independent variable, if there is more than one (multi-valued) independent variable available. For example, if you have calculated reflectance as a function of both incidence angle and wavelength, you must specify whether you wish to save reflectance vs. angle data at a specific wavelength, or reflectance vs. wavelength data at a specific angle. Figure 2.5.1 illustrates:

Figure 2.5.1 The IMD *Save-as-Text* widget associated with a transmittance calculation using three independent variables: angle, wavelength, and layer thickness.

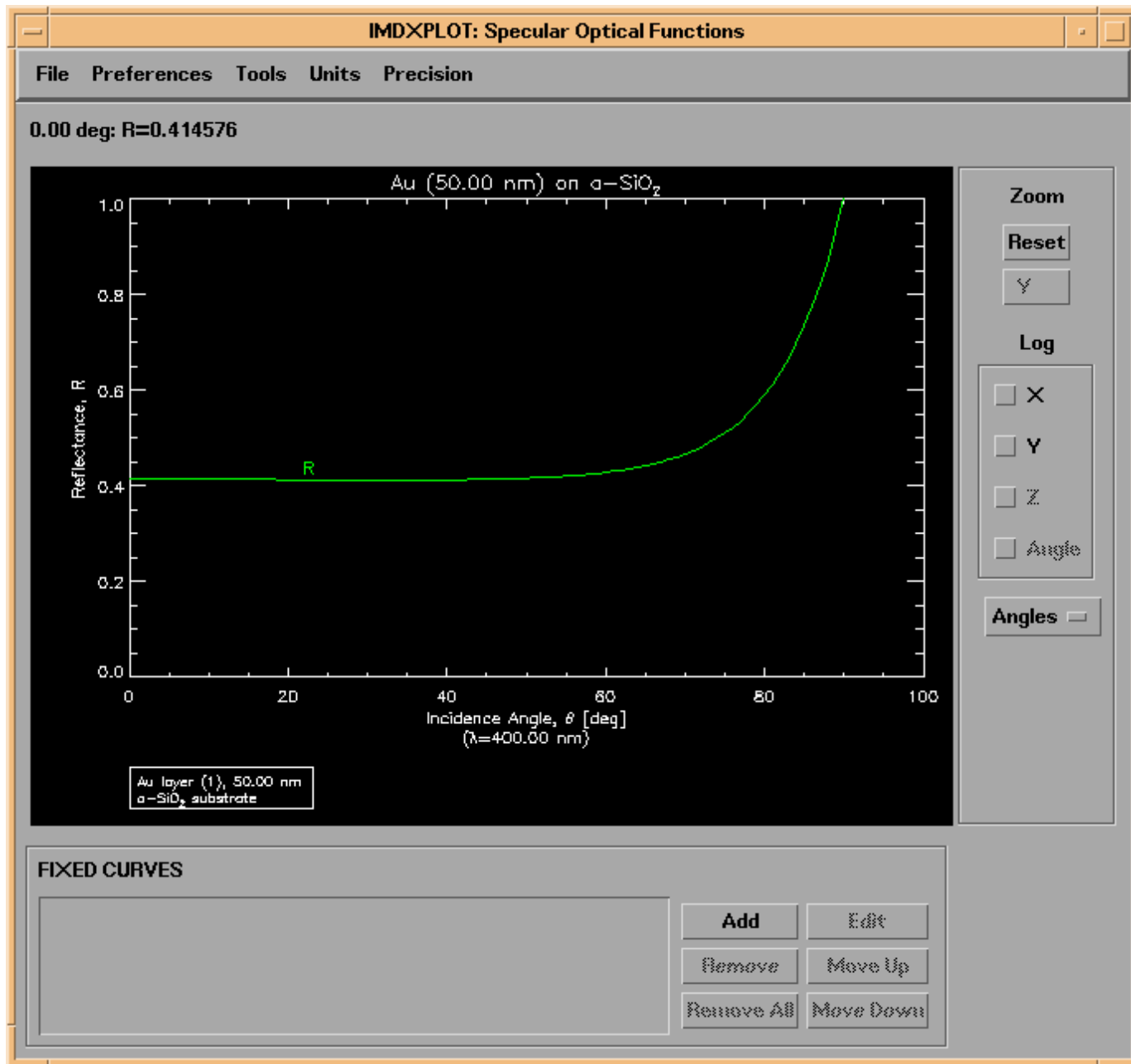
The screenshot shows the 'IMD Save-as-Text' dialog box. It features a menu bar with 'File' and 'Units'. The main area is divided into two sections: 'DEPENDENT VARIABLES' and 'INDEPENDENT VARIABLES'. In the 'DEPENDENT VARIABLES' section, there are five radio button options: 'Average (f,q)' (selected), 's-polarization', 'p-polarization', 'Phase, s-polarization', and 'Phase, p-polarization'. The 'INDEPENDENT VARIABLES' section contains three rows of controls. The first row is for 'Theta', with 'Continuous Variable' checked, a 'Value' field containing '0.00', and an 'Index' field containing '0'. The second row is for 'Lambda', with 'Continuous Variable' unchecked, a 'Value' field containing '253.37', and an 'Index' field containing '11'. The third row is for 'z [Au]', with 'Continuous Variable' unchecked, a 'Value' field containing '50.00', and an 'Index' field containing '0'. At the bottom of the dialog are two buttons: 'Save...' and 'Done'.

VIEWING AND PRINTING THE RESULTS - IMDXPLOT

After the calculation is completed, the results will be displayed graphically in an **IMDXPLOT** widget. The appearance of the **IMDXPLOT** widget depends on the dependent and independent variables you have specified, as will now be described.

Shown in Fig. 2.5.2 is the **IMDXPLOT** widget that results from a calculation of reflectance vs incidence angle for a 50 nm gold film on an amorphous SiO₂ substrate.

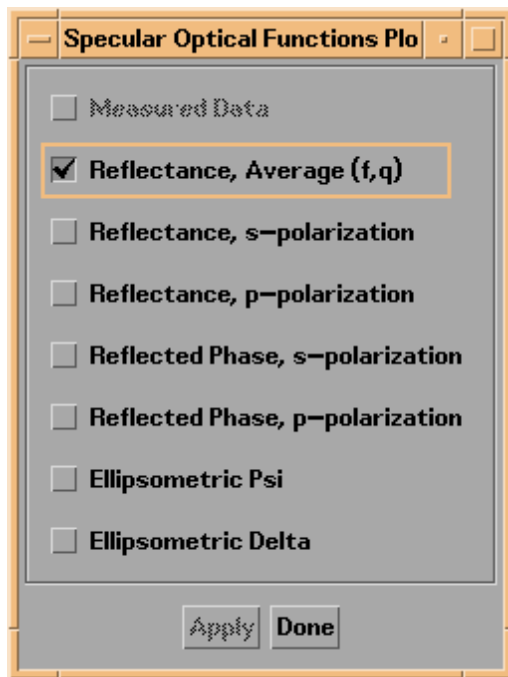
Figure 2.5.2 IMDXPLOT example showing the reflectance of a thin film on a substrate.



For each dependent variable selected in the DEPENDENT VARIABLES area of the main IMD widget, at least three quantities are actually calculated, as previously mentioned: the values of the property for pure s and pure p polarizations, as well as the 'average' value. In the case of reflectance and transmittance, the phases are calculated as well; in the case of reflectance, the ellipsometric psi and delta functions are also computed.

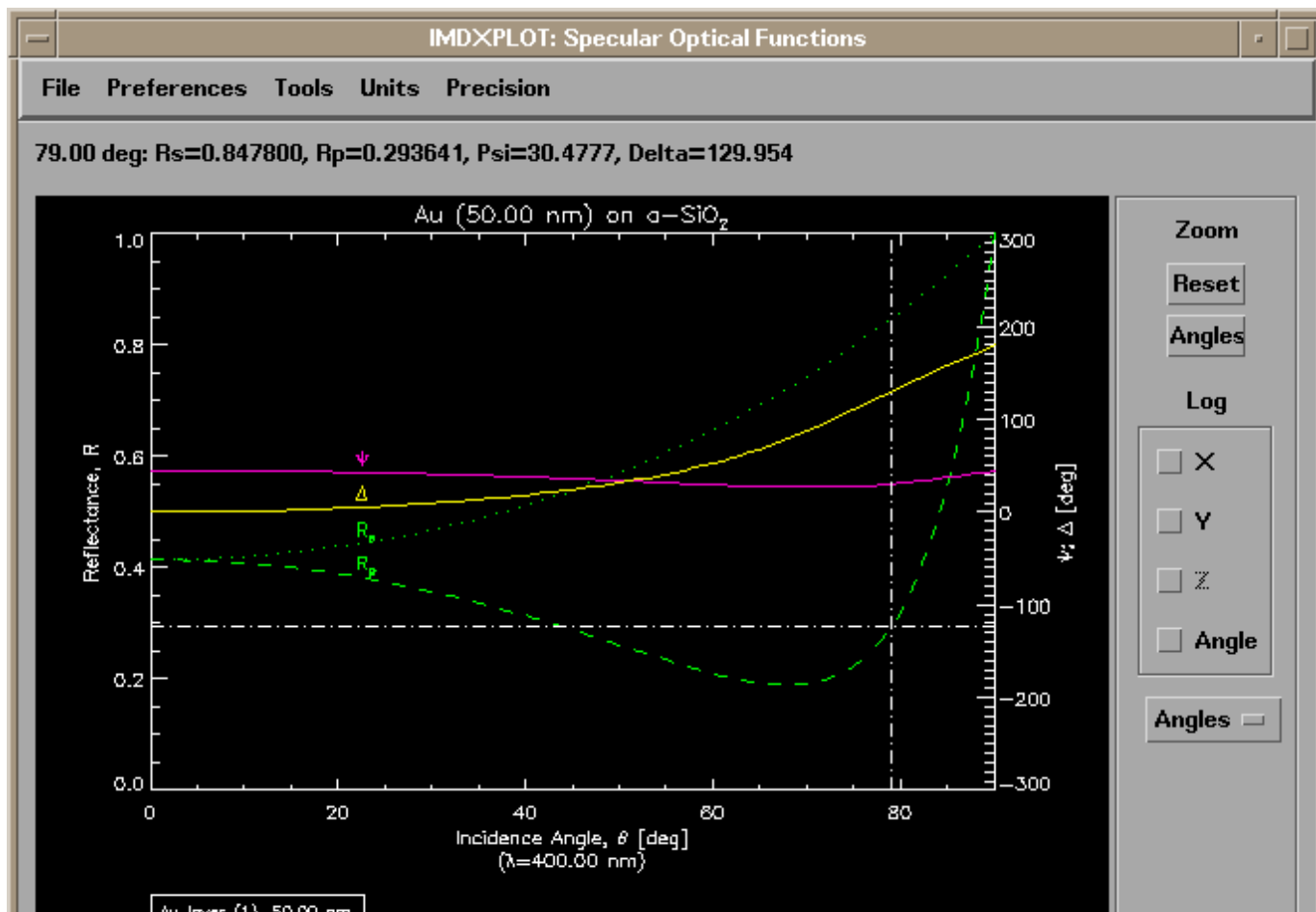
Shown in Figure 2.5.3 is the **Plot Variables** widget associated with the **IMDXPLOT** widget shown in Figure 2.5.2. This widget is accessible from the **Preferences->Plot Variables...** menu option on the **IMDXPLOT** widget. The default setting is to plot only the 'average' reflectance for the specified polarization parameters f and q, as shown:

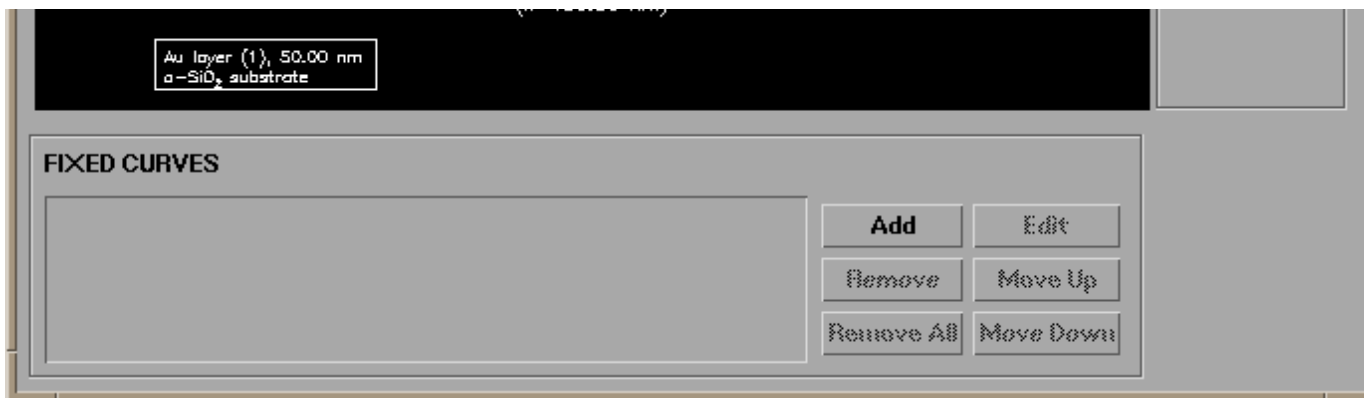
Figure 2.5.3 IMDXPLOT Plot Variables widget



Shown in Figure 2.5.4 is the plot that results after selecting instead as plot variables $R(s)$, $R(p)$, and also the ellipsometric psi and delta functions. I have also changed the colors and linestyles of the different curves using the **Preferences->Plot Variables Styles and Labels...** option, and I have adjusted the axes using the **Preferences->Axes Scaling...** option. The cross-hairs at 79 degrees are due to the fact that I've also selected $R(p)$ as the active 'cursor function'.

Figure 2.5.4 Plot after selecting several Plot Variables.





You can use your mouse to zoom in on a particular region of the plot. Alternatively, more precise axis scaling can be adjusted from the menu items on the IMDXPLO widget; many other aspects of the plot can be adjusted as well: colors, linestyles, thicknesses, plotting symbols, labels and label placement, character size, etc. Once you have adjusted the plot to your liking, you can print it using the **File->Print** menu option.

Note: You can change the default background and plot color, by setting the values of the IDL graphics system variables `!p.background` and `!p.color`. For example, to produce a plot with black lines on a white background (instead of the default white plot on a black background), set `!p.background=255` and `!p.color=0`, prior to plotting your results with IMDXPLO. You can enter these commands either at the IDL prompt, or from within the IDL Commands area of the main IMD widget.

Note: Use the droplist widget (labeled **Angles** in Figure 2.5.4, for example) to the right of the plot area on an IMDXPLO widget to display an optical function vs. q (momentum) rather than incidence or scattering angle.

FIXED CURVES

As a second, and somewhat more complicated example, shown in Figures 2.5.5 and 2.5.6 are **IMDXPLO** widgets corresponding to the results of a calculation of the reflectance of a carbon film vs. angle of incidence, wavelength, and film thickness. There are many different ways to display the results of such a multi-variable calculation. In Figure 2.5.5, I have chosen to display a 1D plot showing Reflectance vs. Incidence Angle. Thus, the **Continuous Variable** box next to the word **Theta** is checked, signifying that **Theta** (incidence angle) is a continuous plot variable, whereas the boxes next to **Lambda** and **z[a-C]** are unchecked, indicating that these parameters are discrete variables. That is, the plot shows the reflectance-vs-angle curves for whichever value of **Lambda** is entered in the box labeled 'Value' to the right of the word **Lambda**. Alternatively, you can position the slider labelled **Index** to view R-vs-Theta curves for different wavelength array indices. On the other hand, in Figure 2.5.6, I've designated both angle and wavelength as continuous variables, and have displayed the results as a 2D surface plot.

Figure 2.5.5 A 1D plot showing the reflectance of a carbon film as a function of incidence angle.

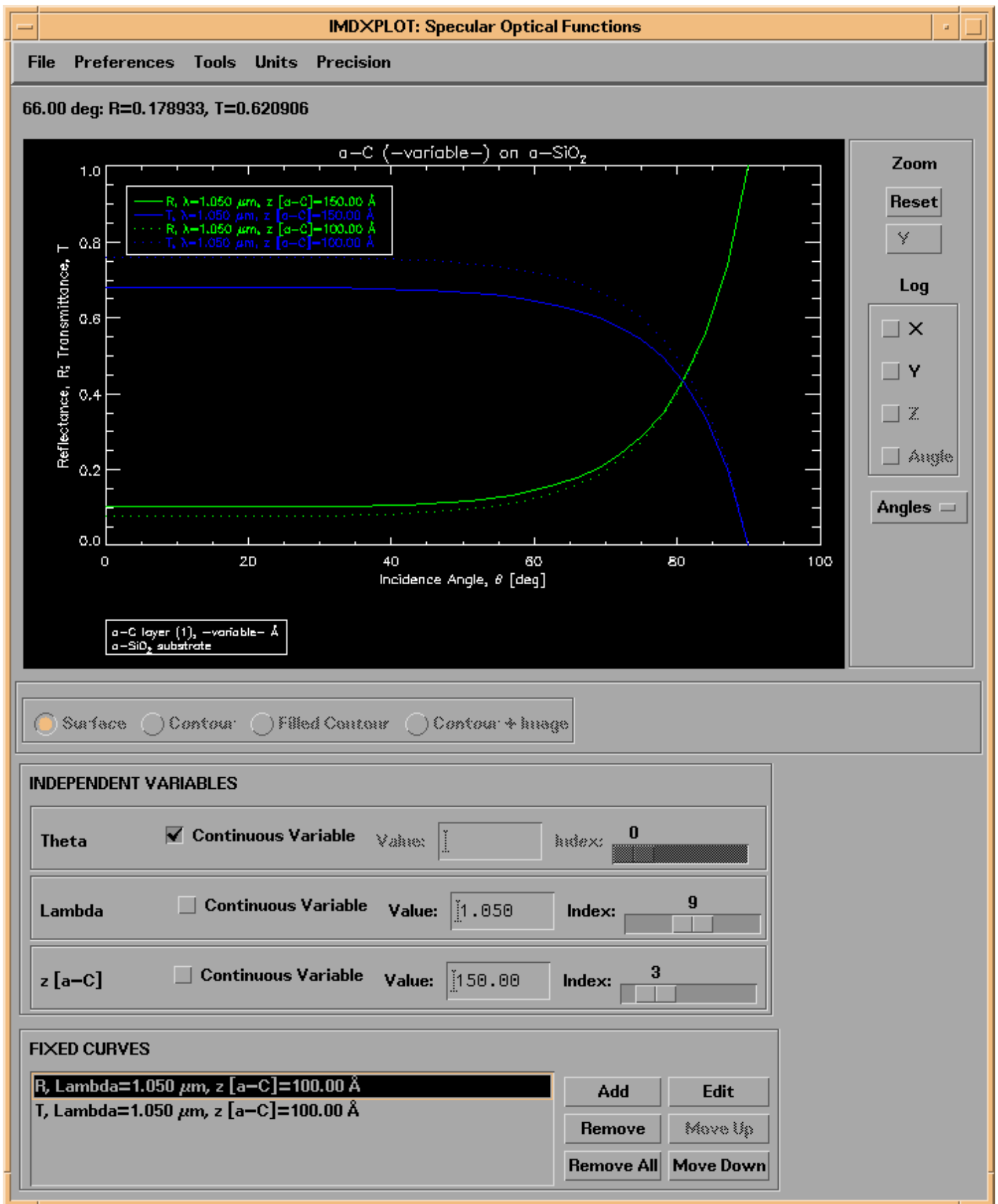
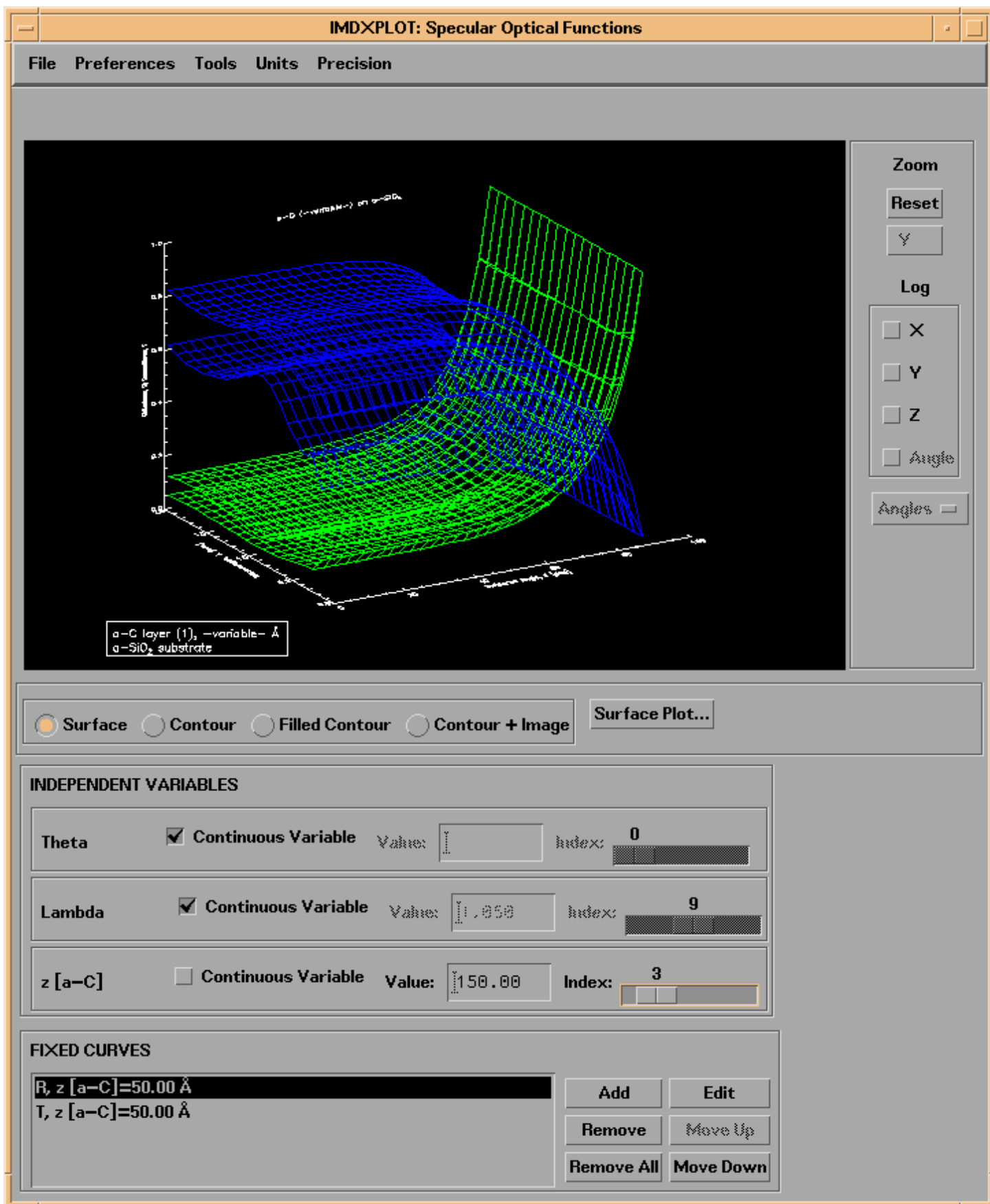


Figure 2.5.6 A 2D surface plot, showing the reflectance of the same carbon film, as a function of both angle and wavelength, and for two different film thicknesses.



The way to display more than one curve at a time, as in Figures 2.5.5 and 2.5.6, is to add "Fixed Curves" to the plot. By pressing the **Add** button in the FIXED CURVES area of the **IMDXPLOT** widget, the currently displayed curves will be added to the list of "Fixed" curves. The appearance (i.e., color, linestyle, etc.) of each fixed curve can be edited by selecting the fixed curve in the usual way: either double-clicking on the line in the *Fixed Curve List* area, or by selecting the curve you wish to edit and pressing the **Edit** button. You can also change the label for the curve, and you can choose to use 'curve labels' (as in Figure 2.5.4, for example), or use a legend (as in Figure 2.5.5.) If you choose to

use a legend, you can adjust the order in which the curves are listed in the legend by using the **Move Up** and **Move Down** buttons in the **FIXED CURVES** area. You can add as many as 30 Fixed Curves to the plot.

Note: You can have more than one **IMDXPLOT** widget open at a time. This makes it easier to compare the results from different types of calculations. But, this also means that *any changes you make in the main IMD widget (i.e., changes to the structure or to the dependent or independent variables) will only affect future instances of IMDXPLOT*. So once a calculation is completed and the **IMDXPLOT** widget is created, you cannot change the data associated with that instance of **IMDXPLOT** (although you can always change the plot appearance, using the **IMDXPLOT Preferences** options.) This also means that any changes you make to the plot using the **IMDXPLOT Preferences** options will only affect that instance if **IMDXPLOT**.

To specify preferences that you want to apply to all future instances of **IMDXPLOT**, use the **Plot->Global Plot Preferences...** option from the main IMD widget menu bar.

Also, you can save the plot appearance changes (and fixed curves) you might have made in **IMDXPLOT** along with the data by using the **File->Save...** option from the **IMDXPLOT** menu bar.

STATISTICS: Estimating film thicknesses, features widths, etc.

You can use the **Tools->Statistics/Region-of-Interest** **IMDXPLOT** menu option to define a region-of-interest, and compute a variety of statistics for whatever optical functions are currently displayed, including measured data. (Loading your measured data into IMD will be discussed in [Chapter 3](#).)

For example, shown in Figure 2.5.7 is the calculated X-ray reflectance of a W/Cr bilayer film, plotted as a function of q_z ; the two dashed vertical lines on this plot refer to the region-of-interest that was defined on the **Statistics** widget shown in Figure 2.5.8. Note that this region-of-interest was digitized to encompass one period of the high-frequency modulation visible in the reflectance curve. In this example, this modulation is due to the total film thickness; thus, the **Corresponding layer thickness** indicated in the **Statistics** widget of Figure 2.5.8 is an estimate of the total film thickness. This technique is especially useful with measured data when trying to fit X-ray reflectance data in order to determine film thicknesses. (The data used to produce Figure 2.5.7 is contained in the file `examples.dir/WCr_bilayer.dat`.)

Figure 2.5.7. The calculated X-ray reflectance of a W/Cr bilayer film. The dashed vertical lines refer to the region-of-interest indicated in Figure 2.5.8.

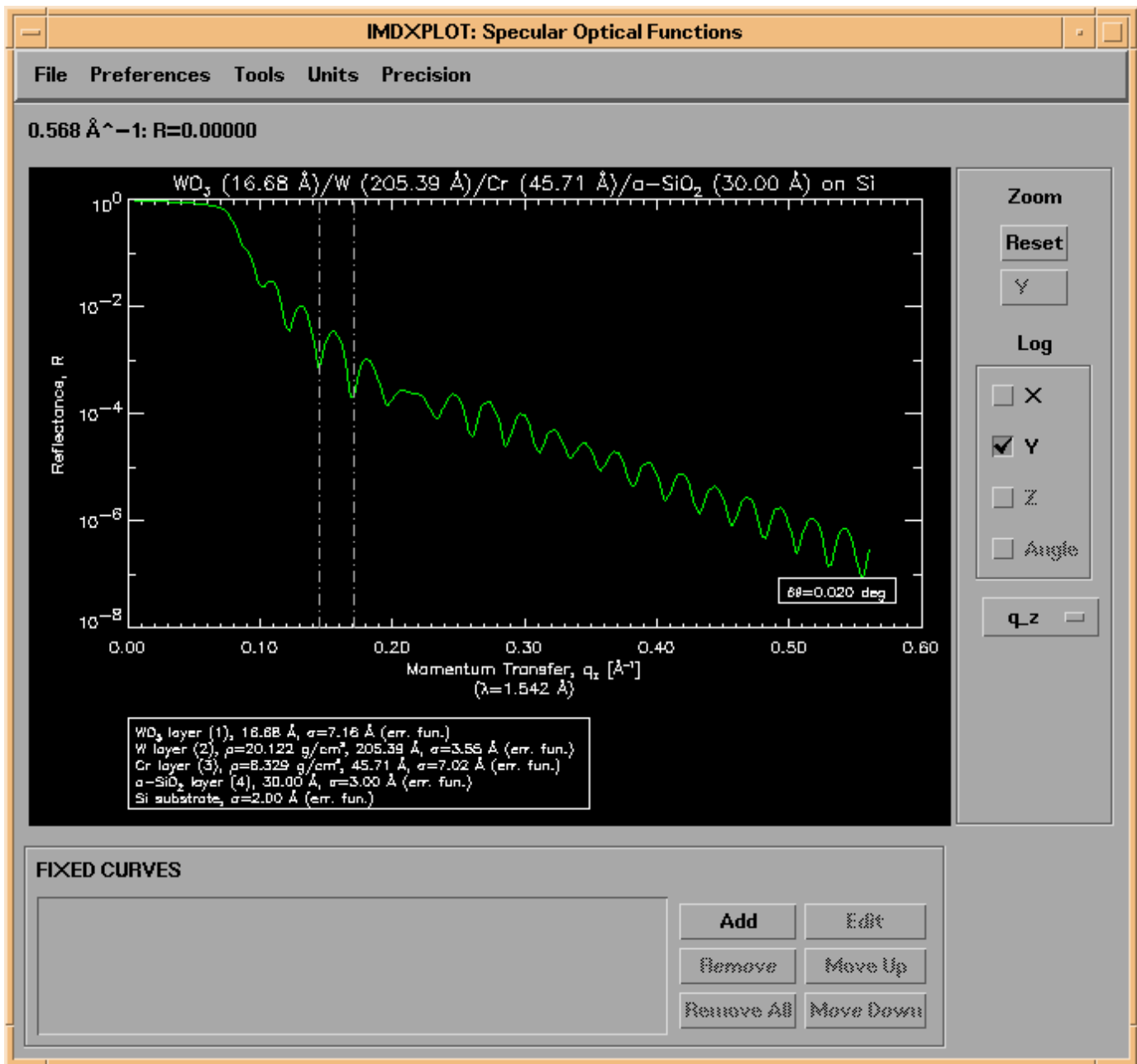


Figure 2.5.8. The **Statistics** widget associated with the IMDXPLOT widget shown in Figure 2.5.7

Specular Optical Functions Statistics

Precision

Function:

Region-Of-Interest

From to \AA^{-1}

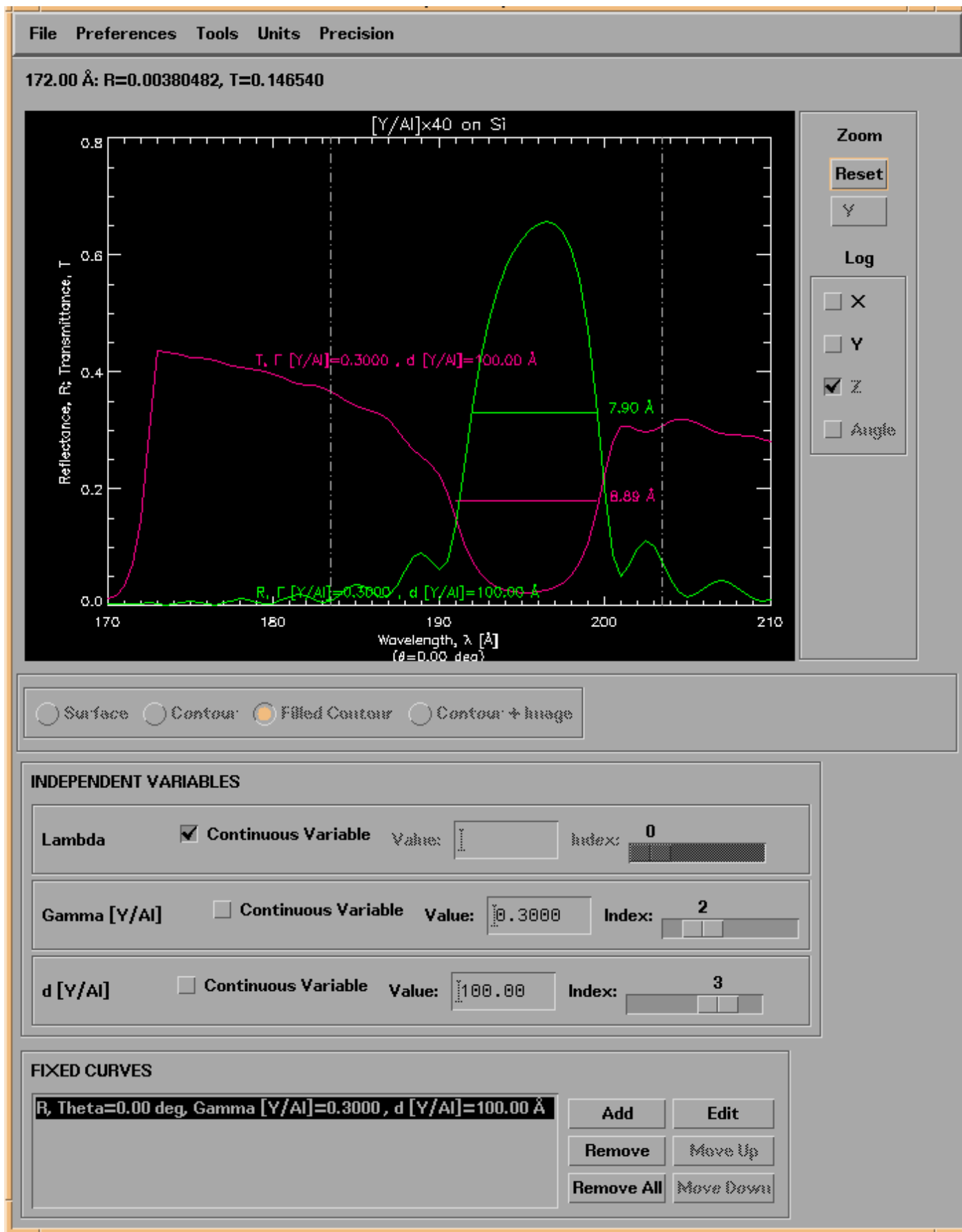
Corresponding layer thickness = 245.46 \AA

Statistics

<input type="checkbox"/> Minimum	<input type="text" value="0.00"/>	<input type="checkbox"/> Maximum	<input type="text" value="0.00"/>
<input type="checkbox"/> Average	<input type="text" value="0.00"/>	<input type="checkbox"/> Integral	<input type="text" value="0.00"/> \AA^{-1}
<input type="checkbox"/> FWHMax	<input type="text" value="0.00"/> \AA^{-1}	<input type="checkbox"/> FWHMin	<input type="text" value="0.00"/> \AA^{-1}

As can be seen in the **Statistics** widget of Figure 2.5.8, six different statistics can be determined: Minimum, Maximum, Average, Integral, Full-Width-Half-Max, and Full-Width-Half-Min (which refers to the width of an 'absorption' feature.) To illustrate, shown in Figure 2.5.9 is the reflectance and transmittance of a Y/Al multilayer film, with the width of the Bragg peak in both functions indicated.

Figure 2.5.9. The reflectance and transmittance of a Y/Al multilayer. The FWHMax of the reflectance, and the FWHMin of the transmittance curves are indicated.



Note: the statistics you select are computed only over the region-of-interest you define.

Note: to display statistics for more than one function simultaneously, as in Figure 2.5.9, you will need to compute the statistics for one function at a time, and then display each function as a Fixed Curve, as described above.

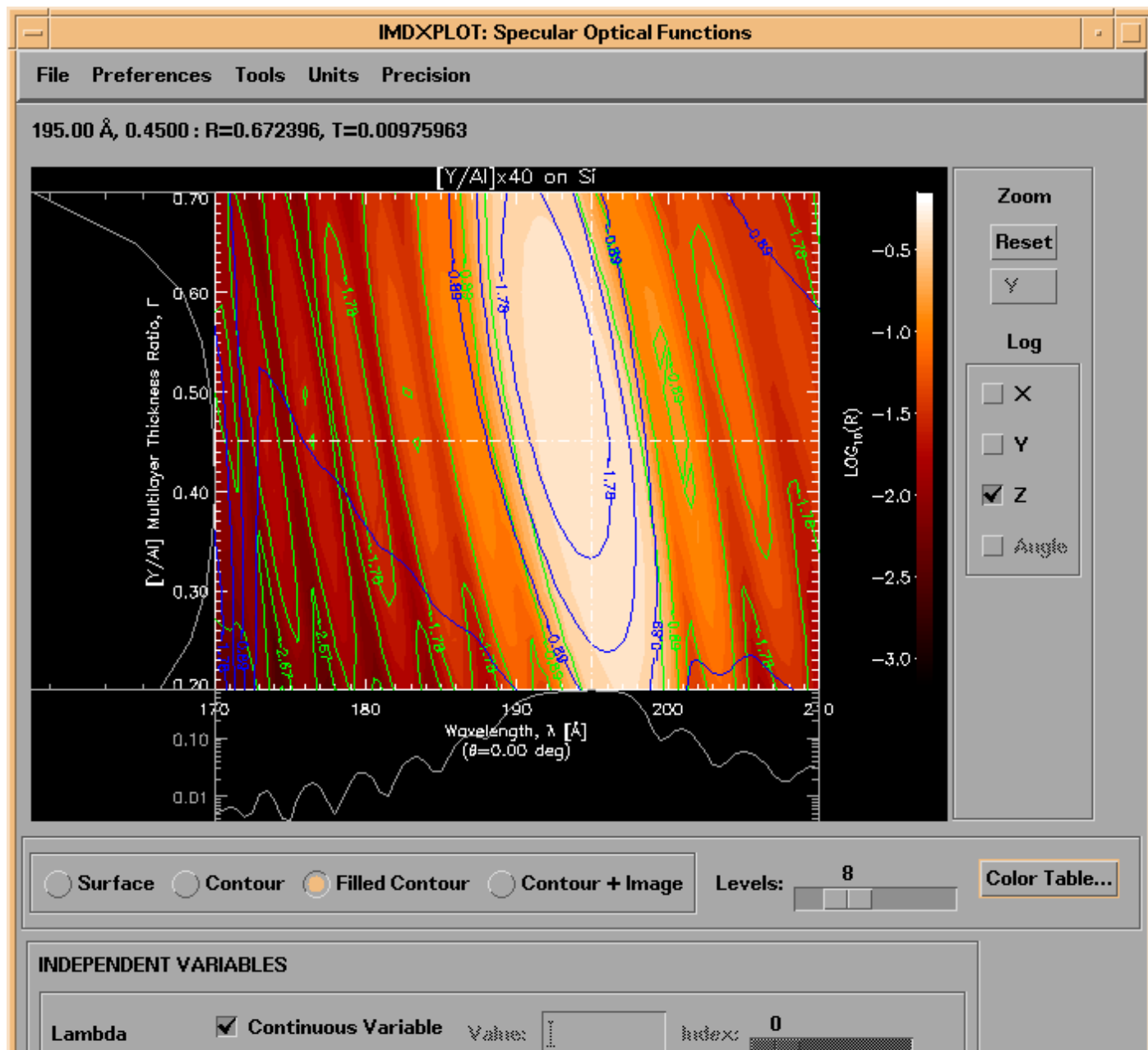
EXAMPLES

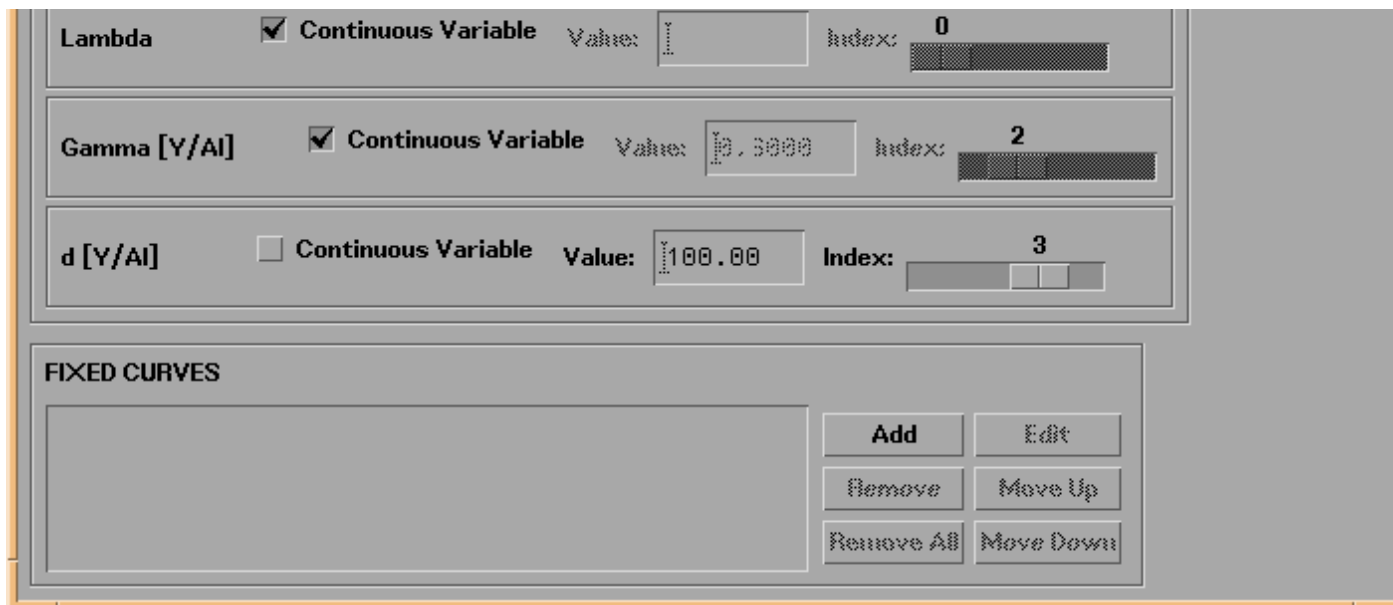
Included here are a few more examples illustrating some of the types of computations and visualizations that are possible in IMD.

Reflectance and transmittance contours of a Y/Al multilayer

Shown in Figure 2.5.10 is the reflectance and transmittance of the same Y/Al multilayer used in Figure 2.5.9. In this case, however, these specular optical functions are displayed as a function of both wavelength and multilayer thickness ratio (Gamma) as color contour plots: contours of constant reflectance are shown in green, contours of constant transmittance are shown in blue, and both sets of contours are overlaid on the a filled contour plot of the reflectance. The grey 1D plots below and to the left of the contour plot are 'live' plots that vary as you move the cursor over the contour plot. (The data used to create this plot is in the file called `examples.dir/YAl.rt.dat.`)

Figure 2.5.10. Reflectance and transmittance contours for a Y/Al multilayer film, as a function of wavelength and layer thickness ratio.

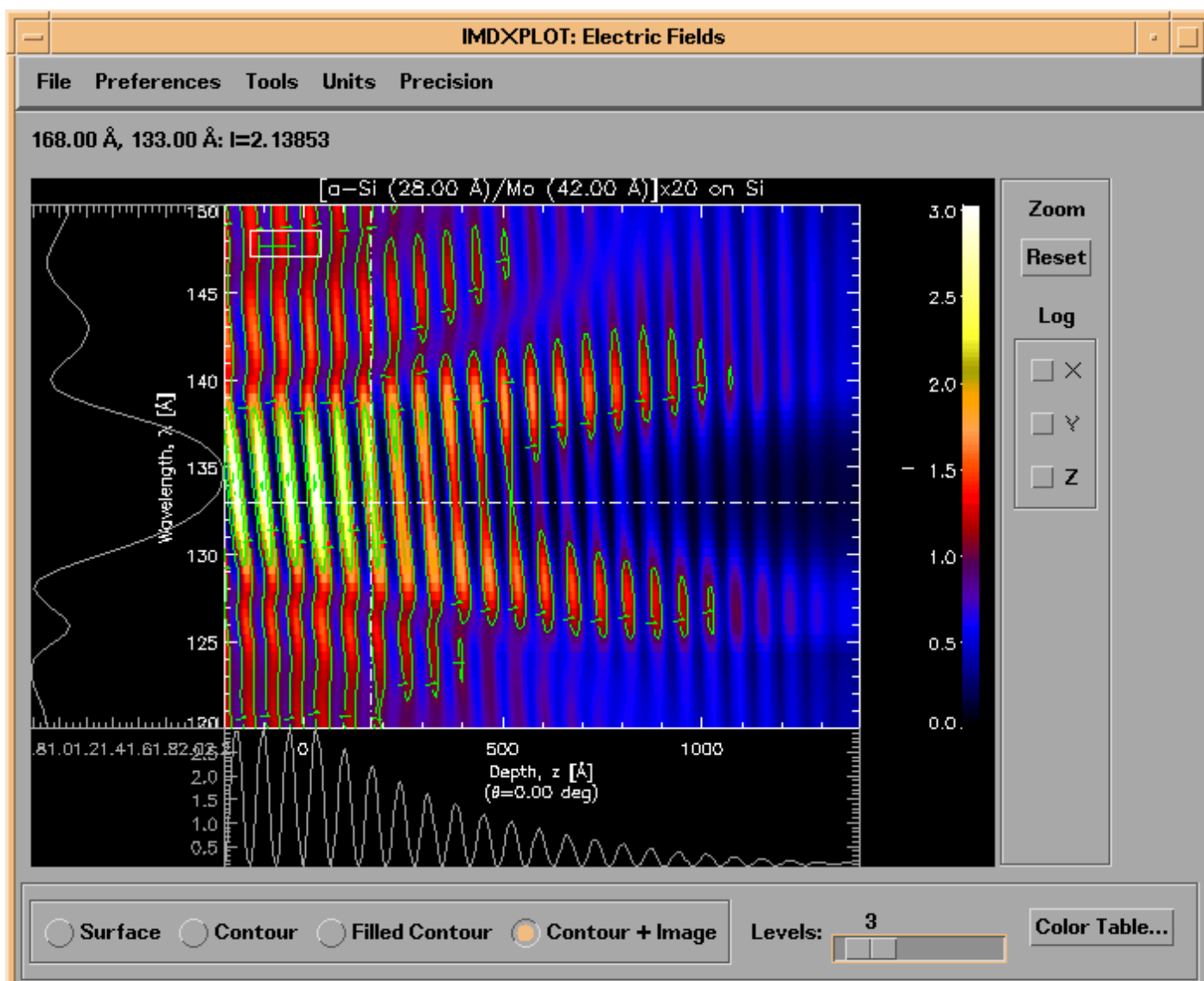


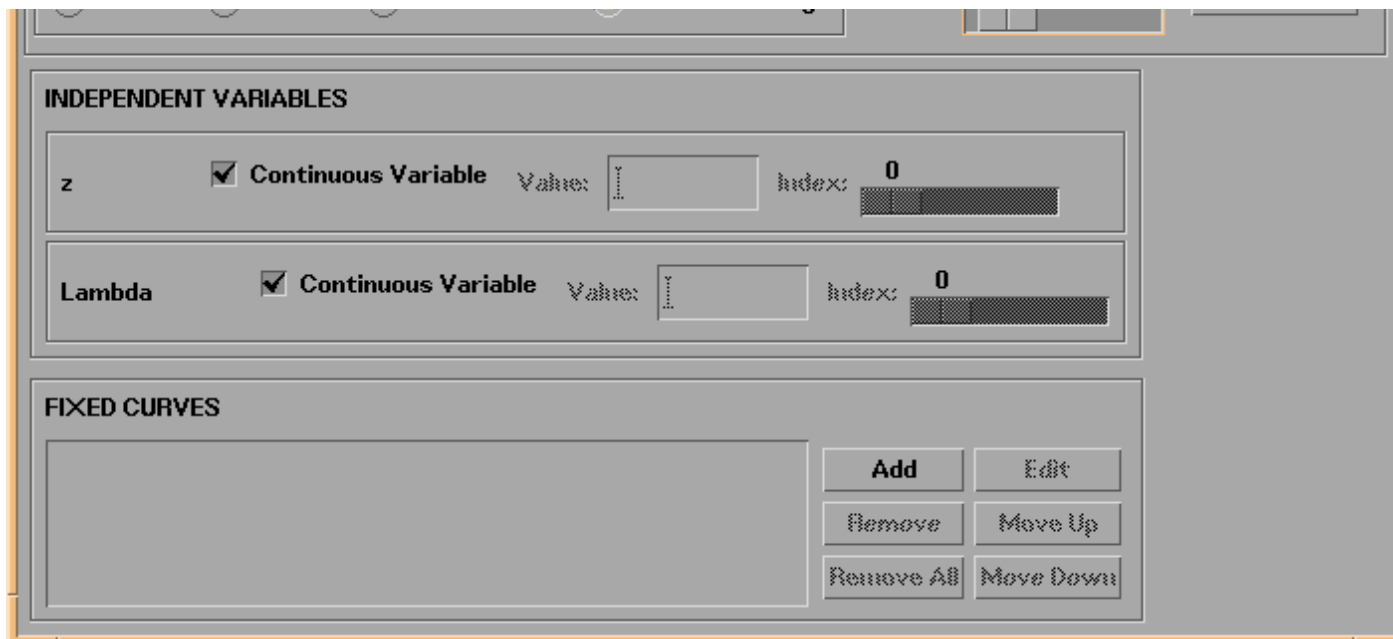


Electric field intensity contours of a Mo/Si multilayer

Similarly, shown in Figure 2.5.11 are the electric field contours for a Mo/Si multilayer film, as a function of wavelength and depth into the film (see the file `examples.dir/SiMo.fields.dat`):

Figure 2.5.11. Electric field intensity contours for a Mo/Si multilayer film.

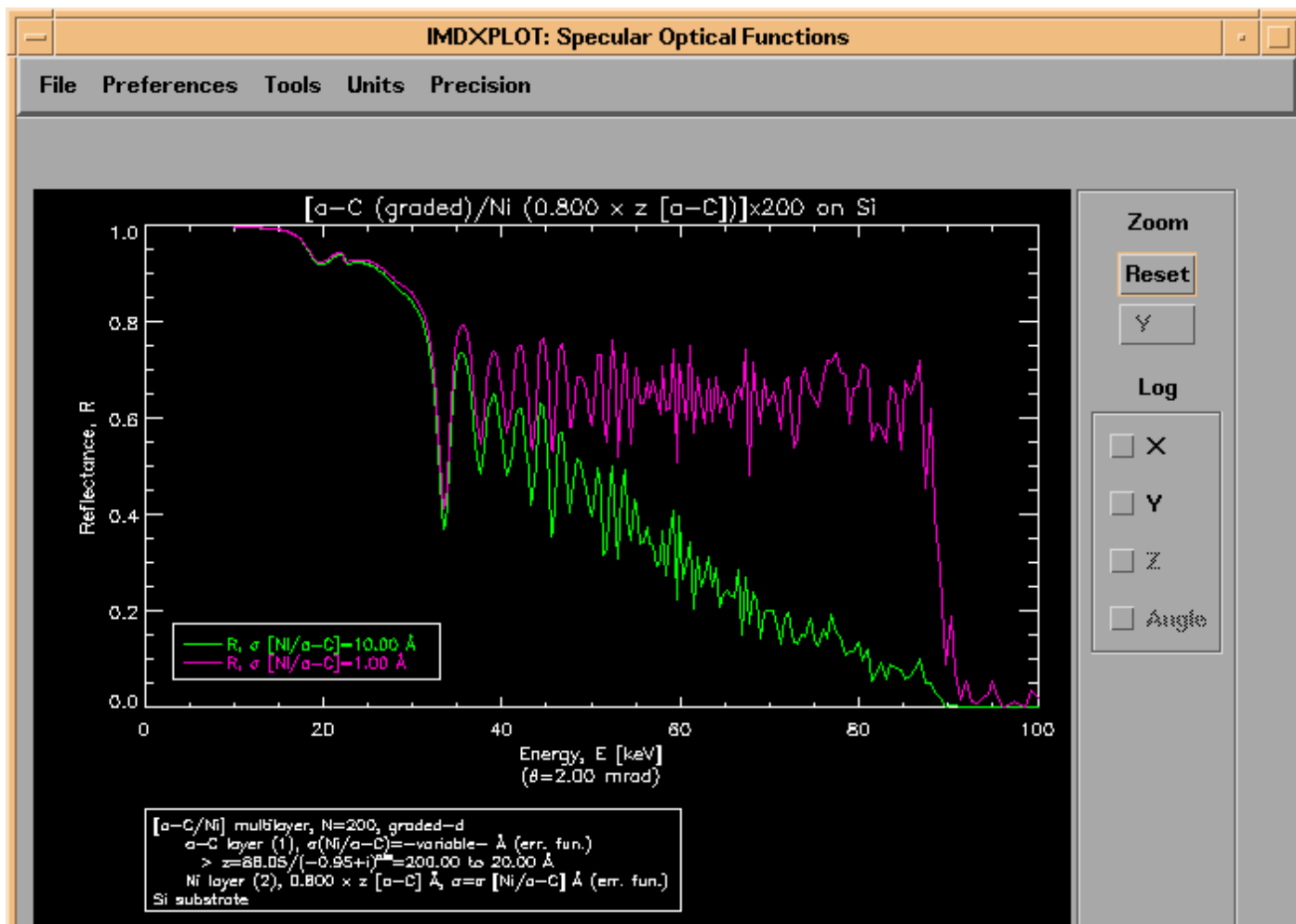


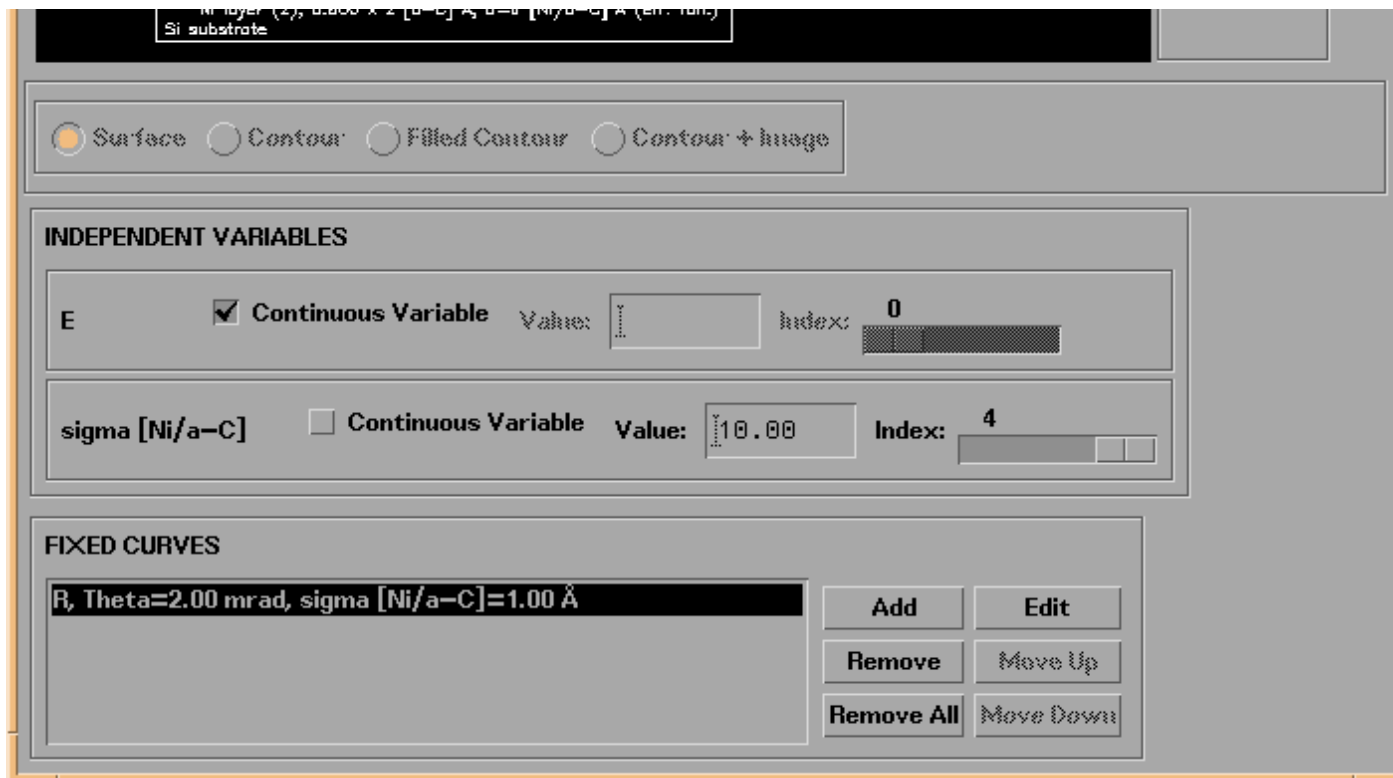


Reflectance of a depth-graded C/Ni multilayer, using coupled parameters

The next example, shown in Figure 2.5.12 (and contained in the file `examples.dir/CNi_graded.dat`), is the grazing incidence X-ray reflectance vs. energy of a graded C/Ni multilayer film, showing the effect of interface roughness/diffuseness on the specular reflectance. This calculation was made by defining two coupled parameters (see Section 2.3): the Ni layer thickness was set to be 0.8 times the C layer thickness (which was graded), and the Ni layer interface width was set equal to the C layer interface width, which itself was defined as an independent variable.

Figure 2.5.12. The grazing incidence X-ray reflectance of a graded C/Ni multilayer, as a function of interface width.

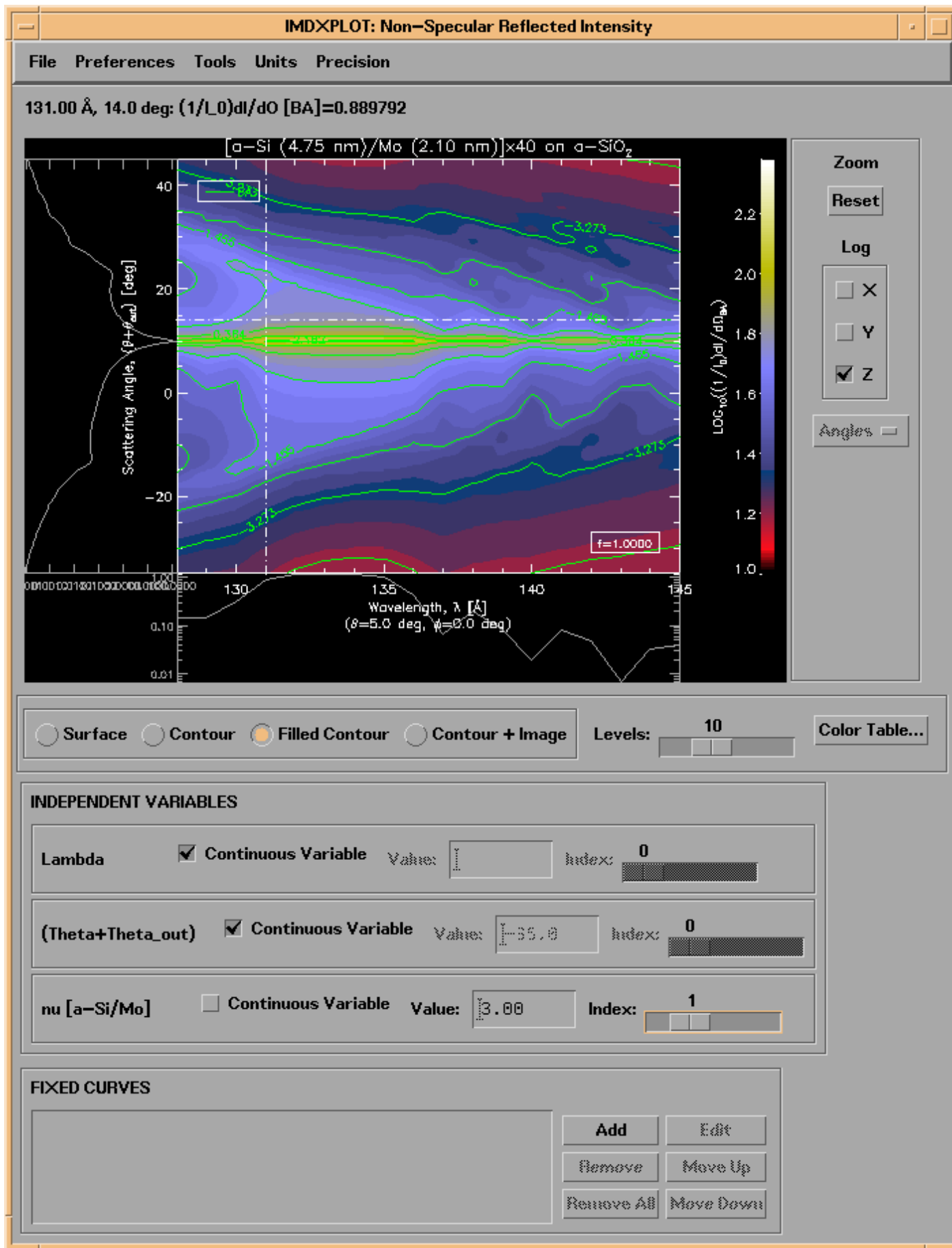




Normal-incidence non-specular reflected intensity for a Mo/Si multilayer, using the Born approximation, with coupled parameters

Figure 2.5.13 shows the result of a calculation of the non-specular reflected intensity for a Mo/Si multilayer film, near normal incidence in the soft X-ray region, computed using the Born approximation vector theory. The Omega/nu/n PSD model was used, and the PSD parameters of the Mo-on-Si interface were coupled to those of the Si-on-Mo interface; the Si-on-Mo relaxation coefficient, nu, was defined as an independent variable. Contours of constant intensity as a function of wavelength and scattering angle are superimposed on a filled color contour plot, and 1D slices are shown below and to the left of the contour plot. (See the file `examples.dir/SiMo.ns_ba.dat`.)

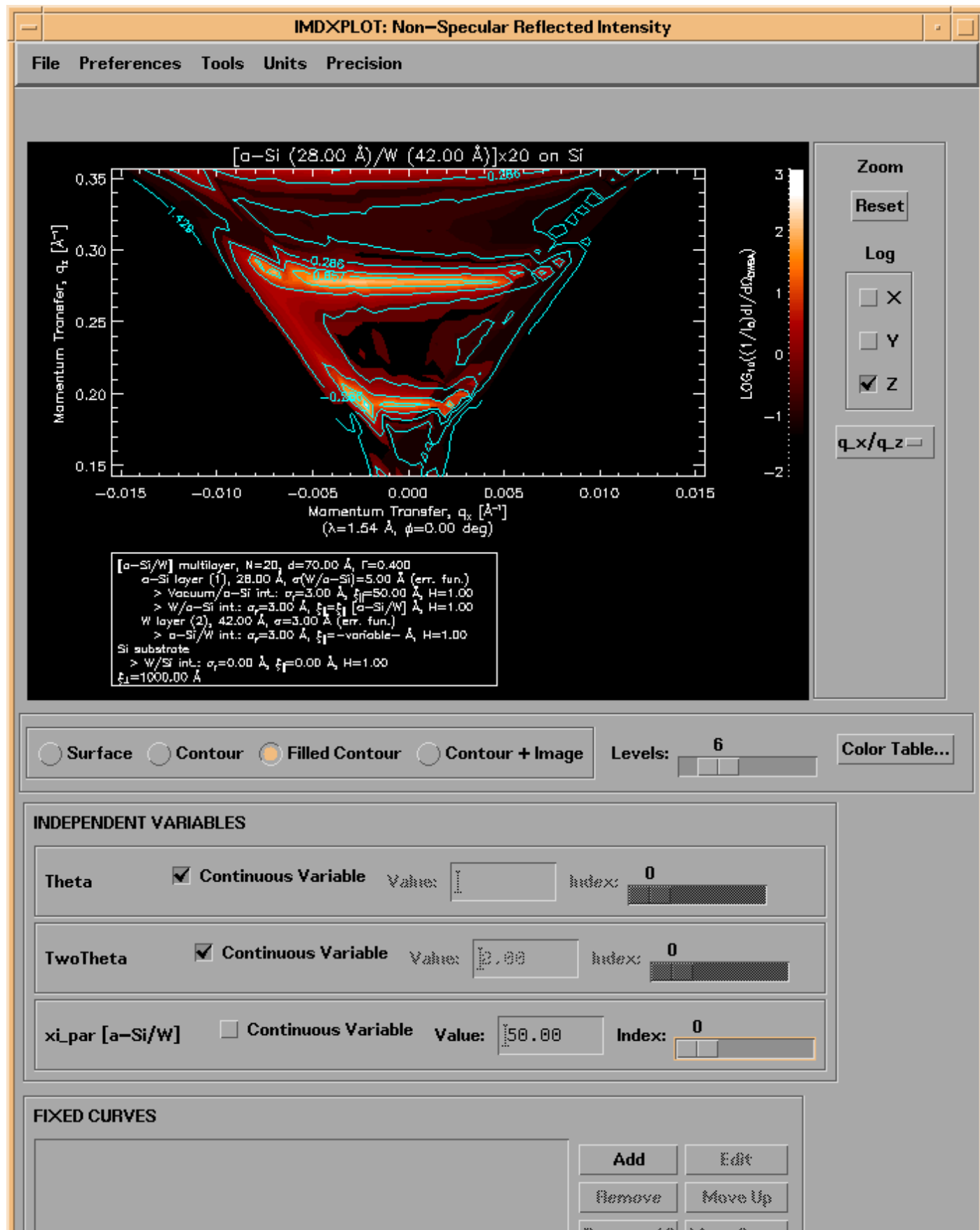
Figure 2.5.13. The non-specular reflected intensity for a Mo/Si multilayer film near normal incidence, computed using the BA theory (see [Section 2.3.](#))



Grazing incidence non-specular reflected intensity of a W/Si multilayer using the distorted-wave Born approximation, with coupled parameters

The last example, shown in Figure 2.5.14, is a plot in q-space of the grazing incidence, non-specular reflected X-ray intensity for a W/Si multilayer calculated with the DWBA theory, as a function of the lateral correlation length. The correlation length of the Si-on-W interface was coupled to that of the W-on-Si interface for this calculation. (See the file `examples.dir/SWi.ns_dwba.dat`.)

Figure 2.5.14. The non-specular reflected intensity for a W/Si multilayer film near grazing incidence, computed using the DWBA theory (see [Section 2.3.](#))





[Back](#) | [Contents](#) | [Next](#)

Chapter 3. Measured Data and Parameter Estimation

In addition to using IMD for modeling, you can also use IMD for parameter estimation (with confidence interval generation) using nonlinear, least-squares curve-fitting, based on the **Chi²** test of fit.

To illustrate, I will present an example showing how to determine the optical constants of a film from reflectance vs. incidence angle measurements.

Note: In IMD you can choose to use either the IDL CURVEFIT function (actually, a slightly modified version,) which is based on the Marquardt algorithm [14] described in reference [15], or the MPFIT function, an implementation of the MINPACK-1 Levenberg-Marquardt algorithm [19], developed by C. B. Markwardt <<http://astrog.physics.wisc.edu/~craigm/idl.html>>

[3.1 Using your measured data](#)

[3.2 Specifying fit parameters](#)

[3.3 Curve-fitting](#)

[3.4 Confidence intervals](#)

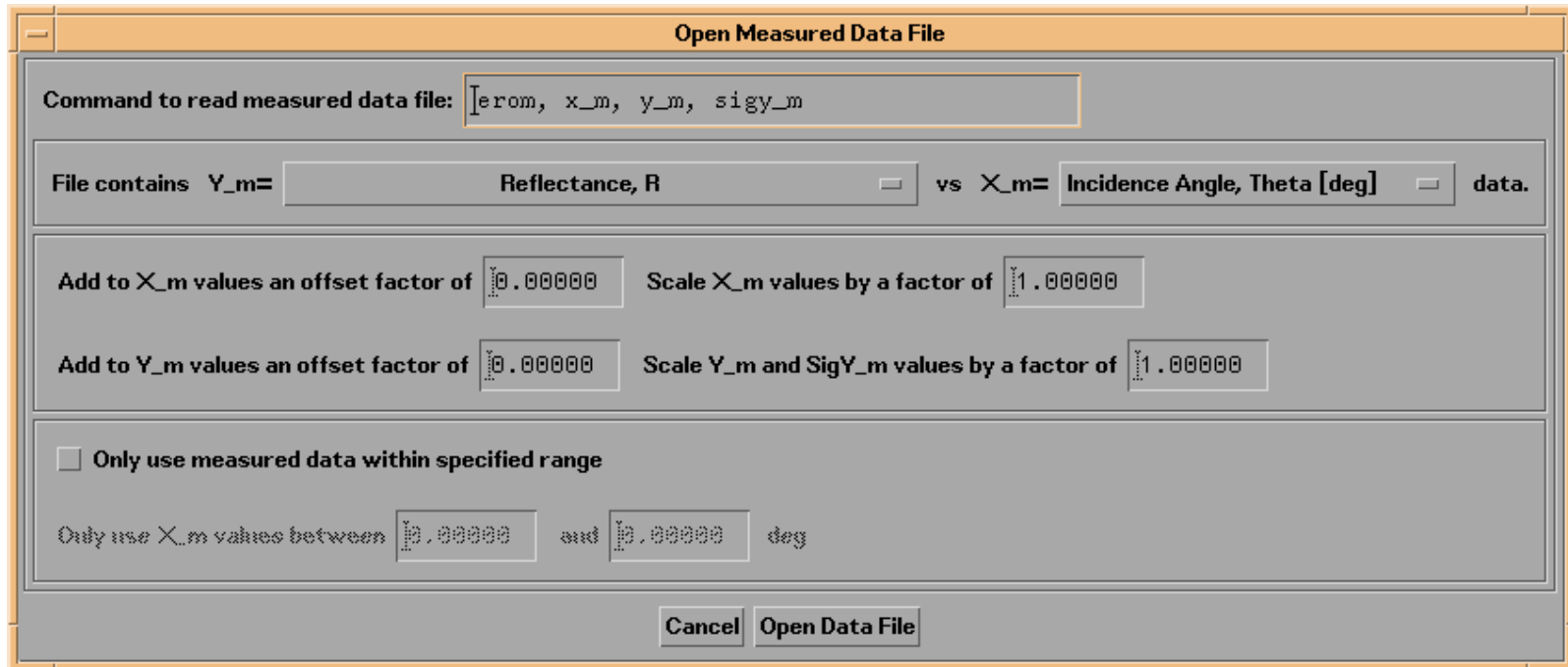
[Back](#) | [Contents](#) | [Next](#)

3.1 Using Your Measured Data

The first step in performing a fit (or just comparing your measured data to IMD calculations) is to load your measured data into IMD. The internal variable names that IMD uses for measured data are **X_m**, **Y_m**, and **SIGY_m**, where **X_m** is the independent variable, **Y_m** is the dependent variable, and **SIGY_m** is the experimental uncertainty in **Y_m**. So the goal here is to get your data inside these variables. (**SIGY_m** is optional - if you don't define it, IMD will just set it to zero.)

The easiest way to load your data into IMD is to use the **File->Open Measured Data File...** option from the main IMD widget menu bar. Figure 3.1.1 shows the widget that appears as a result:

Figure 3.1.1 IMD Open Measured Data File widget



To load in measured data, you must tell IMD what sort of data you have. In the **Open Measured Data** widget (Figure 3.1.1), you must select designations for **X_m** and **Y_m** from a list of available independent and dependent variables; the choices presented will be determined by the independent and dependent variables you have *already* selected in IMD.

For this example, I will illustrate how to read an ASCII file containing reflectance vs. incidence angle data measured for a Au film, 40 nm thick, at a wavelength of 400 nm.

Note: There are files located in the directory called `examples.dir` in the `imd` directory that you can load into IMD in order to follow along with this example. The measured data file, called 'Au_r_vs_th.MEASURED.dat', can be loaded into IMD using the **File->Open Measured Data File...** option, as described below. Use the **File->Open...** option to also read the file `Au_r_vs_th.FIT.dat` into IMD.

After specifying the relevant structure parameters (i.e., Au film, 40 nm thick), and the relevant independent and dependent variables (i.e., reflectance vs. incidence angle) in the main IMD widget, in the **Open Measured Data** widget, select **Reflectance, R** for **Y_m**, and **Incidence Angle, Theta [deg]** for **X_m**.

Note: it's important to set - *before loading the data* - the independent variable **Units** to correspond with what's actually in your file. For instance, if you're reading in data as a function of **Normal incidence angle**, make sure that the **Angle units** are set for **Normal**

Incidence, and not **Grazing Incidence**. Likewise for wavelength/energy or length units.

You can change units to whatever you prefer *after* you load in the data, but IMD needs to know what units are actually in your data file ahead of time.

The final step is to tell IMD what IDL commands to use to actually read the file. Since the file I'm reading in this example is an ASCII file containing three columns of data - angle, reflectance, and uncertainty-in-reflectance - I can use the EROM command (see the documentation for the EROM command, located in the `windt` directory). The IDL command to read in the data is thus 'EROM, X_M, Y_M, SIGY_M'. This command goes in the field labelled **Command to read measured data file:** in the **Open Measured Data File** widget.

Note: If you have data that is in some other format, so that you cannot use the EROM command as described here, then you must enter the appropriate IDL commands in the **Command to read measured data file:** field of the **Open Measured Data File** widget. Consult [Appendix B.3](#) for more details.

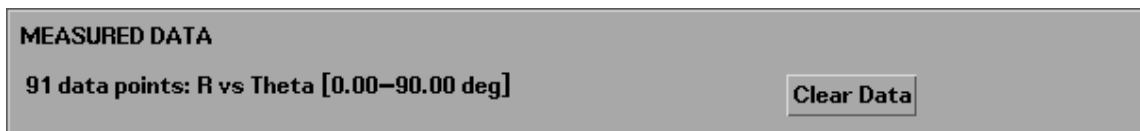
Note: You can add offsets and/or scale factors to your measured data in the **Open Measured Data File** widget (Figure 3.1.1.) This feature can be used, for example, to correct for systematic errors in your data, or to convert measured non-specular reflected X-ray intensity data, normalized to your incident beam intensity, i.e., I/I_0 , to the form $(1/I_0)dI/d\Omega$, which is the quantity that IMD computes. That is, you would divide your values of I/I_0 by your detector solid angle, $d\Omega$.

Note: You can limit the range of measured data by selecting the **Only use measured data within specified range** button, and by entering the `X_m` values that define the range of interest.

Once you have finished with the **Open Measured Data File** widget, press **Open Data File** to actually read the file. In this example, the EROM command will now ask you to select a file to open. If you wish to follow along with this example, then select the file called `Au_r_vs_th.MEASURED.dat` in the `examples.dir` directory.

After the data is read in successfully, the MEASURED DATA area of the main IMD widget will indicate what data has been loaded. In this example, the MEASURED DATA widget looks like this:

Figure 3.1.2: MEASURED DATA area of the main IMD widget after reading in data.



[Back](#) | [Contents](#) | [Next](#)

B.3 Reading measured data files

Contained here are further details on loading your measured data files into IMD.

As described in [section 3.1](#), the easiest way to load your data into IMD is to use the **File->Open Measured Data File...** option from the main IMD widget menu bar. Alternatively, you can use the procedure [IMD_M_RD](#) (described in the previous section) directly from the IDL command line (at the IMD prompt.) But in either case, you must

(a) indicate what type of data your file contains (either by setting the droplist values on the **Open Measured Data File...** widget, or by explicitly setting values for `X_M_PTR` and `Y_M_PTR` when using `IMD_M_RD` from the IDL command line)

and

(b) provide a command string to tell IMD (or `IMD_M_RD`) how to open your measured data file.

The Read-Measured-Data Command String

If your measured data file is an ASCII file containing columns of data, you can use the `EROM` procedure to read the file (see the documentation for `EROM` in the `windt` directory.) If the file is not an ASCII file, or you cannot use `EROM` for some reason, then you will need to write your own IDL procedure (or function) to read your file.

But however you read your measured data file (`EROM` or your own procedure) you must either

(a) explicitly define the IMD variables `X_M`, `Y_M`, and optionally `SIGY_M` in the **Read-Measured-Data Command String**, as in:

```
"EROM, X_M, Y_M, SIGY_M"
```

or

```
"MY_PROCEDURE, X_M, Y_M, SIGY_M"
```

or

(b) use the `IMD_M` common block (see [Appendix B.4](#)) and define `X_M`, `Y_M`, and `SIGY_M` inside the IDL procedure you write to read your data. For example:

```

PRO MY_PRO_TO_READ_MY_DATA

COMMON IMD_M

;; IDL code to read your data goes here

X_M=my_x_data
Y_M=my_y_data

;; and optionally
SIGY_M=my_siggy_data

return
end

```

So that the **Read-Measured-Data Command String** would read simply

```
"MY_PRO_TO_READ_MY_DATA".
```

As indicated in section 3.1, it's important to set - *before loading the data* - the independent variable **Units** to correspond with what's actually in your file. For instance, if you're reading in data as a function of **Normal incidence angle**, make sure that the Angle units are set for **Normal Incidence**, and not **Grazing Incidence**. Likewise for wavelength/energy or length units.

You can change units to whatever you prefer after you load in the data, but IMD needs to know what units are actually in your data file ahead of time, as IMD will convert (i.e., redefine) **X_M** after it reads the file.

But...if you want to get fancy, you can take advantage of the values of the IMD COMMON block variables **IMD.ANGLEUNITS_PTR**, **IMD.PHOTONUNITS_PTR**, or **IMD.LAYERUNITS_PTR**, (see [Appendix B.4](#)) to make sure that your data get converted correctly, regardless of how these pointers might be set. That is, if you know your data file contains, for example, reflectance vs. grazing incidence data, then you might write a procedure like this:

```

PRO MY_PRO_TO_READ_MY_GRAZING_DATA

COMMON IMD
COMMON IMD_M

;; Read an ASCII file of grazing incidence vs reflectance data

EROM, X_M, Y_M

;; Now make sure that the grazing incidence data always gets

```

```
;; converted to normal incidence properly, regardless of how
;; IMD.ANGLEUNITS_PTR is set. That is, if IMD thinks the file
;; contains normal incidence data (IMD.ANGLEUNITS_PTR=0), then make
;; it so, even though the file actually contains grazing incidence
;; data:
```

```
if IMD.ANGLEUNITS_PTR eq 0 then X_M=90-X_M
```

```
return
```

```
end
```

Remember that **X_M** will get converted (redefined) to "internal" units (i.e., normal incidence, or angstroms) after the file is read; this conversion precedes according to the current value of **IMD.X_M**.

Note: Included in the `extras.dir` directory of the imd distribution are some additional IDL procedures that I have used to read in my measured data files; you might wish to use these procedures as starting points for your own procedures.

[Back](#) | [Contents](#) | [Next](#)

B.2 Some IMD functions and procedures

Described below (using standard IDL documentation formatting), are several IMD procedures and functions that you may wish to use directly in IDL. In the documentation for the Graphics routines, you'll find an [example](#) of how to create a plot showing computations stored in separate IMD data files.

- **Computation**

[FRESNEL](#)

[NS_BA](#)

[NS_DWBA](#)

- **Optical constants**

[IMD_F1F2TONK \(procedure\)](#)

[IMD_F1F2TONK \(function\)](#)

[IMD_NK](#)

[XNKPLOT](#) (and the procedure [NKPLOT](#) contained within XNKPLOT)

- **File I/O**

[IMD_RD](#)

[IMD_M_RD](#)

- **Graphics**

[IMDSPLOT](#)

[IMDNPLOT](#)

[IMDFPLOT](#)

[IMDCPLOT](#)

[IMDMPLOT](#)

[IMD_PLOT_LBL](#)

```

;+
; NAME:
;
;   FRESNEL
;
; PURPOSE:
;
;   Compute specular optical functions and electric
;   field intensity for a multilayer stack.
;
; CALLING SEQUENCE:
;
;   FRESNEL, THETA,LAMBDA,NC,Z[,SIGMA,INTERFACE,F,Q]
;
; INPUTS:
;
;   THETA - Scalar or 1-D array of incidence angles, in degrees,
;           measured from the normal.
;
;   LAMBDA - Scalar or 1-D array of wavelengths. Units for LAMBDA
;            are the same as for Z and SIGMA.
;
;   NC - Complex array of optical constants. The dimensions of NC
;        must be (N_ELEMENTS(Z)+2,N_ELEMENTS(LAMBDA)).
;
;   Z - 1-D array of layer thicknesses. Units for Z are the same
;        as for SIGMA and LAMBDA.
;
; OPTIONAL INPUTS:
;
;   SIGMA - Scalar, 1D or 3D array of interface widths. If SIGMA
;            is a scalar, then the same roughness value is applied
;            to each interface. If SIGMA is a 1-D array, it must
;            have (N_ELEMENTS(Z)+1) elements, corresponding to the
;            number of interfaces in the stack. If SIGMA is a 3-D
;            array, it must have
;            (N_ELEMENTS(THETA),N_ELEMENTS(LAMBDA),N_ELEMENTS(Z)+1)
;            elements. Units for SIGMA are the same as for LAMBDA
;            and Z.
;
;   INTERFACE - scalar, 1-D array, or 3-D array of interface
;                roughness profile types.
;
;                INTERFACE=0 corresponds to an error-function
;                interface profile;
;
;                INTERFACE=1 corresponds to an exponential
;                interface profile;
;
;

```


; Note: if neither COMPUTE_TA nor COMPUTE_FIELD is set,
; then only reflectance is computed.
;
;

; ARES - Instrumental angular resolution, in degrees. The
; optical properties (R, T, A) vs. angle will be
; convolved with a Gaussian of width ARES, in
; order to simulate a finite instrumental
; resolution. You must specify three or more
; THETA values to use ARES.
;
;

; PRES - Instrumental spectral resolution, in the same
; units as LAMBDA. The optical properties (R, T,
; A) vs. wavelength will be convolved with a
; Gaussian of width PRES, in order to simulate a
; finite instrumental resolution. You must specify
; three or more LAMBDA values to use PRES.
;
;

; INPUTS FOR FIELD COMPUTATIONS ONLY (i.e., with COMPUTE_FIELD set):
;

; PT_SPACING - The spacing (in same units as Z) between
; field intensity points. If not specified,
; default value of 1 is used.
;
;

; Note that the actual spacing between
; points will not be regular, as it is
; necessary to compute the field intensities
; precisely at the interfaces between
; layers. See DEPTH below.
;
;

; AMBIENT_DEPTH - The depth (in same units as Z) into the
; ambient material (the material above
; the multilayer) for which the field
; intensities are to be calculated.
; If not specified, a default value of 0
; is used.
;
;

; SUBSTRATE_DEPTH - The depth (in same units as Z) into
; the substrate material (the material
; below the multilayer) for which the
; field intensities are to be
; calculated. If not specified, a
; default value of 0 is used.
;
;

; OUTPUTS:
;

; RS - Reflectance for s-polarization.
;

; RP - Reflectance for p-polarization.
;

```

;
;   RA - Average reflectance, =
;         (RS*Q*(1+F)+RP*(1-F))/(F*(Q-1)+(Q+1))
;
;   PRS - Phase of reflected wave for s-polarization.
;
;   PRP - Phase of reflected wave for p-polarization.
;
;   CRS - Complex reflected amplitude for s-polarization.
;
;   CRP - Complex reflected amplitude for p-polarization.
;
;   RHO - Ratio of CRP/CRS
;
;   PSI - Ellipsometric Psi function = ATAN(RHO*CONJ(RHO))
;
;   DELTA - Ellipsometric Delta function =
;           ATAN(IMAGINARY(RHO),DOUBLE(RHO))
;
;   FUNC_USER1,
;
;   FUNC_USER2,
;
;   FUNC_USER3 - Strings specifying the USER1, USER2 and
;               USER3 functions. The IDL EXECUTE function
;               is used to compute these functions, as in:
;               ee=EXECUTE('user1='+func_user1). Thus,
;               these strings must use valid IDL syntax,
;               and must be valid functions of any of the
;               variables and functions internal to the
;               FRESNEL procedure. See Section 2.3 for details.
;
;   USER1,
;
;   USER2,
;
;   USER3 - The user functions determined by the values of
;           associated FUNC_USER* strings described above.
;
;
;   ADDITIONAL OUTPUTS when COMPUTE_TA or COMPUTE_FIELD keywords are set:
;
;   TS - Transmittance for s-polarization.
;
;   TP - Transmittance for p-polarization.
;
;   TA - Average transmittance, =
;         (TS*Q*(1+F)+TP*(1-F))/(F*(Q-1)+(Q+1))
;
;   PTS - Phase of transmitted wave for s-polarization.
;
;   PTP - Phase of transmitted wave for p-polarization.

```

```

;
;       AS - Absorptance for s-polarization.
;
;       AP - Absorptance for p-polarization.
;
;       AA - Average absorptance, =
;           (AS*Q*(1+F)+AP*(1-F))/(F*(Q-1)+(Q+1))
;
; The dimensions of RS, RP, RA, PRS, PRP, TS, TP, TA, PTS, PTP,
; AS, AP, and AA are (N_ELEMENTS(THETA),N_ELEMENTS(LAMBDA)).
;
; ADDITIONAL OUTPUTS WHEN COMPUTE_FIELD IS SET:
;
;       DEPTH - 1-D array of depth values. The number of depth
;              values is
;
;              1+FIX(TOTAL(Z)+AMBIENT_DEPTH+SUBSTRATE_DEPTH)/PT_SPACING
;
;       The depth values are not equally spaced, as it
;       is necessary to calculate the field intensities
;       precisely at the interfaces between layers.
;       If you need an equally spaced DEPTH array,
;       you can interpolate the DEPTH, and INT values.
;
;       INTS - Field intensity for s-polarization.
;
;           Dimensions for INTS, INTP, and INTA are
;           (N_ELEMENTS(THETA),N_ELEMENTS(LAMBDA),N_ELEMENTS(DEPTH))
;
;       INTP - Field intensity for p-polarization.
;
;       INTS - Average field intensity,
;           =(INTS*Q*(1+F)+INTP*(1-F))/(F*(Q-1)+(Q+1))
;
; COMMON BLOCKS:
;
;       COMMON IMD,IMD
;
; PROCEDURE:
;
;       As the names suggest, this procedure uses the Fresnel
;       equations to compute the optical properties of a multilayer as
;       a function of angle and wavelength. All computations are
;       performed in double precision. A straightforward recursion
;       algorithm is used, which is to say that no shortcuts are
;       employed to take advantage of situations in which the
;       multilayer is purely periodic. As such, other algorithms
;       might be faster, but this one is more general.
;
;       If the COMPUTE_TA keyword is set, to compute transmittance and
;       absorptance in addition to reflectance, then the procedure is
;       significantly slower, due to the extra computation required.

```

```

;       If the COMPUTE_FIELD keyword is set, the computation time is
;       longer still.
;
;       Scattering losses due to interfacial roughness or diffuseness
;       are handled according to the methods described in Section 2.2 of
;       of the hypertext IMD documentation.
;
;       Polarization averaging is performed using the function SP2A,
;       usage:
;
;       Result=SP2A(XS,XP,F,Q),
;
;       where F and Q are as defined above, XS and XP are the optical
;       functions for pure s and p polarizations, and Result is the
;       average function. For example, the average reflectance RA is
;       given by:
;
;       
$$RA = (RS * Q * (1 + F) + RP * (1 - F)) / (F * (Q - 1) + (Q + 1))$$

;
;       Instrumental resolution is computed by convolution with a
;       gaussian, using the function INSTRUMENT_RES, usage:
;
;       Result=INSTRUMENT_RES(X,Y,RES,ANGLE=ANGLE,
;                               WAVELENGTH=WAVELENGTH,ENERGY=ENERGY),
;
;       where RES is the width of the gaussian, and X and Y are the
;       independent and dependent variables (e.g., X=THETA, Y=RA).
;       Set ANGLE to convolve reflectance, transmittance, or
;       absorptance vs. angle, WAVELENGTH to convolve r/t/a vs.
;       wavelength, or ENERGY, to convolve r/t/a vs. energy. In the
;       case of ENERGY, both X and RES must be specified in angstroms,
;       but are converted to eV before doing the convolution.
;
; EXAMPLE:
;
;       Compute the reflectance of a gold film, 500 A thick, vs angle,
;       at a wavelength of 4000 A:
;
;       Define THETA=VECTOR(0.,90.,91), an array of angles from 0 to 90
;       degrees, in 1 degree steps.
;
;       Define LAMBDA=4000.
;
;       Using the optical constants for Au at 4000 A, we define
;       NC=[complex(1.,0.),complex(1.658,1.956),complex(1.,0.)],
;       assuming the Au film is surround by vacuum on either side.
;
;       Define Z=[500.]
;
;       FRESNEL, THETA, LAMBDA, NC, Z, RA=RA
;
;       The value for RA we compute in this example corresponds to

```

```

;      unpolarized light.
;
; MODIFICATION HISTORY:
;
;      David L. Windt, Bell Labs, May 1997
;
;      Updated to IMD V4.0, April, 1998
;
;      windt@bell-labs.com
;
;-

```

```

;+
; NAME:
;
;      NS_BA
;
; PURPOSE:
;
;      Procedure to compute the non-specular reflected intensity for
;      a multilayer film, using the Born approximation theory
;      developed by D. Stearns, as described in reference [4].
;
; CALLING SEQUENCE:
;
;      NS_BA, THETA_IN, THETA_OUT, LAMBDA, NC, Z [, F, Q]
;
; INPUTS:
;
;      THETA_IN - Scalar or 1-D array of incidence angles, in
;                degrees, measured from the normal.
;
;      THETA_OUT - Scalar or 1-D array of scattering angles, in
;                 degrees, measured from the normal.
;
;      If THETA_IN is a scalar, then the same value of THETA_IN will
;      be used for every value of THETA_OUT. Similarly, if THETA_OUT
;      is a scalar, then the same value of THETA_OUT will be used for
;      every value of THETA_IN. If THETA_IN and THETA_OUT are both
;      1D arrays, then they must have the same number of elements.
;      In any case, the non-specular reflected intensity is computed
;      for pairs of THETA_IN, THETA_OUT values.
;
;      LAMBDA - Wavelength (scalar).
;
;      NC - Complex array of optical constants. The dimensions of NC
;           must be (N_ELEMENTS(Z)+2)
;
;      Z - 1-D array of layer thicknesses. Units for Z are the same
;          as for SIGMA and LAMBDA.

```

```

;
; OPTIONAL INPUTS:
;
;
; F - Incident polarization factor, defined as the ratio
;       $(I(s)-I(p)) / (I(s)+I(p))$ , where  $I(s)$  and  $I(p)$  are the
;      incident intensities of s and p polarizations. So for pure
;      s-polarization specify  $F=+1$ ; for pure p-polarization
;      specify  $F=-1$ , or for unpolarized incident radiation,
;      specify  $F=0$ .
;
; Q - Polarization analyzer sensitivity, defined as the
;      sensitivity to s-polarization divided by the sensitivity
;      to p-polarization. Specifying a value of q other than 1.0
;      could be used to simulate, for example, the reflectance
;      you would measure using a detector that (for whatever
;      reason) was more or less sensitive to s-polarization than
;      to p-polarization.
;
; KEYWORD PARAMETERS:
;
; INPUTS:
;
; PHI - Scattering plane azimuthal angle. (Scalar.) Default is 0 deg.
;
; MFC_MODEL - an integer specifying the form of the modified
;             Fresnel coefficients to be used to account for
;             interface imperfections. See Section 2.2 for
;             details.
;
; PSD_MODEL - Set PSD_MODEL=0 to use the sigma_r/xi_par/H PSD model.
;             Set PSD_MODEL=1 to use the Omega/nu/n PSD model.
;
; If PSD_MODEL=0, then the following three parameters must be
; supplied:
;
; SIGMA_R - 1D array of interface roughnesses. N_ELEMENTS(Z)+1
;           elements.
;
; XI_PAR - 1D array of interface correlation lengths. N_ELEMENTS(Z)+1
;          elements.
;
; H - 1D array of interface jaggedness factors. N_ELEMENTS(Z)+1
;     elements.
;
; In addition, you can also specify:
;
; XI_PERP - Perpendicular correlation length (scalar).
;
;
; If PSD_MODEL=1, then the following three parameters must be

```

```

;   supplied:
;
;   OMEGA - 1D array of interface volumen
;           elements. N_ELEMENTS(Z)+1 elements.
;
;   NU - 1D array of interface relaxation
;        coefficients. N_ELEMENTS(Z)+1 elements.
;
;   N_ - 1D array of PSD exponents. N_ELEMENTS(Z)+1 elements.
;
;   You can also specify:
;
;   SUBSTRATE_Z - The Z value of the 'substrate', needed to
;                 compute the PSD of the bottom-most interface
;                 when using the Omega/nu/n PSD model.
;
;   Diffuse interfaces can be used when computing the electric
;   field intensities (needed to compute the scattered intensity)
;   by specifying values for SIGMA_D and INTERFACE. The electric
;   fields will be computed from modified Fresnel coefficients,
;   as described in Section 2.2.
;
;   SIGMA_D - 1D array of interface diffuseness factors.
;             SIGMA_D must have N_ELEMENTS(Z)+1 elements.
;
;   INTERFACE - 1D array of interface profiles
;               functions. INTERFACE must have
;               N_ELEMENTS(Z)+1 elements.
;
;               INTERFACE=0 corresponds to an
;               error-function interface profile;
;
;               INTERFACE=1 corresponds to an exponential
;               interface profile;
;
;               INTERFACE=2 corresponds to a linear
;               interface profile;
;
;               INTERFACE=3 corresponds to a sinusoidal
;               interface profile;
;
;               INTERFACE=4 corresponds to a step functoin
;               interface.
;
;   ARES - Instrumental angular resolution, in degrees. The
;          non-specular reflected intensity vs. angle will
;          be convolved with a Gaussian of width ARES, in
;          order to simulate a finite instrumental
;          resolution. You must specify three or more

```

```

;           THETA_IN or THETA_OUT values to use ARES.
;
;   OUTPUTS:
;
;           DIDOMEGA_S - s-polarized component of reflected
;                       intensity.
;
;           DIDOMEGA_P - p-polarized component of reflected
;                       intensity.
;
;           DIDOMEGA_A - polarization-averaged reflected intensity.
;
;           See Section 2.3 for a complete description of these
;           three functions, and how they depend on f and q.
;
;   COMMON BLOCKS:
;
;           COMMON IMD,IMD
;
;   PROCEDURE:
;
;           Instrumental resolution is computed by convolution with a
;           gaussian, using the function INSTRUMENT_RES, usage:
;
;           Result=INSTRUMENT_RES(X,Y,RES,/ANGLE)
;
;           where RES is the width of the gaussian, and X and Y are the
;           independent and dependent variables (e.g., X=THETA,
;           Y=DIDOMEGA_S). Set ANGLE to convolve didomega vs. angle.
;
;   MODIFICATION HISTORY:
;
;           David L. Windt, Bell Labs, April, 1998
;
;           windt@bell-labs.com
;
; -

```

```

;+
;   NAME:
;
;           NS_DWBA
;
;   PURPOSE:
;
;           Procedure to compute the non-specular reflected intensity for
;           a multilayer film, using the distorted-wave Born approximation
;           theory developed by Sinha/Holy/de Boer, described in
;           references 5,6,7 and 8.

```

```

;
; CALLING SEQUENCE:
;
;     NS_DWBA, THETA_IN, THETA_OUT, LAMBDA, NC, Z
;
; INPUTS:
;
;     THETA_IN - Scalar or 1-D array of incidence angles, in
;               degrees, measured from the normal.
;
;     THETA_OUT - Scalar or 1-D array of scattering angles, in
;                degrees, measured from the normal.
;
;     If THETA_IN is a scalar, then the same value of THETA_IN will
;     be used for every value of THETA_OUT. Similarly, if THETA_OUT
;     is a scalar, then the same value of THETA_OUT will be used for
;     every value of THETA_IN. If THETA_IN and THETA_OUT are both
;     1D arrays, then they must have the same number of elements.
;     In any case, the non-specular reflected intensity is computed
;     for pairs of THETA_IN, THETA_OUT values.
;
;
;     LAMBDA - Wavelength (scalar).
;
;     NC - Complex array of optical constants. The dimensions of NC
;          must be (N_ELEMENTS(Z)+2)
;
;     Z - 1-D array of layer thicknesses. Units for Z are the same
;         as for SIGMA and LAMBDA.
;
; KEYWORD PARAMETERS:
;
;     INPUTS:
;
;     PHI - Scattering plane azimuthal angle. (Scalar.) Default is 0.
;
;     MFC_MODEL - an integer specifying the form of the modified
;                 Fresnel coefficients to be used to account for
;                 interface imperfections. See Section 2.2 for
;                 details.
;
;     PSD_MODEL - Set PSD_MODEL=0 to use the sigma_r/xi_par/H PSD model.
;                 Set PSD_MODEL=1 to use the Omega/nu/n PSD model.
;
;
;     If PSD_MODEL=0, then the following three parameters must be
;     supplied:
;
;     SIGMA_R - 1D array of interface roughnesses. N_ELEMENTS(Z)+1
;               elements.
;
;     XI_PAR - 1D array of interface correlation lengths. N_ELEMENTS(Z)+1

```

```

;           elements.
;
;   H - 1D array of interface jaggedness factors. N_ELEMENTS(Z)+1
;       elements.
;
;   In addition, you can also specify:
;
;   XI_PERP - Perpendicular correlation length (scalar).
;
;
;   If PSD_MODEL=1, then the following three parameters must be
;   supplied:
;
;   OMEGA - 1D array of interface volumen
;           elements. N_ELEMENTS(Z)+1 elements.
;
;   NU - 1D array of interface relaxation
;        coefficients. N_ELEMENTS(Z)+1 elements.
;
;   N_ - 1D array of PSD exponents. N_ELEMENTS(Z)+1 elements.
;
;   You can also specify:
;
;   SUBSTRATE_Z - The Z value of the 'substrate', needed to
;                 compute the PSD of the bottom-most interface
;                 when using the Omega/nu/n PSD model.
;
;   Diffuse interfaces can be used when computing the electric
;   field intensities (needed to compute the scattered intensity)
;   by specifying values for SIGMA_D and INTERFACE. The electric
;   fields will be computed from modified Fresnel coefficients,
;   as described in Section 2.2.
;
;           SIGMA_D - 1D array of interface diffuseness factors.
;                   SIGMA_D must have N_ELEMENTS(Z)+1 elements.
;
;           INTERFACE - 1D array of interface profiles
;                      functions. INTERFACE must have
;                      N_ELEMENTS(Z)+1 elements.
;
;                   INTERFACE=0 corresponds to an
;                   error-function interface profile;
;
;                   INTERFACE=1 corresponds to an exponential
;                   interface profile;
;
;                   INTERFACE=2 corresponds to a linear
;                   interface profile;
;
;                   INTERFACE=3 corresponds to a sinusoidal
;                   interface profile;

```

```

;
;           INTERFACE=4 corresponds to a step functoin
;           interface.
;
;
;
;           ARES - Instrumental angular resolution, in degrees. The
;           non-specular reflected intensity vs. angle will
;           be convolved with a Gaussian of width ARES, in
;           order to simulate a finite instrumental
;           resolution. You must specify three or more
;           THETA_IN or THETA_OUT values to use ARES.
;
;   OUTPUTS:
;
;           DIDOMEGA - non-specular reflected intensity.
;
;   COMMON BLOCKS:
;
;           COMMON IMD,IMD
;
;   PROCEDURE:
;
;           Instrumental resolution is computed by convolution with a
;           gaussian, using the function INSTRUMENT_RES, usage:
;
;           Result=INSTRUMENT_RES(X,Y,RES,/ANGLE)
;
;           where RES is the width of the gaussian, and X and Y are the
;           independent and dependent variables (e.g., X=THETA,
;           Y=DIDOMEGA_S). Set ANGLE to convolve didomega vs. angle.
;
;   MODIFICATION HISTORY:
;
;           David L. Windt, Bell Labs, April, 1998
;
;           windt@bell-labs.com
;
; -

```

```

;+
; NAME:
;
;           IMD_F1F2TONK (procedure)
;
; PURPOSE:
;
;           This procedure is a widget interface to the IMD\_F1F2TONK
;           function, and is used to compute optical constants (n,k)

```

```
;          from atomic scattering factors for a compound specified by
;          composition and density.  The resulting optical constants are
;          plotted (using xnkplot; the plot can then be printed using
;          plot_print,) and can be saved to a text file (.nk format).
;
```

```
; CALLING SEQUENCE:
```

```
;          IMD_F1F2TONK
```

```
; COMMON BLOCKS:
```

```
;          IMD
;          IMD_F1F2TONK
```

```
; RESTRICTIONS:
```

```
; See the restrictions for the IMD_F1F2TONK function.
```

```
; PROCEDURE:
```

```
; In this program, the optical constants are computed over a grid of
; 1000 energies, logarithmically spaced from 30 eV to 100 keV.
```

```
; MODIFICATION HISTORY:
```

```
; David L. Windt, Bell Labs, May 1997.
```

```
; windt@bell-labs.com
```

```
; November 1997: renamed from F1F2TONK; brand new widget interface.
```

```
; April 1998: Default grid is now 1000 energies from 30 eV to 100
; keV.
```

```
;-
```

```
;+
```

```
; NAME:
```

```
;          IMD_F1F2TONK (function)
```

```
; PURPOSE:
```

```
;          This function computes optical constants (n,k) from
;          atomic scattering factors for a compound specified
;          by its composition and density.
```

```
; CALLING SEQUENCE:
```

```
;
```

```

;           Result=IMD_F1F2TONK(DENSITY,NUMBER,ELEMENT[ ,WAVELENGTH])
;
;
;

```

```

; INPUT PARAMETERS:
;
;

```

```

;           DENSITY - compound density, in gm/cm3.
;
;

```

```

;           NUMBER - scalar or array of relative concentrations. For example,
;                   to compute the optical constants for Al2O3, set
;                   NUMBER=[2.,3.]
;
;

```

```

;           ELEMENT - scalar or array of chemical element symbols. For example,
;                   to compute the optical constants for Al2O3, set
;                   ELEMENT=['Al','O'].
;
;

```

```

;           WAVELENGTH - vector of wavelengths. If omitted, the optical
;                   constants are computed over a logarithmically-spaced
;                   grid of 500 wavelengths from 0.413 to 413 A (i.e.,
;                   from 30 eV to 30 keV.)
;
;

```

```

; OUTPUTS:
;
;

```

```

;           Result - A complex scalar or 1-D array (the same length
;                   as WAVELENGTH) containing the optical constants (n,k).
;
;

```

```

; KEYWORD PARAMETERS:
;
;

```

```

;           F1F2 - optional input or output array of atomic scattering factors.
;                   Dimensions=[2,N_ELEMENTS(NUMBER),N_ELEMENTS(WAVELENGTH)]; Thus
;                   F1F2(0,0,*) are the F1 values for the first element, and
;                   F1F2(1,0,*) are the F2 values for the first element, and so on.
;                   If F1F2 is dimensioned correctly, then the atomic scattering
;                   factors are not read from the files corresponding to the elements
;                   of the ELEMENT array, but rather the passed values are used.
;                   (So be sure that the F1F2 values are correct!)
;                   Conversely, if F1F2 is undefined (or ill-defined) then the
;                   returned value of F1F2 will contain the F1 and F2 values read
;                   from the atomic scattering factors files.
;
;

```

```

; COMMON BLOCKS:
;
;

```

```

;           IMD
;           IMD_F1F2TONK
;
;

```

```

; RESTRICTIONS:
;
;

```

```

; The program uses atomic scattering factors compiled from the CXRO
; and LLNL websites. (See Section A.3.)
;
;

```

```

; The atomic scattering factor files must be located in the directory
; specified in the file IMDSITECONFIG.PRO, located in the IMD
; directory. However, if the files are not found, the user will be

```

```

; prompted to enter the path leading to these files.
;
; PROCEDURE:
;
; The optical constants are computed according to the principles
; described in the paper "X-ray interactions: photoabsorption,
; scattering, transmission, and reflection at E=50-30,000 eV,
; Z=1-92", B.L. Henke, E. M. Gullikson, and J. C. Davis, Atomic
; Data and Nuclear Data Tables, Vol. 54, No. 2, July 1993. (See
; especially equations (17) and (18).)
;
; MODIFICATION HISTORY:
;
; David L. Windt, Bell Labs, Nov 1997.
; windt@bell-labs.com
;
;-

```

```

;+
; NAME:
;
;     IMD_NK
;
; PURPOSE:
;
;     A function used to read IMD optical constant files (.nk files).
;
; CALLING SEQUENCE:
;
;     Result=IMD_NK(MATERIAL,WAVELENGTH)
;
; INPUTS:
;
;     MATERIAL - A string specifying the name of a valid
;                optical constant file, without the .nk extension.
;
;     WAVELENGTH - A scalar or 1-D array specifying the wavelength
;                  in angstroms.
;
; OUTPUTS:
;
;     Result - A complex scalar or 1-D array (the same length
;              as WAVELENGTH) containing the optical constants (n,k).
;
; COMMON BLOCKS:
;
;     IMD
;     IMD_WIDGET
;
; PROCEDURE:

```

```

;
;       The optical constant file is read, and the data are interpolated
;       (using FINDEX and INTERPOLATE) to get n and k at the specified
;       wavelengths.
;
; MODIFICATION HISTORY:
;
; David L. Windt, Bell Labs, April 1997
; windt@bell-labs.com
;-

```

```

;+
; NAME:
;
;       XNKPLOT
;
; PURPOSE:
;
;       This procedure plots optical constants n,k versus
;       wavelength, and allows the user the ability to adjust some
;       of the plot settings, and print the plot, through a GUI.
;
; CALLING SEQUENCE:
;
;       XNKPLOT[ ,LAMBDA,N,K]
;
; OPTIONAL INPUTS:
;
;       LAMBDA - A 1D vector of wavelength values, in Angstroms
;
;       N, K - 1D vectors of n and k values
;
;       Note: if no inputs are supplied, the use can open a new
;       optical constant file from the File->Open menu option.
;
; RESTRICTIONS:
;
;       Requires widgets; uses lots of stuff in the
;       ~idl/user_contrib/windt directory.
;
; PROCEDURE:
;
;       Note that the procedure called NKPLOT (usage:
;       NKPLOT,LAMBDA,N,K) is the one that actually creates the
;       plot.  NKPLOT can be used on it's own if desired:
;
;       KEYWORDS to nkplot (in addition to most IDL keywords
;       accepted by the plot command):
;
;       XAXIS, NAXIS, KAXIS - 4-element vectors specifying the IDL

```

```

;           [type,range(0),range(1),style] axis
;           values. i.e., type=1 for log plots,
;           etc. For example, to plot n on a
;           linear scale from 0 to 2, and k on a
;           log scale from .1 to 10, specify
;           naxis=[0.,0.,2.,0.],kaxis=[1.,.1,10.,0.]
;
;
;           NSTYLE, KSTYLE - 5-element vectors specifying the IDL
;           [color,linestyle,thick,psym,symsize]
;           values for the n and k curves. For
;           example, to plot n using a red dashed line,
;           specify nstyle=[2,1,0,0,0]
;
;           LABEL_POSITION - a scalar, in the range 0. to 1.,
;           specifying the position along the xaxis
;           for the 'n' and 'k' curve labels. (See
;           the CURVE_LABEL procedure for more
;           details.)
;
;           BANGY_N - the value of the !y system variable set after
;           creating the n-vs-lambda plot. the only reason
;           to use this keyword is to enable subsequent use
;           of the overplot keyword.
;
;           BANGY_K - the value of the !y system variable set after
;           creating the k-vs-lambda plot. the only reason
;           to use this keyword is to enable subsequent use
;           of the overplot keyword.
;
;           OVERPLOT - set this to overplot n and k vs lambda on an
;           existing plot made with nkplot. this keyword
;           must be used with the bangy_n and bangy_k
;           keywords.
;
;           Example: plot two sets of n,k values on the same plot:
;
;
;           NKPLOT,lambda1,n1,k1, $
;                   bangy_n=bangy_n,bangy_k=bangy_k
;           NKPLOT,lambda2,n2,k2, $
;                   bangy_n=bangy_n,bangy_k=bangy_k,/overplot
;
; SIDE EFFECTS:
;
;           TEK_COLOR is used to set the color tables.
;
; COMMON BLOCKS:
;
;           IMD
;           PLOT_PRINT (see ~windt/plot_print.pro)
;

```

```
;
; RESTRICTIONS:
;
; The program uses many procedures found in the
; ~idl/user_contrib/windt directory.
;
; MODIFICATION HISTORY:
;
; David L. Windt, Bell Labs, April 1997
; windt@bell-labs.com
;-

;+
;
; NAME:
;
;     IMD_RD
;
; PURPOSE:
;
;     A function used to open IMD files.
;
; CALLING SEQUENCE:
;
;     Result=IMD_RD([FILE=FILE])
;
; KEYWORD PARAMETERS:
;
;     FILE - The name of the IMD file to open.  If omitted, PICKFILE
;           will be used to get a file name.
;
; OUTPUTS:
;
;     Result - 0 or 1, depending on whether the file was opened
;           successfully or not.
;
; COMMON BLOCKS:
;
;     IMD
;     IMD_PARS
;     IMD_VARS
;     IMD_FPARS
;     IMD_FVARS
;     IMD_NSVARS
;
; RESTRICTIONS:
;
;     Must be used in the IMD environment.
;
;     New versions of IMD will probably not be able to open old IMD
```

```
; files.
;
; PROCEDURE:
;
;   IMD files are saved and opened using the IDL SAVE and RESTORE
;   commands.  The IMD_RD procedure does a few more things than just
;   calling RESTORE, so you should not try to open IMD files using
;   RESTORE directly.
;
; MODIFICATION HISTORY:
;
;   David L. Windt, Bell Labs, April 1997.
;   windt@bell-labs.com
;-
```

```
;+
;
; NAME:
;
;   IMD_M_RD
;
; PURPOSE:
;
;   A procedure to open a measured data file and define the IMD
;   variables X_M, Y_M, and SIGY_M, as well as the pointers X_M_PTR
;   and Y_M_PTR and some other important internal IMD variables.
;
; CALLING SEQUENCE:
;
;   IMD_M_RD, X_M_PTR=X_M_PTR, Y_M_PTR=Y_M_PTR,
;           RD_M_CMD=RD_M_CMD,
;           X_M_SCALE=X_M_SCALE,
;           Y_M_SCALE=Y_M_SCALE,
;           X_M_OFFSET=X_M_OFFSET,
;           Y_M_OFFSET=Y_M_OFFSET
;
;
; INPUTS:
;
;   X_M_PTR - An integer that tells IMD to which independent variable
;             the X_M data refer.  X_M_PTR=0 indicates incidence
;             angle data and X_M_PTR=1 indicates wavelength (or
;             energy) data.  If other independent variables are
;             already defined in the IMD environment, then larger
;             values of X_M_PTR can be set.  The order of the
;             variables listed in the Independent Variables List, on
;             the main IMD widget, correspond to X_M_PTR values.
;
;             If X_M_PTR is omitted, then the data will be assumed
;             have an independent variable corresponding to the
```

```

;           current value if IMD.X_M, i.e., if measured data has
;           already been defined, the new data will be assumed to
;           have the same independent variable, or if no data has
;           been read, IMD.X_M=0, indicating incidence angle data.
;
; Y_M_PTR - An integer that tells IMD which dependent variable the
;           Y_M data refer to. Set
;
;           Y_M_PTR=0 for reflectanc
;           Y_M_PTR=1 for transmittance
;           Y_M_PTR=2 for absorptance
;           Y_M_PTR=3 for psi
;           Y_M_PTR=4 for delta
;           Y_M_PTR=5 for user1
;           Y_M_PTR=6 for user2
;           Y_M_PTR=7 for user3
;           Y_M_PTR=8 for non-specular reflected intensity
;
;
; RD_M_CMD - A string specifying the command to actually read the
;           data file. The command string must obey IDL syntax
;           rules.
;
; OPTIONAL KEYWORD PARAMETERS:
;
; LIMIT_M - Set this keyword to 1 to cause IMD_M_RD to ignore measured
;           data values outside the range specified by the X_M_RANGE
;           keyword if it is set, or by the current value of the
;           IMD.X_M_RANGE. Set this keyword to 0 to use the entire data
;           set. If LIMIT_M is not explicitly set, then the current
;           value of IMD.LIMIT_M is used.
;
; X_M_RANGE - A 2-element array specifying the range of X_M values outside
;           of which the measured data is to be ignored. For example,
;           if the measured data file contains incidence angle data from
;           0 to 90 degrees, but you wish to ignore data from 0 to 5 degrees
;           and from 85 to 90 degrees, then set X_M_RANGE=[5.,85.].
;           If X_M_RANGE is not set, then the current value of IMD.X_M_RANGE
;           is used. Note that X_M_RANGE (and/or IMD.X_M_RANGE) is only
;           used if LIMIT_M (or IMD.LIMIT_M) is set to 1.
;
; X_M_OFFSET - An offset of X_M_OFFSET will be added to the X_M data.
;           Default value is 0.
;
; X_M_SCALE - The X_M data will be multiplied by X_M_SCALE.
;           Default value is 1.
;
; Y_M_OFFSET - An offset of Y_M_OFFSET will be added to the Y_M data.
;           Default value is 0.
;
; Y_M_SCALE - The Y_M data will be multiplied by Y_M_SCALE.
;           Default value is 1.

```

```

;
; COMMON BLOCKS:
;
;   IMD
;   IMD_VARS
;   IMD_PARS
;   IMD_NSVARS
;   IMD_M
;
; RESTRICTIONS:
;
;   If your data does not include experimental uncertainties, SIGY_M,
;   the uncertainty in Y_M, will be set to zero. (In this case, you
;   will not be able to use instrumental weighting when performing
;   curve-fits in IMD.)
;
;   NOTE: You should always use IMD M RD to open a measured data file from
;   the IDL command line, even if you have written a procedure that defines
;   X m, Y m, and SIGY m directly.
;
; PROCEDURE:
;
;   IMD_M_RD will read your data file, and it will set the IMD
;   measured-data-valid flag (IMD.M_VALID) accordingly.
;
;   The measured data file is opened, by using the EXECUTE function
;   with RD_M_CMD as an argument. If RD_M_CMD does not include
;   X_M, Y_M, and optionally SIGY_M explicitly, than the procedure
;   to read the data must contain the IMD_M common block, and
;   these variables must be set inside the procedure.
;
;   Note: The X_M data will be converted to angstroms if X_M refers to
;   wavelengths or lengths, or to degrees from the normal if X_m refers
;   to angles. The conversion will depend on the current values of the
;   IMD internal pointers (IMD.ANGLEUNITS, IMD.PHOTONUNITS_PTR and
;   IMD.LAYERUNITS_PTR; see Appendix B4), so it's important that these
;   pointers are 'pointing' correctly BEFORE READING THE DATA. You should
;   NEVER attempt to set these pointers yourself.
;
;   For example, to read a measured data file containing three
;   columns of data - incidence angle, reflectance, and uncertainty
;   in reflectance - the EROM command could be used, so that the
;   value of RD_M_CMD would be set to
;
;   RD_M_CMD='EROM,X_M,Y_M,SIGY_M'
;
;   Alternatively, if you have an IDL procedure that you have written
;   to read you own measured data files, you would include the IMD_M
;   common block in your procedure (or function) and define X_M, Y_M,
;   and optionally SIGY_M explicitly:
;
;   RD_M_CMD='MY_PRO_TO_READ_MY_DATA'

```

```

;
;   where:
;
;   PRO MY_PRO_TO_READ_MY_DATA
;
;   COMMON IMD_M
;
;   ;; IDL code to read your data goes here
;
;   X_M=my_x_data
;   Y_M=my_y_data
;
;   ;; and optionally
;   SIGY_M=my_siggy_data
;
;   return
;   end
;
; MODIFICATION HISTORY:
;
;   David L. Windt, Bell Labs, April 1997.
;   windt@bell-labs.com
;
;   November 1997: added the LIMIT_M and X_M_RANGE keywords.
;
;   April 1998: added the Y_M_SCALE keyword.
;
; -

```

```

;+
; NAME:
;
;   IMDSPLOT
;   IMDNPLOT
;   IMDFPLOT
;   IMDCPLOT
;
; PURPOSE:
;
;   These four procedures produce 1D and/or 2D plots of specular
;   optical properties (reflectance/transmittance/absorptance
;   etc. ), non-specular reflected intensity, field intensity, and
;   confidence levels, respectively.
;
;   See the KEYWORD and PROCEDURE sections below for details.
;
; CALLING SEQUENCE:
;
;   IMDSPLOT
;   IMDNPLOT

```

```

;      IMDFPLOT
;      IMDCPLOT
;
; KEYWORD PARAMETERS:
;
;      IVINDICES - (IMDSPLOT,IMDNPLOT, IMDFPLOT only) Array indicating
;                  the array indices of independent variables. The
;                  length of IVINDICES is equal to the number of
;                  independent variables that are defined (as indicated
;                  in the Independent Variables list on the IMD
;                  widget). There are always at least two independent
;                  variables - angle and wavelength; in the case of
;                  IMDFPLOT, there are at least three: depth, angle,
;                  and wavelength; in the case of IMDNPLOT, there are
;                  at least four: angle, wavelength, scattering angle,
;                  and scattering plane azimuthal angle (phi).
;
;                  This keyword only has an effect if you're plotting
;                  data that involve more than one multi-valued
;                  independent variable. See the PROCEDURE section
;                  below for details.
;
;      FPINDICES - (IMDCPLOT only) Array indicating the array indices
;                  of fit parameters. Similar to IVINDICES (above.)
;
;      LEVEL - (IMDCPLOT only) the Chi^2 confidence level (from 0-100).
;
;      JOINT - (IMDCPLOT only) 0 for independent confidence intervals,
;              1 for joint confidence intervals.
;
;      OVERPLOT - Don't draw plot axes, just overplot the data.
;
;      S_LABEL_POS - An integer from 0 to 12, indicating the position
;                   for the Structure label. See the PLOT_TEXT
;                   procedure for details.
;
;      FP_LABEL_POS - An integer from 0 to 12, indicating the position
;                   for the Fit Parameters label (IMDSPLOT and
;                   IMDCPLOT only). See the PLOT_TEXT procedure for
;                   details.
;
;      APFQ_LABEL_POS - An integer from 0 to 12, indicating the
;                      position for the Angular Resolution/Spectral
;                      Resolution/ Polarization label. See the
;                      PLOT_TEXT procedure for details.
;
;      CURVE_LABEL_POS - A floating point number from 0 to 1 indicating
;                       the position for curve labels. See the
;                       CURVE_LABEL procedure for details. This
;                       keyword only has an effect if
;                       IMDSPLOT.LEGEND=0 (for IMDSPLOT),
;                       IMDNPLOT.LEGEND=0 (for IMDNPLOT),

```

```

;           IMDFPLOT.LEGEND=0 (for IMDFPLOT), or
;           IMDCPLOT.LEGEND=0 (for IMDCPLOT).
;
; LEGEND_POS - An integer from 0 to 12, indicating the position
;             for the plot legend. See the LEGEND procedure for
;             details. This keyword only has an effect if
;             IMDSPLOT.LEGEND=1 (for IMDSPLOT), IMDFPLOT.LEGEND=1
;             (for IMDFPLOT), or IMDCPLOT.LEGEND=1 (for
;             IMDCPLOT).
;
; CLABEL - String array to label curves using CURVE_LABEL or
;          LEGEND. If non-null, then the values supplied will be
;          used on the plot. Otherwise, the program will return
;          the values automatically generated. These returned
;          values can then be used to label the plot later. This
;          latter behavior is useful when you want to include
;          multiple variables using the OVERPLOT keyword, and you
;          wish to label all the curves using LEGEND; Use of the
;          NO_CLABEL keyword would thus be appropriate.
;
; NO_CLABEL - Don't actually draw the curve labels. (But CLABEL
;            will still contain the strings that would have been
;            labelled.)
;
; FORCE_CLABEL - Force the curve labels to include the independent
;              variable (or fit parameter) values that would
;              otherwise wind up in the subtitle.
;
; LEGEND_STYLE - An N x 5 array, where N is the number of
;               dependent variables on the plot, containing the N
;               values of COLOR, LINSTYLE, THICK, PSYM, and SYMSIZE
;               for each curve. These values can thus be used
;               to instruct LEGEND on how to create a legend
;               to correspond with what was plotted.
;
; DCHI2_LABEL_POS - (1D IMDCPLOTS only) A floating point number from 0
;                  to 1 indicating the position for the Chi^2
;                  curve label. See the CURVE_LABEL procedure
;                  for details.
;
; DCHI2LABEL - (1D IMDCPLOTS only) A string specifying the label
;             to use for the Chi^2 label.
;
; XTITLE
; YTITLE
; PYTITLE (IMDSPLOT only; phase axis)
; ZTITLE (IMDSPLOT, IMDNPLOT, IMDFPLOT only)
; SUBTITLE
; TITLE - The usual graphics keywords. If non-null, then these
;         values will appear on the plot. Otherwise, the program
;         will return the values automatically generated.
;
;

```

```

; XTYPE, XRANGE, XSTYLE
; YTYPE, YRANGE, YSTYLE
; PYTYPE, PYRANGE, PSTYLE, PYTICKS (IMDSLOT only; phase axis)
; ZTYPE, ZRANGE, ZSTYLE (IMDSLOT, IMDNPLOT, IMDFPLOT only)
;     The usual graphics keywords.
;
; YMARGIN0 - Set this to make extra space below a plot to allow
;           for PLOT_TEXT boxes and LEGEND boxes.
;
; HORIZONTAL - The HORIZONTAL keyword for surface plots.
;
; STATS_FLAGS - (IMDSLOT, IMDNPLOT only) a six-element array of
;               flags indicating which statistics are to be
;               computed and displayed (overrides IMDSLOT.STATS_FLAGS
;               or IMDNPLOT.STATS_FLAGS)
;
;               STATS_FLAGS(0): set to compute min
;               STATS_FLAGS(1): set to compute max
;               STATS_FLAGS(2): set to compute average
;               STATS_FLAGS(3): set to compute integral
;               STATS_FLAGS(4): set to compute fwhmax
;               STATS_FLAGS(5): set to compute fwhmin
;
; STATS_FUNCTION - (IMDSLOT, IMDNPLOT only) an integer specifying
;                  which function is to be used when computing
;                  statistics (overrides IMDSLOT.STATS_FUNCTION
;                  or IMDNPLOT.STATS_FUNCTION)
;
;                  for IMDSLOT:
;
;                  STATS_FUNCTION = 0 for average reflectance
;                  STATS_FUNCTION = 1 for s-reflectance
;                  STATS_FUNCTION = 2 for p-reflectance
;                  STATS_FUNCTION = 3 for s-reflected phase
;                  STATS_FUNCTION = 4 for p-reflected phase
;                  STATS_FUNCTION = 5 for psi
;                  STATS_FUNCTION = 6 for delta
;                  STATS_FUNCTION = 7 for average transmittance
;                  STATS_FUNCTION = 8 for s-transmittance
;                  STATS_FUNCTION = 9 for p-transmittance
;                  STATS_FUNCTION = 10 for s-transmitted phase
;                  STATS_FUNCTION = 11 for p-transmitted phase
;                  STATS_FUNCTION = 12 for average absorptance
;                  STATS_FUNCTION = 13 for s-absorptance
;                  STATS_FUNCTION = 14 for p-absorptance
;                  STATS_FUNCTION = 15 for user1
;                  STATS_FUNCTION = 16 for user2
;                  STATS_FUNCTION = 17 for user3
;
;                  for IMDNPLOT:
;
;                  STATS_FUNCTION = 0 for didomega_baa

```

```

;           STATS_FUNCTION = 1 for didomega_bas
;           STATS_FUNCTION = 2 for didomega_bap
;           STATS_FUNCTION = 3 for didomega_dwba
;
; ROI_FLAG - (IMDSPLIT, IMDNPLOT only) set to 1 to display
;             region-of-interest lines.
;
; ROI_RANGE - (IMDSPLIT, IMDNPLOT only) a two-element array
;             specifying the region-of-interest array indices of
;             the X-axis plot variable.
;
; TD_PARS - a 2-element array indicating what type of 2D plot
;            draw: For a surface plot, set TD_PARS(0)=0; for a
;            contour plot, TD_PARS(0)=1; for a filled contour
;            plots, set TD_PARS(0)=2; and for a cont_image plot
;            (using the CONT_IMAGE procedure in the windt library),
;            set TD_PARS(0)=3. TD_PARS(1) is the number of contour
;            levels to draw when TD_PARS(0) is greater than 0.
;
; QSPACE - a scalar flag indicating that an angle axis or axes are
;           to be plotted in momentum space instead of real
;           space.
;
;           For IMDNPLOT,
;
;           QSPACE=1 => 1D plot vs. q_x
;           QSPACE=2 => 1D plot vs. q_y
;           QSPACE=3 => 1D plot vs. q_z
;           QSPACE=4 => 2D plot vs. q_x vs q_y
;           QSPACE=5 => 2D plot vs. q_x vs q_z
;           QSPACE=6 => 2D plot vs. q_y vs q_z
;
;           For IMDSPLIT, IMDFPLOT and IMDCPLOT, a QSPACE value
;           greater than one results in a 1D or 2D plot vs. q_z.
;
;           If lambda (or phi) are plot variables, momentum space
;           plots are not possible.
;
; The following keywords determine which dependent variables
; are plotted
;
; IMDSPLIT only:
;
; PLOT - an array of flags indicating which functions to plot:
;
; PLOT(0) - Plot average reflectance (overrides IMDSPLIT.RA)
; PLOT(1) - Plot s-reflectance (overrides IMDSPLIT.RS)
; PLOT(2) - Plot p-reflectance (overrides IMDSPLIT.RP)
; PLOT(3) - Plot reflected s-phase (overrides IMDSPLIT.PRS)
; PLOT(4) - Plot reflected p-phase (overrides IMDSPLIT.PRP)
; PLOT(5) - Plot ellipsometric psi (overrides IMDSPLIT.PSI)

```

```

; PLOT(6) - Plot ellipsometric delta (overrides IMDSPLOT.DELTA)
; PLOT(7) - Plot average transmittance (overrides IMDSPLOT.TA)
; PLOT(8) - Plot s-transmittance (overrides IMDSPLOT.TS)
; PLOT(9) - Plot p-transmittance (overrides IMDSPLOT.TP)
; PLOT(10) - Plot transmitted s-phase (overrides IMDSPLOT.PTS)
; PLOT(11) - Plot transmitted p-phase (overrides IMDSPLOT.PTP)
; PLOT(12) - Plot average absorptance (overrides IMDSPLOT.AA)
; PLOT(13) - Plot s-absorptance (overrides IMDSPLOT.AS)
; PLOT(14) - Plot p-absorptance (overrides IMDSPLOT.AP)
; PLOT(15) - Plot user1 function (overrides IMDSPLOT.USER1)
; PLOT(16) - Plot user2 function (overrides IMDSPLOT.USER2)
; PLOT(17) - Plot user3 function (overrides IMDSPLOT.USER3)
;
; IMDNPLOT only:
;
; PLOT - an array of flags indicating which functions to plot:
;
; PLOT(0) - Plot didomega_baa (overrides IMDNPLOT.BAA)
; PLOT(1) - Plot didomega_bas (overrides IMDNPLOT.BAS)
; PLOT(2) - Plot didomega_bap (overrides IMDNPLOT.BAP)
; PLOT(3) - Plot didomega_dwba (overrides IMDNPLOT.DWBA)
;
; IMDFPLOT only:
;
; PLOT_FA - Plot average field intensity (overrides IMDFPLOT.FA)
; PLOT_FS - Plot s-field intensity (overrides IMDFPLOT.FA)
; PLOT_FP - Plot p-field intensity (overrides IMDFPLOT.FA)
;
; The following keywords are all 5-element arrays, specifying
; how the dependent variables are to appear. The 5-elements
; correspond to the [COLOR, LINESYLE, THICK, PSYM, SYMSIZE]
; graphics keywords.
;
; IMDSPLOT only:
;
; RASTYLE - average reflectance style
; RSSTYLE - s-reflectance style
; RPSTYLE - p-reflectance style
; PRSSTYLE - s-reflected phase style
; PRPSTYLE - p-reflected phase style
; TASTYLE - average transmittance style
; TSSTYLE - s-transmittance style
; TPSTYLE - p-transmittance style
; PTSSTYLE - s-transmitted phase style
; PTPSTYLE - p-transmitted phase style
; AASTYLE - average absorptance style
; ASSTYLE - s-absorptance style
; APSTYLE - p-absorptance style
;
; IMDFPLOT only:
;
; FASTYLE - average field intensity style

```

```
; FSSTYLE - s-field intensity style
; FPSTYLE - p-field intensity style
; ISTYLE - interface line style (PSYM and SYMSIZE are ignored)
;
; NOINTERFACE - Set to inhibit IMDFPLOT from drawing the interface
;               lines.
;
; IMDCPLOT only:
;
; CSTYLE - Chi^2 style (PSYM and SYMSIZE are ignored for contour
;                  plots)
;
; PTSTYLE - Best fit point style (only PSYM and SYMSIZE are used.)
;
;
; PROCEDURE/EXAMPLES:
;
; If you have calculated optical properties, field intensities or
; chi^2 values for only one independent variable (or fit
; parameter), then you need not worry about the following
; discussion. Just type IMDSPLIT, IMDFPLOT, or IMDCPLOT at the
; command line and a plot will appear.
;
; On the other hand....
;
; In the case of IMDSPLIT and IMDFPLOT, if more than one
; (multi-valued) independent variable is available, or in the case
; of IMDCPLOT, if more than one (multi-valued) fit parameter is
; available, the value of the IMD common block variable
; IMDSPLIT.IV, IMDFPLOT.IV, or IMDCPLOT.FP determines what is
; actually plotted. These three variables are bit-wise flags that
; indicate whether or not an independent variable (or fit
; parameter) is to be used as a continuous plot variable, or as a
; discrete plot variable. That is, if bit 0 of IMDSPLIT.IV is
; set, then the optical functions will be plotted versus incidence
; angle; if bit 1 is set, then the optical functions will be set
; versus wavelength (or energy). If other independent variables
; are available (as listed in the Independent Variables List on
; the main IMD widget), then other bits can be set as well.
; Similarly for IMDFPLOT.IV, except bit 0 now refers to depth, bit
; 1 to incidence angle, bit 2 to wavelength, etc. IMDCPLOT.FP
; works the same way, except each bit corresponds to an available
; fit parameter that has been varied to construct the Chi^2 array.
;
; If two bits of IMDSPLIT.IV, IMDFPLOT.IV or IMDCPLOT.FP are
; set, then a surface plot (or a contour plot in the case of
; IMDCPLOT) will be created.
;
; You will also need to set the value of IVINDICES (or FPINDICES
; in the case of IMDCPLOT), in order to specify discrete independent
; variables or fit parameters.
;
```

```
; EXAMPLE 1
;
; Suppose you've computed reflectance vs incidence angle vs
; wavelength, for 20 incidence angles and 30 wavelengths. The IMD
; reflectance variable (R) will thus be a 20x30 element array. To
; plot Reflectance vs Incidence Angle, for the wavelength
; corresponding to the 12th element of the wavelength array,
; use the following commands:
;
; IMD> imdsplot.iv=1
; IMD> imdsplot,ivindices=[0,12]
;
; Alternatively, to plot reflectance vs. wavelength, for the
; angle corresponding to the 9th element of the angle array,
; type:
;
; IMD> imdsplot.iv=2
; IMD> imdsplot,ivindices=[9,0]
;
; Finally, to produce a surface plot of reflectance vs angle vs
; wavelength:
;
; IMD> imdsplot.iv=3
; IMD> imdsplot
;
; EXAMPLE 2
;
; Here's how to plot the results from two separate IMD calculations
; on the same plot:
;
; IMD> rd=imd_rd(file='file1.dat')
; IMD> imdsplot
; IMD> rd=imd_rd(file='file2.dat')
; IMD> imdsplot,/overplot
;
; Of course you'll probably want to make use of some of the other
; keywords, in order to properly label and distinguish between
; the two data sets. For example, instead of the above, you
; might try something like:
;
; IMD> rd=imd_rd(file='file1.dat')
; IMD> imdsplot,clabel=['File 1'],s_label_pos=0
; IMD> rd=imd_rd(file='file2.dat')
; IMD> imdsplot,/overplot,clabel=['File 2'],rastyle=[2,0,0,0,0]
;
; MODIFICATION HISTORY:
;
; David L. Windt, Bell Labs, April 1997.
;
; Many changes to IMD V4.0 - April, 1998.
;
; windt@bell-labs.com
```

;-

;+

;

; NAME:

;

; **IMDMPLOT**

;

; PURPOSE:

;

; Produce plots of measured data.

;

; CALLING SEQUENCE:

;

; IMDMPLOT

;

; KEYWORD PARAMETERS:

;

; The XTITLE, YTITLE, SUBTITLE, TITLE, CHARSIZE, OVERPLOT,
; CURVE_LABEL_POS, LEGEND_POS, NO_LABEL, CLABEL and QSPACE
; keywords work the same way as for IMDSPLIT/IMDNPLOT.

;

; In addition, the MSTYLE keyword is an array specifying [COLOR,
; LINSTYLE, THICK, PSYM, and SYMSIZE values for the measured
; data.

;

; EXAMPLE:

;

; Here's how to open an IMD data file, open a measured data file
; containing reflectance vs. incidence angle data, plot the IMD
; data, and overplot your measured data:

;

; IMD> rd=imd_rd(file='file.dat')

; IMD> imdsplot

; IMD> imd_m_rd,rd_m_cmd='erom,x_m,y_m,sigy_m',x_m_ptr=0,y_m_ptr=0

; IMD> imdmplot,/overplot

;

;

; MODIFICATION HISTORY:

;

; David L. Windt, Bell Labs, April 1997.

;

; April, 1998: Many changes upgrading to IMD V4.0.

;

; windt@bell-labs.com

;-

;+

; NAME:

```
;
;   IMD_PLOT_LBL
;
; PURPOSE:
;
;   A procedure to add labels to a plot.
;
; CALLING SEQUENCE:
;
;   IMD_PLOT_LBL, /OPLOT or /FPLOT or /CPLOT
;
; INPUTS:
;
;   OPLOT, FPLOT, CPLOT - indicates what type of plot to label.
;
; KEYWORD PARAMETERS:
;
;   S_LABEL_POS
;   FP_LABEL_POS
;   APFQ_LABEL_POS
;
;   See the description of these keywords in the
;   IMDSPLOT/IMDFPLOT/IMDCPLOT documentation above.
;
;   Setting these keywords overrides the current value of the
;   corresponding flags:
;
;   IMDSPLOT.S_LABEL,IMDFPLOT.S_LABEL,  IMDCPLOT.S_LABEL;
;
;   IMDSPLOT.FP_LABEL,  IMDCPLOT.FP_LABEL;
;
;   IMDSPLOT.APFQ_LABEL,IMDFPLOT.APFQ_LABEL,  IMDCPLOT.APFQ_LABEL;
;
; MODIFICATION HISTORY:
;
;   David L. Windt, Bell Labs, April 1997.
;   windt@bell-labs.com
;-
```

[Back](#) | [Contents](#) | [Next](#)

Appendix B- Notes for IDL programmers

(Be warned that if you don't do much IDL programming, you might be frightened by what's contained in B.2 and especially B.3)

[B.1 Customizing the installation](#)

[B.2 Some IMD functions and procedure](#)

[B.3 Reading measured data files](#)

[B.4 IMD common block variables](#)

[Back](#) | [Contents](#) | [Next](#)

B.4 IMD COMMON block variables

Listed here, for those of you who might actually be interested in such things, are all the IMD COMMON blocks. All of these COMMON block variables are accessible from the IDL command line, whenever you see the IMD prompt. I'm only going to describe the variables that you really ought to be concerned with (to the extent that you wish to be concerned.)

Click [here](#) to go directly to the COMMON IMD_VARS section, containing the variables you are most likely to use when defining user-functions (as described in [Section 2.3](#)).

```

; COMMON IMD, $
;   IMD,IMDHOME,IMD_NKPATH,IMD_NKPATH_PTR,$
;   IMDSPLOT,IMDSPLOT_FC,IMDSPLOT_BANGPY,$
;   IMDNPLOT,IMDNPLOT_FC,$
;   IMDFPLOT,IMDFPLOT_FC,$
;   IMDCPLOT,IMDCPLOT_FC,$
;   IMDPRINT
;
; -----
;
; IMD - A structure largely controlling the behavior of IMD. The only
;       tags you might need to be concerned with are:
;
;
; IMD.ANGLEUNITS_PTR - Pointer for angle units: 0=normal, 1=grazing.
;
; IMD.PHOTONUNITS_PTR - Pointer for photon units: 0=A, 1=nm, 2=um, 3=eV, 4=keV.
;
; IMD.LAYERUNITS_PTR - Pointer for layer (length) units: 0=A, 1=nm, 2=um
;
;
; IMD.Y_M - Measured data dependent variable pointer.
;
; IMD.X_M - Measured data independent variable pointer.
;
; IMD.RD_M_CMD - Read measured data command.
;
; IMD.LIMIT_M - Flag to indicate whether or not to limit measured data.
;
; IMD.X_M_RANGE - 2-element array specifying the X_M range of valid measured data.
;
; IMD.X_M_OFFSET - Offset factor to be added to X_M data.
;
; IMD.X_M_SCALE - Scale factor to be applied to X_M data.
;
; IMD.Y_M_OFFSET - Offset factor to be added to Y_M data.

```

```
;  
;  
; IMD.Y_M_SCALE - Scale factor to be applied to Y_M data.  
;  
;  
; -----  
;  
;  
; IMDSPLOT - A structure controlling the behavior of the IMDSPLOT  
;           procedure, containing the following tags:  
;  
;  
; IMDSPLOT.XAXIS - 4-element array corresponding to TYPE, RANGE(0:1), and STYLE  
; IMDSPLOT.YAXIS - 4-element array corresponding to TYPE, RANGE(0:1), and STYLE  
; IMDSPLOT.PYAXIS - 4-element array corresponding to TYPE, RANGE(0:1), and STYLE  
; IMDSPLOT.ZAXIS - 4-element array corresponding to TYPE, RANGE(0:1), and STYLE  
; IMDSPLOT.IV - Bit-wise flag for independent variables.  
; IMDSPLOT.IVINDICES - Array indices for independent variables.  
; IMDSPLOT.M - Plot measured data flag  
; IMDSPLOT.RA - Plot average reflectance flag  
; IMDSPLOT.RS - Plot s-reflectance flag.  
; IMDSPLOT.RP - Plot p-reflectance flag.  
; IMDSPLOT.PRS - Plot s-reflected phase flag.  
; IMDSPLOT.PRP - Plot p-reflected phase flag.  
; IMDSPLOT.PSI - Plot ellipsometric psi flag.  
; IMDSPLOT.DELTA - Plot ellipsometric delta flag.  
; IMDSPLOT.TA - Plot average reflectance flag  
; IMDSPLOT.TS - Plot s-transmittance flag.  
; IMDSPLOT.TP - Plot p-transmittance flag.  
; IMDSPLOT.PTS - Plot s-transmitted phase flag.  
; IMDSPLOT.PTP - Plot p-transmitted phase flag.  
; IMDSPLOT.AA - Plot average absorptance flag  
; IMDSPLOT.AS - Plot s-absorptance flag.  
; IMDSPLOT.AP - Plot p-absorptance flag.  
; IMDSPLOT.USER1 - Plot user1 flag.  
; IMDSPLOT.USER2 - Plot user2 flag.  
; IMDSPLOT.USER3 - Plot user3 flag.  
; IMDSPLOT.RASTYLE - Style parameters for average reflectance  
; IMDSPLOT.RSSTYLE - Style parameters for s-reflectance  
; IMDSPLOT.RPSTYLE - Style parameters for p-reflectance  
; IMDSPLOT.PRSSTYLE - Style parameters for s-reflected phase  
; IMDSPLOT.PRPSTYLE - Style parameters for p-reflected phase  
; IMDSPLOT.PSISTYLE - Style parameters for psi  
; IMDSPLOT.DELTASTYLE - Style parameters for delta  
; IMDSPLOT.TASTYLE - Style parameters for average transmittance  
; IMDSPLOT.TSSTYLE - Style parameters for s-transmittance  
; IMDSPLOT.TPSTYLE - Style parameters for p-transmittance  
; IMDSPLOT.PTSSTYLE - Style parameters for s-transmitted phase  
; IMDSPLOT.PTPSTYLE - Style parameters for p-transmitted phase  
; IMDSPLOT.AASTYLE - Style parameters for average absorptance  
; IMDSPLOT.ASSTYLE - Style parameters for s-absorptance  
; IMDSPLOT.APSTYLE - Style parameters for p-absorptance  
; IMDSPLOT.USER1STYLE - Style parameters for user1  
; IMDSPLOT.USER2STYLE - Style parameters for user2  
; IMDSPLOT.USER3STYLE - Style parameters for user3
```

```

; IMDSPLOT.MSTYLE - Style parameters for average reflectance
; IMDSPLOT.MCLABEL - Curve label for measured data.
; IMDSPLOT.MCURVE_LABEL_POS - Curve label position for measured data.
; IMDSPLOT.TITLE - Title
; IMDSPLOT.AUTO_TITLE - Automatically generate titles.
; IMDSPLOT.SUBTITLE - Subtitle
; IMDSPLOT.AUTO_SUBTITLE - Automatically generate subtitles.
; IMDSPLOT.XTITLE - Xtitle
; IMDSPLOT.AUTO_XTITLE - Automatically generate xtitle
; IMDSPLOT.YTITLE - Ytitle
; IMDSPLOT.AUTO_YTITLE - Automatically generate ytitle
; IMDSPLOT.PYTITLE - Phase title
; IMDSPLOT.AUTO_PYTITLE - Automatically generate phase title
; IMDSPLOT.ZTITLE - Ztitle
; IMDSPLOT.AUTO_ZTITLE - Automatically generate ztitle
; IMDSPLOT.CHARSIZE - Charsize
; IMDSPLOT.S_LABEL_POS - Position for structure label
; IMDSPLOT.APFQ_LABEL_POS - Position for ares/pres/f/q label
; IMDSPLOT.FP_LABEL_POS - Position for fit parameters label
; IMDSPLOT.LEGEND:0 - 0: use curve_label, 1: use legend, -1: no legend
; IMDSPLOT.CURVE_LABEL_POS - Curve_label position
; IMDSPLOT.CLABEL - Curve labels
; IMDSPLOT.LEGEND_POS - Position for legend.
; IMDSPLOT.BANGX - Private copy of !x
; IMDSPLOT.BANGY - Private copy of !y
; IMDSPLOT.BANGZ - Private copy of !z
; IMDSPLOT.BANGPY - Private copy of !y used for phase plots
; IMDSPLOT.BANGP - Private copy of !p
; IMDSPLOT.WXSIZE - Plot window X size
; IMDSPLOT.WYSIZE - Plot window Y size
; IMDSPLOT.QSPACE - Flag for q-space plots
; IMDSPLOT.THREED - Flag for type of 2D plot.
; IMDSPLOT.C_NLEVELS - Number of contour levels for contour plots.
; IMDSPLOT.HORIZONTAL- Horizontal keyword to surface
; IMDSPLOT.CURSOR_VALUE - Cursor function pointer.
; IMDSPLOT.STATS_FUNCTION - Statistics function pointer.
; IMDSPLOT.STATS_FLAGS - Array of flags for computing statistics
; IMDSPLOT.STATS - Array of statistics values.
; IMDSPLOT.STATS_PRECISION - Array of integers specifying statistics
;                               display precision
; IMDSPLOT.ROI_RANGE - 2-element array of substrates for ROI
; IMDSPLOT.ROI_MARK_FLAG - flag to indicate that the ROI is in the
;                               process of being marked.
; IMDSPLOT.ROI - flag to indicate ROI.
;
; -----
;
; IMDNPLOT - A structure controlling the behavior of the IMDNPLOT
;           procedure, containing the following tags:
;
; IMDNPLOT.XAXIS - 4-element array corresponding to TYPE, RANGE(0:1), and STYLE

```

```
; IMDNPLOT.YAXIS - 4-element array corresponding to TYPE, RANGE(0:1), and STYLE
; IMDNPLOT.ZAXIS - 4-element array corresponding to TYPE, RANGE(0:1), and STYLE
; IMDNPLOT.IV - Bit-wise flag for independent variables.
; IMDNPLOT.IVINDICES - Array indices for independent variables.
; IMDNPLOT.M - Plot measured data flag
; IMDNPLOT.BAA - Plot didomega_baa
; IMDNPLOT.BAS - Plot didomega_bas
; IMDNPLOT.BAP - Plot didomega_bap
; IMDNPLOT.DWBA - Plot didomega_dwba
; IMDNPLOT.BAASTYLE - Style parameters for didomega_baa
; IMDNPLOT.BASSTYLE - Style parameters for didomega_bas
; IMDNPLOT.BAPSTYLE - Style parameters for didomega_bap
; IMDNPLOT.DWBASTYLE - Style parameters for didomega_dwba
; IMDNPLOT.MSTYLE - Style parameters for average reflectance
; IMDNPLOT.MCLABEL - Curve label for measured data.
; IMDNPLOT.MCURVE_LABEL_POS - Curve label position for measured data.
; IMDNPLOT.TITLE - Title
; IMDNPLOT.AUTO_TITLE - Automatically generate titles.
; IMDNPLOT.SUBTITLE - Subtitle
; IMDNPLOT.AUTO_SUBTITLE - Automatically generate subtitles.
; IMDNPLOT.XTITLE - Xtitle
; IMDNPLOT.AUTO_XTITLE - Automatically generate xtitle
; IMDNPLOT.YTITLE - Ytitle
; IMDNPLOT.AUTO_YTITLE - Automatically generate ytitle
; IMDNPLOT.PYTITLE - Phase title
; IMDNPLOT.AUTO_PYTITLE - Automatically generate phase title
; IMDNPLOT.ZTITLE - Ztitle
; IMDNPLOT.AUTO_ZTITLE - Automatically generate ztitle
; IMDNPLOT.CHARSIZE - Charsize
; IMDNPLOT.S_LABEL_POS - Position for structure label
; IMDNPLOT.APFQ_LABEL_POS - Position for ares/pres/f/q label
; IMDNPLOT.FP_LABEL_POS - Position for fit parameters label
; IMDNPLOT.LEGEND:0 - 0: use curve_label, 1: use legend, -1: no legend
; IMDNPLOT.CURVE_LABEL_POS - Curve_label position
; IMDNPLOT.CLABEL - Curve labels
; IMDNPLOT.LEGEND_POS - Position for legend.
; IMDNPLOT.BANGX - Private copy of !x
; IMDNPLOT.BANGY - Private copy of !y
; IMDNPLOT.BANGZ - Private copy of !z
; IMDNPLOT.BANGP - Private copy of !p
; IMDNPLOT.WXSIZE - Plot window X size
; IMDNPLOT.WYSIZE - Plot window Y size
; IMDNPLOT.QSPACE - Flag for q-space plots
; IMDNPLOT.THREED - Flag for type of 2D plot.
; IMDNPLOT.C_NLEVELS - Number of contour levels for contour plots.
; IMDNPLOT.HORIZONTAL- Horizontal keyword to surface
; IMDNPLOT.CURSOR_VALUE - Cursor function pointer.
; IMDNPLOT.STATS_FUNCTION - Statistics function pointer.
; IMDNPLOT.STATS_FLAGS - Array of flags for computing statistics
; IMDNPLOT.STATS - Array of statistics values.
; IMDNPLOT.STATS_PRECISION - Array of integers specifying statistics
```

```

;                               display precision
;  IMDNPLOT.ROI_RANGE - 2-element array of substrates for ROI
;  IMDNPLOT.ROI_MARK_FLAG - flag to indicate that the ROI is in the
;                               process of being marked.
;  IMDNPLOT.ROI - flag to indicate ROI.
;
; -----
;
;  IMDFPLOT - A structure controlling the behavior of the IMDFPLOT
;              procedure, containing the following tags:
;
;  IMDFPLOT.XAXIS - 4-element array corresponding to TYPE, RANGE(0:1), and STYLE
;  IMDFPLOT.YAXIS - 4-element array corresponding to TYPE, RANGE(0:1), and STYLE
;  IMDFPLOT.ZAXIS - 4-element array corresponding to TYPE, RANGE(0:1), and STYLE
;  IMDFPLOT.IV - Bit-wise flag for independent variables.
;  IMDFPLOT.IVINDICES - Array indices for independent variables.
;  IMDFPLOT.FA - Plot average field intensity flag
;  IMDFPLOT.FS - Plot s-field intensity flag.
;  IMDFPLOT.FP - Plot p-field intensity flag.
;  IMDFPLOT.FASTYLE - Style parameters for average field intensity
;  IMDFPLOT.FSSTYLE - Style parameters for s-field intensity
;  IMDFPLOT.FPSTYLE - Style parameters for p-field intensity
;  IMDFPLOT.TITLE - Title
;  IMDFPLOT.AUTO_TITLE - Automatically generate titles.
;  IMDFPLOT.SUBTITLE - Subtitle
;  IMDFPLOT.AUTO_SUBTITLE - Automatically generate subtitles.
;  IMDFPLOT.XTITLE - Xtitle
;  IMDFPLOT.AUTO_XTITLE - Automatically generate xtitle
;  IMDFPLOT.YTITLE - Ytitle
;  IMDFPLOT.AUTO_YTITLE - Automatically generate ytitle
;  IMDFPLOT.ZTITLE - Ztitle
;  IMDFPLOT.AUTO_ZTITLE - Automatically generate ztitle
;  IMDFPLOT.CHARSIZE - Charsize
;  IMDFPLOT.S_LABEL_POS - Position for structure label
;  IMDFPLOT.APFQ_LABEL_POS - Position for ares/pres/f/q label
;  IMDFPLOT.LEGEND:0 - 0: use curve_label, 1: use legend, -1: no legend
;  IMDFPLOT.CURVE_LABEL_POS - Curve_label position
;  IMDFPLOT.CLABEL - Curve labels
;  IMDFPLOT.LEGEND_POS - Position for legend.
;  IMDFPLOT.BANGX - Private copy of !x
;  IMDFPLOT.BANGY - Private copy of !y
;  IMDFPLOT.BANGZ - Private copy of !z
;  IMDFPLOT.BANGP - Private copy of !p
;  IMDFPLOT.WXSIZE - Plot window X size
;  IMDFPLOT.WYSIZE - Plot window Y size
;  IMDFPLOT.QSPACE - Flag for q-space plots
;  IMDFPLOT.THREED - Flag for type of 2D plot.
;  IMDFPLOT.C_NLEVELS - Number of contour levels for contour plots.
;  IMDFPLOT.HORIZONTAL- Horizontal keyword to surface
;
; -----

```

```

;
; IMDCPLOT - A structure controlling the behavior of the IMDCPLOT
;           procedure, containing the following tags:
;
; IMDCPLOT.XAXIS - 4-element array corresponding to TYPE, RANGE(0:1), and STYLE
; IMDCPLOT.YAXIS - 4-element array corresponding to TYPE, RANGE(0:1), and STYLE
; IMDCPLOT.FP - Bit-wise flag for fit parameters.
; IMDCPLOT.FPINDICES - Array indices for fit parameters.
; IMDCPLOT.CSTYLE - Style parameters for Chi^2.
; IMDCPLOT.PTSTYLE - Style parameters for best-fit point
; IMDCPLOT.TITLE - Title
; IMDCPLOT.AUTO_TITLE - Automatically generate titles.
; IMDCPLOT.SUBTITLE - Subtitle
; IMDCPLOT.AUTO_SUBTITLE - Automatically generate subtitles.
; IMDCPLOT.XTITLE - Xtitle
; IMDCPLOT.AUTO_XTITLE - Automatically generate xtitle
; IMDCPLOT.YTITLE - Ytitle
; IMDCPLOT.AUTO_YTITLE - Automatically generate ytitle
; IMDCPLOT.CHARSIZE - Charsize
; IMDCPLOT.S_LABEL_POS - Position for structure label
; IMDCPLOT.APFQ_LABEL_POS - Position for ares/pres/f/q label
; IMDCPLOT.FP_LABEL_POS - Position for fit parameters label
; IMDCPLOT.LEGEND:0 - 0: use curve_label, 1: use legend, -1: no legend
; IMDCPLOT.CURVE_LABEL_POS - Curve_label position
; IMDCPLOT.CLABEL - Curve labels
; IMDCPLOT.JOINT - 0 for independent, 1 for joint confidence intervals
; IMDCPLOT.LEVEL - Confidence level
; IMDCPLOT.DCHI2_LABEL_POS - Curve_label position for Delta(Chi^2)
; IMDCPLOT.DCHI2LABEL - Curve labels for Delta(Chi^2)
; IMDCPLOT.LEGEND_POS - Position for legend.
; IMDCPLOT.BANGX - Private copy of !x
; IMDCPLOT.BANGY - Private copy of !y
; IMDCPLOT.BANGZ - Private copy of !z
; IMDCPLOT.BANGP - Private copy of !p
; IMDCPLOT.WXSIZE - Plot window X size
; IMDCPLOT.WYSIZE - Plot window Y size
; IMDCPLOT.QSPACE - Flag for q-space plots
; IMDCPLOT.THREED - Flag for type of 2D plot.
; IMDCPLOT.C_NLEVELS - Number of contour levels for contour plots.
;

```

```

; COMMON IMD_PARS, $
;   IV,FP,FP_C,AMBIENT,AMBIENT_NC,AMBIENT_F1F2,
;   LAYER,LAYER_NC,LAYER_F1F2,SUBSTRATE,SUBSTRATE_NC,SUBSTRATE_F1F2, $
;   IV0,AMBIENT0,AMBIENT_NC0,AMBIENT_F1F20,
;   LAYER0,LAYER_NC0,LAYER_F1F20,SUBSTRATE0,SUBSTRATE_NC0,SUBSTRATE_F1F20,
;   SEED
;

```

```

; You shouldn't be concerned with any variables in IMD_PARS.

```

;

```

; COMMON IMD_VARS, $
;   THETA, LAMBDA, IDVAR, FITPAR, CHI_2, NC, Z, SIGMA, SIGMA_FROM_PSD,
;   INTERFACE, F, Q, ARES, PRES, $
;   R, RS, RP, PRS, PRP, PSI, DELTA,
;   T, TS, TP, PTS, PTP, A, AS, AP,
;   USER1, USER2, USER3
;
; THETA - Incidence angles, in degrees from normal.
;
; LAMBDA - Wavelengths, in angstroms.
;
; IDVAR - A structure containing independent variable arrays.
;         Each tag of IDVAR is an array. i.e., IDVAR.IV0 = Theta,
;         IDVAR.IV1 = Lambda, etc.
;
; FITPAR - Similar to IDVAR, but for Fit Parameters.
;
; CHI_2 - Array of Chi^2 values.  Dimensions are given by the
;         number of tags to FITPAR
;
; NC - Complex array of indices of refraction.  Dimensions are equal to
;      N_ELEMENTS(Z)+2 by N_ELEMENTS(LAMBDA)
;
; Z - 1D array of layer thicknesses, in angstroms.
;
; SIGMA - 1D array of interface roughnesses.
;
; SIGMA_FROM_PSD - 1D array of flags indicating that the SIGMA value
;                 for that interface is to be computed from the PSD.
;
; INTERFACE - 1D array of interface profile pointers
;
; F - Polarization factor
;
; Q - Polarization analyzer sensitivity
;
; ARES - Angular resolution, in degrees.
;
; PRES - Spectral resolution, in angstroms.
;
; R, RS, RP - Reflectance
;
; PRS, PRP - Reflected phases.
;
; PSI, DELTA - Ellipsometric Psi and Delta.
;
; T, TS, TP - Transmittance

```

```

;
; PTS, PTP - Transmitted phases
;
; A, AS, AP - Absorptance
;
; USER1, USER2, USER3 - User-defined functions.
;
; Note: the dimensions of the optical properties are determined by the
; number of independent variables.

```

```

;
; COMMON IMD_FPARS,PT_SPACING,AMBIENT_DEPTH,SUBSTRATE_DEPTH
;
; Field calculation parameters. Don't mess with these.
;

```

```

; COMMON IMD_FVARS,DEPTH,INT,INTS,INTP
;
; DEPTH - Depth array (for field intensities)
;
; INT, INTS, INTP - Field intensities.
;
; Note: the dimensions of the field intensities are determined by the
; number of independent variables.

```

```

; COMMON IMD_NSVARS,Q_RANGE, $
; THETA_IN,THETA_OUT,PHI, $
; PSD_XI_PERP,SIGMA_D, $
; PSD_SIGMA_R,PSD_XI_PAR,PSD_H, $
; PSD_OMEGA,PSD_NU,PSD_N, $
; DIDOMEGA_DWBA,DIDOMEGA_BAA,DIDOMEGA_BAS,DIDOMEGA_BAP
;
; THETA_IN - Multi-dimensional array of Theta_in values, in degrees
; from normal.
;
; THETA_OUT - Multi-dimensional array of Theta_out values, in
; degrees from normal.
;
; PHI - Scattering plane azimuthal angle, in degrees.
;
; PSD_XI_PERP - Perpendicular correlation length, used with the
; sigma_r/xi_par/H PSD model.
;
; SIGMA_D - 1D array of interface diffuseness values.
;

```

```

; PSD_SIGMA_R - 1D array of interface roughnesses.
;
; PSD_XI_PAR - 1D array of interface correlation lengths.
;
; PSD_H - 1D array of interface jaggedness factors.
;
; PSD_OMEGA - 1D array of interface volume element parameters.
;
; PSD_NU - 1D array of interface relaxation parameters.
;
; PSD_N - 1D array of interface PSD exponents.
;
; DIDOMEGA_DWBA - Non-specular reflected intensity computed from the
;                 DWBA
;
; DIDOMEGA_BAS - s-polarized component of non-specular reflected
;                 intensity computed using the BA.
;
; DIDOMEGA_BAP - p-polarized component of non-specular reflected
;                 intensity computed using the BA.
;
; DIDOMEGA_BAA - polarization-averaged non-specular reflected
;                 intensity computed using the BA.

```

```

;
; COMMON IMD_M,X_M,Y_M,SIGY_M
;
; X_M, Y_M, SIGY_M - Measured data (in internal units, i.e., angstroms,
;                 degrees, etc.)

```

```

;
; COMMON IMD_F1F2,ATWT_LIST,ELEMENT_LIST, $
;   F1F2_COMPOUND_NAME,F1F2_DENSITY,F1F2_NUMBER,F1F2_ELEMENT, $
;   F1F2_LAMBDA,F1F2_N,F1F2_K,F1F2_AUTOPLT
;
; These are all variables used by the IMD_F1F2TONK function.  You shouldn't
; mess with any of these.
;

```

```

;
; COMMON IMD_WIDGET, $
;   MAINW,AMBW,LAYW,SUBW,IVW,OPEN_MW,FITW,CPW,FPW, $
;   PMFCW,PPSDW,PSAVW,PFLDW,NKVIEWW,PNKPATHW,PRINTW,F1F2W
;
; Widget ids.  You definitely shouldn't mess with these.

```

```
;  
; COMMON IMD_STR, $  
; IV_STR,CP_STR,FP_STR,AMBIENT_STR,LAYER_STR,SUBSTRATE_STR  
;  
; Structure variable templates. You definitely shouldn't mess with  
; these.
```

[Back](#) | [Contents](#)

Appendix A - Optical Constants

[A.1 The IMD optical constants database](#)

[A.2 Using your own optical constants](#)

[A.3 Creating new X-ray optical constants](#)

[Back](#) | [Contents](#) | [Next](#)

Chapter 4. Problem solving and reporting bugs

Should you encounter a situation in which IMD stops running, the easiest thing to do is to start over from scratch. That is, exit IDL, remove the IMD default configuration file, named `imdsave.dat`, and start IDL and IMD again. If you believe you have discovered a problem with IMD, please let me know about it. Also, I'd be most interested to hear about any suggestions you might have for future improvements.

Note: Please understand that specifying many layers and many independent variables can easily result in very large arrays which might consume memory exceeding what is available to IDL. Should IDL run out of memory during a computation, you can try adjusting the value of the `SP_MAX_ARRAY_SIZE` and/or `NS_MAX_ARRAY_SIZE` variables, as described in [Appendix B.1](#)

Note: There is a *huge* number of bugs in IDL 5.0 for Windows and Macintosh. You are **strongly** encouraged to upgrade to IDL 5.1/5.2: you will see a dramatic difference!

I can be reached at windt@bell-labs.com. If you're reporting a problem, be sure to include as many details about the problem as you can.

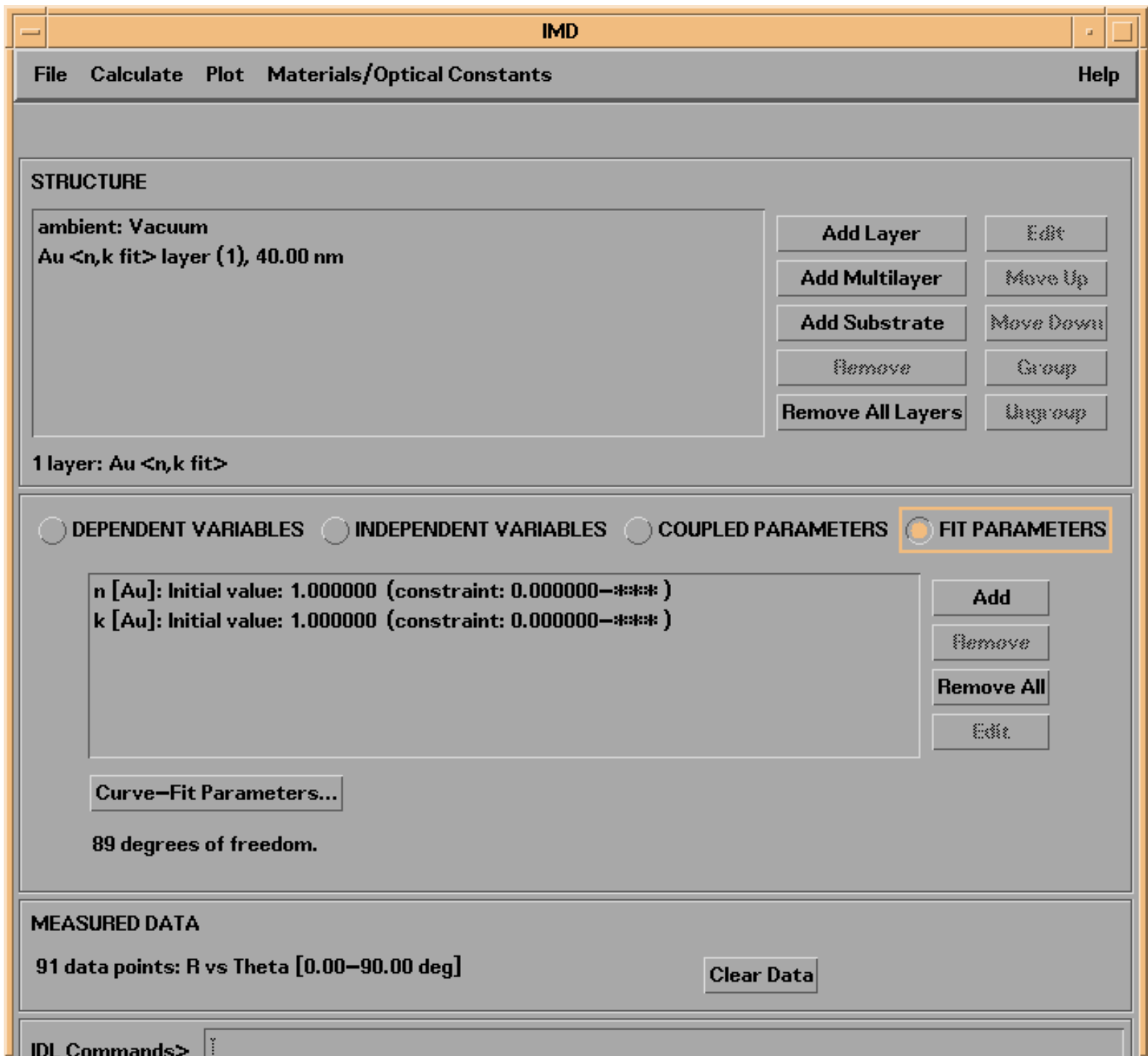
[Back](#) | [Contents](#) | [Next](#)

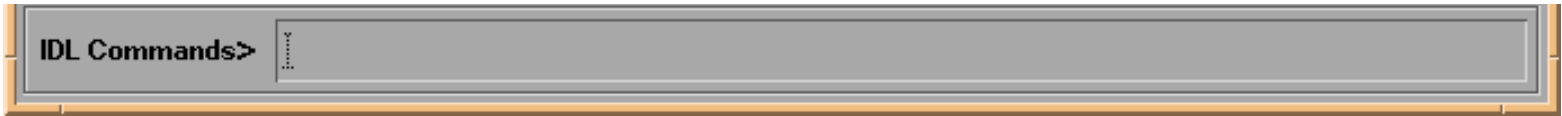
3.2 Specifying Fit Parameters

To perform a fit to your measured data, you must specify which parameters you wish to vary. As in the case of selecting independent variables, any parameters that describe the structure or the incident 'beam' can be chosen to be fit parameters (so long as they are not already designated as independent variables or coupled parameters.) So before specifying fit parameters, make sure the structure and independent variables are defined appropriately.

Continuing with our example (having already specified the structure as a single Au film, 40 nm thick,) to designate fit parameters select the FIT PARAMETERS button on the main IMD widget, as in Figure 3.2.1:

Figure 3.2.1 The main IMD widget as it appears when the FIT PARAMETERS button is selected.





Now press the **Add** button on the FIT PARAMETERS page. You will be presented with the list of available fit parameters. You can choose as many parameters as you like, so long as the number of data points available is greater than the number of fit parameters.

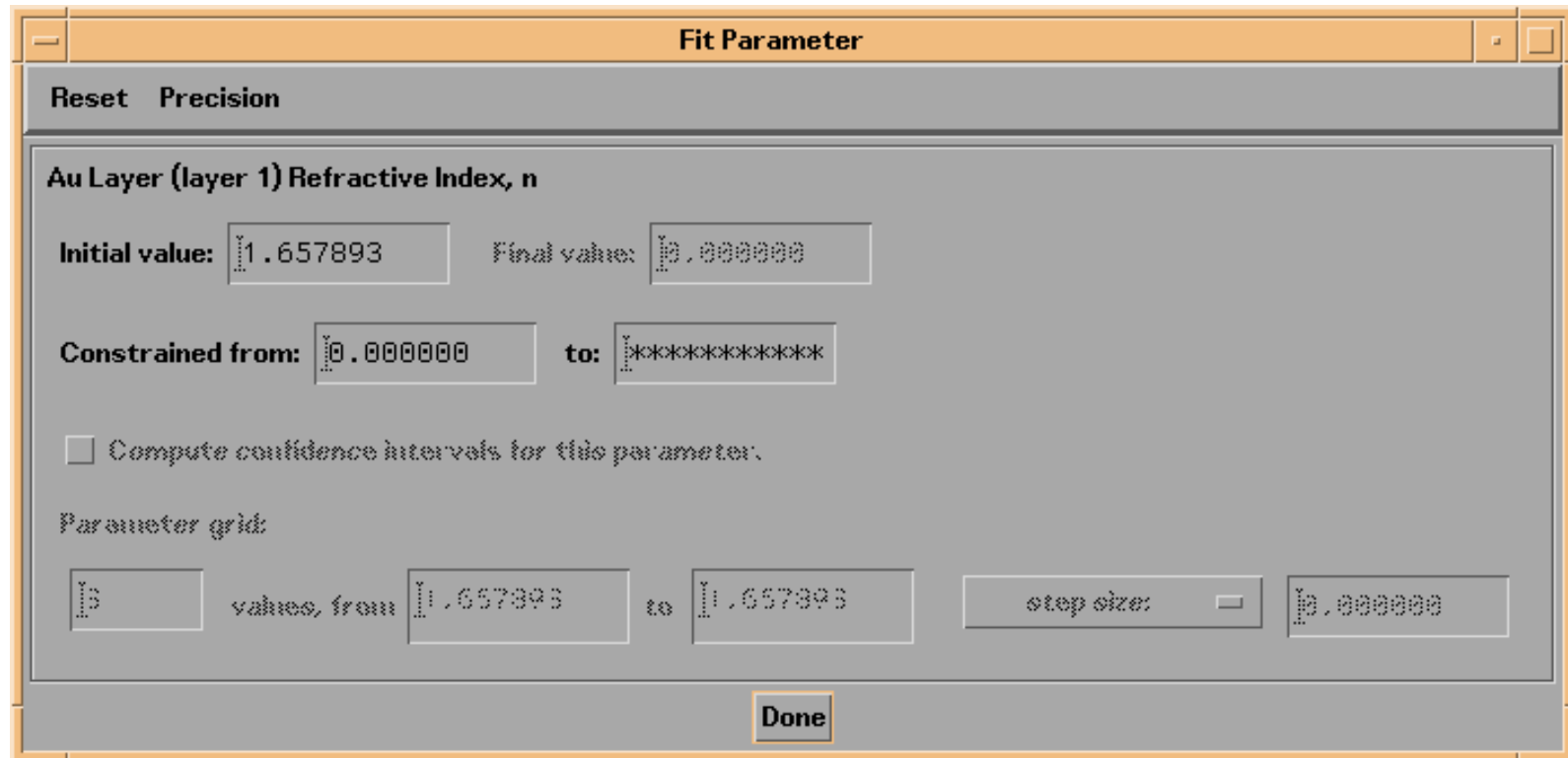
Note: The structure parameters you choose as fit parameters will be indicated as such in the *Structure List* after the fit is completed.

In this example, I will choose two fit parameters: the refractive index, **n**, and the extinction coefficient, **k** of the Au film.

For each fit parameter selected, IMD will create a **Fit Parameter** widget that allows you to specify an initial value for the parameter, and, optionally, constraints on the range of acceptable fit values.

Figure 3.2.2 shows the **Fit Parameter** widget corresponding to the refractive index of Au. The initial value is automatically set to the value of **n** for Au at 400 nm obtained from the IMD optical constant database, i.e., **n**=1.657893. Likewise, the initial value for **k** is automatically set to 1.95601.

Figure 3.2.2 **Fit Parameter** widget example.



Note: It's important to specify initial parameter values that are as close to the actual values as possible, or else the

fitting algorithm may not converge. Although the actual parameter values are usually unknown (which is probably why you're doing a fit), try to make as good a guess as you can.

For our example, to make things (slightly) more interesting, I will set the initial values for **n** and **k** to be far from the actual values; I'll choose initial values of **(n,k)=(1.,1.)**. To see what happens in this thrilling example, go to the [Next](#) page...

[Back](#) | [Contents](#) | [Next](#)

3.3 Curve-Fitting

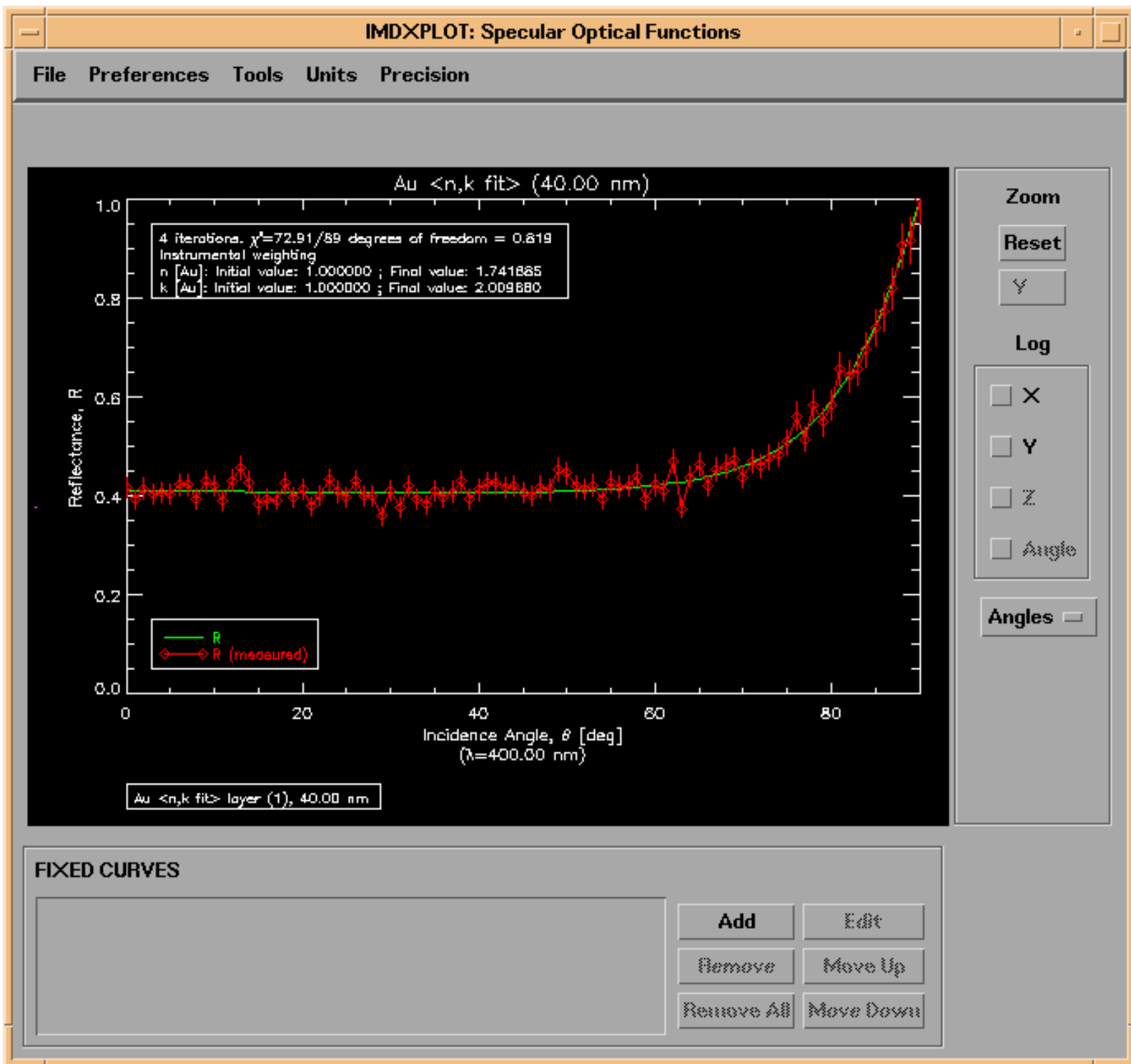
Once the initial values (and optionally parameter constraints) have been set, select **Calculate->Fit Optical Properties to Measured Data** to perform the fit. A new widget will appear indicating the progress of the fit with each iteration.

Once the calculation is completed, the results will be saved to an IMD file automatically, unless you have disabled this feature in the **File->Preferences->Auto-Save...** menu option.

Note: You can choose to save the measured data along with the calculation by selecting this option in the **File->Preferences->Auto Save...** menu option.

The results of our example are shown in Figure 3.3.1. The fit results are listed on the plot, showing the number of iterations, the final **Chi²** value, and the initial and final values of the fit parameters. The fit results are also indicated on the FIT PARAMETERS section of the main IMD widget, and the individual **Fit Parameters** widgets are updated to show the final fit parameter values as well.

Figure 3.3.1 Fit results.

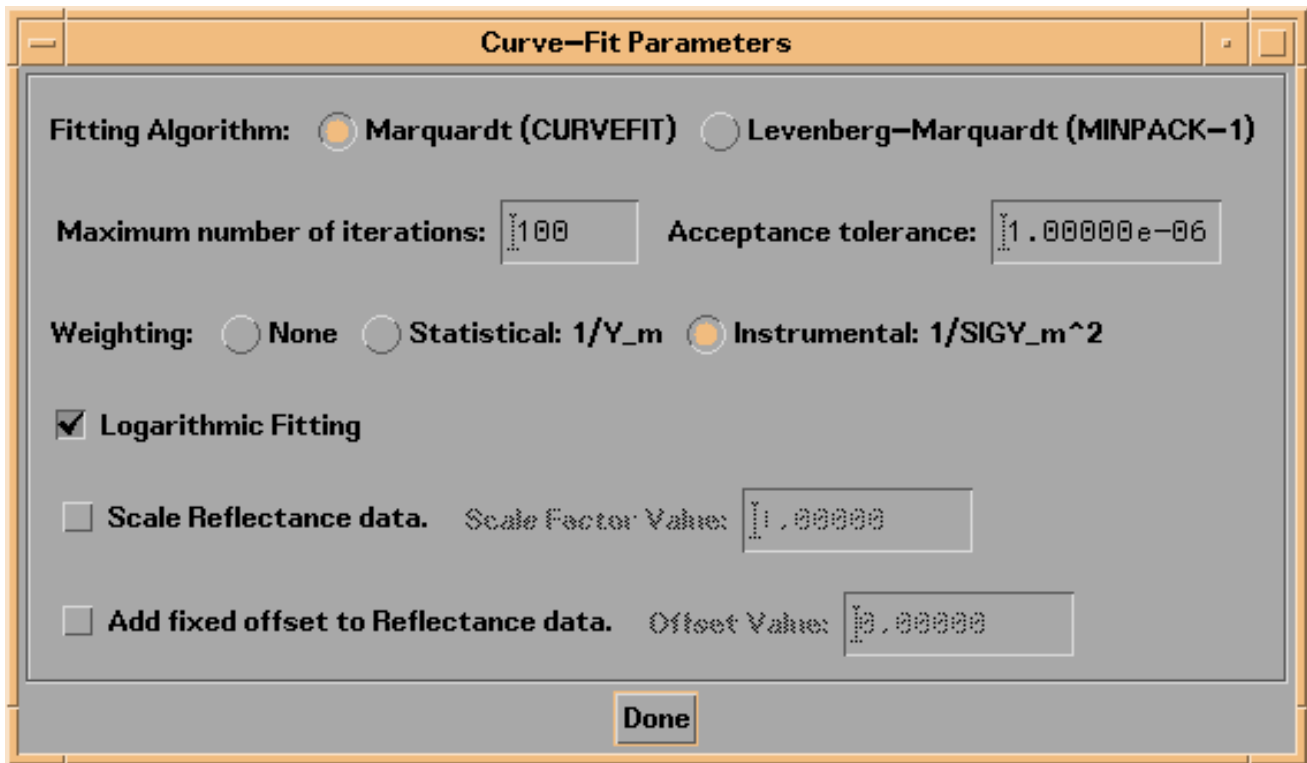


There are several other parameters that you can adjust on the **Curve-Fit Parameters** widget which affect how the fit is performed. This widget is shown in Figure 3.3.2, and is accessible by pressing the **Curve-Fit Parameters...** button in the FIT PARAMETERS section of the main IMD widget.

- You can choose to use either the Marquardt (CURVEFIT) or Levenberg-Marquardt (MINPACK-1) fitting algorithms.
- You can limit the **Maximum number of iterations**, and you can specify the **Acceptance tolerance**: the fitting will stop when the decrease in the (reduced) χ^2 statistic is less than the **Acceptance tolerance** in one iteration.

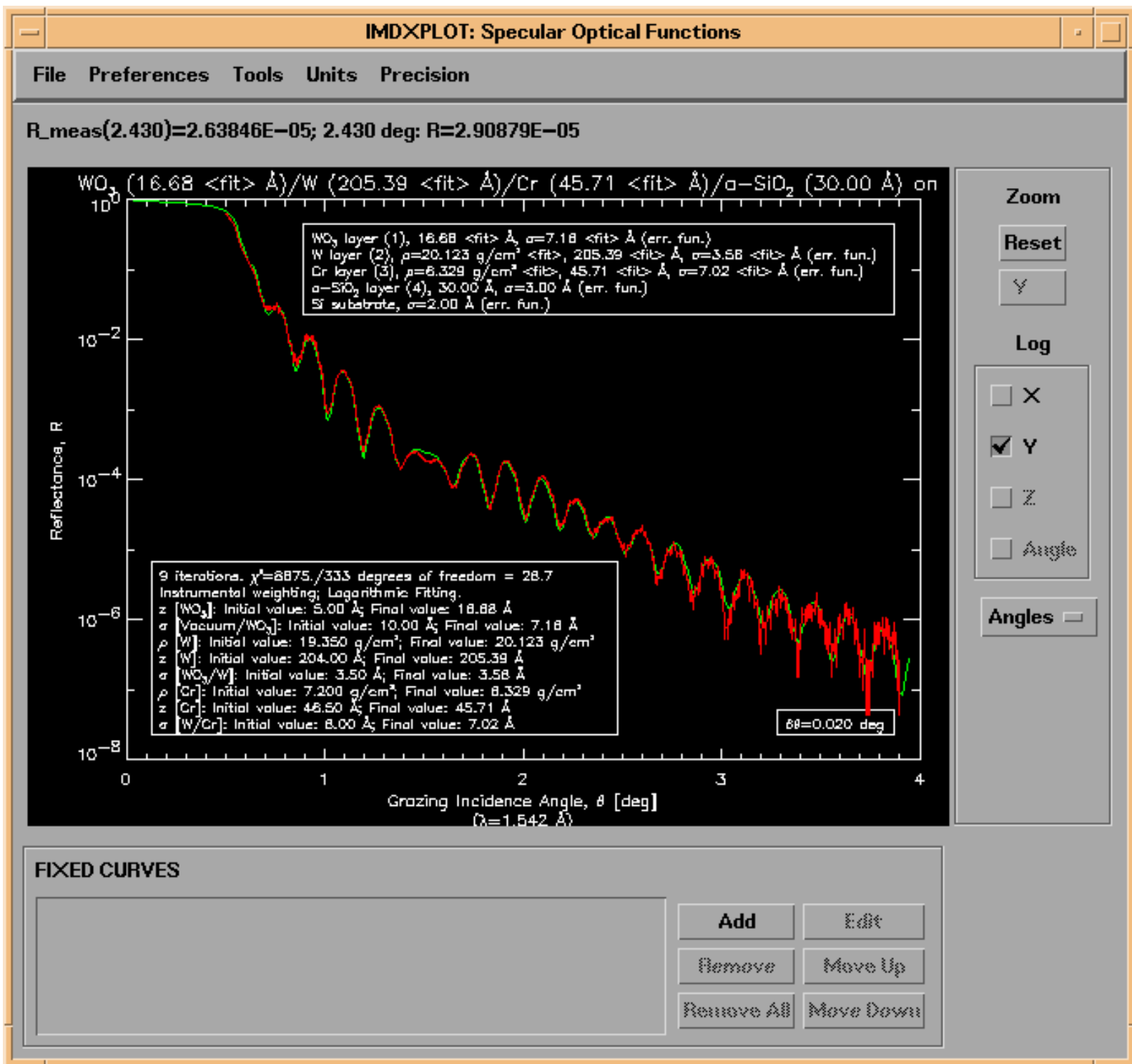
- You can designate the **Weighting** factor: if you have loaded in measured data that includes estimated uncertainties (non-zero **SIGY_m**), then you should use **Instrumental weighting: $1/\text{SIGY}_m^2$** . Otherwise, you can use either **Statistical weighting: $1/Y_m$** , or no weighting. (See reference [15] for more details.)
- You can select **Logarithmic Fitting**, in which case the χ^2 function will be computed from the logarithms of the calculated and measured optical functions.
- You can add a fixed **offset** and/or **scale factor** to the dependent variable, to account for a possible systematic error in your data; or, you can set the offset and/or scale factor values to be fit parameters if desired (using the **Add** button on the FIT PARAMETERS section of the main IMD widget).

Figure 3.3.2. The **Curve-Fit Parameters** widget.



The results of a more complicated fitting example are shown in Figure 3.3.3. In this case, the X-ray reflectance of a W/Cr bilayer film was fit, using eight fit parameters. (The IMD file used to produce this plot is called `examples.dir/WCr_bilayer.FIT.imd`; the measured data file is called `examples.dir/WCr_bilayer.MEASURED.dat`.)

Figure 3.3.3. Fit to X-ray reflectance data of a W/Cr bilayer film



3.4 Confidence Intervals

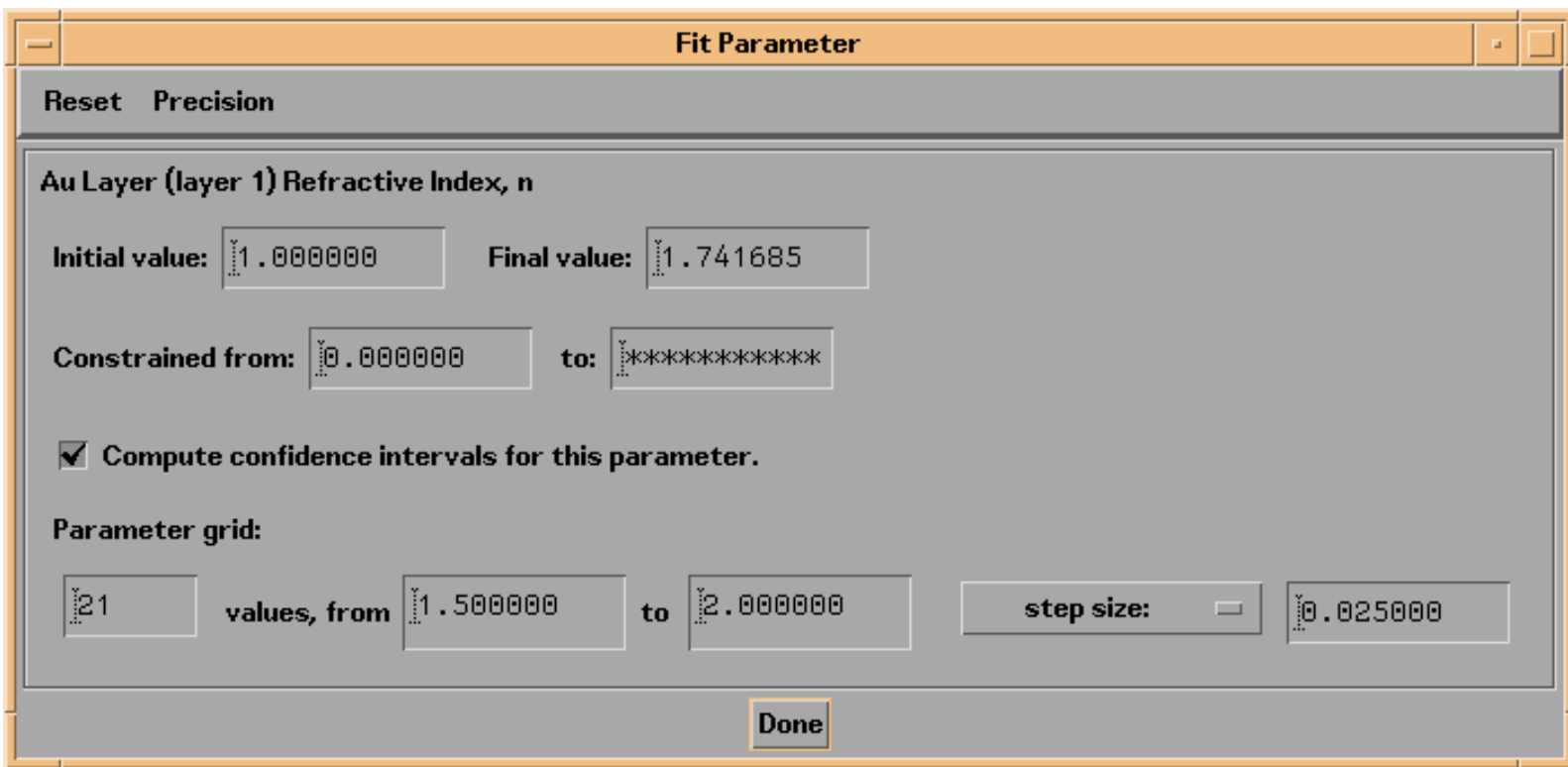
The abbreviated discussion of confidence intervals presented in this section is based largely on the methods described in references [16] and [17]. Please consult those papers for a full discussion.

To quote Lampton, et al., *"In parameter estimation, it is the **range** of parameter values to which a theory is restricted that is the useful result of an experiment. The discrete best-fitting values of the parameters are essentially statistical artifacts subject to a variety of correlated random errors originating in the counting statistics of the original data. If an experiment could be repeated without systematic changes, best-fitting parameter values would differ, while their properly derived allowed ranges will overlap."*

Once you have performed a fit, IMD can compute independent and joint confidence interval estimates on the fit parameters. The confidence intervals are estimated by computing the value of the **Chi²** statistic on a grid of points in parameter-space. Although there is no limit on the number of fit-parameters you can select when performing curve-fitting in IMD, due to the limit of 8-dimensional arrays imposed by IDL, you can only compute 8-dimensional confidence intervals. (If this is a problem for you, then you're probably doing something you shouldn't be doing anyway.)

To compute confidence intervals, you must first designate which fit parameters are to be included in the parameter space to be examined. So, for each parameter of interest, you must check the box labelled **Compute confidence intervals for this parameter**, in the associated **Fit Parameter** widget. Shown in Figure 3.4.1 is the **Fit Parameter** widget for the refractive index, **n** of the Au film in the example of the previous section.

Figure 3.4.1 Fit Parameter widget for refractive index, n



For each fit parameter you select, you must specify the parameter grid over which the **Chi²** statistic is to be computed. To illustrate, in figure 3.4.1, because the best fit value for **n** is approximately 1.66, I have selected 21 parameter values, ranging from **n**=1.5 to 2.0. Similarly, I have selected 21 values for **k**, ranging from 1.9 to 2.1 (not shown.)

Once you have completed the parameter grid specifications for all fit parameters of interest, select the **Calculate->Compute Confidence Intervals** option from the main IMD widget. IMD will then iterate through each of the parameter values throughout the parameter-space grid you have defined, and compute the value of **Chi²**.

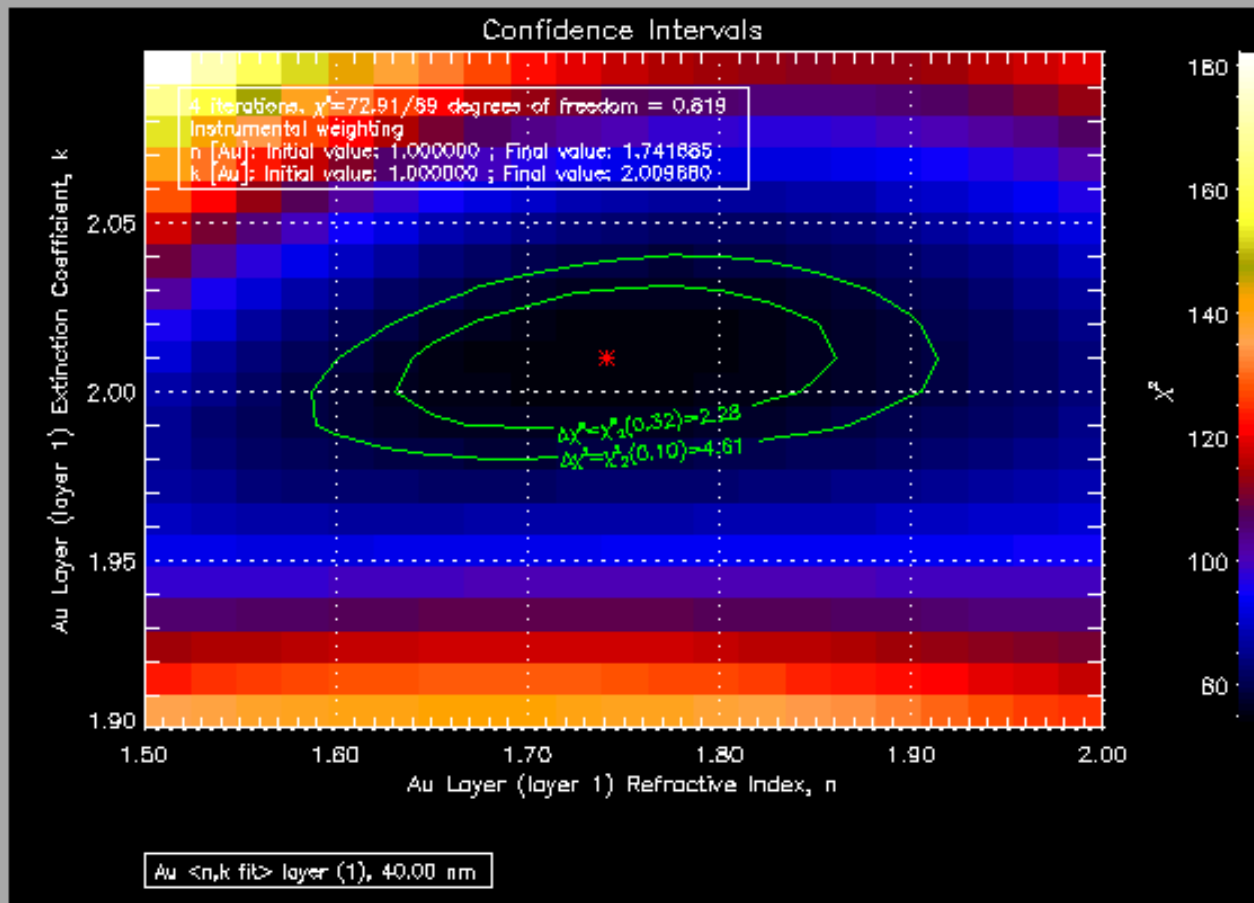
The actual method used to compute **Chi²** at each point in the parameter space you have defined depends on what fraction of the fit parameters you have specified for confidence interval generation. That is, if you have elected to compute confidence intervals for all of the fit parameters used to perform the fit, then IMD will simply compute the value of the optical function for each of the parameter values, and compare it with the measured data in order to compute the value of **Chi²** at that point in parameter space. On the other hand, if you have selected only some of the parameters for confidence interval generation, then IMD will perform a non-linear, least-squares fit to the data at each of the points in the parameter-space grid you have defined, *with the remaining fit parameters used as adjustable parameters to minimize **Chi²** at that point in parameter space*. This latter option is useful if, for example, your fit parameters consist of a mix of 'interesting' and 'uninteresting' parameters. As an example, if you have derived optical constants, **n** and **k**, from reflectance vs. incidence angle data, and have also used a **Reflectance Offset** as a fit parameter to account for some offset in your data, then you might wish to compute confidence intervals for **n** and **k**, but not for the **Reflectance Offset**.

After the calculation is completed, the results will be saved to an IMD file automatically, unless you have disabled this feature in the **File->Auto-Save Preferences** menu.

The confidence intervals will be displayed in another **IMDXPLOT** widget, as shown, for example in Figure 3.4.2:

Figure 3.4.2 Confidence Intervals plot.





Zoom
 Reset
 Log
 ×
 ↵

Contour
 Filled Contour
 Contour + Image

Color Table...

CONFIDENCE LEVEL

Display %
 joint
 confidence interval.

FIT PARAMETERS

n [Au]
 Continuous Variable
 Value:
 Index:

k [Au]
 Continuous Variable
 Value:
 Index:

FIXED CURVES

90.00% joint conf.



By checking the **Continuous Variable** boxes next to each of the fit parameters (in the FIT PARAMETERS area of the **IMDXPLOT** widget,) you can display either 1D plots of **Chi²** versus the parameter value, or 2D contour plots showing contours of constant **Chi²**. You can use the **Value** and **Index** widgets for non-continuous fit parameters to display **Chi²** plots for discrete parameter values, and you can use the **FIXED CURVES** buttons to overlay multiple confidence intervals on the same plot.

The area of the **IMDXPLOT** widget labelled **CONFIDENCE LEVEL** allows you to adjust which confidence level is displayed, and, if you have computed confidence intervals for more than one parameter, whether independent or joint confidence intervals are shown. These adjustments determine the value of **Delta(Chi²)** that is displayed on the plots. That is, the confidence interval corresponds to the region in parameter space for which the value of the **Chi²** statistic is less than the minimum value (i.e., the value at the best-fit point) plus an amount **Delta(Chi²)**. For example, if you have computed confidence intervals for 2 fit parameters, then the 68% joint confidence interval corresponds to **Delta(Chi²) = 3.5**, which is the value of the **Chi²** function for 2 parameters with significance $1-.68=.32$. (Please refer to Lampton et al. for further details.)

Shown in Figure 3.4.2 are 68% and 90% joint confidence intervals for **n** and **k**, for the example we have been discussing. The meaning of these contours is the following: there is a 68% (90%) probability that the true values of **n** and **k** both lie within the green (red) region displayed in the figure.

[Back](#) | [Contents](#) | [Next](#)

1.4 Starting IMD

Before you attempt to start IMD, make sure that the `imd` directory is included in your IDL Path. Consult the IDL manuals for instructions on how to do this.

To start IMD, at the IDL prompt type:

```
IDL> .run imdstart
```

This will load IMD and launch the main IMD program. If you exit IMD and wish to run it again during the same IDL session, at the IDL prompt type:

```
IMD> imd
```

Note: You can define `NORUN=1` before executing `'.run imdstart'`, to inhibit automatic execution of the `imd` procedure.

Note: On Unix platforms, the `IDL_DEVICE` environment variable must be set to 'X'.

[Back](#) | [Contents](#) | [Next](#)